Tomas Bata University in Zlín
Faculty of Applied Informatics

Ing. Libor Pekař

Control of Time Delay Systems – An Algebraic Approach

Řízení systémů se zpožděním – Algebraický přístup

Doctoral Thesis

Advisor: prof. Ing. Roman Prokop, CSc.

Study programme: Chemical and Process Engineering
Study course: Technical Cybernetics

Zlín, Czech Republic, 2013

Acknowledgements

I would like to express gratefulness to my supervisor, prof. Roman Prokop, CSc., for his helpful and kind guidance and valuable advices during my Ph.D. studies.

Next, the warmest word of thanks must be dedicated to my loving wife (in memoriam), a beautiful daughter, a girlfriend and to all my enduring family.

Last but not least, my thanks go to my colleagues from Tomas Bata University in Zlín for creating a comfortable working environment.

The work was supported by the Ministry of Education, Youth and Sports of the Czech Republic under grant no. MSM 7088352102 and by the European Regional Development Fund under the project CEBIA-Tech No. CZ.1.05/2.1.00/03.0089, which are also very gratefully acknowledged.

RESUMÉ

Předložená disertační práce se zabývá problematikou řízení jednorozměrných systémů se zpožděními v algebraickém smyslu v okruhu speciálních meromorfních funkcí, jeho využitím v procesu autotuningu a laděním získaných anizochronních regulátorů.

Popis systémů se vstupně výstupním a/nebo vnitřním zpožděním, jakož i návrh struktury regulátorů, je založen na využití revidovaného a rozšířeného okruhu stabilních a ryzích kvazipolynomiálních meromorfních funkcí. Množina všech stabilizujících regulátorů je určena řešením lineární diofantické rovnice (Bézoutovy rovnosti) spolu s Youla-Kučerovou parametrizací v uvedeném okruhu. Postup umožňuje zajištění vnitřní stability regulačního obvodu, asymptotické sledování průběhu žádané hodnoty a kompenzaci poruchy modelované na vstupu řízené soustavy. Jednou z výhod je, že v nominálním případě lze užitím netriviálního uzavřeného regulačního obvodu docílit konečného spektra některých přenosových funkcí. Metoda je doplněna odvozením podmínek stability pro vybrané kvazipolynomy, neboť tato znalost je zásadní pro správný postup návrhu, a zobecněného Nyquistova kritéria pro systémy se zpožděním a speciální strukturu řízení.

Práce dále obsahuje návrh několika postupů ladění získaných anizochronních regulátorů, jmenovitě spojité posouvání pólů uzavřeného regulačního obvodu, kvazioptimální umístění dominantních pólů v levé komplexní polorovině a rozložení spektra při požadovaném překmitu přechodové funkce.

Pro nalezení dostatečně přesného modelu řízené soustavy jsou taktéž analyticky odvozeny vztahy pro identifikaci neznámých parametrů modelu z reléového experimentu s využitím relé typu nasycení, čímž práce zasahuje do oblasti autotuningu.

Pro inženýrské využití spojitých řídicích algoritmů na číslicovém počítači jsou stručně popsány možnosti jejich diskretizace a zjednodušení a vybrané postupy implementovány na anizochronní regulátory.

Součástí práce jsou příklady objasňující popsané teoretické poznatky a výsledky simulací v prostředí MATLAB/Simulink.

V neposlední řadě disertace prezentuje výsledky reálných identifikačních a řídicích experimentů na laboratorním modelu zaokruhované tepelné soustavy vykazujícím výrazná vnitřní zpoždění, doplněny o základní analýzu robustní stability a kvality regulace z hlediska robustnosti, čímž je verifikována praktická využitelnost použitého přístupu.

SUMMARY

The presented dissertation thesis is focused on control of single-input single-output time delay systems by algebraic means in the ring of special meromorphic functions, on its use in the autotuning and on the tuning of obtained anisochronic controllers.

Time delay systems description as well as controller design is based on the utilization of the extended and revised ring of stable proper quasipolynomial meromorphic functions. The solution of a Diophantine equation (Bézout identity) together with Youla-Kučera parameterization in the ring constitutes the set of all stabilizing controllers. The approach enables to satisfy inner feedback system stability, asymptotic reference tracking and input disturbance attenuation. A benefit of the methodology is that one can acquire a finite spectrum of some feedback transfer functions using a non-trivial control system. Contrariwise, a sufficiently accurate model of the controlled process is needed. Proven stability conditions for some quasipolynomials (since it is crucial for the correct controller design) and a generalized Nyquist criterion for time delay systems and a special control system structure are derived as well.

The thesis then comprises design of selected controller tuning approaches for the obtained anisochronic controllers. Namely, a continuous feedback system spectrum shifting, a quasioptimal dominant pole placement and a pole placement when a desired transfer function overshoot is prescribed. Some original ideas are involved in the methods.

Analytically derived formulas for the identification of unknown model parameters from feedback-relay experiment with saturation relay in order to find a sufficiently accurate process model are presented as well.

For real-world applications with digital computers, control algorithms ought to be discretized and simplified; hence, some approaches are briefly described and implemented.

A numerous examples together with MATLAB/Simulink results clarify theoretic statements throughout the thesis. Selected complex examples involve.

Last but not least, results of identification and control of a laboratory heating plant with significant delays, with a basic robust stability and robust performance analysis, are presented in the thesis, which clearly affirms the practical applicability of the approach.

CONTENT

LIST OF FIGURES **12**

LIST OF TABLES **17**

LIST OF SYMBOLS AND ABBREVIATIONS **18**

1 INTRODUCTION **29**

1.1 MOTIVATION AND BACKGROUND 29

1.2 OVERVIEW OF THE THESIS 30

2 ACTUAL STATE OF RESEARCH AND THEORETICAL BACKGROUND **32**

2.1 MODELS OF LINEAR TDS 32

2.1.1 State space description *33*

2.1.2 Input-output description as a transfer function (matrix) *34*

2.1.3 Operator-based description of autonomous TDS *35*

2.2 POLES AND ZEROS, STABILITY OF TDS 37

2.2.1 Poles and zeros *38*

2.2.2 Stability of TDS *39*

2.3 ALGEBRAIC DESCRIPTION OF TDS 45

2.3.1 Theoretical background, basic algebraic notions *45*

2.3.2 Fields, rings and modules for description of TDS *52*

2.3.3 R_{MS} ring *56*

2.4 ALGEBRAIC CONTROL OF TDS 57

2.4.1 TDS stabilizability and controllability *58*

2.4.2 Overview of algebraic methods in control of TDS *61*

2.4.3 Control of TDS in the R_{MS} ring *65*

2.5 CONTROL SYSTEM STRUCTURES 66

2.5.1 1DoF control structure *66*

2.5.2 TFC control structure *67*

2.6 TUNING OF CONTROLLERS FOR TDS 67

2.6.1 Finite spectrum assignment *68*

2.6.2 Static pole placement for TDS *69*

2.6.3 Continuous pole placement for TDS *73*

2.6.4 Optimal pole placement minimizing the spectral abscissa *78*

2.7 ROBUST STABILITY AND ROBUST PERFORMANCE 81

2.7.1 Nominal performance *83*

2.7.2 Robust stability ... *84*
2.7.3 Robust performance ... *85*
2.8 FUNDAMENTALS OF RELAY AUTOTUNING ... 87
2.8.1 Relay feedback test ... *87*
2.8.2 Model parameters identification ... *89*
2.8.3 Saturation relay ... *91*
2.8.4 Artificial delay for identification of more parameters ... *93*
2.8.5 Use of relay transient ... *94*
2.9 CONTROLLER DISCRETIZATION ... 95
2.9.1 State space methods ... *95*
2.9.2 Input-output methods ... *100*
3 GOALS OF THE THESIS ... 103
4 ALGEBRAIC CONTROLLER DESIGN IN RMS ... 105
4.1 R_{MS} RING ... 105
4.1.1 Revision of the ring ... *105*
4.1.2 Coprime factorization and the Bézout identity ... *110*
4.1.3 Basic properties of the ring ... *115*
4.2 OBJECTIVES IN CONTROLLER DESIGN ... 119
4.3 DERIVATION OF CONTROLLERS FOR 1DOF ... 119
4.3.1 Closed loop stabilization ... *120*
4.3.2 Reference tracking and load disturbance rejection ... *122*
4.4 DERIVATION OF CONTROLLERS FOR TFC ... 126
4.4.1 Closed loop stabilization ... *127*
4.4.2 Solution decomposition ... *127*
4.4.3 Load disturbance rejection and reference tracking ... *128*
4.4.4 Quasi-finite spectrum assignment ... *131*
4.5 STABILITY ANALYSIS OF SELECTED RETARDED QUASIPOLYNOMIALS ... 132
4.6 GENERALIZED NYQUIST CRITERION FOR TDS ... 151
4.6.1 1DoF control structure ... *151*
4.6.2 TFC control structure ... *158*
4.7 EXAMPLES ... 159
4.7.1 Stable system ... *159*
4.7.2 Integration system ... *162*
4.7.3 Unstable system ... *170*

4.7.4 Non-stepwise reference and/or disturbance ... 171

5 TUNING OF ANISOCHRONIC CONTROLLERS ... 178

5.1 ESTIMATION OF A STEP RESPONSE OVERSHOOT ... 178

5.2 CONTINUOUS POLE PLACEMENT FOR DESIRED OVERSHOOT ... 183

5.3 SELF-ORGANIZING MIGRATION ALGORITHM ... 186

5.4 NELDER-MEAD ITERATIVE OPTIMIZATION ALGORITHM ... 189

5.5 STUDY CASE: A SKATER ON THE SWAYING BOW ... 192

5.5.1 Controller structure design ... 193

5.5.2 Desired maximum overshoot ... 195

5.5.3 Spectral abscissa minimization ... 201

6 RELAY FEEDBACK IDENTIFICATION TEST ... 208

6.1 FREQUENCY-DOMAIN SOLUTION ... 208

6.2 TIME-DOMAIN SOLUTION ... 209

7 REAL PLANT APPLICATION EXAMPLE ... 212

7.1 DESCRIPTION OF A LABORATORY HEATING CIRCUIT SYSTEM ... 212

7.2 MODEL OF A LABORATORY HEATING CIRCUIT SYSTEM ... 213

7.2.1 Analysis of the model plant dynamics ... 215

7.2.2 Linearization of the model in the vicinity of the operation point ... 217

7.2.3 Parameters identification ... 222

7.3 DESIGN OF A CONTROLLER FOR THE PLANT IN R_{MS} ... 231

7.3.1 1DoF control structure ... 232

7.3.2 TFC control structure ... 233

7.4 RELAY FEEDBACK IDENTIFICATION TEST ... 236

7.4.1 Frequency-domain solution ... 237

7.4.2 Time-domain solution ... 238

7.4.3 Use of relay transient ... 238

7.4.4 Comparison of the results ... 239

7.4.5 Design of controllers in R_{MS} for the relay-identified model ... 241

7.5 CONTROLLERS SIMPLIFICATION ... 242

7.5.1 Using dominant poles and zeros ... 243

7.5.2 Using the Padé approximation ... 244

7.6 ROBUST ANALYSIS OF CONTROLLERS ... 245

7.6.1 1DoF control structure ... 246

7.6.2 TFC control structure ... 248

7.7 CONTROLLERS TUNING AND SIMULATION EXPERIMENTS 255
7.8 DISCRETE-TIME IMPLEMENTATION 265
7.9 FEEDBACK CONTROL APPLIED TO THE LABORATORY PLANT 269
7.9.1 Original controllers using the R_{MS} ring 270
7.9.2 Relay test based controllers using the R_{MS} ring 272
7.9.3 Simplified controllers using the Padé approximation 279
7.10 DISCUSSION AND SUMMARY 282
8 CONTRIBUTIONS AND FURTHER DIRECTIONS 283
9 CONCLUSION 285
REFERENCES 287
LIST OF AUTHOR'S RELATED PUBLICATIONS 310
AUTHOR'S CURRICULUM VITAE 320

LIST OF FIGURES

Fig. 2.1 1DoF control system structure *66*

Fig. 2.2 TFC control system structure *67*

Fig. 2.3 Bode plots expressing the meaning of $W_M(s)$ *for Example 2.6*..... *83*

Fig. 2.4 The graphical interpretation of nominal performance *84*

Fig. 2.5 The graphical interpretation of robust stability *85*

Fig. 2.6 The graphical interpretation of robust performance *86*

Fig. 2.7 Relay-feedback test scheme *88*

Fig. 2.8 Asymmetric (biased) relay static characteristics..... *89*

Fig. 2.9 Relay with hysteresis static characteristics *90*

Fig. 2.10 Dominant input-output time delay estimation *90*

Fig. 2.11 Saturation relay static characteristics..... *91*

Fig. 2.12 Relay input and output signals for saturation relay *92*

Fig. 4.1 Root loci of the rightmost poles of $G_1(s)$ *from (4.3)* *107*

Fig. 4.2 Clarification of Lemma 4.11..... *135*

Fig. 4.3 For $a\vartheta \le 1$, *the Mikhaylov plot of* $m_1(s)$ *must lie in the first and the fourth quadrant (left) or in the first and second quadrant (right)*..... *138*

Fig. 4.4 Crossover frequency for $m_1(s)$ *138*

Fig. 4.5 The difference between ω_C *(left) and* $\omega_0 \neq \omega_C$ *(right)*..... *145*

Fig. 4.6 Explanation of Observation 4.1..... *145*

Fig. 4.7 MATLAB/Simulink scheme of controller (4.169)..... *161*

Fig. 4.8 Smith predictor structure..... *162*

Fig. 4.9 Simulation control responses of $u_0(t)$ *(left) and* $y(t)$ *(right) for* $b=1$, $\tau=5$, $\gamma=0.75$ *using controllers (4.180)*..... *166*

Fig. 4.10 Simulation control responses of $u_0(t)$ *(left) and* $y(t)$ *(right) for* $b=1$, $\tau=5$, $\gamma=0.75$, $m_0=0.4$, $\varphi=500$ *using controllers (4.183)*..... *166*

Fig. 4.11 Simulation control responses of $u_0(t)$ *(left) and* $y(t)$ *(right) for* $b=1$, $\tau=5$, $\gamma_1=\gamma_2=0.75$, $m_0=0.4$, *using polynomial approach with optimal LQ controllers* *167*

Fig. 4.12 Reconfigured TFC control system structure..... *168*

Fig. 4.13 Simulation control responses of $u_0(t)$ (left) and $y(t)$ (right) for $b=1$, $\tau=5$, $m_0=0.4$ using controllers (4.188) and (4.194) *169*

Fig. 4.14 Simulation control responses of $u_0(t)$ (left) and $y(t), w(t)$ (right) for $a=b=6.5\cdot10^{-2}$, $\tau=15.3$, $\vartheta=6.7$ using controllers (4.212) and (4.215) *174*

Fig. 4.15 Simulation control responses for $a=b=6.5\cdot10^{-2}$, $\tau=15.3$, $\vartheta=6.7$ using controller (4.222) *177*

Fig. 5.1 Reference-to-output step response characteristics and the maximum overshoot *180*

Fig. 5.2 Maximum overshoots $\Delta h_{WY,m,\max}(\xi_\alpha,\xi_z)$ (left) and normalized maximum-overshoot times $t_{\max,norm}(\xi_\alpha,\xi_z)$ (right) for $\xi_\alpha=[0.1,2]$, $\xi_z=\{0.2,0.4,0.6,0.8,1\}$ *181*

Fig. 5.3 Maximum overshoots $\Delta h_{WY,m,\max}(\xi_\alpha,\xi_z)$ (left) and normalized maximum-overshoot times $t_{\max,norm}(\xi_\alpha,\xi_z)$ (right) for $\xi_\alpha=[0.1,2]$, $\xi_z=\{2,3,4,5,10\}$ .. *181*

Fig. 5.4 Maximum overshoots $\Delta h_{WY,m,\max}(\xi_\alpha,\xi_z)$ (left) and normalized maximum-overshoot times $t_{\max,norm}(\xi_\alpha,\xi_z)$ (right) for $\xi_\alpha=[2,10]$, $\xi_z=\{0.2,0.4,0.6,0.8,1\}$ *182*

Fig. 5.5 Maximum overshoots $\Delta h_{WY,m,\max}(\xi_\alpha,\xi_z)$ (left) and normalized maximal-overshoot times $t_{\max,norm}(\xi_\alpha,\xi_z)$ (right) for $\xi_\alpha=[2,10]$, $\xi_z=\{2,3,4,5,10\}$ ... *182*

Fig. 5.6 Maximum overshoots $\Delta h_{WY,m,\max}(\xi_\alpha,\xi_z)$ (left) and normalized maximal-overshoot times $t_{\max,norm}(\xi_\alpha,\xi_z)$ (right) for $\xi_\alpha=[1.5,4.5]$, $\xi_z=\{2.8,3,3.2,3.4,3.6\}$ - A detailed view on "small" overshoots *183*

Fig. 5.7 Roller skater on a controlled swaying bow *193*

*Fig. 5.8 Evolution of **K** using the PPSA – version 1* *196*

Fig. 5.9 Evolution of $\alpha(\mathbf{K})$ (left) and $|\sigma_1-s_1|$ (right) using the PPSA – version 1 .... *197*

*Fig. 5.10 Evolution of **K** using the PPSA – version 2* *198*

Fig. 5.11 Evolution of $|\sigma_1-s_1|$ (left) $|\zeta_1-z_1|$ (right) using the PPSA – version 2 ..... *199*

Fig. 5.12 Evolution of $\alpha_P(\mathbf{K})$ (left) $\alpha_N(\mathbf{K})$ (right) using the PPSA – version 2 ..... *199*

Fig. 5.13 Step responses comparison of results of the PPSA *200*

Fig. 5.14 Evolution of real parts of the rightmost roots of (5.38) using the QCSA *202*

Fig. 5.15 A detailed view on Fig. 5.14 for the iterations range of i = 600-1750 ..... *202*

Fig. 5.16 Evolution of $\mathbf{K}$ *for (5.38) and (5.55) using the QCSA* *203*

Fig. 5.17 Evolution of real parts of the rightmost roots of (5.38) using the QCSA within the iteration range $i \in [3000, 3520]$ *204*

Fig. 5.18 Evolution of $\alpha(\mathbf{K})$ *using the NM for* h_j *= {1, 10, 100} from i = 3305*..... *204*

Fig. 5.19 Evolution of $\alpha(\mathbf{K})$ *using the EGSA for* $\Delta\lambda = 10^{-5}$ *from i = 3305* *205*

Fig. 5.20 Evolution of $\alpha(\mathbf{K})$ *using the SOMA for* $Rad = \{1, 10\}$ *from i = 3305*..... *206*

Fig. 5.21 Evolution of $\alpha(\mathbf{K})$ *using the NM (*d_j *= 100), EGSA (*$\Delta\lambda = 10^{-5}$*) and SOMA (Rad = 10) in the calculation time range starting from i = 3305* .. *206*

Fig. 7.1 A photo (left) and a scheme (right) of a laboratory heating model..... *212*

Fig. 7.2 Heater power step change responses *222*

Fig. 7.3 Comparison of measured and calculated K_{H0} *225*

Fig. 7.4 Comparison of measured and calculated $\dot{m}_0$ *226*

Fig. 7.5 Comparison of measured and calculated K_{C0} *228*

Fig. 7.6 Static characteristics $\vartheta_{HO}(u_P)$, $\vartheta_{CI}(u_P)$, $\vartheta_{CO}(u_P)$, *for P = 300 W,* $u_C = 3\,\mathrm{V}$, $\vartheta_A = 24\,^\circ\mathrm{C}$ *229*

Fig. 7.7 Static characteristics $\vartheta_{HO}(u_C)$, $\vartheta_{CI}(u_C)$, $\vartheta_{CO}(u_C)$, *for P = 300 W,* $u_P = 5\,\mathrm{V}$, $\vartheta_A = 24\,^\circ\mathrm{C}$ *229*

Fig. 7.8 Static characteristics $\vartheta_{HO}(P)$, $\vartheta_{CI}(P)$, $\vartheta_{CO}(P)$, *for* $u_P = 5\,\mathrm{V}$, $u_C = 3\,\mathrm{V}$, $\vartheta_A = 24\,^\circ\mathrm{C}$ *230*

Fig. 7.9 Comparison of measured (dotted) and calculated (solid) step responses for the settings $u_P = 5\,\mathrm{V}$, $u_C = 3\,\mathrm{V}$, $\Delta P = 300\,\mathrm{W}$, *on/off fan is on*..... *231*

Fig. 7.10 MATLAB/Simulink scheme of controller (7.46)..... *234*

Fig. 7.11 Step responses of the original model (7.40) vs. approximating models (6.1) via relay-feedback test..... *240*

Fig. 7.12 Nyquist plots of the original model (7.40) vs. approximating models (6.1) via relay-feedback test..... *241*

Fig. 7.13 Determination of $|W_M(\mathrm{j}\omega)|$ *246*

Fig. 7.14 Robust stability verification for 1DoF..... *247*

Fig. 7.15 Nominal performance – determination of $|W_P(\mathrm{j}\omega)|$ *for 1DoF* *247*

Fig. 7.16 Robust performance test for 1DoF *248*

Fig. 7.17 Robust stability verification for TFC..... *251*

Fig. 7.18 Nominal performance $|S_0(j\omega)|$ [dB] for various m_0, m_1, γ for TFC – part 1 ..... *252*

Fig. 7.19 Nominal performance $|S_0(j\omega)|$ [dB] for various m_0, m_1, γ for TFC – part 2 ..... *253*

Fig. 7.20 Nominal performance – determination of $|W_P(j\omega)|$ for TFC *253*

Fig. 7.21 Robust performance test (7.76) for TFC *254*

Fig. 7.22 Simulation control responses of $u_0(t)$ (left) and $y(t)$ (right) for 1DoF structure) with controller (7.46) *256*

Fig. 7.23 Values of δ and ρ according to (7.85) and (7.86), respectively, for $\lambda = 0.25$ *258*

Fig. 7.24 Simulation control responses of $\Delta u_0(t)$ (left) and $\Delta y(t)$ (right) for the TFC structure with controllers (7.55) - $\gamma \in 0.4$ *258*

Fig. 7.25 Simulation control responses of $\Delta u_0(t)$ (left) and $\Delta y(t)$ (right) for the TFC structure with controllers (7.55) - $\gamma \in 0.8$ *259*

Fig. 7.26 A detailed view on overshoots of $\Delta y(t)$ from Fig. 7.24 ..... *259*

Fig. 7.27 A detailed view on overshoots of $\Delta y(t)$ from Fig. 7.25 ..... *260*

Fig. 7.28 Simulation control responses of $\Delta u_0(t)$ (left) and $\Delta y(t)$ (right) for the 1DoF structure with controllers (7.46) vs. (7.59) *261*

Fig. 7.29 Simulation control responses of $\Delta u_0(t)$ (left) and $\Delta y(t)$ (right) for the TFC structure with controllers (7.55) vs. (7.60) - $m_1 = 0.005, \gamma = 0.4$ *262*

Fig. 7.30 Simulation control responses of $\Delta u_0(t)$ (left) and $\Delta y(t)$ (right) for 1DoF structure with controllers (7.46) vs. (7.90) *263*

Fig. 7.31 Simulation control responses of $\Delta u_0(t)$ (left) and $\Delta y(t)$ (right) for the TFC structure with controllers (7.55) vs. (7.91) and (7.93) *264*

Fig. 7.32 Simulation control responses of $\Delta u_0(t)$ (left) and $\Delta y(t)$ (right) for the 1DoF structure with controllers (7.46) vs. (7.94) *265*

Fig. 7.33 Simulation control responses of $\Delta u_0(t)$ (left) and $\Delta y(t)$ (right) for TFC structure with controllers (7.55) vs. (7.95) *265*

Fig. 7.34 Measured vs. simulated control responses of $\Delta u_0(t)$ for the 1DoF structure with controller (7.46) *270*

Fig. 7.35 Measured vs. simulated control responses of $\Delta y(t)$ for the 1DoF structure with controller (7.46) *271*

Fig. 7.36 Measured vs. simulated control responses of $\Delta u_0(t)$ for the TFC structure with controllers (7.55) *271*

Fig. 7.37 Measured vs. simulated control responses of $\Delta y(t)$ for the TFC structure with controllers (7.55) *272*

Fig. 7.38 Symmetrical on-off relay test *273*

Fig. 7.39 Biased relay test *274*

Fig. 7.40 Step responses comparison of measured data vs. relay based model using the time domain solution *275*

Fig. 7.41 Step responses comparison of measured data vs. relay based model using the time domain solution *276*

Fig. 7.42 Measured vs. simulated control responses of $\Delta u_0(t)$ for the 1DoF structure with controller (7.59) *277*

Fig. 7.43 Measured vs. simulated control responses of $y(t)$ for the 1DoF structure with controller (7.59) *278*

Fig. 7.44 Measured vs. simulated control responses of $\Delta u_0(t)$ for the TFC structure with controllers (7.60) *278*

Fig. 7.45 Measured vs. simulated control responses of $y(t)$ for the TFC structure with controllers (7.60) *279*

Fig. 7.46 Measured vs. simulated control responses of $\Delta u_0(t)$ for the 1DoF structure with controller (7.94) *280*

Fig. 7.47 Measured vs. simulated control responses of $y(t)$ for the 1DoF structure with controller (7.94) *280*

Fig. 7.48 Measured vs. simulated control responses of $\Delta u_0(t)$ for the TFC structure with controllers (7.95) *281*

Fig. 7.49 Measured vs. simulated control responses of $y(t)$ for the TFC structure with controllers (7.95) *281*

LIST OF TABLES

Tab. 4.1 ISE and ISTE criteria values for $b=1,\ \tau=5,\gamma=0.75,\ \varphi=500$ *using controllers (4.180)* *165*

Tab. 4.2 ISE and ISTE criteria values for $b=1,\ \tau=5,\gamma=0.75,m_0=0.4,\ \varphi=500$ *using controllers (4.183)* *166*

Tab. 4.3 ISE and ISTE criteria values for $b=1,\ \tau=5,\ \gamma_1=\gamma_2=0.75,$ $m_0=0.4,\varphi=500$ *using polynomial approach with optimal LQ controllers..* *167*

Tab. 4.4 ISE and ISTE criteria values for $b=1,\ \tau=5,m_0=0.4,\varphi=500$ *using controllers (4.188) and (4.194)* *169*

Tab. 7.1 Measurements of steady-state temperatures for $u_C=3\,\mathrm{V}$ *223*

Tab. 7.2 Measurements of "quasi" steady-state temperatures for $u_C=3\,\mathrm{V}$ *224*

Tab. 7.3 Measured relation $\dot{m}_0(u_P)$ *225*

Tab. 7.4 Measured relation $K_{H0}(u_P,P)$ *[W·K^{-1}]* *225*

Tab. 7.5 Measurements of steady-state temperatures for various $u_C,\ P=300\,\mathrm{W},$ $u_P=5\,\mathrm{V}$ *227*

Tab. 7.6 Measured relation $K_{C0}(u_C)$ *228*

Tab. 7.7 Measured delays as functions of u_P *230*

Tab. 7.8 Frequency-domain solution with saturation relay and artificial delay *238*

Tab. 7.9 Time-domain solution with saturation relay and artificial delay *238*

Tab. 7.10 Solution by the use of the relay transient *239*

Tab. 7.11 Comparison of relay experiment results *241*

Tab. 7.12 Robust performance fulfillment for TFC – yes (Y), no(N) *255*

Tab. 7.13 ISE and ISTE criteria values for controller (7.46) with $\varphi=10$ *256*

Tab. 7.14 Values of δ *and* ρ *according to (7.85) and (7.86), respectively* *257*

Tab. 7.15 Comparison of simulated and measured relay tests data *273*

Tab. 7.16 Time domain solution via NM method *275*

Tab. 7.17 Results of the use of the relay transient with $y_0=36$ *276*

LIST OF SYMBOLS AND ABBREVIATIONS

Symbols

■	end of a lemma, theorem, definition, remark, observation or example
□	end of a proof
\	set relative complement
$\varnothing$	empty set
$\lvert\cdot\rvert$	cardinality of a set, absolute value, modulus, gain
$\lVert\cdot\rVert$	a matrix norm
$:=$	definition
$\equiv$	identity
$\hat{=}$	transformation (correspondence)
$\preceq$	a partial order, ordering
$\subseteq$	set inclusion
$\cup$	union
$\cap$	intersection
1	multiplicative identity element
$a(s)$	plant transfer function denominator as a (quasi)polynomial
α	real part of a complex number
$\alpha(\mathbf{K})$	spectral abscissa
A	amplitude of a plant output for limit cycles
$\tilde{A}$	amplitude of a plant output from ATV^{+} test

$\mathbf{A}_i$, $\widetilde{\mathbf{A}}(\tau)$, $\mathbf{B}_i$, $\widetilde{\mathbf{B}}(\tau)$, $\mathbf{C}$, $\widetilde{\mathbf{C}}(\tau)$, $\mathbf{H}_i$	state matrices
$A(s)$	plant transfer function denominator in $H_\infty(\mathbb{C}^+)$, R_{MS}, R_{PS} (after coprime factorization)
$\mathcal{A}$	infinitesimal generator
$b(s)$	plant transfer function numerator as a (quasi)polynomial
B^+, B^-, B	(upper, lower) amplitude of a relay output
$B(s)$	plant transfer function numerator in $H_\infty(\mathbb{C}^+)$, R_{MS}, R_{PS} (after coprime factorization)
$\mathcal{B}$	behavior
C	space of continuous functions
$\overline{C}_D(\boldsymbol{\eta})$	safe upper bound
$\mathbb{C}$	set of all complex numbers
$\mathbb{C}^k$	k-dimensional space of complex numbers
$\mathbb{C}_0^-$, $\mathbb{C}^-$, $\mathbb{C}_0^+$, $\mathbb{C}^+$	set of complex numbers from the open and closed left half-plane, and the open and closed right half-plane, respectively
$d(t)$, $D(s)$	load disturbance and its Laplace image, respectively
δ	delta transform operator
D	a disk in the complex plane
$\mathfrak{D}$	a region in the complex plane
$\Delta(s)$	perturbation function

e	identity element of a group
$\mathbf{e}_i$	i-th Euclidean unit vector
ε	arbitrarily small positive real number
$e(t),\ E(s)$	control error and its Laplace image, respectively
$\mathcal{E}$	ring of pseudopolynomials
η_i	lumped delays
$\boldsymbol{\eta}$	vector of delays
φ^+	closed Jordan curve (in anti-clockwise direction)
ϕ_D	phase lag by artificial delay
$\Phi(\mathbf{K})$	an objective (cost) function
γ	variable associated with δ
γ_{ij}	weighting controller parameters
G	a group
$G(s)$	plant transfer function, perturbed plant transfer function
$G(\mathrm{j}\omega)$	a transfer fucntion in the frequency domain
$G_{RD}(z), G_{QD}(z)$	discretized controllers‘ transfer functions
$G_0(s)$	nominal plant transfer function, inner feedback transfer function
$G_O(s), L(s)$	open loop transfer function
$G_{DE}(s)$	disturbance-to-error transfer function
$G_{DY}(s)$	disturbance-to-output transfer function

$G_Q(s), G_R(s)$	controllers' transfer functions
$\overline{G}_Q(s)$, $\overline{\overline{G}}_Q(s)$, $\overline{G}_R(s)$	simplified controllers' transfer functions
$G_{WE}(s)$, $S_0(s)$, $S(s)$	reference-to-error transfer function (nominal) sensitivity function
$G_{WY}(s)$, $T_0(s)$, $T(s)$	reference-to-output transfer function (nominal) complementary sensitivity function
$\mathbf{G}(s)$	plant transfer functions matrix
$h_{WY}(t)$	reference-to-output step response function
H_C	set of all entire functions
$H_\infty(\mathbb{C}^+)$	Hardy space of functions analytic and bounded in the right half-plane
i	iteration step
$i_{WY}(t)$	reference-to-output impulse function
I	a set of indexes
Im	imaginary part
I	an ideal
$\mathbf{I}$	unit matrix
$I(\delta)$	discrete-time (delta) integrator
j	imaginary unit
J_{ISE}, J_{ISTE}	values of ISE and ISTE criteria, respectively
k	plant static gain, static characteristics direction (slope) for saturation relay, discretization step
$k_{\min}$	lower bound on k (for saturation relay)

k_u	ultimate gain
$\mathbf{K}$, $\mathbf{K}_{num}$, $\mathbf{K}_{den}$	vector of controller parameters (in the controller transfer function numerator and denominator, respectively)
$\mathbf{K}^*$, $\mathbf{K}_{opt}$	vector of optimal controller parameters
$\Delta\lambda$	discretization step
L	maximum value of lumped delay
L_1, L_2, L_∞	Lebesgue spaces and norms
$\mathcal{L}$	Laplace transform
m	a multiplicity
Δm	a multiplicity difference
m_0, m_1, m_2	controller real (selectable) coefficients
$m_0(s)$	characteristic (quasi)polynomial of a plant
$m(s)$	characteristic (quasi)polynomial of a closed loop
$M_0(s)$	characteristic meromorphic function
M	number of migration rounds
n	system order
n_C, n_R	number of complex conjugate pairs and real poles, respectively
ni	number of iterations
n_{sp}, n_{sz}	number of currently shifted poles and zeros, respectively
N	number of discrete samples

N_H	number of lumped delays
N_U	number of unstable poles (zeros) or conjugate pairs
$\mathbb{N}$	set of all natural numbers
O_R	relative order
p	pole multiplicity
$p_N(s), p_D(s)$	numerator and denominator (quasi)polynomial of $P(s)$, respectively
P	a partially ordered set, population
$P(s)$	controller transfer function denominator in R_{MS} or R_{PS}
$P_H(t)$	heater power
$\mathbf{P}_R$	reachability matrix
q	quotient, shifting operator
q_0	crossover gain
q_C	critical gain
$Q(s),\ R(s)$	controller transfer function numerator in R_{MS} or R_{PS}
r	reminder, number of controller parameters
r_{num}, r_{den}	number of free controller parameters in the transfer function numerator and denominator, respectively
r_Ω	spectral radius

$r_1,...,r_M$	independent delays
R	a ring
$R(A)$	describing function of a relay
Re	real part
R_{MS}	ring of proper and stable (retarded) quasipolynomial meromorphic functions
R_{PS}	ring of stable and proper rational functions
$\mathbb{R}^k$	*k*-dimensional space of real numbers
$\mathbb{R}^+$	positive real numbers
$\mathbb{R}[s]$	a polynomial in s over real numbers
$\mathbb{R}[s,z]$	a 2-D polynomial (a polynomial in s and z over real numbers)
$\mathbb{R}(s)$	a rational function in s over real numbers
$\mathbb{R}(s,z)$	a rational function in s and z over real numbers
$\mathcal{R}$	ring of polynomials in $\exp(-\tau s)$ over Θ
s	complex variable (from the Laplace transform)
$\bar{s}$	complex conjugate of s
s_0 , s_i, σ_i	system (or transfer function) poles
ρ	sampling radius
S	a ground set, simplex
$\mathbf{S}$	sensitivity matrix
t	time variable

$t_{\max}, t_{\max,norm}$	time to step response maximum peak overshoot and its normed value, respectively
t_f	final time
t_O	time to step response peak overshoot
$t_N(s), t_D(s)$	numerator and denominator (quasi)polynomial of $T(s)=Q(s)+R(s)$, respectively
τ , T	distributed delay, input-output delay
τ^+	artificial delay
ϑ	internal delay
T_s , T_0	sampling period
T_u	ultimate period
$\mathcal{T}(t)$	solution operator
Θ	ring generated by entire functions from the transformation of distributed delays
$\mathbf{u}(t)$	vector of inputs
$u(t)$, $U(s)$	control signal (manipulated input) and its Laplace image, respectively
$\overline{U}(s)$	Fourier image of decayed $u(t)$
$\mathbf{U}(s)$	vector of transformed inputs
$\mathbf{v}_{PRT}$	perturbation vector
$\mathbf{x}(t)$	vector of state variables
$\xi(t)$	initial state vector

$\boldsymbol{x}_t$	vector of state variables from the Banach space within the range $t \in [0, \tau]$
X	Banach space of continuous functions
$\tilde{X}$	Hilbert product space
$w(t),\ W(s)$	reference value and its Laplace image, respectively
$W_M(s),\ W_P(s)$	weight functions
$\mathbf{y}(t)$	vector of outputs
$y(t),\ Y(s)$	plant output signal and its Laplace image, respectively
$\overline{Y}(s)$	Fourier image of decayed $y(t)$
$\mathbf{Y}(s)$	vector of transformed outputs
z	complex number, variable from the z-transform
$\mathbb{Z}$	integers
ω	frequency, imaginary part of a complex number
ω_0	crossover frequency
ω_C	critical frequency
ω_u	ultimate frequency
Ω	a set

Abbreviations

1-D, 2-D	one-dimensional, two-dimensional
1DoF	One-Degree-of-Freedom
A/D	Analog/Digital
ATV, ATV$^+$	Autotune Variation (plus)
BIBO	Bounded Input Bounded Output
CTCR	Clustering Treatment of Characteristic Roots
DC	Direct (stationary) Component
DDS	Delay Dependent Stability
deg	degree
den	denominator
DFT	Discrete Fourient Transform
DTFT	Discrete-Time Fourient Transform
DIS	Delay Independent Stability
EGSA	Extended Gradient Sampling Algorithm
FDE	Functional Differential Equation
FFT	Fast Fourier Transform
FSA	Finite Spectrum Assignment
GCD	Greatest Common Divisor
IMC	Internal Model Control
ISE	Integrated Squared Error
ISTE	Integrated Squared Time Error
LCM	Least Common Multiple
LQ	Linear-Quadratic

LM	Levenberg-Marqurdt
LMS	Linear Multistep
LTI	Linear Time-Invariant
MIMO	Multi-Input Multi-Output
MS	Microsoft
num	numerator
NM	Nelder-Mead
ODE	Ordinary Differential Equation
PC	Personal Computer
PID	Proportional–Integral–Derivative (controller), Principal Ideal Domain
PP	Pole Placement
PPSA	Pole-Placement Shifting based controller tuning Algorithm
QCSA	Quasi-Continuous Shifting Algorithm
R-K	Runge-Kutta
SISO	Single-Input Single-Output
SOMA	Self-Organizing Migration Algorithm
TDS	Time Delay System(s)
TFC	Two Feedback Controllers
UFD, UFR	Unique Factorization Domain (Ring)

Besides aforementioned more or less general symbols and abbreviations, there are also other ones used “locally”, i.e. for the only purpose, in the thesis. Their meaning should be always clear from the context.

1 INTRODUCTION

In this introductory chapter, an explanation of the work motivation and the background of the problem dealt with in this thesis are presented. The structure of the thesis is also introduced.

1.1 Motivation and background

It is a well known fact that a large number of both hypothetic and real-life processes and systems in a wide spectrum of human activities (e.g. in biology, chemistry, economics, mechanics, information technologies, etc.) are affected by delay as their generic part. Delay within the meaning of a lag or latency has been usually assumed to take effect in input-output relations only, and moreover, in a one time instant. However, this conception is somewhat restrictive in effort to fit and model the real plant dynamics since in many cases delay appears in process inner feedback loops (or/and it can be of a distributed or nature).

Time delay systems (TDS), also called hereditary, anisochronic, or systems with aftereffect or dead-time, involve delays as other dynamical elements, besides integrators. Hence, instead of ordinary differential equations (ODEs), these systems are described by equations with deviating arguments or so-called differential-difference equations which belong to the class of infinite dimensional functional differential equations (FDEs). Anisochronic models serve not only for description of systems in which the inner loops are really delayed but they (even of low order) can adequately fit the dynamics of many conventional high-order systems. In contrast to undelayed linear time-invariant (LTI) systems, linear TDS have some surprising features, namely, they own an infinity spectrum, which makes these systems difficult to control and resistant to many “classical” controllers. Delay significantly deteriorates the dynamics and performance of feedback control loops, and control theory has been dealing with the problem of delay effect on the feedback system since its nascence.

Although it may appear that the simplest approach consists in replacing TDS by some finite dimension approximations, it is not a convenient solution in general since it

leads to a higher degree of complexity and one looses the process dynamics information. Therefore, naturally, other approaches to control of TDS ought to be developed utilizing non-approximated (notwithstanding linear) process model to keep information about dynamics expressed by delays.

Algebraic structures in their charming and attractive elegance proved to be suitable and effective tools for system dynamics description and control system design. Modern control theory has been adopting algebraic approaches and parlance, which are based on TDS description in a suitable field, ring or module and the subsequent operation in the algebraic structure, for decades.

This work is focused on theory, simulation and practical application problems related to control of single-input single-output (SISO) linear TDS designed through the general solutions of Diophantine equations in the revised and extended ring of proper and stable quasipolynomial meromorphic functions (R_{MS}).

1.2 Overview of the thesis

The content of this work is divided into nine main chapters. In an attempt to facilitate the orientation in the text for reader, a simple guideline throughout the thesis is provided.

This first, introductory, part is intended for explaining the motivation for writing the thesis and background of the issue, and it includes the thesis overview.

In the second chapter, the current state of the research and theoretical background devoted to description, analysis and algebraic control of LTI TDS and to some controller tuning principles, and basics of autotuning including references to recent and momentous literature are introduced.

The main goals of the thesis follow in the third chapter.

The fourth (and the principal) part starts with the analysis and revision of the R_{MS} set followed by the derivation of controllers in R_{MS} for two control system structures. Moreover, it includes many examples to illustrate given problems.

Next, the fifth part presents the application of selected tuning approaches usable in an effort to set the unknown (free) anisochronic controller parameters appropriately. Pole placement methods are accentuated.

In the sixth chapter, the fundamentals of the relay feedback experiment due to TDS model parameters identification are utilized where a saturation relay and the Fourier transform are taken into account.

The subsequent, seventh, section presents results of identification and algebraic control experiments realized on real laboratory model of a circuit heating system. The chapter contains a mathematical model of the process, its linearization, controller design in R_{MS} and its tuning, controller robust analysis, simplification and digital implementation, in sequence. Moreover, controller design for simple models obtained from the relay test and that for simplified (finite-dimensional) controller structures are introduced. Simulation experiments facilitate the selection of the suitable controller for the final real-time control trial.

The aim of the eighth chapter is to sum up main contributions of the thesis both for science community and practical applications, and to foreshadow further direction in the research.

The final, ninth, chapter concludes the whole work.

References to the sources drawn in the work, the list of author's publications associated with the subject of the thesis and his curriculum vitae are naturally placed at the end of the work.

2 ACTUAL STATE OF RESEARCH AND THEORETICAL BACKGROUND

2.1 Models of linear TDS

Linear time-invariant time delay systems (LTI TDS) have usually been assumed to contain delay elements in input-output relations only. All the system dynamics has been hence modeled by point accumulations in the form of a set of ordinary differential equations. The Laplace transform then results in a transfer function expressed by a serial combination of a delayless term and a delay. However, this conception is somewhat restrictive in effort to fit the real plant dynamics because inner feedbacks are often of time-distributed or delayed nature.

Anisochronic (or *hereditary*) TDS models, on the other hand, offer a more universal dynamics description applying both integrators and delay elements either in lumped or distributed form so that delays appear on the left side of a differential equation which is no longer *ordinary* (ODE) but rather *functional* (FDE) - this brings the concept of *internal* (or *state*) delays. In the further text, an abbreviation TDS means LTI TDS containing state delays with or without input-output delays.

Already Volterra formulated differential equations incorporating the past states when he was studying predator-pray models [170]. The theory of these models was then developed by Bellman and Cooke [6], Krasovskii [67], Kolmanovskii and Nosov [66], Zítek [195], Górecki et al. [47] , Marshall et al. [86] and especially by Hale and Verduyn Lunel [50] and Niculescu [106], to name a few. Aftereffect phenomenon is included in many processes, e.g. in chemical processes [198], heat exchange networks [197], in internal combustion engines with catalytic converter [142], in models of mass flow in sugar factory [42], in metallurgic processes [100], etc. Plenty of references to examples of processes with internal delays, covering a wide range of human activities (e.g. biology, chemistry, economics, communication and information technologies, etc.) are introduced in [65], [106], [141]. Capabilities and advantages of this class of models and controllers for modeling and process control were broadly discussed in [83]. TDS models can be used not only for description of those systems embodying internal delays but they are successfully

capable to express the dynamics of high-order systems and processes even without apparent delays [151], [173], [205], which simplifies the processes description.

2.1.1 State space description

In the LTI case, TDS can be described by state and output functional differential equations in the following form [47], [141]

$$\begin{aligned}\frac{\mathrm{d}\mathbf{x}(t)}{\mathrm{d}t} &= \sum_{i=1}^{N_H}\mathbf{H}_i\frac{\mathrm{d}\mathbf{x}(t-\eta_i)}{\mathrm{d}t}+\mathbf{A}_0\mathbf{x}(t)+\sum_{i=1}^{N_A}\mathbf{A}_i\mathbf{x}(t-\eta_i)+\mathbf{B}_0\mathbf{u}(t)+\sum_{i=1}^{N_B}\mathbf{B}_i\mathbf{u}(t-\eta_i)\\ &\quad+\int_0^L\left[\tilde{\mathbf{A}}(\tau)\mathbf{x}(t-\tau)+\tilde{\mathbf{B}}(\tau)\mathbf{u}(t-\tau)\right]\mathrm{d}\tau \qquad (2.1)\\ \mathbf{y}(t) &= \mathbf{C}\mathbf{x}(t)+\int_0^L\tilde{\mathbf{C}}(\tau)\mathbf{x}(t-\tau)\mathrm{d}\tau\end{aligned}$$

where $\mathbf{x}\in\mathbb{R}^n$ is a vector of state variables, $\mathbf{u}\in\mathbb{R}^m$ stands for a vector of inputs, $\mathbf{y}\in\mathbb{R}^l$ represents a vector of outputs, $\mathbf{A}_i$, $\tilde{\mathbf{A}}(\tau)$, $\mathbf{B}_i$, $\tilde{\mathbf{B}}(\tau)$, $\mathbf{C}$, $\tilde{\mathbf{C}}(\tau)$, $\mathbf{H}_i$ are matrices of compatible dimensions, $0\le\eta_i\le L$ are *lumped* (discrete) delays and convolution integrals express *distributed* delays. If $\mathbf{H}_i\neq\mathbf{0}$ for any i = 1,2,...N_H, model (2.1) is called *neutral*; on the other hand, if $\mathbf{H}_i=\mathbf{0}$ for every i = 1,2,...N_H, so-called *retarded* model is obtained. It should be noted that the state of model (2.1) is given not only by a vector of state variables in the current time (in one time instant), but also by a segment of the last model history of state and input variables, i.e. $\mathbf{x}(t+\tau)$, $\mathbf{u}(t+\tau)$, $\tau\in\langle -L,0\rangle$.

Model (2.1) can also be expressed in more consistent functional form using Riemann-Stieltjes integrals so that both lumped and distributed delays are under one convolution [141], [195], [205]

$$\frac{\mathrm{d}\mathbf{x}(t)}{\mathrm{d}t}=\int_0^L\mathrm{d}\bar{\mathbf{A}}_N(\tau)\frac{\mathrm{d}\mathbf{x}(t-\eta_i)}{\mathrm{d}t}+\int_0^L\mathrm{d}\bar{\mathbf{A}}_R(\tau)\mathbf{x}(t-\tau)+\int_0^L\mathrm{d}\bar{\mathbf{B}}(\tau)\mathbf{u}(t-\tau),\ \mathbf{y}(t)=\int_0^L\mathrm{d}\bar{\mathbf{C}}(\tau)\mathbf{x}(t-\tau) \qquad (2.2)$$

Contrariwise, integrals in (2.1) can be rewritten into sums using the Laplace transform, which is suitable for model implementation in computers and simulations. Under some assumptions, see [141], the transform correspondence is the following

$$\mathcal{L}\left[\int_0^L \mathbf{F}(\tau)g(t-\tau)\mathrm{d}\tau\right] = g(s)\int_0^L \mathbf{F}(\tau)\exp(-s\tau)\mathrm{d}\tau + \mathbf{F}_0(s) \tag{2.3}$$

where

$$\begin{aligned}
&g(s) = \mathcal{L}[g(t)] = \int_0^\infty g(\tau)\exp(-s\tau)\mathrm{d}\tau,\\
&\mathbf{F}_0(s) = \mathcal{L}[\mathbf{F}_0(t)] = \int_0^\infty \mathbf{F}_0(\tau)\exp(-s\tau)\mathrm{d}\tau,\ \mathbf{F}_0(t) = \int_t^L \mathbf{F}(\tau)\varphi(t-\tau)\mathrm{d}\tau,\\
&g(\tau) = \varphi(\tau), \tau \in [-L, 0],\ \mathbf{F}(\cdot) \in \left\{\tilde{\mathbf{A}}(\cdot), \tilde{\mathbf{B}}(\cdot), \tilde{\mathbf{C}}(\cdot)\right\},\ g(\cdot) \in \{x(\cdot), u(\cdot), y(\cdot)\}
\end{aligned} \tag{2.4}$$

Subsequent utilization of the reverse Laplace transform instructs how to realize a model. For the scalar case of $\mathbf{F}(\tau)$, explicit relations between convolution integrals for distributed delays with

$$\begin{aligned}
F_\varphi(\tau) &= \tau^{(i)}\exp(\tau\,\mathrm{Re}\,\sigma)\cos(\tau\,\mathrm{Im}\,\sigma)\\
F_\psi(\tau) &= \tau^{(i)}\exp(\tau\,\mathrm{Re}\,\sigma)\sin(\tau\,\mathrm{Im}\,\sigma)
\end{aligned} \tag{2.5}$$

and derivatives of functions

$$\varphi_\sigma(s) = 0.5(\theta_\sigma + \theta_{\bar{\sigma}}), \psi_\sigma(s) = 0.5\mathrm{j}(\theta_\sigma - \theta_{\bar{\sigma}}), \theta_\sigma(s) = \frac{1-\exp(-\tau(s-\sigma))}{s-\sigma}, \sigma \in \mathbb{C} \tag{2.6}$$

was presented in [16]. Note that $\bar{\sigma}$ stands for the complex conjugate of σ and $t^{(i)}$ denotes the *i*-th derivative of *t*. $\theta_\sigma(s)$ is an entire function with $\theta_\sigma(\sigma) = \tau$.

Alternatively, one can use a numeric approximation of convolutions in (2.1) or (2.2) to get state and output equations containing lumped delays only, which can, however, destabilize even a stable system, see [141] and reference herein. Another possibility is to introduce a new state variable $\mathbf{z}(t) = \left[\mathbf{x}(t) \quad \frac{\mathrm{d}\mathbf{x}(t)}{\mathrm{d}t}\right]^{\mathrm{T}}$, see e.g. [143].

2.1.2 Input-output description as a transfer function (matrix)

Considering model (2.1) and zero initial conditions, the following input-output description of a general multi-input multi-output (MIMO) system in the form of the transfer matrix using the Laplace transform is obtained

$$
\begin{aligned}
\mathbf{Y}(s) &= \mathbf{G}(s)\mathbf{U}(s) = \frac{\mathbf{C}(s)\mathrm{adj}[s\mathbf{I}-\mathbf{A}(s)]\mathbf{B}(s)}{\det[s\mathbf{I}-\mathbf{A}(s)]}\mathbf{U}(s) \\
\mathbf{A}(s) &= s\sum_{i=1}^{N_H}\mathbf{H}_i \exp(-s\eta_i) + \mathbf{A}_0 + \sum_{i=1}^{N_A}\mathbf{A}_i \exp(-s\eta_i) + \int_0^L \tilde{\mathbf{A}}(\tau)\exp(-s\tau)\mathrm{d}\tau \\
\mathbf{B}(s) &= \mathbf{B}_0 + \sum_{i=1}^{N_B}\mathbf{B}_i \exp(-s\eta_i) + \int_0^L \tilde{\mathbf{B}}(\tau)\exp(-s\tau)\mathrm{d}\tau \\
\mathbf{C}(s) &= \mathbf{C} + \int_0^L \tilde{\mathbf{C}}(\tau)\exp(-s\tau)\mathrm{d}\tau
\end{aligned}
\qquad (2.7)
$$

The main advantage of the TDS system description in the form of the transfer function lies in its practical usability when system analysis and control design. All transfer functions in **G**(*s*) (or a transfer function in SISO case) have identical denominator in the form

$$
m_0(s) = \mathrm{num}\det[s\mathbf{I}-\mathbf{A}(s)] = \mathrm{num}M_0(s) = s^n + \sum_{i=0}^{n}\sum_{j=1}^{h_i} m_{ij}s^i \exp(-s\eta_{ij}), \eta_{ij} \geq 0 \qquad (2.8)
$$

where prefix num means the numerator of the determinant, and $\sum_{j=1}^{h_n} m_{nj}\exp(-\eta_{nj}s) \neq$ constant holds for a neutral system; otherwise, the system is retarded. The expression on the right-hand side of (2.8) represents a so-called *quasipolynomial* [36]. Indeed, $M_0(s)$ is a ratio of quasipolynomials (i.e. a meromorphic function) in general due to distributed state (internal) delays, and all roots of the denominator of $M_0(s)$ are those of the numerator in this case. As a consequence, a transfer function (in a SISO case) can be expressed as a meromorphic function as well.

2.1.3 Operator-based description of autonomous TDS

In order to comprehend a chapter of this thesis, let us briefly introduce another possible (autonomous) TDS description and some associated notions. When investigating on e.g. stability of TDS, the operator-based state space description of an autonomous system can be advantageous, see [10], [29], [50], [171], [187].

Consider e.g. autonomous state part of (2.1), i.e.

$$\frac{\mathrm{d}\mathbf{x}(t)}{\mathrm{d}t}=\sum_{i=1}^{N_H}\mathbf{H}_i\frac{\mathrm{d}\mathbf{x}(t-\eta_i)}{\mathrm{d}t}+\mathbf{A}_0\mathbf{x}(t)+\sum_{i=1}^{N_A}\mathbf{A}_i\mathbf{x}(t-\eta_i)+\int_0^L\tilde{\mathbf{A}}(\tau)\mathbf{x}(t-\tau)\mathrm{d}\tau \tag{2.9}$$

and introduce the state and its derivative

$$\boldsymbol{x}_t=\mathbf{x}(t+\tau),\dot{\boldsymbol{x}}_t=\dot{\mathbf{x}}(t+\tau)=\frac{\mathrm{d}\mathbf{x}(t+\tau)}{\mathrm{d}t},\ \tau\in[-L,0] \tag{2.10}$$

in the Banach space of continuous real function on the defined interval

$$X=C([-L,0],\mathbb{R}^n) \tag{2.11}$$

provided with the supremum norm of the initial function $\mathbf{x}(t)=\boldsymbol{\xi}(t),t\in[-L,0]$, i.e., $\|\boldsymbol{\xi}\|=\max_{-T\le\tau\le0}|\boldsymbol{\xi}(\tau)|$, and that of its derivative as well.

Let the *solution operator* $\mathcal{T}(t),t\ge0$ on the Banach space be defined by

$$\mathcal{T}(t)\boldsymbol{\xi}=\boldsymbol{x}_t,\ \boldsymbol{\xi}\in X \tag{2.12}$$

The family of $\{\mathcal{T}(t)\}_{t\ge0}$ is strongly continuous semigroup [116], [171] with *infinitesimal generator* $\mathcal{A}:\mathcal{D}(\mathcal{A})\subseteq X\to X$ given by

$$\mathcal{A}\ \boldsymbol{\xi}=\dot{\boldsymbol{\xi}}=\lim_{t\to0}(\mathcal{T}(t)\boldsymbol{\xi}-\boldsymbol{\xi})/t \tag{2.13}$$

with domain

$$\mathcal{D}(\mathcal{A})=\left\{\boldsymbol{\psi}\in X:\dot{\boldsymbol{\psi}}\in X,\dot{\boldsymbol{\psi}}(0)=\sum_{i=1}^{N_H}\mathbf{H}_i\dot{\boldsymbol{\psi}}(-\eta_i)+\mathbf{A}_0\boldsymbol{\psi}(0)+\sum_{i=1}^{N_A}\mathbf{A}_i\boldsymbol{\psi}(-\eta_i)+\int_0^L\tilde{\mathbf{A}}(\tau)\boldsymbol{\psi}(-\tau)\mathrm{d}\tau\right\} \tag{2.14}$$

Then (2.9) can be written as a Cauchy problem in the operator form [29].

$$\begin{aligned}&\boldsymbol{x}_0=\boldsymbol{\xi}\\&\frac{\mathrm{d}\boldsymbol{x}_t}{\mathrm{d}t}=\mathcal{A}\,\boldsymbol{x}_t,\ t>0\end{aligned} \tag{2.15}$$

A survey of some other (predominantly state space) models of TDS is introduced in [141]. Moreover, in this thesis, selected algebraic-based models over fields and rings are depicted in Subchapters 2.3 and 4.1.

2.2 Poles and zeros, stability of TDS

Formula (2.8) expresses the characteristic quasipolynomial of system (2.1), the meaning of which is as similar as for delay-free systems, i.e. the solution of $m_0(s)=0$ determines zero points of the transfer function denominator. In principle, there are two cases when the set these solutions do not equal to the system poles. First, the realization of the system (or an appropriate model) is not minimal, so that in the SISO case there is a common factor in the numerator and the denominator of the transfer function, as known for finite-dimensional systems. Second (which is specific for TDS), there is an effect of a distributed delay which results in a common root of the numerator and denominator of the transfer function, yet there is no common factor which can be reduced. The following example [74] clarifies the latter case for distributed input-output delays.

Example 2.1

Consider the transfer function

$$G(s)=\frac{Y(s)}{U(s)}=\frac{1-\exp(1)\exp(-s)}{s-1} \tag{2.16}$$

The common root of the numerator and denominator, $\sigma=1$, is unstable (see Subchapter 2.2.2). Although the is no stable realization in the form (2.1) only with lumped delays, there exists a realization using convolutions (distributed delays) which is stable

$$y(t)=\int_0^1 \exp(\tau)u(t-\tau)\mathrm{d}\tau \tag{2.17}$$

since it is defined via a finite integral. ■

2.2.1 Poles and zeros

In the further text, poles and zeros will mean transfer function poles and zeros, for the simplicity. More precisely for a SISO case, *poles* σ_i, $i \in \mathbb{N}$ of LTI TDS are solutions of the equation

$$M_0(s) = \det[s\mathbf{I} - \mathbf{A}(s)] = 0 \tag{2.18}$$

Zeros $\zeta_i, i \in \mathbb{N}$ are given by the solution of

$$G(s) = \frac{\mathbf{C}(s)\mathrm{adj}[s\mathbf{I} - \mathbf{A}(s)]\mathbf{B}(s)}{\det[s\mathbf{I} - \mathbf{A}(s)]} = 0 \tag{2.19}$$

where the matrices $\mathbf{A}(s)$, $\mathbf{B}(s)$, $\mathbf{C}(s)$ are defined in (2.7). This definition ignores possible common roots of a numerator and denominator of the transfer function since they do not influence the system dynamics. The role of poles and zeros is the same as for delay-free systems, so that they decide about system stability and phase minimality, respectively.

Due to transcendental character of $M_0(s)$ caused by functionality of its exponential terms, the number of poles is infinite; however, as for delay-free systems, spectrum $\Omega := \{\sigma_i\}_{i=1}^{\infty}$ decides about asymptotic system stability. Spectral properties of retarded and neutral systems significantly differ; according to [6] poles occur in chains depending of the type of a system. For systems of retarded type, poles satisfy $\mathrm{Re}\,\sigma_i \to -\infty$ and thus there are only finitely many poles in any right half-plane; whereas poles of a neutral type system lie in a band centered on the imaginary axis, which implies that it owns an infinite number of poles with $\mathrm{Re}\,\sigma_i > a$ for some finite real *a*. Note that there also exist systems of *advanced* type satisfying $\mathrm{Re}\,\sigma_i \to \infty$.

Locations of poles can be done using a gridding procedure [174], [176] or via discretization methods [12], [39], [77], estimating either the solution operator or the infinite dimensional generator, among others.

Stability notions of both retarded and neutral TDS systems together with a brief overview of the literature dealing with this topic are introduced in the following subchapter.

2.2.2 Stability of TDS

We introduce some stability notions and preliminaries for TDS with respect to different properties of retarded and neutral systems to understand the literature overview and the further text of the thesis.

Delay independent stability (DIS) means that delay(s) may cover the full range $[0,\infty]$, whereas in *delay-depended stability* (DDS) one considers that the finite interval $\tau \in [\tau_1, \tau_2]$ is taken into account.

Considering the characteristic equation (2.18), a TDS is *asymptotically stable* if all poles are located in the open left half-plane, $\mathbb{C}_0^-$, i.e. there is no *s* satisfying

$$M_0(s) = 0 \tag{2.20}$$

with $\operatorname{Re} s \geq 0$ for retarded TDS and $\operatorname{Re} s \geq \alpha, \alpha < 0$ for neutral ones. This definition agrees with *exponential* stability for TDS.

In the case of neutral systems, one has to be more careful when deciding about stability since there may be infinite braches of poles tending to the imaginary axis. Strictly negative roots of the characteristic (quasi)polynomial (or meromorphic function), thus, do not guarantee a satisfactory stable behavior of a system from the asymptotic (and robust) point of view. Let us introduce an associated difference equation and two stability notions for neutral TDS which are close to each other in the meaning.

Given a SISO neutral TDS (2.9), an *associated difference equation* is defined as

$$\mathbf{x}(t) - \sum_{i=1}^{N_H} \mathbf{H}_i \mathbf{x}(t-\eta_i) = 0 \tag{2.21}$$

A neutral TDS is said to be *formally* stable if

$$\operatorname{rank}\left[I - \sum_{i=1}^{N_H} \mathbf{H}_i \exp(-s\eta_i) \right] = n, \forall s : s \geq 0 \tag{2.22}$$

see e.g. in [18], [75]. It also means that system (2.9) has only a finite number of poles in the right complex half-plane [137]. Clearly from (2.21) and (2.22), a system is formally stable if characteristic equation

$$m_{0,D}(s) = \det\left[I - \sum_{i=1}^{N_H} \mathbf{H}_i \exp(-s\eta_i) \right] = 0 \tag{2.23}$$

expressing the spectrum of the difference equation has all roots in $\mathbb{C}_o^-$.

The feature of a neutral TDS that rightmost solution of (2.23) is not continuous in its delays [52] gives rise to another (yet a germane) stability notion. *Strong* stability of the difference equation (2.21) means that it remains exponentially stable when subjected to small variations in delays (i.e. a TDS remains formally stable). A system is strongly stable if and only if

$$\gamma_0 := \max\left\{ r_\Omega\left(\sum_{i=1}^{N_H} \mathbf{H}_i \exp(\mathrm{j}\theta_i) \right) : \theta_i \in [0, 2\pi), 1 \le i \le N_H \right\} < 1 \tag{2.24}$$

where $r_\Omega(\cdot)$ denotes the spectral radius. Alternatively, the necessary and sufficient strong stability condition in the Laplace transform can be formulated as

$$\sum_{j=1}^{h_n} |m_{nj}| < 1 \tag{2.25}$$

see e.g. [50], [208] where m_{nj} are coefficients for the highest *s*-power in (2.8). A sufficient condition for this type of stability is e.g.

$$\sum_{i=1}^{N_H} \|\mathbf{H}_i\| < 1 \tag{2.26}$$

where $\|\cdot\|$ is a matrix norm. A strongly stable system is robust against infinitesimal changes in delays of a neutral TDS which can destroy asymptotic stability of the difference equation.

The practical connection between these two stability notions is that a control feedback with a formally unstable system may not be strongly stable [141]. Clearly, a strongly stable TDS is formally stable.

Let us mention other stability terms useful when dealing with algebraic description and control of TDS, namely H_∞ stability and BIBO stability.

A system is H_∞ stable if its transfer function $G(s)$ lies in the space $H_\infty(\mathbb{C}^+)$ of functions analytic and bounded in the right complex half-plane, i.e. providing the finite norm

$$\|G\|_\infty := \sup\{|G(s)| : \mathrm{Re}\, s \geq 0\} < \infty \tag{2.27}$$

see e.g. [115]. That is, the system has finite $L_2(0,\infty)$ to $L_2(0,\infty)$ gain where $L_2(0,\infty)$ norm of an input or output signal $h(t)$ is defined as

$$\|h(t)\|_2 := \sqrt{\int_0^\infty |h(t)|^2 \,\mathrm{d}t} \tag{2.28}$$

Notice, for instance, that a transfer function having no pole in the right complex half-plane but a sequence of poles with real part converging to zero can be H_∞ unstable due to unbounded gain at the imaginary axis [115].

The notion of *BIBO* (Bounded Input Bounded Output) stability is stronger than the preceding one and usually more difficult to analyze. A SISO TDS is BIBO stable if a bounded input $|u(t)| < M_1$, $t < 0$, $M_1 \in \mathbb{R}$ produces a bounded output $|y(t)| < M_2, t < 0$, $M_2 \in \mathbb{R}$; in other words, it has a finite L_∞ gain. It holds that the system is BIBO stable if its transfer function is an element of a commutative Banach algebra $\mathcal{L}(L_1 + \mathbb{R}\delta)$ of Laplace transforms of functions of the form

$$h(t) = h_a(t) + \sum_{i=1}^{\infty} h_i \delta(t - \tau_i), t \geq 0 \tag{2.29}$$

where $h_a(t) \in L_1(0,\infty)$, i.e.

$$\int_0^\infty |h_a(t)| \mathrm{d}t < \infty \tag{2.30}$$

$h_i \in \mathbb{R}$, $\tau_0 = 0, \tau_i > 0$, for $i > 0$, $\delta(t)$ stands for the Dirac delta function, and

$$\sum_{i=1}^{\infty} |h_i| < \infty \tag{2.31}$$

BIBO stability implies H_∞ stability [27], [75].

Finally, before a brief overview of basic and some recent literature resources is presented, let us mention *interdependences* of delays [89]. Generally, in many practical application delays are not independent from each other. Assume that N delays $\tau_i, i = 1,2,..., N$ depend on $M \le N$ so-called independent delays $r_1,..., r_M$ as

$$\tau_i = \sum_{j=1}^{M} \gamma_{ij} r_j = \boldsymbol{\gamma}_i^T \mathbf{r} \tag{2.32}$$

where $\boldsymbol{\gamma}_i = [\gamma_{i1}, \gamma_{i2}, ... \gamma_{iM}]^T \in \mathbb{N}^M$ are non-zero vectors with non-negative integer coefficients and $\mathbf{r} \in (0, \infty)^N$. The numbers $r_1,..., r_M$ are *rationally independent* if and only if

$$\sum_{j=1}^{M} n_j r_j = 0, n_j \in \mathbb{Z} \tag{2.33}$$

implies $n_j = 0, j = 1,2,..., M$. For example, two numbers are rationally independent if and only if their ratio is an irrational number. Otherwise they are *rationally dependent*.

A special case of (2.32), *fully independent* delays, corresponds to $M = N$, $\boldsymbol{\gamma}_i = \mathbf{e}_i$, the j-th unity vector in $\mathbb{R}^N$ and $\tau_1,..., \tau_N$ are rationally independent delays. In another special case where $M = 1$, the delays $\tau_1,..., \tau_N$ are called *commensurate*, as they are natural multiples of the same number r_1. For example, the numbers $1, \pi$, $1 + \pi$ are rationally dependent (not rationally independent), yet not commensurate (Michiels and Niculescu, 2007a).

Without any attempt to be exhaustive, we refer now to some of recent stability analysis approaches and literature resources.

Stability of retarded systems with only one delay was studied e.g. in [109], [140] based on the well known Rekasius transform (substitution) $\exp(-\tau_i s) \to (1 - T_i s)/(1 + T_i s), T_i \in \mathbb{R}^+$ mapping exponentials to rational functions which holds true exactly for $s = \mathrm{j}\omega$ and serves to find the position where the roots cross the

imaginary axis. In [107], [159] a second order retarded TDS and in [153] a third order one with two delays waere studied. In the last reference, where the authors utilized their CTCR (Clustering Treatment of Characteristic Roots) algorithm, non-commensurate delays and DDS together with a type of delay interdependence in the characteristic quasipolynomial (called *cross-talking*) were considered. Tools of CTCR and the Rekasius mapping were also used in [26] to investigate DIS of retarded TDS with multiple delays via sufficient elimination of T_i by means of a special discriminant and the Déscartes rule of signs. There was also recalled that stability of a delay-free system is a necessary condition for DIS here. A similar problem for TDS with parametric uncertainties and non-commensurate delays was solved in [40] providing a huge literature overview and a sufficient DIS condition. Some DIS and DDS criteria for retarded TDS with multiple uncertain delays were established in [189] by using both the time-domain and the frequency-domain methods. DIS for retarded TDS with multiple delays was studied in [91] where the authors discussed delay interference phenomenon. Robust stability measures using so-called stability radius were introduced in [93].

Concerning stability of neutral systems, to name just a few recent contributions, the notion of *safe upper bound* on roots of the difference equations was introduced in [94] and further developed in [96]. In the latter, a necessary and sufficient condition for strong stability was also given and rationally dependent delays were considered. The notion of so-called *p-stability* (including small delays, model errors, discretization etc.) was established and developed in [95]. DDS of neutral TDS with multiple yet commensurate delays was studied in [41] providing so-called stability windows and location of all crossing frequencies and unstable poles. The authors utilized a mapping $\exp(-\mathrm{j}\omega\tau) \to \exp(-\mathrm{j}\theta),\ \theta \in [0,\pi]$, instead of the Rekasius transform to obtain a simpler imaginary axis crossing analysis.

A huge overview of methods based predominantly on Ljapunov-Krasovskii approaches can be found in [141]. There were also published some monographs about TDS stability and related problems, e.g. [48], [92], [188], during the last decade.

Many of the methods mentioned above are complex and hard to implement. In this thesis we utilize the *argument-increment based stability criterion* (also called the *argument*

principle or the *Mikhaylov stability criterion*) for TDS applied to retarded systems e.g. in [47], [104], [196] and to neutral ones in [208].

Let φ^+ denotes a closed Jordan curve enclosing the region $\mathfrak{D} \in \mathbb{C}$ in the positive direction. The number N_D of zeros of $m_0(s)$ of retarded type inside $\mathfrak{D}$ is given by

$$N_D = \frac{1}{2\pi \mathrm{j}} \int_{\varphi^+} \frac{\dot{m}_0(s)}{m_0(s)} \mathrm{d}s = \frac{1}{2\pi} \Delta_{\varphi^+} \arg m_0(s) \tag{2.34}$$

A more useful and practical formula when studying stability of retarded quasipolynomials was presented e.g. in [47]. If $m_0(0) > 0$ and $m_0(s) \neq 0$ for any imaginary $s = \mathrm{j}\omega$, $\omega \in \mathbb{R}$, then

$$N_U = \frac{n}{2} - \frac{1}{\pi} \Delta_{s=\mathrm{j}\omega, \omega \in [0,\infty)} \arg m_0(s) \tag{2.35}$$

where N_U is the number of roots of $m_0(s)$ in $\mathbb{C}^+$ and n stands for the highest s-power in $m_0(s)$. If all the zeros are located in $\mathbb{C}_0^-$, i.e. $N_U = 0$, (2.35) results in

$$\Delta_{s=\mathrm{j}\omega, \omega \in [0,\infty)} \arg m_0(s) = \frac{n\pi}{2} \tag{2.36}$$

which (taking mutual implication) agrees with the well known Mikahylov stability criterion used by some authors when control of TDS as well, e.g. [197], [125].

Analysis of neutral TDS is a rather more complicated due to the absence of a limit of $\Delta \arg m_0(s)$; however, it holds true the following [208]. Consider a quasipolynomial $m_0(s)$ of neutral type as in (2.8) satisfying $m_0(0) > 0$, $m_0(s) \neq 0$ for any imaginary $s = \mathrm{j}\omega$, $\omega \in \mathbb{R}$, and (2.25). Then $m_0(s)$ is strongly and asymptotically stable if and only if

$$\frac{n\pi}{2} - \Phi \leq \Delta_{s=\mathrm{j}\omega, \omega \in [0,\infty)} \arg m_0(s) \leq \frac{n\pi}{2} + \Phi \tag{2.37}$$

where

$$\Phi = \arcsin\left(\sum_{j=1}^{h_n} \left| m_{nj} \right| \right) \tag{2.38}$$

Although both criteria are used to the characteristic quasipolynomial $m_0(s)$ to determine whether all its roots are located in $\mathbb{C}_0^-$, they can also be useful when dealing with zeros of the characteristic meromorphic function $M_0(s)$ (for distributed internal delays) simply by subtraction the phase change of the numerator and denominator, i.e.

$$\Delta \arg M_0(s) = \Delta \arg \operatorname{num} M_0(s) - \Delta \arg \operatorname{den} M_0(s) \tag{2.39}$$

If both quasipolynomials are of retarded type, one abides by (2.36); otherwise (i.e. the numerator is of neutral type yet strongly stable), (2.37) and (2.38) are considered. Moreover, *n* must be taken as a relative degree of $M_0(s)$ as

$$n = \deg \operatorname{num} M_0(s) - \deg \operatorname{den} M_0(s) \tag{2.40}$$

This vague statement above is going to be precised in Subchapter 4.6 dealing with the derivation of a generalized Nyquist criterion for TDS.

2.3 Algebraic description of TDS

2.3.1 Theoretical background, basic algebraic notions

Prior to a brief overview of particular algebraic structures utilized by some authors when analysis (and/or synthesis) of TDS, it is convenient to introduce some basic algebraic notions being used in this thesis and their elementary properties if useful [144], [185].

A *group*, *G*, is an algebraic structure with binary operation · satisfying:

a) For each $a, b \in G$, it holds that $a \cdot b \in G$.

b) For all $a, b, c \in G$, $(a \cdot b) \cdot c = a \cdot (b \cdot c) \in G$ (associativity).

c) There exists an element $e \in G$, such that for every element $a \in G$, it holds that $a = a \cdot e = e \cdot a \in G$ (*identity element, neutral element*).

d) For each $a \in G$, there exists an element $b \in G$ such that $a \cdot b = b \cdot a = e \in G$ (*inverse element*).

A set satisfying a) and b) only from the definition above, i.e. without a necessity of identity and inverse elements, is called a *semigroup*. If one requires the existence of an identity element, a so-called *monoid* is obtained. A group with the commutative property, i.e.

e) For each $a,b \in G$, $a \cdot b = b \cdot a \in G$

is called a *commutative* (abelian) group.

A *ring, R*, is a set with two binary operations +, · (generally interpreted as addition and multiplication) for which it holds true the following:

a) *R* is a commutative group under addition with an identity element denotes as 0.

b) For any $a,b,c \in R$, $(a+b)\cdot c = a \cdot b + a \cdot c \in R$ and $c \cdot (a+b) = c \cdot a + c \cdot b \in R$ (left and right distributivity).

c) For every $a,b,c \in R$, it holds that $(a \cdot b)\cdot c = a \cdot (b \cdot c) \in R$ (Associativity of multiplication).

Some authors add another property of a ring as:

d) There exists $1 \in R$ such that for every $a \neq 0 \in R$, $a \cdot 1 = 1 \cdot a \in R$ (multiplicative identity).

If d) holds, then a ring is a commutative group under + and a commutative monoid under ·, together with distributivity. In a *commutative ring*, the commutative property holds also for multiplication.

A *unit* of the ring (or an *invertible element*) is $a \neq 0 \in R$, for which there exists $a^{-1} \in R$, such that $a \cdot a^{-1} = a^{-1} \cdot a = 1$. If all elements of a ring are units, the ring is called a *field*.

It is said that $b \in R$ *divides* $a \in R$ (i.e. $b \mid a$) if there exists $q \in R$, such that $a = q \cdot b$. Two elements $a,b \in R$ are *associated* if $b \mid a$ and $a \mid b$.

Let *R* be a commutative ring and $a,b \in R$. A *common divisor* $c \in R$ of *a*, *b* is an element of the ring, for which $c \mid a$ and $c \mid b$. $d \in R$ is the *greatest common divisor* (GCD)

of a, b if for every common divisor $c \in R$ of $a,b \in R$ it holds that $c \mid d$. The GCD is determined unambiguously except for associativity.

A nonzero noninvertible element a of a commutative ring R is called *irreducible* if it is divisible solely by a unit or any element associated with a. In some rings, so-called *prime elements* generalizing prime numbers are introduced. A prime elements is a nonzero noninvertible $a \in R$, such that if $a \mid (b \cdot c)$ for some $b,c \in R$, then always $a \mid b$ or $a \mid c$. Every prime element is irreducible, the converse is not true in general.

A ring R in which every nonzero noninvertible $a \in R$ can be uniquely decomposed in a (finite) product of irreducible or prime elements (except for the ordering and associativity) is called a unique factorization ring (UFR).

A commutative ring with identity (under multiplication) such that for any two elements $a \neq 0 \in R$ and $b \neq 0 \in R$ it holds that $a \cdot b \neq 0$ is called an *integral domain*. An UFR which is an integral domain is labeled as a unique factorization domain (UFD).

A *field of fractions* of an integral domain R (at least with one element) is the "smallest" field containing R, such that necessary elements satisfying the divisibility (by a nonzero element) are added. An element c of this field can be expresses in the form $c = a/b$ where $a,b \in R$, $b \neq 0$.

An *ideal* I (of the ring R) is a subset of R with the following properties:

a) For every $a,b \in I$, it holds that $a + b \in I$.

b) For each $a \in I$ and $r \in R$, $a \cdot r \in I$.

It holds that an intersection of ideals is an ideal as well. Let $M = \{a_1, a_2, ...a_n\} \subseteq R$, then an intersection of all ideals of R containing M is called an ideal *generated by M*. It is also the "smallest" ideal including M. Ideals of the form $aR = \{a \cdot r \mid r \in R\}$, i.e. those generated by (the only one) element a, are called *principal*.

If every ideal of an integral domain is principal, a so-called *principal ideal domain* (PID) is obtained. It holds true that every PID is UFD; however, the converse is not true in general.

A *Noetherian* ring R is primarily defined as that satisfying the so-called finite ascending chain condition. Equivalently, it is possible to circumscribe the term as follows: A ring R is Noetherian if its every ideal is finitely generated, i.e. $n=|M|$ is a finite number.

A (left) *module* (or *R-module*) M over the ring R is a commutative group satisfying:

a) For every $r\in R$, $a,b\in M$, it holds that $r\cdot(a+b)=r\cdot a+r\cdot b\in M$.

b) For every $r,s\in R$, $a\in M$, $(r+s)\cdot a=r\cdot a+s\cdot a\in M$.

c) For every $r,s\in R$, $a\in M$, $(r\cdot s)\cdot a=r\cdot(s\cdot a)\in M$.

d) If there exists a multiplicative identity $1\in R$, and $a\in M$, then $1\cdot a=a\in M$

Modules are similar to vector spaces, yet in modules, coefficients are taken from rings, not from fields. A *free module* is that with a basis. For instance, since nonzero elements in a ring are not necessarily invertible, a relation $\sum_{i=1}^{n} r_i\cdot a_i=0, r_i\in R, a_i\in M$, where M is a free module, does not imply that each r_i is the linear combination of the remaining ones [24].

A *partially ordered set* (poset) is defined as an ordered pair $P=(S,\preceq)$ where S is called the ground set of P and $\preceq$ is the partial order of P. A relation $\preceq$ is a poset on S if:

a) For all $a\in S$, $a\preceq a$ (reflexivity)

b) For $a,b\in S$, if $a\preceq b$ and $b\preceq a$, then $a\equiv b$ (antisymmetry)

c) For $a,b,c\in S$, $a\preceq b$ and $b\preceq c$ implies $a\preceq b$ (transitivity)

From a PID, a *Bézout domain* is distinguished in which every *finitely* generated ideal is principal. In a Bézout domain, PID is UFD and viceversa. Thus, a PID admits the existence of an infinitely generated ideal which is principal.

In a Bézout domain *R*, for every pair $a,b \in R$ (or generally for a finite set of elements) there exists the $d = \mathrm{GCD}(a,b)$ which meets the *Bézout identity* (or more generally a *linear Diophantine equation*)

$$a \cdot x + b \cdot y = d,\ x,y \in R \tag{2.41}$$

A solution $x,y \in R$ is not determined uniquely but (an infinitely many) solutions of (2.41) are given by the parameterization

$$\begin{aligned} x &= x_0 \pm z \cdot \frac{b}{d} \\ y &= y_0 \mp z \cdot \frac{a}{d} \end{aligned} \tag{2.42}$$

where $\{x_0, y_0\}$ is a particular solution of (2.41) and $z \in R$.

If (2.41) is solved for any $c \in R$ on the right-hand side instead of $\mathrm{GCD}(a,b)$, it is necessary to verify whether there exists $\mathrm{GCD}(a,b)$ (especially in a ring which is not Bézout or PID) for which $\mathrm{GCD}(a,b) \mid c$.

The Bézout identity can be solved e.g. using a *generalized* (extended) *Euclidean algorithm* which can be described as follows. Let a,b be given and the task is to find $d = \mathrm{GCD}(a,b)$ and a pair x,y according to (2.41). The iterative procedure can be written as

$$\begin{aligned} &r_i = r_{i-2} - \lfloor q_i \rfloor \cdot r_{i-1} \\ &r_{i-2} \geq r_{i-1} \geq r_i \\ &i = 3,4,\ldots,n \end{aligned} \tag{2.43}$$

i.e. the current reminder r_i of the division can be expressed by preceding reminders r_{i-1}, r_{i-2} and using the whole quotient $q_i = r_{i-2} / r_{i-1}$.

In every step of the algorithm, it is possible to write the following identity

$$r_i = a \cdot x_i + b \cdot y_i \tag{2.44}$$

where x_i, y_i are from the ring. The first two reminders are chosen as

$$r_1 = a = a \cdot 1 + b \cdot 0$$
$$r_2 = b = a \cdot 0 + b \cdot 1 \qquad (2.45)$$

The desired $d = \mathrm{GCD}(a,b)$ then equals the last nonzero reminder, $r_n \neq 0,\ r_{n+1} = 0, n < \infty$.

The whole procedure can be expressed in a table (matrix) form as follows

$$\left[\begin{array}{cc|c} 1 & 0 & a \\ 0 & 1 & b \end{array}\right] \sim \begin{array}{c} \text{elementary} \\ \text{row} \\ \text{matrix} \\ \text{operations} \end{array} \sim \left[\begin{array}{cc|c} v & t & 0 \\ x & y & d \end{array}\right] \qquad (2.46)$$

The result is determined by two Diophantine equations

$$a \cdot v + b \cdot t = 0$$
$$a \cdot x + b \cdot y = d \qquad (2.47)$$

In the case when (2.41) is solved for any fixed $c \in R$ on the right-hand side instead of $d = \mathrm{GCD}(a,b)$ it is possible (if a solution exists) to use the extended Euclidean algorithm again in the following two possibilities:

1) To use scheme (2.46) for $c \in R$ instead of $d = \mathrm{GCD}(a,b)$. Generally, it is not necessary to achieve the zero element on the upper right matrix corner.

2) Obviously

$$a \cdot x + b \cdot y = d \quad / \frac{c}{d}$$
$$a\frac{xc}{d} + b\frac{yc}{d} = c \qquad (2.48)$$
$$ax_1 + b \cdot y_1 = c$$

Hence, $\mathrm{GCD}(a,b)$, x,y are found using (2.46) first, and subsequently, the following substitution is used

$$x_1 = x\frac{c}{d},\ y_1 = y\frac{c}{d} \qquad (2.49)$$

to get the desired solution.

For the necessity and comprehension of the further text, some basic notions from the complex functions analysis ought to be introduced.

A *holomorphic function* is a complex-valued function of a single (or multiple) complex variable defined on a region $\mathfrak{D} \subseteq \mathbb{C}$ which is infinitely complex differentiable (i.e. there exists all complex derivatives) at any point $z_0 \in \mathfrak{D}$.

The term holomorphic function is often used interchangeably with or compared to an *analytic function* which is generally a complex-valued function of a single (or multiple) complex variable defined on a region $\mathfrak{D} \subseteq \mathbb{C}$, in which the Taylor series expansion exists at every point $z_0 \in \mathfrak{D}$. That is, a series $T(z) = \frac{1}{i!} \sum_{i=0}^{\infty} f^{(i)}(z_0)(z - z_0)^i$ converges to $f(z)$ for every point z from a neighborhood of z_0. For complex functions, a holomorphic function implies an analytic function. A function holomorphic on all $\mathbb{C}$ is called *entire*.

An *isolated singularity* of a complex function $f(z)$ is a point z_0, in which the function is not differentiable; however, there exists an open disk *D* centered at z_0 such that $f(z)$ is holomorphic on the disk excluding z_0. There are several types of isolated singularities. A *pole* is an isolated singularity z_0 of $f(z)$ such that $f(z)$ converges uniformly to infinity for $z \to z_0$. Thus, if there exists the improper limit $\left|\lim_{z \to z_0} f(z)\right| = \infty$, then there exists also $n \in \mathbb{N}$, so that $\left|\lim_{z \to z_0} (z - z_0)^n f(z)\right| < \infty$. A *removable singularity* is another type of an isolated one for which $\left|\lim_{z \to z_0} f(z)\right| \neq \infty$. In this case, it is possible to define $f(z_0) = \lim_{z \to z_0} f(z)$, so that $f(z)$ becomes holomorphic. An *essential singularity* represents the last type of an isolated singularity which evinces “peculiar” behavior within the neighborhood of the singularity, and it holds that the limit $\lim_{z \to z_0} f(z)$ does not exist here.

A *meromorphic function* is a complex-valued function of a complex variable which is holomorphic on an open subset $\mathfrak{D} \subseteq \mathbb{C}$ except a set of poles. The function can be expressed as a ratio of two holomorphic functions.

2.3.2 Fields, rings and modules for description of TDS

The nascence of algebraic methods in description of TDS is connected with fields, namely with systems over fields [58], which can be written in the (retarded) state-space form

$$\begin{aligned}\dot{\mathbf{x}}(t) &= \mathbf{A}\mathbf{x}(t) + \mathbf{B}\mathbf{u}(t)\\ \mathbf{y}(t) &= \mathbf{C}\mathbf{x}(t)\end{aligned} \tag{2.50}$$

where elements of $\mathbf{A}, \mathbf{B}, \mathbf{C}$ are from a fixed field and $\dot{\mathbf{x}}(t) = \frac{\mathrm{d}\mathbf{x}(t)}{\mathrm{d}t}$.

The next step was to further generalize the concept of linear systems, to include the case in which coefficients belong to a ring. The first, general, in-depth research into the properties of systems over rings was constituted in [145], [146]. One of the primordial attempts to utilize ring theory to infinite-dimensional linear systems was made by Kamen 0\[59] where an operator theory was presented, the particular case of systems defined via rings of distributions. Namely, the ring Θ generated by the entire functions $\theta_\sigma(s)$ defined in (2.6), their derivatives and 1 was introduced there. Ring models for TDS with lumped delays was published in [102].

In [156], linear systems over commutative rings, especially TDS, were intensively studied. The author i.a. presented the simplest TDS over rings, those with commensurate delays where the introduction of the operator $\delta x(t) := x(t-\tau)$, where τ represents the smallest delay, yields state matrix entries in the ring of polynomials $\mathbb{R}[\delta]$. In more details, let the model be

$$\begin{aligned}\dot{\mathbf{x}}(t) &= \sum_{k=0}^{N} \mathbf{A}_k \mathbf{x}(t-k\tau) + \mathbf{B}_k \mathbf{u}(t-k\tau)\\ \mathbf{y}(t) &= \sum_{k=0}^{N} \mathbf{C}_k \mathbf{x}(t-k\tau)\end{aligned} \tag{2.51}$$

then state and output matrices in (2.50) read

$$\mathbf{A} = \sum_{k=0}^{N} \mathbf{A}_k \delta^k, \mathbf{B} = \sum_{k=0}^{N} \mathbf{B}_k \delta^k, \mathbf{C} = \sum_{k=0}^{N} \mathbf{C}_k \delta^k \tag{2.52}$$

Using a substitution $\delta^k \to \exp(-k\tau s)$, one can obtain the Laplace transform form of the state model for TDS with commensurate delays. If delays are not commensurate, we need to define a finite set of delay operators $\delta_1, \delta_2, ..., \delta_N$ resulting in a ring $\mathbb{R}[\delta_1, \delta_2, ..., \delta_N]$. Some authors, e.g. Youla (1968), introduced the field $\mathbb{R}(\delta_1, \delta_2, ..., \delta_N)$ of rational functions in $\mathbb{R}[\delta_1, \delta_2, ..., \delta_N]$ in order to study networks with transmission lines (i.e. delayed systems). Reachability and observability of a general system with coefficients over a ring are analyzed in [156] as well.

Conte and Perdon [22] further studied the realization of such systems. These authors also developed the geometrical approach to the study of dynamical systems with coefficients over a ring concerning TDS. The overview of the methodology was presented in [24]. In this framework, the main tool lies in the view that $\mathbf{x}(t), \mathbf{u}(t), \mathbf{y}(t)$ in (2.51) are free *R*-modules.

Concerning input-output maps, which are substantive for the aims of this thesis, Sontag [156] and Morse [102] mentioned the conception of 2-D systems which naturally arises from the transfer function of a TDS with commensurate delays over a ring (2.51), (2.52). Translation the state-space description into the transfer function according to the first formula in (2.7) results in a rational function in s and $\exp(-\tau s)$. This expresses that two operators are used here, i.e. the integrator and the delay operator, which are algebraically independent (due to the fact that the exponential term is a transcendental function) in the meaning of that there is no nontrivial linear combination of s and $\exp(-\tau s)$ over real numbers equaling to zero. Thus, the ring $\mathbb{R}[s, \exp(-\tau s)]$ of quasipolynomials, which is isomorphic to the ring of real polynomials in two variables (a so-called 2-D polynomial) $\mathbb{R}[s, z]$, is obtained. Quasipolynomials defined in (2.8) do not coincide with those introduced above since commensurate delays only are considered here. This concept was further studied and developed e.g. in [44], [101]. It holds that any two coprime elements in $\mathbb{R}[s, \exp(-\tau s)]$ have a finite number of common zeros, see e.g. [74].

However, some authors pointed out that the use of quasipolynomials does not permit to effectively handle some stabilization and control tasks, thus other rings based on quasipolynomials for TDS with commensurate delays were introduced.

For instance, Bréthé and Loiseau [16], Loiseau [74] established the following rings: A ring $\mathcal{R} = \Theta \cup \mathbb{R}\left[\exp(-\tau s)\right] = \Theta[\exp(-\tau s)]$ of all linear combinations, with real coefficients, of distributed delays from Θ and lumped delays, and a ring $\mathcal{E} = \mathcal{R}[s] = \Theta \cup \mathbb{R}\left[s, \exp(-\tau s)\right]$ of so-called *pseudopolynomials* which consists of Laplace transforms of operators that are generated using derivatives, lumped and distributed delays. Any element $T(s) \in \mathcal{E}$ can be written in the (coprime) form $T(s) \in N(s, \exp(-\tau s))/D(s)$, $N(s, \exp(-\tau s)) \in \mathbb{R}\left[s, \exp(-\tau s)\right]$, $D(s) \in \mathbb{R}\left[s\right]$. Two pseudopolynomials are coprime if and only if there are neither their common zeros nor factors in the form $\exp(-k\tau s)$. Ring $\mathcal{R}[s]$ is not isomorphic to $\mathcal{R}[x]$, which means that the variables are not algebraically independent (transcendental) over $\mathcal{R}$, see an example in [16]. Moreover, it is a Bézout domain, yet not an Euclidean ring nor a Noetherian ring nor a UFD. Notice that $\mathcal{E}$ and $\mathbb{R}\left[s, \exp(-\tau s)\right]$ share the same field of fractions, i.e. $\mathbb{R}\left(s, \exp(-\tau s)\right)$. The transfer function can then be expresses as a fraction of two pseudopolynomials.

Behavioral approach, as it was introduced for dynamical systems in [186], was presented by Gluessing-Lueerssen [46] for TDS, again with commensurate delays. In contrast to above mentioned works, the author considered systems in the behavioral point of view instead of systems over rings. A behavior is the kernel of a delay-differential operator. More precisely, consider equations in the scalar case in the form

$$\sum_{j=0}^{L}\sum_{i=0}^{N} p_{ij} x^{(i)}(t-j) = 0 \tag{2.53}$$

where $p_{ij}, t \in \mathbb{R}$, $x^{(i)}(t)$ denotes the *i*-th derivative of the function $x(t)$: $\mathbb{R} \to \mathbb{R}$. Behaviors $\mathcal{B}$ are those functions $x(t)$ satisfying (2.53). Alternatively, $\mathcal{B} = \ker \widetilde{P}$ where $P = \sum_{j=0}^{L}\sum_{i=0}^{N} s^i z^j \in \mathbb{R}\left[s, z\right]$ and $\widetilde{P}$ denotes the associated delay-differential operator, i.e.

$\tilde{P}x(t) = \sum_{j=0}^{L}\sum_{i=0}^{N} p_{ij} x^{(i)}(t-j)$. It is stated in [46] that it is algebraically more adequate to consider the ring $\mathbb{R}[s, z, z^{-1}]$ instead of $\mathbb{R}[s, z]$. There is also defined the ring

$$\mathcal{H} := \{p \in \mathbb{R}(s)[z, z^{-1}] \mid p(s, z) \in H_C\} \tag{2.54}$$

as the appropriate domain in order to translate relations between behaviors, lying between $\mathbb{R}[s, z, z^{-1}]$ and $\mathbb{R}(s)[z, z^{-1}]$, where the latter means the ring of polynomials in z, z^{-1} with the coefficients in rational functions in s with real parameters, and H_C is the set of all entire functions. It was proved that $\mathcal{H}$ is not a UFD and not a Noetherian ring; however, it is a Bézout ring.

However, delays are naturally real-valued and thus the limitation to commensurate delays is rather restrictive for real applications [94]. Dealing with rings for input-output maps of TDS with even non-commensurate delays, it is crucial for this thesis to mention here the family of approaches (originally developed for delayless systems) utilizing a field of fractions where the transfer function is expressed as a ratio of two coprime (or relatively prime) elements of a suitable ring [28], [69], [167]. The process of finding such coprime pair is called a *coprime factorization*.

One of such rings for continuous-time systems is the ring of stable and proper rational functions, R_{PS}, [69], [138]. An element of this ring is defined as a ratio of two polynomials in s over $\mathbb{R}$ where the denominator polynomial is Hurwitz stable (i.e. free of roots located in the closed right half-plane including imaginary axis) and, moreover, the ratio is proper (i.e. the s-degree of the numerator is less or equal to the denominator). Alternatively, the element of R_{PS} is analytic and bounded for $\mathrm{Re}\, s \geq 0$ including infinity, i.e. it lies in $H_\infty(\mathbb{C}^+)$. Such a definition is, however, not sufficient for TDS since e.g., as demonstrated in Example 2.1, the Laplace form of a stable system including in $H_\infty(\mathbb{C}^+)$ can have an unstable denominator.

The utilization of R_{PS} in description (and control) of TDS requires a rational approximation of a general meromorphic transfer function as a first step of a coprime

factorization, for instance, by a substitution of the exponential terms, $\exp(-\tau s) \approx X(s) \in \mathbb{R}(s)$.

An example of a coprime factorization in R_{PS} follows.

Example 2.2

Consider a stable TDS with distributed delays governed by the transfer function (2.16). The use of e.g. the first order Padé rational approximation results in

$$G(s) = \frac{Y(s)}{U(s)} \approx \frac{0.5s(1+\exp(1))+1-\exp(1)}{(s-1)(0.5s+1)} = \frac{b(s)}{a(s)} \tag{2.55}$$

where $a(s)$, $b(s) \in \mathbb{R}[s]$. Notice that the common root $s = -1$ characterizing the delay distribution in this example vanished after the rationalization. An addition, although the relative order of the transfer function is preserved, the absolute one has increased. To establish coprime factors $A(s) = a(s)/m(s)$, $B(s) = b(s)/m(s)$, $m(s) \in \mathbb{R}[s]$ (with no zero in $\mathbb{C}^+$), $A(s) \in R_{PS}$, $B(s) \in R_{PS}$, one has to realize the divisibility condition in R_{PS}: Any $A(s) \in R_{PS}$ divides $B(s) \in R_{PS}$ if and only if all unstable zeros (including $s \to \infty$) of $A(s)$ are those of $B(s)$. Inclusion of infinity in the condition gives rise to the requirement $\deg m(s) = \deg a(s) = 2$, and moreover, there is no s with $\mathrm{Re}\, s \geq 0$ satisfying $m(s) = 0$. ■

The main drawback of the ring, i.e. the necessity of a rational approximation, induces the idea of introduction a similar, yet rather different, ring avoiding this operation.

2.3.3 R_{MS} ring

The original definition of the ring of proper and stable retarded quasipolynomial (RQ) meromorphic functions, R_{MS}, is the subject of this subchapter [199]. The basic idea for its introduction proceeds from the following ideas. First, as mentioned above in the previous subchapter, a rational approximation of the transfer function in the form of a ratio of two quasipolynomials is required for the use of the ring R_{PS}. This operation brings a loss of system dynamics information, as can be seen from Example 2.2. Second, from the

practical point of view, there is no reason to be limited to commensurate delays in a model, thus, a more universal description ought to be introduced. Third, authors took into account the fact that two variables, *z* and *s*, are not independent from the functional point of view, thus, a one-dimensional (1-D) instead of 2-D approach can be used. Last but not least, as stated above, quasipolynomials in the transfer function do not permit to effectively handle some stabilization and control tasks such as impulse-free stability and controller properness and parameterization.

An element $T(s) \in R_{MS}$ is represented by a proper fraction of two quasipolynomials

$$T(s) = \frac{y(s)}{x(s)} \tag{2.56}$$

where a denominator $x(s)$ is a quasipolynomial of degree *n* and a numerator can be factorized as

$$y(s) = \tilde{y}(s)\exp(-\tau s) \tag{2.57}$$

where $\tilde{y}(s)$ is a quasipolynomial of degree *l* and $\tau > 0$. $x(s)$ is stable, which means that there is no zero of $x(s)$, s_0, such that $\operatorname{Re} s_0 \geq 0$. Moreover, the ratio is proper, i.e. $l \leq n$.

Obviously, the condition $\tau > 0$ is too restrictive (or more likely a misprint); the inequality $\tau \geq 0$ would be more natural instead. The original definition of R_{MS} has some drawbacks; especially, it does not constitute a ring, which requires making some changes in the definition as presented in Subchapter 4.1.1. Namely, although the retarded structure of TDS is considered only, the minimal ring conditions require the use of neutral quasipolynomials at least in the numerator of $T(s)$. Moreover, the original definition brings problems when comprising models with distributed delays and handling the coprime factorization.

2.4 Algebraic control of TDS

Algebraic approaches of control systems theory aim at changing differential equations into algebraic ones, thanks to the use of the Laplace transform.

2.4.1 TDS stabilizability and controllability

Let us briefly mention notions of controllability and stabilizability of TDS which present differences compared to finite dimensional systems [141]. First, controllability means to reach a function $\boldsymbol{x}_t$ within the time range $[t-T,t]$ instead of a point $\mathbf{x}(t)$ at one time instant. As second, delays introduce the existence of a required minimum reaching time, e.g. a system with input-output delay *T* can not be controlled within time *T*.

The concept of controllability is not unique here. Richard [141] provides an overview of different controllability definitions, including $\mathcal{M}_2$-controllability, absolute controllability, $(\psi,\mathbb{R}^n)$-controllability, spectral controllability, $\mathbb{R}^n$-controllability and ring-controllability and presents the chain of implications between some of them as well. However, all the statements are made in the state space and most of the definitions hold for models with commensurate delays, which is almost useless for the purpose of this thesis.

The definition of the *spectral controllability* mentioned above can be extended to non-commensurate delays as follows. The system (2.1) with matrices (2.7) is spectrally controllable if and only if

$$\operatorname{rank}[s\mathbf{I} - \mathbf{A}(s), \mathbf{B}(s)] = n, \ \forall s \in \mathbb{C} \tag{2.58}$$

see [111], [205]. Alternatively, the criterion can be formulated as

$$\operatorname{rank}[\mathbf{B}(s), \mathbf{A}(s)\mathbf{B}(s), \mathbf{A}^2(s)\mathbf{B}(s), \ldots \mathbf{A}^{n-1}(s)\mathbf{B}(s)] = n, \ \forall s \in \mathbb{C} \tag{2.59}$$

where on the left-hand side is the well known spectral controllability (reachability) matrix $\mathbf{P}_R := [\mathbf{B}, \mathbf{AB}, ..., \mathbf{A}^{n-1}\mathbf{B}]$.

In e.g. [24] two different notions of reachability of TDS over a ring are defined and distinguished: Given the obvious reachability matrix $\mathbf{P}_R$, the system is *weakly reachable* if $\mathbf{P}_R$ has full rank, whereas it is said *reachable* if $\mathbf{P}_R$ is (right) invertible over *R*. For example, it is easy to prove that a system $\dot{\mathbf{x}}(t) = u(t-\tau) = \delta u(t)$ is weakly reachable and not reachable over $\mathbb{R}[\delta]$. Clearly, the condition (2.59) agrees with the weak reachability.

It was proved in [158] - although for commensurate delays only - that if the system is spectrally controllable, then it is *ring controllable*, i.e. any element of the appropriate *R*-module can be reached by the feedback from any initial state.

A similar notion of the (finite) *spectrum assignability* for TDS with commensurate delays (which can be extended to those with non-commensurate ones) was introduced by Sontag [156] and Spong and Tarn [158]. Intuitively, the system is spectral assignable if there exists a finite number of state feedback controller parameters (with appropriate controller and control system structures) such that the closed-loop spectrum contains arbitrary (but fixed) poles. Bretheé and Loiseau [16] proved that TDS (with commensurate point delays) is finite spectrum assignable if and only if it is spectrally controllable.

If one wants to assign only stable poles, the spectral assignability turns to the (spectral) *stabilizability*, i.e. the necessary and sufficient condition for the stabilizability is

$$\operatorname{rank}[s\mathbf{I} - \mathbf{A}(s), \mathbf{B}(s)] = \operatorname{rank}[\mathbf{B}(s), \mathbf{A}(s)\mathbf{B}(s), \mathbf{A}^2(s)\mathbf{B}(s), \ldots \mathbf{A}^{n-1}(s)\mathbf{B}(s)] = n, \ \forall s \in \mathbb{C}^+ \tag{2.60}$$

However, since the condition is based on the state space description, it depends on the system realization as shown in the following example.

Example 2.3

Consider an integrator with distributed input-output delay governed by functional differential equation

$$\dot{y}(t) = \int_0^1 u(t-\tau)\mathrm{d}\tau \tag{2.61}$$

By introduction of a state variable $x(t) = y(t)$, (2.61) represents the state equation as well. Using the Laplace transform on the convolution, the following image of the equation is obtained

$$sX(s) = \frac{1-\exp(-s)}{s}U(s) = B(s)U(s) \tag{2.62}$$

Hence, the system is stabilizable since $\operatorname{rank} B(s) = 1$ for all complex *s*.

Contrariwise, by derivation, model (2.61) becomes

$$\ddot{y}(t) = u(t) - u(t-1) \tag{2.63}$$

the "direct" state space realization of which is

$$\dot{\mathbf{x}}(t) = \begin{bmatrix} 0 & 1 \\ 0 & 0 \end{bmatrix} \mathbf{x}(t) + \begin{bmatrix} 0 \\ 1 \end{bmatrix} u(t) + \begin{bmatrix} 0 \\ -1 \end{bmatrix} u(t-1) \tag{2.64}$$

which yields the stabilizability test as

$$\operatorname{rank}[\mathbf{B}(s), \mathbf{A}(s)\mathbf{B}(s)] = \operatorname{rank} \begin{bmatrix} 0 & 1-\exp(-s) \\ 1-\exp(-s) & 0 \end{bmatrix} = 0, \; s = \pm k 2\pi \mathrm{j}, k \in \mathbb{N} \tag{2.65}$$

Obviously, the system is not (spectrally) stabilizable. ■

The stabilization of systems over rings was the aim of [37], [49].

The most important result for the stabilization of TDS in input-output space, namely for *BIBO stabilization*, which is crucial for this work, was presented e.g. in [75], [155]. The system is said to be BIBO stabilizable if there exists a feedback loop such that the closed-loop system is BIBO stable, see Subchapter 2.2.2. Then it holds the following necessary condition:

Let TDS be in the form of the transfer function

$$G(s) = \frac{b(s)}{a(s)} \tag{2.66}$$

where $a(s), b(s)$ are quasipolynomials as in (2.8). Then if the system is BIBO stabilizable, then it admits a Bézout factorization over $H_\infty(\mathbb{C}^+)$, i.e. there exist $A(s), B(s), P(s), Q(s) \in H_\infty(\mathbb{C}^+)$, such that

$$G(s) = \frac{B(s)}{A(s)} \tag{2.67}$$

$$A(s)P(s) + B(s)Q(s) = 1 \tag{2.68}$$

Further, if the system is BIBO stabilizable, then any coprime factorization (2.67), having no common factor on $H_\infty(\mathbb{C}^+)$, is also Bézout. Moreover, two elements $A(s), B(s) \in H_\infty(\mathbb{C}^+)$ form a Bézout factorization if and only if

$$\inf_{\mathrm{Re}\, s \geq 0} \left(|A(s)| + |B(s)| \right) > 0 \tag{2.69}$$

In fact, a coprime factorization does not guarantee a Bézout factorization as clarified in the following example. In such cases the system is not BIBO stabilizable.

Example 2.4

A TDS of neutral type has a transfer function

$$G(s) = \frac{Y(s)}{U(s)} = \frac{b(s)}{a(s)} = \frac{1}{(1-\exp(-s))(s+1)} \tag{2.70}$$

Clearly, a pair

$$B(s) = \frac{1}{s+2}, A(s) = \frac{(1-\exp(-s))(s+1)}{s+2} \tag{2.71}$$

has no nontrivial (non-unit) common factor, i.e. it is coprime. However, $|A(\pm k2\pi\mathrm{j})| = 0, k \in \mathbb{N}$, and $\lim_{k\to\infty} |B(\pm k2\pi\mathrm{j})| = 0$, hence (2.69) does not holds true and the system is not BIBO stabilizable. ■

As stated in [75] for neutral-type TDS, a system that is not formally stable is not BIBO stable nor stabilizable. However, this is not true exactly, as shown in [115].

2.4.2 Overview of algebraic methods in control of TDS

Algebraic control and controller design methods for TDS generally follow algebraic analytic approaches described in Subchapter 2.3.2. Without being exhaustive, an overview of some methods and literature sources follows.

One of the first algebraic results in the area of control of TDS was presented by Sontag [156]. As mentioned above, he studied the reachability, coefficient- and pole-assignability of TDS with lumped and commensurate delays, originating from the

possibility of deriving methods and techniques from the framework of systems with coefficients over the field of real numbers. Similar results were published e.g. in [102], [157]. A general algebraic solution to the problem of control of linear systems over arbitrary commutative rings by dynamic output feedback is given in [38]. Mounier [103] considered tracking problems and Picard et al. [135], [136] dealt with precompensation feedback loop for TDS and the model matching, respectively.

Kamen et al. [62] studied stabilization of TDS with non-commensurate delays by finite dimensional controllers where it was shown there that a spectrally stabilizable time-delay system can always be stabilized using a finite-dimensional compensator obtained by a rational approximation. In [63], the existence and construction of proper stable Bézout factorizations of transfer function matrices for TDS with commensurate time delays in terms of a specialized ring of lumped and distributed delays was introduced. Furthermore, regarding 2-D systems, let us mention works of Morf et al. [101], who found a constructive results for 2-D polynomial matrices factorization, Šebek [160], [161] investigated procedures for the characteristic polynomial assignment (by a transformation into 1-D polynomials) and asymptotic tracking via solving two linear equations in 2-D polynomials.

These approaches above adopt the concept of Diophantine equations (originally derived for discrete-time systems) which can be found throughout the algebraic control theory, particularly in the form of the Bézout identity [69], [167], see Subchapter 2.3.1.

Algebras for distributed LTI systems were introduced in [27].

A geometrical approach was developed and applied to a number of control problems e.g. in [23], [55], [57]. In [24] the geometric approach via ring and modules algebra for systems over rings was used to provide the solution of problems such as disturbance decoupling and block decoupling.

In the framework of a behavioral approach for control of TDS, the controllability criterion for, generally, multivariable systems with commensurate yet even distributed delays using ranks of associated matrices was introduced and proved in the most significant work by Gluessing-Lueerssen [46]. This criterion generalizes the spectral controllability test for time-delay state-space systems as in (2.58).

In [16], the ring $\mathcal{R}[s]$ was utilized to solve the task of the finite spectrum assignment for SISO TDS with lumped commensurate delays via a state feedback with convolution integrals (distributed delays), so-called Volterra integrals of type (2.3). Bézout-type identity with 2-D polynomial matrices was used there.

The results of author's long-standing work and research on algebraic control of TDS with commensurate delays were summarized and reviewed in [74]. The author pointed out that algebraic approaches fail to give a constructive procedure for stabilizing TDS and the use of distributed delays in the feedback can lead to effective procedures solving this problem, see also [83], [183]. Exact model matching (including disturbance rejection) in $\mathbb{R}[s,\exp(-\tau s)]$, $\mathbb{R}[s,\exp(\tau s)]$ and $\mathbb{R}(\exp(\tau s))[s]$ for retarded and neutral TDS, respectively, was one of the topics solved in the paper. The second part of the contribution dealt with the stabilization of TDS using the ring of pseudopolynomials, $\mathcal{E}$, see Subchapter 2.3.2, the realization over $\mathcal{R}$ of a fraction of elements in $\mathcal{E}$, and with the pole placement using $\mathcal{E}$. It was recalled there that a system is stabilizable if the plant transfer function numerator and denominator have no unstable common zero - compare with (2.69). Another finding states that there always exists a stable realization over $\mathcal{R}$, however, over $\mathbb{R}[\exp(-\tau s)]$ does not, see Example 2.3.

The strongest result about $\mathcal{E}$ constructively proved in [74] is the following. For two coprime elements of $\mathcal{E}$, say $a(s), b(s)$, there exist a pair $x(s), y(s) \in \mathcal{E}$ satisfying $a(s)x(s)+b(s)y(s)=1$, see (2.68) for the comparison.

Stabilization and synthesis of the so-called fractional exponential systems has been worked out e.g. in [9].

Surveys [141], [183] focused on advances in control of TDS also includes overview of some algebraic methods, particularly in robust control of systems with commensurate delays.

The main result of [75], that neutral TDS that are not formally stable are not BIBO stabilizable, has already been introduced above, see Subchapter 2.4.1, where the authors employed the algebra of Laplace transform elements from $H_\infty(\mathbb{C}^+)$. This finding,

however, holds for strictly proper systems, i.e. proper systems can have a Bézout coprime factorization, see example $G(s)=s/(s+s\exp(-s)+1)$ in [160]. The authors provided stabilizing procedure for state-space models via distributed feedback of the form as in [16].

A generalization of a so-called structure at infinity (closely related to the coprime factorization) and the introduction of non-equivalent notions of proper and biproper fractions for both retarded and neutral TDS with commensurate delays (in 2-D) were presented in [30]. In the paper, advantages of the use of pseudopolynomials for distributed delays were mentioned as well.

Partington and Bonet [115], in their very attractive paper, studied H_∞ and BIBO stabilizability of neutral SISO TDS with one internal delay. They paid their attention to controlled systems with limit case for strong (and formal) (in)stability, $\sum_{j=1}^{h_i}|m_{nj}|=1$, see (2.25). The authors stated that in [75] it had actually been proven that formally unstable neutral TDS can not be exponentially stabilized. However, they disproved that such systems can not be BIBO stable. For instance, it was proved there that a system with transfer function $G_0(s)=1/(s+s\exp(-s)+1)\notin H_\infty(\mathbb{C}^+)$ and it is not BIBO stable, yet $G(s)=G_0(s)/(s+1)\in H_\infty(\mathbb{C}^+)$ but still not BIBO stable, and $G(s)=G_0(s)/(s+1)^k\in H_\infty(\mathbb{C}^+)$ and is BIBO stable for $k \geq 4$. For all there three systems, the Bézout factorization condition (2.69) can not be satisfied. In extension to [75], they showed that many neutral systems can not be stabilized in an H_∞ sense. Moreover, it was proved that any H_∞-stabilizable SISO system can be stabilized by a proper controller of a finite dimension (compare to [62]). The authors opened the question of the existence of an infinite-dimensional controller for such systems. Although no algebraic methods are used in the work, the results are fruitful for this thesis.

A novel controller parameterization that reflect the Internal Model Control (IMC) structure for both, SISO and MIMO TDS, independent on the coprime factorization, was proposed in [194].

A robust control based algebraic approach, namely via a structured singular value, applied to three practical problems was introduced in [31].

2.4.3 Control of TDS in the R_{MS} ring

As mentioned above, this thesis intends primarily to use the ring of stable and proper meromorphic functions, R_{MS}, or its revised form, more precisely, therefore the overview of selected contributions dedicated to control in this ring follows. Notice that the conception of R_{MS} has not been finalized in many of these papers.

A control methodology for retarded TDS with non-commensurate delays based on the R_{MS} ring was introduced in [199]. Besides a conventional control loop with the Bézout identity and the Youla-Kučera parameterization for system stabilization and asymptotical tracking of stepwise reference, the affine parameterization was adopted. The idea of the affine parameterization in R_{MS} was extended in [201], [202]. In the former paper, the authors solved asymptotic stability, (again stepwise) reference tracking and disturbance rejection followed by the shifting of the closed-loop poles [171]. The cascade controller scheme for unstable plants plays the important role here. The latter one dealt with state-feedback pre-stabilization supported by a finite-dimensional observer and followed by the affine parameterization again. The methodology provides a finite spectrum assignment of the control loop. A specific cascade control structure satisfying the disturbance compensation presented in [203] improved the ideas introduced in the papers above.

To name just a few contributions by the author of this thesis related to controller design in R_{MS}, control of unstable retarded TDS and that of integrating processes with dead time by two feedback controllers were designed in [131] and [122] respectively. The link between relay-based autotuning and controller design was set e.g. in [130], [139]. Reference tracking and disturbance rejection of non-stepwise external inputs with delayed plants and two feedback controllers were solved in [129]. However, some authors' (mainly early) papers suffer from mistakes and inaccuracies.

Yet, as pointed in [124], the algebraic structure defined in [199] does not constitute a ring and, moreover, neutral-type system structures ought to be included in the definition.

2.5 Control system structures

An essential step in controller design is the selection of the control system structure, hence, the description of control system structures utilized in this thesis follows. The first one agrees with the simple negative feedback loop, whereas the second one introduces a secondary (slave) controller making the task of load disturbance rejection easier and better to solve. Moreover, it will be shown later that this control structure enables to guarantee a (quasi)finite spectrum assignment.

2.5.1 1DoF control structure

One-Degree-of-Freedom (1DoF) system structure is depicted in Fig. 2.1, where , $W(s)$ is the Laplace transform of the reference signal, $D(s)$ stands for that of the load disturbance, $E(s)$ is transformed control error, $U(s)$ represents the plant input, and $Y(s)$ is the plant output controlled signal in the Laplace transform. The plant transfer function is depicted as $G(s)$, and $G_R(s)$ stands for a controller in the scheme.

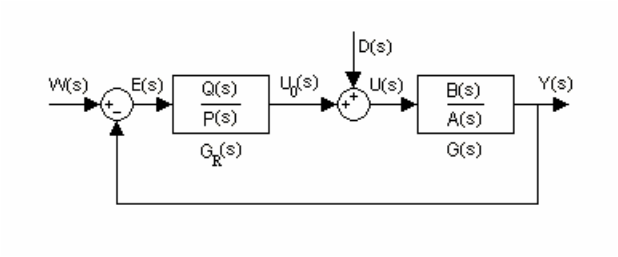

Fig. 2.1 1DoF control system structure

Let $G(s)=B(s)/A(s)$ and $G_R(s)=Q(s)/P(s)$, then the following basic transfer function can be derived in the control system in general

$$\begin{aligned} G_{WY}(s)&=\frac{Y(s)}{W(s)}=\frac{B(s)Q(s)}{M(s)}, G_{DY}(s)=\frac{Y(s)}{D(s)}=\frac{B(s)P(s)}{M(s)},\\ G_{WE}(s)&=\frac{E(s)}{W(s)}=\frac{A(s)P(s)}{M(s)}, M(s)=A(s)P(s)+B(s)Q(s) \end{aligned} \tag{2.72}$$

2.5.2 TFC control structure

Two-Feedback-Controllers (TFC) control system, see e.g. [112], is another controller structure, displayed in Fig. 2.2. The transformed signals and transfer functions have the same meaning as for 1DoF and $G_Q(s)$ states for the transfer function of the secondary (slave) controller in the inner feedback loop.

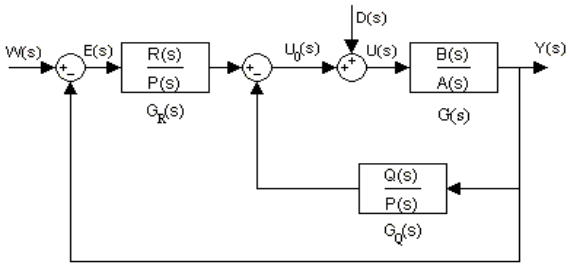

Fig. 2.2 TFC control system structure

In the structure, the following transfers can be derived

$$\begin{aligned} &G_{WY}(s)=\frac{Y(s)}{W(s)}=\frac{B(s)R(s)}{M(s)},\ G_{DY}(s)=\frac{Y(s)}{D(s)}=\frac{B(s)P(s)}{M(s)},\\ &G_{WE}(s)=\frac{E(s)}{W(s)}=\frac{A(s)P(s)+B(s)Q(s)}{M(s)},\ G_{DE}(s)=\frac{E(s)}{D(s)}=-\frac{B(s)P(s)}{M(s)},\\ &M(s)=A(s)P(s)+B(s)\big(Q(s)+R(s)\big) \end{aligned} \tag{2.73}$$

where

$$G_R(s)=\frac{R(s)}{P(s)},\ G_Q(s)=\frac{Q(s)}{P(s)} \tag{2.74}$$

Obviously, 1DoF and TFC coincide if and only if $G_Q(s)=0$.

2.6 Tuning of controllers for TDS

A suitable setting (of free parameters) of finally derived controller(s) is another important task in controller design.

The most of tuning approaches have dealt with an optimal setting of the state feedback. For instance, Linear-Quadratic (LQ) optimal control was proposed e.g. in [45], [47], [82]. Yet, these approaches are marked by the enormous complexity of the control laws. An interesting idea of the state-feedback controller tuning by the change of delays in the feedback was proposed e.g. in [110].

Regarding output-feedback control, the stabilizing effect of delayed feedback was pointed out in [1]. The optimal modulus principle for TDS via classical PID controllers was implemented in [205]. A dead-beat (i.e. that guaranteeing the minimal number of control actions) controller for discrete-time TDS models was derived in [183]. H_∞ optimal control of TDS based on operator methods and frequency domain descriptions of systems was solved in [43]. The LQ control technique ensuring asymptotical tracking of step reference and step load disturbance attenuation for stable, integrating and unstable plants with input-output delay based on delay approximation and the polynomial approach was presented in [32].

An overview of some other (rather controller design) methods was presented in [141]. A detailed PID controllers design for systems with time delay was published in [150]. A number of results on control and tuning of systems with input-output delays were published as well, see e.g. [108], [169] and references therein.

As a pole placement tuning methodology is concerned in this thesis, a basic overview of pole placement (PP) and finite spectrum assignment (FSA) methods for TDS ought to be presented.

2.6.1 Finite spectrum assignment

A FSA methodology for SISO linear systems with delays in state and/or control variables was introduced in [83] for the first time. The authors utilized a feedback law involving convolutory integrals over past and present values of input and state variables (i.e. distributed delays in the feedback). The results were extended by Watanabe [183], however, the procedure is too complex.

As mentioned above, Brethé and Loiseau [16] proposed an algebraic approach by means of pseudopolynomials based on the Bézout identity.

A comprehensive treatment of FSA for controlled plants with input-output delays was made in [164], [180].

2.6.2 Static pole placement for TDS

Extending the system PP task to TDS brings a rather different problem in comparison to finite-dimensional systems. The crucial difference lies mainly in the fact that the characteristic quasipolynomial has an infinite number of zeros, yet a finite number of (free) controller parameters. Hence, in the contrary to FSA, the aim of PP is to place some (dominant) poles of, generally, infinite spectrum instead of to design control law resulting in a finite-dimensional feedback. The problem was already formulated in [113]. The notion “static” in this subchapter heading expresses PP strategies assigning poles “at once” to the prescribed positions without iterations. For spectrally controllable systems, it is possible to place as many poles as free controller parameters are available.

A specific and crucial problem for TDS is that the poles dominancy must be checked, e.g. using methods introduced in Subchapter 2.2.1 or via a conformal mapping technique and the Mikhailov (or Nyquist) criterion [197], [200]. Indeed, any attempt to place poles too left in the complex plane results to moving the rest of the spectrum to the right. The dominancy can be understand in the classical sense as the smallest distance of real parts of poles from the imaginary axis, or via the calculation of poles residues as it was introduced e.g. in [206].

Pole assignment problem for controllable TDS has been solved in [71] where a systematic procedure was derived.

Frequency domain pole assignment employing conformal mapping for a general class of delays expressed by convolutions of the form (2.2) was proposed in [197]. Dominant pole placement for TDS with input-output delay and the PID controller based on the ultimate gain and ultimate frequency from the Nyquist plot was presented e.g. in [181], [182], [200] and improved in [73]. In [169], the same problem, however, in the Laplace domain was solved.

A simple method of designing state variable feedback in TDS assigning the dominant system poles on prescribed positions was presented e.g. in [206]. Look at the idea in more details. Consider the closed-loop characteristic quasipolynomial $m(s,\mathbf{K})$ with a vector $\mathbf{K}$ of r unknown (free) controller parameters as

$$\mathbf{K} = [K_1, K_2, ..., K_r]^T \in \mathbb{R}^r \tag{2.75}$$

If the aim is to assign n_R real feedback poles, σ_i, i = 1...n_R, into prescribed positions, the following set of linear algebraic equations are to be solved

$$m(\sigma_i, \mathbf{K}) \approx m(\sigma_i, \mathbf{K}_0) + \sum_{j=1}^{r} \Delta K_j \left[\frac{\partial m(s,\mathbf{K})}{\partial K_j} \right]_{\substack{s=\sigma_i \\ \mathbf{K}=\mathbf{K}_0}} = 0, i = 1...n_R \tag{2.76}$$

where $\mathbf{K}_0$ is a vector of arbitrary parameters values (ideally) near the desired $\mathbf{K}$ and ΔK_j represent the parameters increments (i.e. $\mathbf{K} = \mathbf{K}_0 + \Delta\mathbf{K}$). The left-hand side equality in (2.76) comes if $m(s,\mathbf{K})$ is linear with respect to $\mathbf{K}$, which is usual in linear control, and the sensitivity functions do not depend on $\mathbf{K}$.

In case of complex conjugate poles, it is necessary to solve real and imaginary parts of (2.76) separately as

$$\begin{aligned} \mathrm{Re}\{m(\sigma_i, \mathbf{K})\} &\approx \mathrm{Re}\left\{ m(\sigma_i, \mathbf{K}_0) + \sum_{j=1}^{r} \Delta K_j \left[\frac{\partial m(s,\mathbf{K})}{\partial K_j} \right]_{\substack{s=\sigma_i \\ \mathbf{K}=\mathbf{K}_0}} \right\} = 0 \\ \mathrm{Im}\{m(\sigma_i, \mathbf{K})\} &\approx \mathrm{Im}\left\{ m(\sigma_i, \mathbf{K}_0) + \sum_{j=1}^{r} \Delta K_j \left[\frac{\partial m(s,\mathbf{K})}{\partial K_j} \right]_{\substack{s=\sigma_i \\ \mathbf{K}=\mathbf{K}_0}} \right\} = 0, \; i = 1...n_C \end{aligned} \tag{2.77}$$

where n_C expresses the number of prescribed complex conjugate pairs.

Equations (2.76) or (2.77) have a unique solution if $r = n_R$ or $r = 2n_c$, respectively, and they are linearly independent. If the intention is to place less poles than the number of free parameters is, i.e. $r > n_R$ or $r > 2n_C$, respectively, sets (2.76) or (2.77) are to be solved using so-called Moore-Penrose pseudoinverse, [134], minimizing the norm

$$\left\|\mathbf{K}\right\|_2 = \sum_{i=1}^{r} K_i^2 \tag{2.78}$$

Contrariwise, if $r < n_R$ or $r < 2n_C$, respectively, it is not possible to place poles to the prescribed positions exactly, and the pseudoinverse provides the least squares minimization

$$\Delta\mathbf{K} = \arg\min \sum_{i=1}^{n_R} \left(m(\sigma_i, \mathbf{K}_0) + \sum_{j=1}^{r} \Delta K_j \left[\frac{\partial m(s,\mathbf{K})}{\partial K_j} \right]_{\substack{s=\sigma_i \\ \mathbf{K}=\mathbf{K}_0}} \right)^2$$

$$\Delta\mathbf{K} = \arg\min \sum_{i=1}^{n_C} \left(\begin{array}{l} \left(\mathrm{Re}\left\{ m(\sigma_i, \mathbf{K}_0) + \sum_{j=1}^{r} \Delta K_j \left[\frac{\partial m(s,\mathbf{K})}{\partial K_j} \right]_{\substack{s=\sigma_i \\ \mathbf{K}=\mathbf{K}_0}} \right\} \right)^2 \\ + \left(\mathrm{Im}\left\{ m(\sigma_i, \mathbf{K}_0) + \sum_{j=1}^{r} \Delta K_j \left[\frac{\partial m(s,\mathbf{K})}{\partial K_j} \right]_{\substack{s=\sigma_i \\ \mathbf{K}=\mathbf{K}_0}} \right\} \right)^2 \end{array} \right) \tag{2.79}$$

In case of prescribed multiple poles of *p*-th order, formulas (2.76) or (2.77) not only for $m(s,\mathbf{K})$ but also for

$$m^{(l)}(s,\mathbf{K}) = \mathrm{d}^l m(s,\mathbf{K}) / \mathrm{d}s^l, l = 1,2,..., p-1 \tag{2.80}$$

must hold.

Alternatively, if linearity of the algebraic equations is not required, one can solve a set on non-linear algebraic equations

$$\left[\frac{\mathrm{d}^{l_i}}{\mathrm{d}s^{l_i}} m(\sigma_i, \mathbf{K}) \right]_{s=\sigma_i} = 0,\ \mathrm{Re}\left[\frac{\mathrm{d}^{l_j}}{\mathrm{d}s^{l_j}} m(\sigma_j, \mathbf{K}) \right]_{s=\sigma_j} = 0,\ \mathrm{Im}\left[\frac{\mathrm{d}^{l_j}}{\mathrm{d}s^{l_j}} m(\sigma_j, \mathbf{K}) \right]_{s=\sigma_j} = 0$$
$$l_i = 0,1..., p_i - 1, i = 1,2,...n_R, l_j = 0,1..., p_j - 1,\ j = 1,2,...n_C \tag{2.81}$$

without linearization (2.76), (2.77); however, it requires a rather more sophisticated computational methods, e.g. the well known Newton method.

An example demonstrating the pole assignment procedure follows.

Example 2.5

Consider the characteristic quasipolynomial

$$m(s) = s + a\exp(-\tau s) \tag{2.82}$$

The task is to find a pair $\{a,\tau\}$ when a prescribed pair of roots of (2.82), $\sigma = \alpha \pm \mathrm{j}\omega$, is given. The exact analytic solution (meeting the requirements of the positivity of $\{a,\tau\}$ and the negativity of σ) reads

$$a = |\sigma|\exp\left(\frac{\alpha}{\omega}\arccos\left(-\frac{\alpha}{|\sigma|}\right)\right),\ \tau = \frac{1}{\omega}\arccos\left(-\frac{\alpha}{|\sigma|}\right) \tag{2.83}$$

Compare now the solution with (2.77) in the working point $[a,\tau] = [1,1]$.

$$\begin{aligned} m(\sigma,[a,\tau]) &\approx \sigma + \exp(-\sigma) + \Delta a[\exp(-\tau\sigma)]_{\tau=1} + \Delta\tau[-a\sigma\exp(-\tau\sigma)]_{\substack{\tau=1\\a=1}} \\ &= \sigma + \exp(-\sigma) + \Delta a(\exp(-\sigma)) + \Delta\tau(-\sigma\exp(-\sigma)) \end{aligned} \tag{2.84}$$

where $a = 1 + \Delta a,\ \tau = 1 + \Delta\tau$. By decomposition into real and imaginary parts, (2.84) becomes

$$\begin{aligned} &\Delta a(\exp(-\alpha)\cos\omega) - \Delta\tau\exp(-\alpha)(\alpha\cos\omega + \omega\sin\omega) = -(\alpha + \exp(-\alpha)\cos\omega) \\ &-\Delta a(\exp(-\alpha)\sin\omega) + \Delta\tau\exp(-\alpha)(\alpha\sin\omega - \omega\cos\omega) = \exp(-\alpha)\sin\omega - \omega \end{aligned} \tag{2.85}$$

For example, let $\sigma = -1 \pm \mathrm{j}0.5$, then (2.83) gives $a = 0.4423, \tau = 0.9273$. In contrast to that, (2.85) reads

$$\begin{aligned} &2.3855\Delta a + 1.7339\Delta\tau = -1.3855 \\ &-1.3032\Delta a - 2.496\Delta\tau = 0.8032 \end{aligned} \tag{2.86}$$

which results in $\Delta a = -0.5591, \Delta\tau = -0.0299$, i.e. $a = 0.4409, \tau = 0.9701$. Contrariwise, a quasipolynomial with $a = 0.4409, \tau = 0.9701$ has the dominant pair of roots as $\sigma = -0.9269 \pm \mathrm{j}0.5612$. ■

So-called σ-stabilizability (roughly speaking – closed loop spectrum is to be located left from the prescribed value $-\sigma < 0$ determining exponential decay) was addressed in [99] for retarded TDS and in [64] for neutral ones. A similar problem was

solved in [168] for a delay-free DC servomotor controlled by a delayed feedback using shaping of the characteristic quasipolynomial with the dominant poles analysis.

Pole placement issues for TDS were also partially investigated e.g. in [47], [82], [184].

2.6.3 Continuous pole placement for TDS

The mentioned specific feature of TDS that placing the desired dominant poles may cause the effect that unexpected dominant poles emerge somewhere to the right of the desired ones has induced the investigation of iterative (shifting) algorithms pushing the undesirable poles to the left. Although this class of approaches has been developed for state feedback control, it can be applied to output controllers effortlessly.

Let us describe basic steps of algorithms introduced in [90], [171] which have the common idea, yet utilize a rather different tools. The core of algorithms, called also Quasi-Continuous Shifting Algorithm (QCSA), combines the estimation of poles locations with changing controller parameters based either on the prescription of new desired poles positions or on the sensitivity (tendency) of current poles. The method starts with the static pole placement introduced in 2.6.2 where initial closed-loop poles positions are set. Let n_S denotes the number of shifted dominant poles, then n_S (or more) dominant are to be found. Exactly n_S poles are then moved left (in real axis) with appropriately short distance. The number of shifted poles can be increased if necessary (e.g. when the algorithm is cycled). The differences between the two approaches [90], [171] lie in the way how to induce the shifting and in the number of possibly shifted poles. Naturally, it depends also on whether a feedback has retarded or neutral character, see [94].

A short description and a summarization of the two algorithm variants of QCSA follow. Consider the idea of [171] for single roots first. Equation (2.76) and (2.77) can be written in the matrix form as

$$\mathbf{A}\Delta\mathbf{K} = \mathbf{b} \tag{2.87}$$

where

$$\mathbf{A}=\begin{bmatrix} a_{1,1} & a_{1,2} & \cdots & a_{1,r} \\ a_{2,1} & a_{2,2} & \cdots & a_{2,r} \\ \vdots & \vdots & \ddots & \vdots \\ a_{n_R,1} & a_{n_R,2} & \cdots & a_{n_R,r} \\ a_{R,1,1} & a_{R,1,2} & \cdots & a_{R,1,r} \\ a_{R,2,1} & a_{R,2,2} & \cdots & a_{R,2,r} \\ \vdots & \vdots & \ddots & \vdots \\ a_{R,n_C,1} & a_{R,n_C,2} & \cdots & a_{R,n_C,r} \\ a_{I,1,1} & a_{I,1,2} & \cdots & a_{I,1,r} \\ a_{I,2,1} & a_{I,2,2} & \cdots & a_{I,2,r} \\ \vdots & \vdots & \ddots & \vdots \\ a_{I,n_C,1} & a_{I,n_C,2} & \cdots & a_{I,n_C,r} \end{bmatrix},\ \mathbf{b}=\begin{bmatrix} b_1 \\ b_2 \\ \vdots \\ b_{n_R} \\ b_{R,1} \\ b_{R,2} \\ \vdots \\ b_{R,n_C} \\ a_{I,1} \\ a_{I,2} \\ \vdots \\ b_{I,n_C} \end{bmatrix}$$

$$a_{i,j}=\left[\frac{\partial m(s,\mathbf{K})}{\partial K_j}\right]_{\substack{s=\alpha_i+\Delta\alpha_i \\ \mathbf{K}=\mathbf{K}_0}},\ a_{R,i,j}=\mathrm{Re}\left[\frac{\partial m(s,\mathbf{K})}{\partial K_j}\right]_{\substack{s=\alpha_i+\mathrm{j}\omega_i+\Delta\alpha_i \\ \mathbf{K}=\mathbf{K}_0}},\ a_{I,i,j}=\mathrm{Im}\left[\frac{\partial m(s,\mathbf{K})}{\partial K_j}\right]_{\substack{s=\alpha_i+\mathrm{j}\omega_i+\Delta\alpha_i \\ \mathbf{K}=\mathbf{K}_0}}$$

$$b_i=m(\alpha_i+\Delta\alpha_i,\mathbf{K}_0),\ b_{R,i}=\mathrm{Re}\{m(\alpha_i+\mathrm{j}\omega_i+\Delta\alpha_i,\mathbf{K}_0)\},b_{R,i}=\mathrm{Im}\{m(\alpha_i+\mathrm{j}\omega_i+\Delta\alpha_i,\mathbf{K}_0)\} \tag{2.88}$$

where $\sigma_i=\alpha_i, i=1...n_R$ are current real poles, $\sigma_i=\alpha_i\pm\mathrm{j}\omega_i, i=1...n_C$ mean complex conjugate pairs of poles, $\mathbf{K}_0$ represents the vector of actual controller parameters and $\Delta\alpha_i<0$ stands for a shift of real parts of poles. Hence, a new vector of controller parameters $\mathbf{K}=\mathbf{K}_0+\Delta\mathbf{K}$, or $\mathbf{K}=\mathbf{K}_0+\mathrm{Re}\,\Delta\mathbf{K}$, is calculated using the pseudoinverse

$$\Delta\mathbf{K}=\mathbf{A}^{+}\mathbf{b} \tag{2.89}$$

based on the chosen value of $\Delta\alpha_i$. In every iteration step it is necessary to check the prescribed poles dominancy. Naturally, one can use nonlinear equations (2.81); however, it requires more complex calculations.

If n_S denotes the number of currently shifted poles, it must hold that $n_S=n_R+2n_C\le r$, i.e. one controller parameter can move one pole, not the whole conjugate.

The case of a *p*-multiple pole can be easily solved similarly as in (2.88) where $p-1$ *s*-derivatives of $m(s,\mathbf{K})$ are to be used to calculate appropriate rows in $\mathbf{A},\mathbf{b}$.

The methodology published in [90] utilized an extrapolation

$$\underbrace{m(\sigma_i,\mathbf{K}_0)}_{=0}+\Delta\sigma_i\left[\frac{\partial m(s,\mathbf{K})}{\partial s}\right]_{\substack{s=\sigma_i\\ \mathbf{K}=\mathbf{K}_0}}+\Delta K_j\left[\frac{\partial m(s,\mathbf{K})}{\partial K_j}\right]_{\substack{s=\sigma_i\\ \mathbf{K}=\mathbf{K}_0}}=0,\ i=1...n_S,\ j=1...r \tag{2.90}$$

yielding

$$\frac{\Delta\sigma_i}{\Delta K_j}\approx-\left[\frac{\partial m(s,\mathbf{K})}{\partial s}\right]^{-1}_{\substack{s=\sigma_i\\ \mathbf{K}=\mathbf{K}_0}}\left[\frac{\partial m(s,\mathbf{K})}{\partial K_j}\right]_{\substack{s=\sigma_i\\ \mathbf{K}=\mathbf{K}_0}} \tag{2.91}$$

A matrix

$$\mathbf{S}=\left[\frac{\Delta\sigma_i}{\Delta K_j}\right]\in\mathbb{R}^{\,n_S\times r} \tag{2.92}$$

is so-called sensitivity matrix which enables to estimate parameters changes according to

$$\Delta\mathbf{K}=\mathbf{S}^{+}\Delta\boldsymbol{\sigma} \tag{2.93}$$

where $\Delta\boldsymbol{\sigma}=\left[\Delta\sigma_1,\Delta\sigma_2,...,\Delta\sigma_{n_S}\right]^T$.

It holds that

$$\frac{\Delta\,\mathrm{Re}\,\sigma_i}{\Delta K_j}=\mathrm{Re}\left\{\frac{\Delta\sigma_i}{\Delta K_j}\right\} \tag{2.94}$$

thus, if poles are shifted in the real axis only, it can be calculated

$$\Delta\mathbf{K}=\left(\mathrm{Re}\,\mathbf{S}\right)^{+}\mathrm{Re}\{\Delta\boldsymbol{\sigma}\} \tag{2.95}$$

The advantage of this technique is that up to $2r$ (complex conjugate) poles can be shifted, since one controller parameter can be used to adjust a real pole or a pair of (both) complex conjugate poles. Unfortunately, in case of a *p*-multiple pole, the technique fails and one can consider a pole a “nest” of close single poles.

Prior to an algorithm summarization, a specific of neutral TDS ought to be mentioned. Since there exist vertical strips of characteristic roots the position of which in

the real axis is not continuous with respect to delays, the so called safe upper bound has been defined [94]. The notion expresses the real number that is definitely higher than the real part of the rightmost strip even considering small changes in delays. If such number is strictly negative, the system is strongly stable and thus it can be stabilized safely. More precisely, define $c_D(\boldsymbol{\eta})$ as

$$c_D(\boldsymbol{\eta}) := \sup\{\mathrm{Re}\, s : m_D(s) = 0\} \tag{2.96}$$

where $\boldsymbol{\eta}$ is the vector of N_H delays and $m_D(s)$ is the characteristic quasipolynomial (2.23) related to the associated difference equation (2.21). As mentioned in Subchapter 2.2.2, $c_D(\boldsymbol{\eta})$ is not continuous with respect to $\boldsymbol{\eta}$ and it expresses the real part of the rightmost strip of poles of a neutral TDS. The safe upper bound $\overline{C}_D(\boldsymbol{\eta}) \in \mathbb{R}$ is defined as follows

$$\overline{C}_D(\boldsymbol{\eta}) := \lim_{\varepsilon \to 0^+} \sup\{c_D(\boldsymbol{\eta} + \delta\boldsymbol{\eta}) : \|\delta\boldsymbol{\eta}\| < \varepsilon\} \tag{2.97}$$

It holds that $\overline{C}_D(\boldsymbol{\eta}) \geq c_D(\boldsymbol{\eta})$ and $\overline{C}_D(\boldsymbol{\eta})$ is continuous in the delays. It has been proved in [94] that the quantity $\overline{C}_D(\boldsymbol{\eta})$ is the unique zero of the strictly decreasing function

$$c \in \mathbb{R} \to f(c, \boldsymbol{\eta}) - 1 \tag{2.98}$$

where $f(c, \boldsymbol{\eta})$ is defined as

$$f(c, \boldsymbol{\eta}) := \max_{\boldsymbol{\theta} \in [0, 2\pi]^{N_H}} r_\Omega\left(\sum_{i=1}^{N_H} \mathbf{H}_i \exp(\mathrm{j}\theta_i - c\eta_i) \right) \tag{2.99}$$

where $r_\Omega(\cdot)$ means the spectral radius. It is possible to estimate an upper bound on $\overline{C}_D(\boldsymbol{\eta})$ using the fact that

$$f(c, \boldsymbol{\eta}) \leq \sum_{i=1}^{N_H} \|\mathbf{H}_i\| \exp(-c\eta_i) \tag{2.100}$$

as the unique solution of the equation

$$\sum_{i=1}^{N_H} \|\mathbf{H}_i\| \exp(-c\eta_i) = 1 \tag{2.101}$$

If the control law can not change any of $\mathbf{H}_i$ (or, equivalently any of m_{nj}, see (2.25)), one can concentrate on the characteristic roots (poles) with the real part larger than $\overline{C}_D(\boldsymbol{\eta})$, since the value of $\overline{C}_D(\boldsymbol{\eta})$ can not be adjusted in this case. It holds that all poles in the half-plane $\mathrm{Re}\, s \geq \overline{C}_D + \varepsilon, \varepsilon > 0$, lie in a compact (i.e. closed and bounded) set and the number of these roots is finite [52], [94]. Hence only isolated poles right from the value of $\overline{C}_D(\boldsymbol{\eta})$ can be taken into account when shifting. In the contrary, if $\mathbf{H}_i$ can be changed, the value of $\overline{C}_D(\boldsymbol{\eta})$ varies and it must be recalculated in every iteration step; however, there is still no reason to deal with the characteristic roots left from $\overline{C}_D(\boldsymbol{\eta})$. The knowledge of $\overline{C}_D(\boldsymbol{\eta})$ prevents to spend much control action to poles with smaller real part which are useless for feedback stabilization.

The case $\overline{C}_D(\boldsymbol{\eta}) > 0$ agrees with strong instability, and if it is not possible to improve $\overline{C}_D(\boldsymbol{\eta})$, one can give the controller tuning up.

To sum up, the basic steps of the algorithms follow.

Algorithm 2.1

Input: The characteristic quasipolynomial $m(s,\mathbf{K})$ with an initial setting $\mathbf{K}_0$, initialize the counter as $i = 1$, $\mathbf{K}_i = \mathbf{K}_0$.

Step 1: If $m(s,\mathbf{K})$ is of a neutral type and coefficients for the highest s-power m_{nj} can not be modified, determine whether $\gamma_0 < 1$. If not, give up.

Step 2: Set the number of shifted poles $n_S = 1$, compute $\overline{C}_D(\boldsymbol{\eta})$ and choose $\varepsilon > 0$ if $m(s,\mathbf{K})$ is neutral.

Step 3: Compute the rightmost roots σ of $m(s,\mathbf{K})$, or those with $\mathrm{Re}\,\sigma \geq \overline{C}_D(\boldsymbol{\eta}) + \varepsilon$ in the neutral case.

Step 4: Choose the desired poles shifts $\Delta\boldsymbol{\sigma}$ of n_S rightmost poles and compute the pseudoinverse (2.89), or equivalently, calculate the sensitivity matrix (2.92) and the pseudoinverse (2.95). Update $\mathbf{K}_{i+1} = \mathbf{K}_i + \Delta\mathbf{K}_i$.

Step 5: Monitor the rightmost uncontrolled poles, or those with $\mathrm{Re}\,\sigma \geq \overline{C}_D(\boldsymbol{\eta}) + \varepsilon$. If necessary (e.g. when the rightmost poles are close to each other), increase n_S. Stop when stability is reached or if $n_S = r$. In neutral case, the algorithm stops also when the leftmost from the controlled characteristic roots reaches $\overline{C}_D(\boldsymbol{\eta})$. Otherwise, increment the counter *i* and go to Step 3.

Output: The vector of controller parameters $\mathbf{K}$ and the positions of the rightmost poles. ■

Recall that $m(s)$ as the closed loop transfer function denominator quasipolynomial in the case of distributed delays also contains roots which are not system poles and they can not be shifted by any mean. These roots are common zeros of the numerator and denominator of the characteristic meromorphic function $M(s)$ introduced in (2.8), see Example 2.1. Hence, it would be more suitable to consider $M(s)$ instead of $m(s)$ in the algorithm.

2.6.4 Optimal pole placement minimizing the spectral abscissa

The basic aim of the continuous pole placement is to gradually refine the positions of the rightmost poles in the real axis by arbitrarily small changes in the controller parameters. This process can be viewed as the optimization of the so-called spectral abscissa which is defined as

$$\alpha(\mathbf{K}) := \max_i \{\mathrm{Re}(\sigma_i) : m(\sigma_i) = 0\} \tag{2.102}$$

Thus, the objective is to solve the optimization problem

$$\min_{\mathbf{K}} \alpha(\mathbf{K}) \tag{2.103}$$

or to reach $\alpha(\mathbf{K})$ to be strictly negative at least.

Again, in case of distributed delays, one ought to take $M(s)$ instead of $m(s)$.

The problem was solved e.g. in [166] where state feedback controller design and the Extended Gradient Sampling Algorithm (EGSA), see [17], for the abscissa

minimization have been used to retarded TDS with lumped delays. It has been pointed out in the paper that a complex optimization algorithm ought to be used instead of a standard one, say, the well known steepest descent algorithm, when dealing with this task.

The reason lies in some spectral abscissa function properties. The first problem arises from the fact that $\alpha(\mathbf{K})$ is non-convex, i.e. it may have multiple local minima. It is clear that with such behavior the global minimum is hard to find, and many optimization algorithms will converge to a local minimum. The second difficulty is that $\alpha(\mathbf{K})$ is non-smooth with respect to parameter changes in points where more then one real poles or conjugate pairs are with the maximum real part [90], [166]. At these points the function $\alpha(\mathbf{K})$ is hence not differentiable. As third, the function is non-Lipschitz, for example, at points where the maximum real part has multiplicity greater than one [17]. However, it is assumed that the spectral abscissa is differentiable almost everywhere.

An extension of the paper referenced above to neutral state feedback was attempted to do in [88], [172]. The limitation (2.24) or (2.25) due to strong stability requires introducing a rather different objective function than (2.103) leading to a constrained optimization problem (in the input-output formulation)

$$\min_{\mathbf{K}} \alpha(\mathbf{K}), \sum_{j=1}^{h_n} |m_{nj}| < 1 \tag{2.104}$$

Note that in the state space, (2.24) is taken instead of (2.25). A restriction of the objective function can be included as a penalty subfunction. In [88], the following option is made

$$\Phi(\mathbf{K}) = \alpha(\mathbf{K}) + \lambda \left(\sum_{j=1}^{h_n} |m_{nj}(\mathbf{K})| \right)^2 \tag{2.105}$$

where $\Phi(\mathbf{K})$ is the objective function and λ represents a weighting parameter. This conception, however, does not guarantee that the restriction (2.25) holds true. A rather more suitable option would be

$$\Phi(\mathbf{K}) = \alpha(\mathbf{K}) + \lambda \left(1 - \varepsilon - \sum_{j=1}^{h_n} |m_{nj}(\mathbf{K})| \right)^2 \tag{2.106}$$

where $0 < \varepsilon << 1$, for which holds the following theorem. If $\{\lambda_i\}$ is an increasing sequence with $\lim_{i\to\infty} \lambda_i = \infty$ and $\varepsilon \to 0$, then $\Phi(\mathbf{K}^*) \leq \Phi(\mathbf{K}_{i+1}, \lambda_{i+1}) \leq \Phi(\mathbf{K}_i, \lambda_i)$, where $\mathbf{K}^*$ is the optimal solution of the minimization of (2.106) and it holds that

$$\lim_{\lambda_i\to\infty}\left(1-\varepsilon-\sum_{j=1}^{h_n}\left|m_{nj}(\mathbf{K})\right|\right)^2 = 0 \text{, i.e. } \sum_{j=1}^{h_n}\left|m_{nj}(\mathbf{K})\right| \to 1-\varepsilon \tag{2.107}$$

see e.g. [3].

Another possibility is to introduce a barrier function, e.g. as

$$\Phi(\mathbf{K}) = \alpha(\mathbf{K}) - \lambda \ln\left(1-\sum_{j=1}^{h_n}\left|m_{nj}(\mathbf{K})\right|\right) \tag{2.108}$$

as utilized in [172], yet for a state feedback controller.

The spectral abscissa minimization for a general class of retarded TDS described by (2.2) (without the neutral term) using a state-feedback controller was presented in [97]. The method application follows two steps. First, a number of rightmost poles, smaller than the number of controlled one, is directly assigned, which makes some controller parameters constrained. Second, the remaining degrees of freedom in the space of controller parameters are used to shift the rest of the spectrum as far to the left as possible, again by the EGSA. If the prescribed poles are not dominant after shifting, new poles positions are to be selected.

In [127] a similar idea was independently introduced. In contrast to [97] , there are nevertheless some differences. Firstly, the approach presented in [127] uses the input-output space of meromorphic Laplace transfer functions, whereas the one in [97] deals purely with the state space. Second, poles are initially placed in desired positions unambiguously according to the estimated maximal overshoot; however, they can leave their positions during the shifting. The dominant poles move to the prescribed ones and the rest of the spectrum is pushed to the left again by minimization of an objective function (including the spectral abscissa), without the requirement of resetting the selection of assigned poles. Last but not least, the Self-Organizing Migration Algorithm (SOMA), see [192], is utilized as a minimization technique. For more details, see Subchapters 5.1 - 5.3.

Note that the closed-loop zeros can be optimized in the similar way as poles are, because of the fact that zeros placed too right in the complex plane cause undesirable high oscillations, see details e.g. in [127].

2.7 Robust stability and robust performance

Robust analysis constitutes a set of possible tools for controller quality and performance evaluation, particularly when an ideal plant mathematical model does not match the real system behavior perfectly. The existence of a *family* of models gives rise to the notion of model *uncertainty* which can be formulated as a *structured* or *unstructured* uncertainty. Robustness means that a certain characteristics (e.g. internal stability) of a control system valid for a *nominal* plant model holds also for a family of models in the neighborhood of the nominal one. Basic robust analysis tasks are *robust stability* and *robust performance*. Robust stability agrees with the requirement that the asymptotic stability of a control feedback loop is preserved for all models from the family. Robust performance is usually expressed by a weighted limitation on (reference or disturbance) control errors under perturbations in the frequency domain.

We pay attention to unstructured uncertainty, more precisely *multiplicative disk uncertainty* which enables to develop simple general analytic methods and results. Let $G_0(s)$ be the nominal plant transfer function and $G(s)=[1+\Delta(s)W_M(s)]G_0(s)$ be a family of perturbed transfer functions. Here $W_M(s)$ is a fixed stable weight function expressing the uncertainty frequency distribution. Perturbation $\Delta(s)$ is a variable stable transfer function satisfying $\|\Delta(s)\|_\infty \le 1$. Moreover, $G(s)$ and $G_0(s)$ have the same number of unstable poles. It holds that

$$\left|\frac{G(\mathrm{j}\omega)}{G_0(\mathrm{j}\omega)}-1\right| \le |W_M(\mathrm{j}\omega)|, \forall\omega \tag{2.109}$$

which means that $G(\mathrm{j}\omega)/G_0(\mathrm{j}\omega)$ lies in the disk with center 1 and radius $|W_M(\mathrm{j}\omega)|$. The weight function is selected so that it covers all systems from the family

$$\max_{G(s)}\left|\frac{G(\mathrm{j}\omega)}{G_0(\mathrm{j}\omega)}-1\right|\le|W_M(\mathrm{j}\omega)|,\forall\omega \tag{2.110}$$

For instance, $W_M(s)$ can be taken as follows [154]

$$W_M(s)=\frac{Ts+r_0}{\frac{T}{r_\infty}s+1} \tag{2.111}$$

where r_0 and r_∞ are relative uncertainties for the steady state (ω = 0) and high frequencies (typically $\omega>2$), respectively, and $1/T$ means an approximate frequency wherein the uncertainty almost reaches its upper bound. The following example demonstrates the construction [70].

Example 2.6

A process of bleaching in the stationery industry can be modeled by the transfer function

$$G(s)=\frac{1}{2s+1}\exp((-0.1+\tau)s),\tau\in[0,0.9] \tag{2.112}$$

where τ arises from neglecting of a fast plant dynamics. Equation (2.112) expresses the family of models for which $\tau=0$ agrees with the nominal model, whereas $\tau\in(0,0.9]$ gives rise to perturbation models. Hence

$$\left|\frac{G(\mathrm{j}\omega)}{G_0(\mathrm{j}\omega)}-1\right|=|\exp(-\tau\mathrm{j}\omega)-1|\le|W_M(\mathrm{j}\omega)|,\forall\omega \tag{2.113}$$

In [70], $W_M(s)$ was chosen as

$$W_M(s)=\frac{2.1s}{s+1} \tag{2.114}$$

A comparison of Bode plots of the weighting function and normalized perturbations according to (2.113) is displayed in Fig. 2.3.

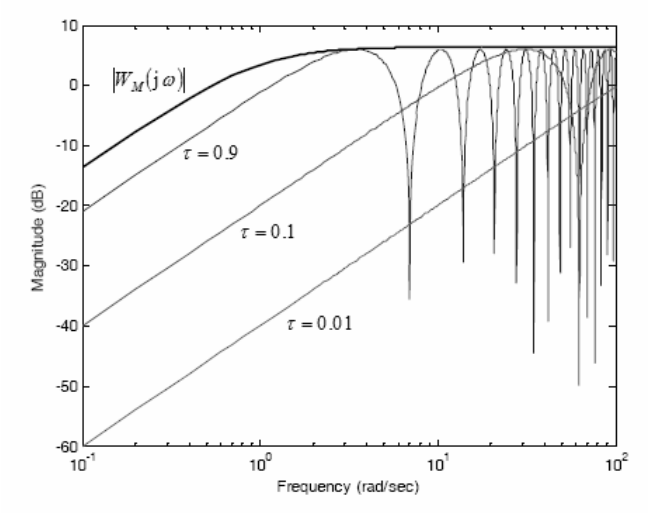

Fig. 2.3 Bode plots expressing the meaning of $W_M(s)$ for Example 2.6

■

2.7.1 Nominal performance

Consider a simple feedback loop as in Fig. 2.1. The (nominal) sensitivity function $S_0(s) = G_{WE}(s) = E(s)/W(s)$ is a very good closed-loop performance indicator. The frequency-depended gain bound on $S_0(j\omega)$ is a typical performance requirement. Usually, $|S_0(j\omega)|$ has small values for $\omega \to 0$; however, there is a peak on middle frequencies causing noise amplification. Hence, the elimination of this peak improves control quality and it can be formulated by the upper bound $1/|W_P(j\omega)|$ as follows

$$|S_0(j\omega)| < 1/|W_P(j\omega)|, \forall \omega \Leftrightarrow \|W_P(j\omega)S_0(j\omega)\|_\infty < 1 \qquad (2.115)$$

A graphical interpretation of the nominal performance condition (2.115) can be obtained using some simple calculations and it means that the distance of the Nyquist plot of the (nominal) open loop $L_0(j\omega) = G_R(j\omega)G_0(j\omega)$ from the critical point -1 is less then the maximal value of $|W_P(j\omega)|$, see a sketch in Fig. 2.4. [35]

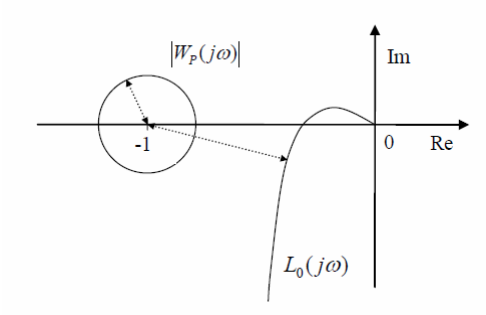

Fig. 2.4 The graphical interpretation of nominal performance

The weight function $|W_P(\mathrm{j}\omega)|$ (or more precisely $1/|W_P(\mathrm{j}\omega)|$) is chosen according to user requirements and can be constructed similarly as in (2.111).

2.7.2 Robust stability

As mentioned above, the closed-loop system is called robustly stable if it is stable for the whole family of perturbed plant models. For multiplicative uncertainty, the feedback system as in Fig. 2.1 is robustly stable if and only if

$$\|W_M(\mathrm{j}\omega)T_0(\mathrm{j}\omega)\|_\infty < 1 \tag{2.116}$$

where $T_0(s) = G_{WY}(s) = Y(s)/W(s)$ is the so-called (nominal) complementary sensitivity function, see e.g. [35].

The graphical interpretation of condition (2.116) can be easily obtained by some calculation

$$\left\| \frac{W_M(\mathrm{j}\omega)L_0(\mathrm{j}\omega)}{1+L_0(\mathrm{j}\omega)} \right\|_\infty < 1 \Leftrightarrow |W_M(\mathrm{j}\omega)L_0(\mathrm{j}\omega)| < |L_0(\mathrm{j}\omega) - (-1)|, \forall\omega \tag{2.117}$$

It means that the number of open-loop Nyquist plot encirclements must be the same for the whole family of perturbed plants, see Fig. 2.5, according to [33].

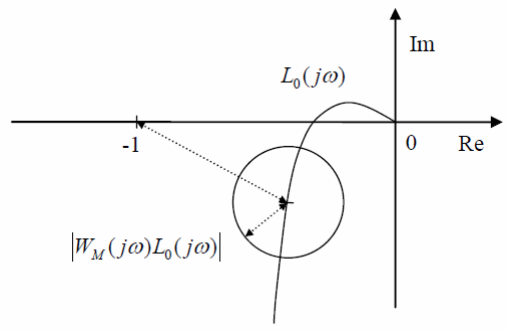

Fig. 2.5 The graphical interpretation of robust stability

The graphical interpretation can serve for the robust stability condition derivation for other control system loops, see Subchapter 7.6.

2.7.3 Robust performance

The general notion of robust performance is that both, internal stability and performance, should hold for the whole family of perturbed plants. The robust performance condition should therefore be

$$\|W_M(\mathrm{j}\omega)T_0(\mathrm{j}\omega)\|_\infty < 1 \text{ and } \|W_P(\mathrm{j}\omega)S(\mathrm{j}\omega)\|_\infty < 1 \tag{2.118}$$

The combination of the two conditions in (2.118) gives

$$\big\|\,|W_M(\mathrm{j}\omega)T_0(\mathrm{j}\omega)| + |W_P(\mathrm{j}\omega)S_0(\mathrm{j}\omega)|\,\big\|_\infty < 1 \tag{2.119}$$

The following sketch of proof of (2.119), which can be found e.g. in [35], can provide direction for derivation of robust performance condition when other feedback loops are used, see Subchapter 7.6 again.

Assume

$$\|W_P(\mathrm{j}\omega)S(\mathrm{j}\omega)\|_\infty < 1 \tag{2.120}$$

hence

$$
\begin{aligned}
&|W_P(\mathrm{j}\omega)S(\mathrm{j}\omega)|<1,\forall\omega \\
&\Leftrightarrow \left|\frac{W_P(\mathrm{j}\omega)}{1+L_0(\mathrm{j}\omega)+\Delta(\mathrm{j}\omega)W_M(\mathrm{j}\omega)L_0(\mathrm{j}\omega)}\right|<1,\forall\omega \\
&\Leftrightarrow \left|\frac{W_P(\mathrm{j}\omega)S_0(\mathrm{j}\omega)}{1+\Delta(\mathrm{j}\omega)W_M(\mathrm{j}\omega)T_0(\mathrm{j}\omega)}\right|<1,\forall\omega
\end{aligned}
\tag{2.121}
$$

Since $|1+\Delta(\mathrm{j}\omega)W_M(\mathrm{j}\omega)T_0(\mathrm{j}\omega)|\geq 1-|W_M(\mathrm{j}\omega)T_0(\mathrm{j}\omega)|$, the worst case is

$$
\max|W_P(\mathrm{j}\omega)S(\mathrm{j}\omega)|=\frac{|W_P(\mathrm{j}\omega)S_0(\mathrm{j}\omega)|}{1-|W_M(\mathrm{j}\omega)T_0(\mathrm{j}\omega)|},\forall\omega \tag{2.122}
$$

Therefore, from (2.120), the robust performance condition (2.119) holds.

The graphical interpretation of (2.119) is depicted in Fig. 2.6, see [33].

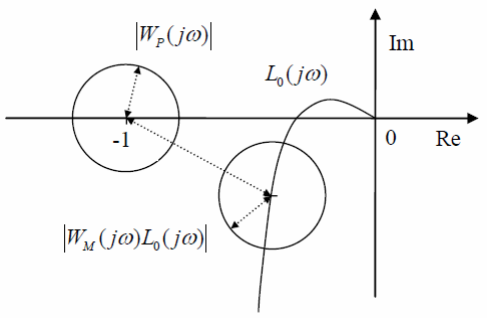

Fig. 2.6 The graphical interpretation of robust performance

A compromise condition, between nominal and robust performance, is

$$
\left\|\sqrt{|W_P(\mathrm{j}\omega)S_0(\mathrm{j}\omega)|^2+|W_M(\mathrm{j}\omega)T_0(\mathrm{j}\omega)|^2}\right\|_\infty<1 \tag{2.123}
$$

since it holds that

$$
\begin{aligned}
&\max\left(|W_P(\mathrm{j}\omega)S_0(\mathrm{j}\omega)|,|W_M(\mathrm{j}\omega)T_0(\mathrm{j}\omega)|\right)\leq\sqrt{|W_P(\mathrm{j}\omega)S_0(\mathrm{j}\omega)|^2+|W_M(\mathrm{j}\omega)T_0(\mathrm{j}\omega)|^2} \\
&\leq|W_P(\mathrm{j}\omega)S_0(\mathrm{j}\omega)|+|W_M(\mathrm{j}\omega)T_0(\mathrm{j}\omega)|
\end{aligned}
\tag{2.124}
$$

2.8 Fundamentals of relay autotuning

By autotuning (i.e. automatic tuning), a set of methods which enable the controller to be tuned automatically on demand from an operator or an external signal is meant [2], [53]. Industrial experience has clearly indicated that this is highly desirable and useful feature. The whole procedure usually consists of two basic steps: Process model parameters identification followed by controller tuning; however, some approaches do not require explicit model identification.

The beginning of autotuning is linked up with the very famous work of Ziegler and Nichols [193] where, besides the PID controller tuning rule, an interesting identification procedure based on the information on the *critical gain* and the *critical frequency* was introduced. This is often referred to as the trial-and-error procedure. Historically, other methodologies were investigated as well, for example, the Cohen-Coon method [20], which requires an open-loop test on the process and it is thus inconvenient to apply. The disadvantage of other methods is e.g. the need of large setpoint change, see details in [53]. A set of methods called *selftuning* [8], which performs at-once or continual plant identification and adaptively reset controller parameters, usually requires a priori information about the time scale of the process dynamics to be provided (due to a sampling period) and is time and computer-memory consumptive.

2.8.1 Relay feedback test

The relay feedback autotuning (identification) test performing limit cycle oscillations, which does not have shortcomings mentioned above, was successfully applied to the autotuning of PID controllers in [2] and it is widely used and in practice as a well applicable technique. It is robust, easy to implement, timesaving, easy to use and close-loop control which keeps the process close to the setpoint. The classical relay-feedback loop scheme with a symmetrical relay is depicted in Fig. 2.7.

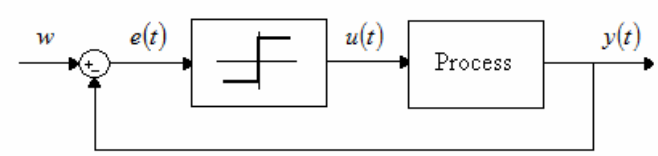

Fig. 2.7 Relay-feedback test scheme

If the process is stabilizable and has a phase lag of at least π radians, the process input $u(t)$ and output $y(t)$ are logged until the system reaches stationary oscillations, the amplitude A of error $e(t)$ equals the amplitude of $y(t)$ and the phase shift between $e(t)$ and $y(t)$ is $-\pi$. Hence, the *ultimate period* T_u is obtained from oscillations, which gives the information about the critical point, together with the *ultimate gain* which is approximately given by

$$k_u = \frac{4B}{\pi A} \tag{2.125}$$

where B is the relay amplitude. The *ultimate* (critical) *frequency* is close to the value of $\omega_u = 2\pi / T_u$. Formula (2.125) comes from linearization of the relay output via the Fourier series approximation when upper harmonic components of the signal are neglected, since a relay is a non-linear element and it can be linearized for linear theory approaches, details can be viewed e.g. in [191].

However, the original relay feedback test - sometimes called ATV (Autotune Variation), see [76], [191] – has two basic drawbacks. First, due to an approximation, the estimation of the critical point is not accurate enough for some processes, such as those with large time delays [179]. For example, there is an error of 23% for a first order unstable system with input-output delay. Second, the basic test enables to estimate only single point of the frequency characteristics. Hence, there have been investigated and developed many advanced techniques, which should eliminate the two mentioned deficiencies. Much research has been undertaken in identifying multiple points on the process frequency response, for instance, inserting of an integral or a delay element into the open loop [148], [163], see Subchapter 2.8.4, an analytic expression of some quantities

in input and output signals [79], [177], a utilization of a damping element [178] or a decomposition into transient and stationary cycle parts [179] followed by the discrete Fourier transform (DFT) - or the discrete-time Fourier transform (DTFT), more precisely - or the fast Fourier transform (FFT), see Subchapter 2.8.5, or the use of a parasitic relay [53] or a saturation relay [149], [191], see details in Subchapter 2.8.3, etc.

2.8.2 Model parameters identification

As mentioned above, the relay feedback experiment can be utilized for model parameters identification. An asymmetric (biased) relay, after removing stationary components, enables to estimate the static gain of the system according to

$$k = \frac{\int_{t}^{t+T_u} y(\theta)d\theta}{\int_{t}^{t+T_u} u(\theta)d\theta}, \; T_u = \frac{2\pi}{\omega_u} \tag{2.126}$$

see [76], [171]. The static characteristic of a biased relay is displayed in

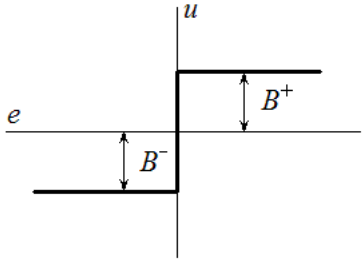

Fig. *2.8*, where $B^+ \neq B^-$.

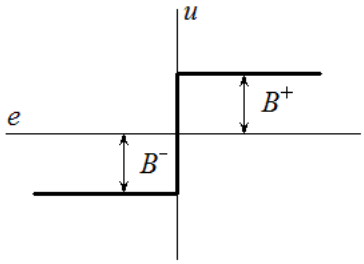

Fig. 2.8 Asymmetric (biased) relay static characteristics

Nevertheless, this estimation of k can be inaccurate, due to e.g. model nonlinearities or a shift of the operation point.

A relay with hysteresis of value ε, the static characteristics of which is displayed in Fig. 2.9, is another type of an on-off relay which is suitable for noise elimination while autotuning experiment; however, it causes a phase shift, thus the estimation of ω_u is not accurate – the found point lies at a frequency smaller then the ultimate one.

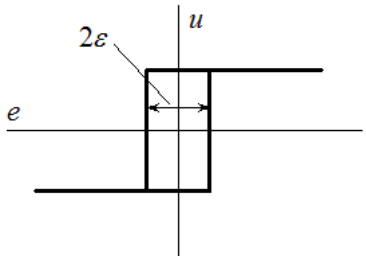

Fig. 2.9 Relay with hysteresis static characteristics

Dominant input-output delay, say τ, [191], can be estimated as a lag between the change of $u(t)$ and the maximum (minimum) value of $y(t)$ within the period, which is clear from Fig. 2.10. Good results are given using a relay with hysteresis here.

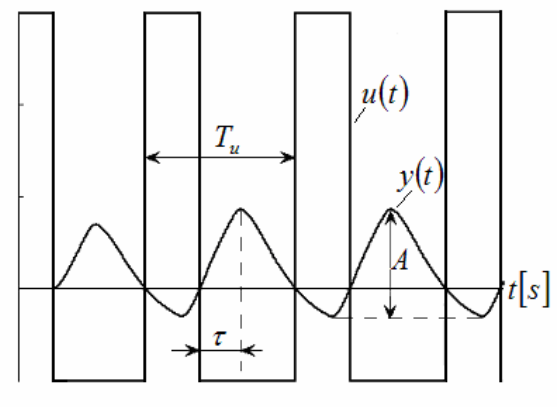

Fig. 2.10 Dominant input-output time delay estimation

Let $G(s)$ be the controlled system transfer function and $R(A)$ the describing (linearized) function of a relay (or a nonlinear element, in general), then for sustained oscillation holds $R(A)G(\mathrm{j}\omega_u) = -1 + 0\,\mathrm{j}$, or equivalently

$$\left|R(A)G(\mathrm{j}\omega_u)\right| = 1, \arg\left[R(A)G(\mathrm{j}\omega_u)\right] = -\pi \tag{2.127}$$

which describes one point at the open-loop Nyquist plot giving rise to the estimation of two plant model parameters by the solution of it. As mentioned above, an estimation of two or more points requires using a special technique.

In [117], [173], the relay-feedback experiment was used to identification of a stable time-delay model of the first order with one input-output and one internal delay, where an additional (artificial) delay was utilized. Moreover, an approach based on a time-domain description instead of frequency one leading to the solution of nonlinear algebraic equations was introduced in [117]. Due to, generally, an ill-conditioned set of equations and multimodality of its solution, it would be useful to solve the equations by some advanced methods, such as the SOMA [192] or the Nelder-Mead (NM) method [105], see Subchapters 5.3 and 5.4.

2.8.3 Saturation relay

Model parameters estimation can be improved by a saturation relay [149], [191], the static characteristics of which is depicted in Fig. 2.11.

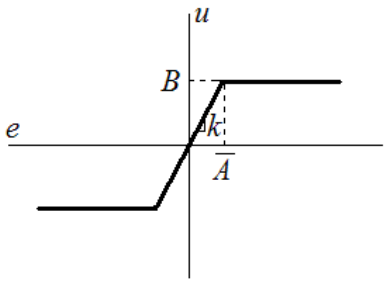

Fig. 2.11 Saturation relay static characteristics

Its advantage lies in the feature that relay output is not stepwise (i.e. with an abrupt slope change at the zero point), but it provides a smooth transient around the zero point. The relay input signal $e(t)$ is multiplied by k up to the limit value B of $u(t)$, hence $u(t)$ is (ideally) in the form of a harmonic (sine) waves with an upper and lower limit. The output of the nonlinear element $u(t)$ looks like a truncated sinusoidal wave, see Fig. 2.12. The

height of the relay output response is limited by $B = k\overline{A}$; the meaning of $\overline{A}$ is clear from the figure.

Obviously, the ideal case is that when $u(t)$ has the shape of $e(t)$ while $\overline{A} = A$, where A is the amplitude of $e(t)$. In this case, the ultimate gain equals the value of k exactly. Another limit case arrives when $k \to \infty$ which agrees with the standard on-off relay.

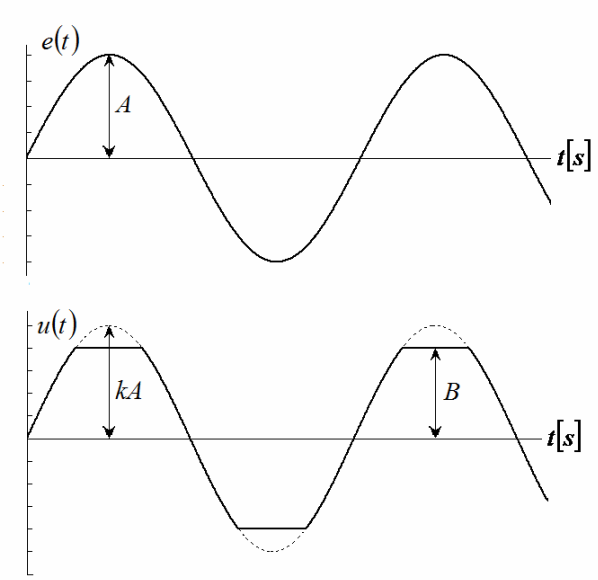

Fig. 2.12 Relay input and output signals for saturation relay

The describing function of the relay can be obtained from the Fourier series expansion of $u(t)$ and $e(t)$ as follows

$$R(A) = k_u = \frac{2B}{\pi\overline{A}}\left(\arcsin\left(\frac{\overline{A}}{A}\right) + \frac{\overline{A}}{A}\sqrt{1-\left(\frac{\overline{A}}{A}\right)^2}\right) \tag{2.128}$$

Hence, the aim is to find k (or $\overline{A}$) such that $\overline{A} = A$ which provides the exact critical gain estimation. On the other hand, there is also a potential problem that can make the test fail. If the slope of the static characteristics k is too small, or equivalently, if $\overline{A} > A$, a limit cycle may not exist. To avoid this, there has been proposed a two-step

procedure finding a rough estimate of the lower bound on k, say $k_{\min}$, followed by a saturation relay test [149], [191]:

1) Select the height of the relay B (manipulated input).

2) Use an ideal relay (set the slope to a large value) to estimate k_u according to (2.125). Set $k_{\min} = k_u$.

3) Calculate the slope of the saturation relay $k = 1.4k_{\min}$.

4) Use the saturation relay with calculated k.

5) Find ω_u from the relay feedback test and compute the ultimate gain from (2.128).

2.8.4 Artificial delay for identification of more parameters

As mentioned above, the standard relay feedback test enables to identify only one point at the Nyquist curve, i.e. two unknown parameters of the model, and the estimation of other model parameters requires a special technique.

One of the possibilities is to use the ATV$^+$ (Autotune Variation Plus) [72], [84], [148]. The first step of the ATV$^+$ procedure is a standard relay test. The second step introduces an artificial delay τ^+ between the relay and the process.

The overall phase shift is $-\pi$, however only a part of this is attributed to the process, as τ^+ is characterized by the phase leg $\phi_D = \tilde{\omega}_u \tau^+$ where $\tilde{\omega}_u$ is a new ultimate frequency. The new amplitude $\tilde{A}$ of the output can be read as well. Every next setting of τ^+ determines one point of the Nyquist curve, hence, one needs to set the number $\lceil n/2 - 1 \rceil$ of various values of τ^+ where n is the number of unknown model parameters.

In [72] the following setting was suggested

$$\tau^+ = \frac{5\pi}{12\omega_u} \tag{2.129}$$

where ω_u means the ultimate frequency with no artificial delay.

2.8.5 Use of relay transient

In [54], there was proposed a technique that could obtain multiple points on the process frequency response in a step test by removing stationary components followed by applying the DFT, DTFT, or FFT to the remaining signals there. The procedure was improved in [178] where a method that can identify multiple points simultaneously under one relay test was proposed, the description of which follows.

Using a standard relay test, $u(t)$ and $y(t)$ are recorded from the initial time until the system reaches a stationary oscillation and they are subjected to exponential decaying as

$$\begin{aligned} \bar{u}(t) &= u(t)\exp(-at) \\ \bar{y}(t) &= y(t)\exp(-at) \end{aligned} \tag{2.130}$$

Obviously, $\bar{u}(t)$ and $\bar{y}(t)$ will decay to zero for $a > 0$ and $t \to \infty$.

The Fourier transform applied to (2.130) results in

$$\begin{aligned} \bar{U}(\mathrm{j}\omega) &= \int_0^\infty \bar{u}(t)\exp(-\mathrm{j}\omega t)\mathrm{d}t = \int_0^\infty u(t)\exp(-at)\exp(-\mathrm{j}\omega t)\mathrm{d}t = U(\mathrm{j}\omega + a) \\ \bar{Y}(\mathrm{j}\omega) &= \int_0^\infty \bar{y}(t)\exp(-\mathrm{j}\omega t)\mathrm{d}t = \int_0^\infty y(t)\exp(-at)\exp(-\mathrm{j}\omega t)\mathrm{d}t = Y(\mathrm{j}\omega + a) \end{aligned} \tag{2.131}$$

Hence

$$G(\mathrm{j}\omega + a) = \frac{\bar{Y}(\mathrm{j}\omega)}{\bar{U}(\mathrm{j}\omega)} = \frac{Y(\mathrm{j}\omega + a)}{U(\mathrm{j}\omega + a)} \tag{2.132}$$

$\bar{U}(\mathrm{j}\omega)$ and $\bar{Y}(\mathrm{j}\omega)$ can be computed at discrete frequencies with DTFT as

$$\begin{aligned} \bar{U}(\mathrm{j}\omega) &= \mathrm{DTFT}(\bar{u}(t)) = T\sum_{k=0}^{N-1} \bar{u}(kT)\exp(-\mathrm{j}\omega_l kT),\ l = 1,2,...,m \\ \bar{Y}(\mathrm{j}\omega) &= \mathrm{DTFT}(\bar{y}(t)) = T\sum_{k=0}^{N-1} \bar{y}(kT)\exp(-\mathrm{j}\omega_l kT),\ l = 1,2,...,m \end{aligned} \tag{2.133}$$

where T is the sampling interval, N means the number of samples and $t_f = (N-1)T$ expresses the final time when the value of $\bar{u}(t)$ (or $\bar{y}(t)$) is sufficiently small.

Usually, $m = N/2$ and $\omega_l = 2\pi l/(NT)$, see e.g. (Wang *et al.*, 1999a). If, moreover, $N = 2^n, n \in \mathbb{N}$, then the standard FFT can be used for faster computing.

The method can identify accurate frequency response points as many as desired with one relay experiment.

2.9 Controller discretization

A sampled-data approximation of TDS is needed e.g. in computation of the system spectrum when the infinite spectrum is transformed into a finite one, the order of which depends on the sampling period and a discretization method, or for a computer realization of anisochronic controllers. The latter case is the primarily motivation for the following brief framework overview of basic ideas of discretization of TDS, both in a state and an input-output space, since the author intended to use the discrete-time algorithms for a laboratory experiment.

A number of methods is based on a state-space description, see e.g. (2.1). Moreover, almost all of them consider retarded systems with or without distributed delays, hence, these systems are assumed below. The differences for neutral systems are briefly mentioned throughout the following subchapter. Although equation (2.1) describes a controlled plant, the approaches can be treated analogously for controllers.

2.9.1 State space methods

Prior to a discretization itself, an interpolation of point delays and an approximation of distributed delays ought to be introduced. Since a value of delay $0 \le \eta_i \le L$ in (2.1) is not an integer multiple of a sampling period T_s, delayed quantities $x(t-\eta_i)$ and $u(t-\eta_i)$ must be interpolated by these quantities yet with delays $\tau_k = kT_s, k = 0,1,...H$, where $H = \lceil L/T_s \rceil$ and L is the highest delay value of the system. Linear interpolation is the simplest and for practical purposes sufficient interpolation method given by

$$x(t-\eta_i) \approx (1-\alpha_i)x(t-\tau_{d,i}) + \alpha_i x(t-\tau_{d+1,i}) \tag{2.134}$$

where $d_i = \lfloor \eta_i / T_s \rfloor, \tau_{d,i} = d_i T_s$, $\tau_{d+1,i} = (d_i + 1)T_s$, $\tau_{d,i} \le \eta_i \le \tau_{d+1,i}$ and a weighting coefficient $\alpha_i = (\eta_i - \tau_{d,i})/T_s \in [0,1]$

A rather neglected task is the comprisal of distributed delays (i.e. convolution integrals) in the model and their subsequent approximation by lumped delays followed by the use of formula (2.134). One possibility is to use the idea [143] mentioned in Subchapter 2.1.1. Alternatively, in [165] the following approximation was proposed

$$\int_0^L g(t)h(t-\tau)\mathrm{d}\tau \approx \frac{L}{N}\sum_{i=1}^{N}\beta_i g\left(i\frac{L}{N}\right)h\left(t-i\frac{L}{N}\right) \tag{2.135}$$

where $\sum_{i=1}^{N}\beta_i = N/L$. For instance, the well known Simpson's numerical integration method agrees with $\beta_1 = N/(12L)$, $\beta_2 = N/(3L)$, $\beta_3 = N/(6L)$, $\beta_4 = N/(3L)$, $\beta_5 = N/(12L)$. Note that even some very good convolution integral approximation can lead to an unstable control action in case of a delayed feedback, see [165].

Now look at the discretization itself. Let

$$\left[x(t-\tau_{d,i})\right]_{t=kT_s} = x_{k-d\,i} \tag{2.136}$$

and likewise for $u(t-\tau_{d,i})$ analogously. Then the right-hand side of a retarded system (2.1) can be written in a discrete form

$$\mathbf{f}_k = \sum_{l=0}^{H_A+1}\hat{\mathbf{A}}_l\mathbf{x}_{k-l} + \sum_{l=0}^{H_B+1}\hat{\mathbf{B}}_l\mathbf{u}_{k-l} \tag{2.137}$$

where H_A, H_B are maxima of corresponding integers d_i according to (2.136), $H = \max(H_A, H_B)$ and it holds that $\hat{\mathbf{A}}_l$ and $\hat{\mathbf{B}}_l$ are linear combinations of $\mathbf{A}_i$ and $\mathbf{B}_i$, respectively.

For a simple discrete approximation of TDS, it is sufficient to use a numeric method for the solution of

$$\left[\frac{\mathrm{d}\mathbf{x}(t)}{\mathrm{d}t}\right]_{t=kT_s} = \mathbf{f}_k \tag{2.138}$$

in the following form [171], [175]

$$\mathbf{x}_{k+1} = \mathbf{x}_k + T_s \Phi(\mathbf{f}_k) \tag{2.139}$$

where functional $\Phi(\mathbf{f}_k)$ is determined by the solution method, for instance, (the implicit) Trapezoidal method reads $\Phi(\mathbf{f}_k) = 0.5\mathbf{f}_{k+1} + 0.5\mathbf{f}_k$, the Euler implicit method agrees with $\Phi(\mathbf{f}_k) = \mathbf{f}_{k+1}$, it is also possible to consider higher order Runge-Kutta (R-K) methods etc. Generally, implicit numerical methods provide better approximation than the explicit ones. Thanks to the TDS model linearity, $\Phi(\mathbf{f}_k)$ is a linear combination of $\mathbf{f}_{k-m}, m = -1,0,1,2...$

A suitable value of the sampling period T_s is questionable. It is necessary to take account of process (or controller) and external inputs dynamics. The smaller T_s yields the better approximation and stability of the numerical method, yet there is higher round-off error and computational requirements. The problem has been discussed e.g. in [39].

Although the aim of this subchapter is to provide an easy-handling discretization, instead of the best one, the author has to mentione some more sophisticated discrete approximations based on discretization of the solution operator or that of the infinitesimal generator, see Subchapter 2.1.3., which serve mainly for spectrum estimation.

Consider an autonomous TDS only since the input part of the model can be governed simply as in (2.137). For discrete approximation of the solution operator, it is necessary consider the whole system state $\boldsymbol{x}_t \in X$ defined in (2.10) instead of $\mathbf{x}(t)$, or its discrete form, more precisely

$$\boldsymbol{x}_t \to \mathbf{x}_k = \left[\mathbf{x}_k, \mathbf{x}_{k-1}, \ldots, \mathbf{x}_{k-H_A+1}, \mathbf{x}_{k-H_A}\right]^T \tag{2.140}$$

determining the system state at the step *k* as

$$\boldsymbol{x}_{k+1} = \boldsymbol{\Phi}\boldsymbol{x}_k \tag{2.141}$$

where $\boldsymbol{\Phi} \in \mathbb{R}^{(H_A+1)n \times (H_A+1)n}$ is the discrete approximation of the solution operator $\mathcal{T}(t)$. Formula (2.141) is the discrete form of

$$\boldsymbol{x}_{t+T_s} = \mathcal{T}(T_s)\boldsymbol{x}_t \tag{2.142}$$

The first row of the matrix $\boldsymbol{\Phi}$ is determined by (2.139) and the others usually have a simple form such that corresponding elements of vectors $\boldsymbol{x}_{k+1}$ and $\boldsymbol{x}_k$ equals. Particular forms of $\boldsymbol{\Phi}$ for the Euler explicit, Euler implicit and Trapezoidal methods can be found e.g. in [171]. The application of the R-K methods has been introduced in [12] without the distributed delay term and in [13] with this term. The distributed delay case by using Linear Multistep (LMS) methods was proposed e.g. in [77]. A revision of LMS methods and their comparison with R-K schemes was introduced in [10]. All these methods are called *pseudospectral*.

An alternative – so-called *spectral* – approach, introducing the generalized Fourier projection represented by the Hilbert product space $\tilde{X} = \mathbb{C}^n \times L_2([-L,0), \mathbb{C}^n)$, instead of the classic interpolation in the Banach space (2.11), was proposed in [11]. More precisely, the initial function is $\mathbf{x}(0) = \mathbf{p}$, $\mathbf{x}(t) = \boldsymbol{\xi}(t), t \in [-L,0)$, $(\mathbf{p}, \boldsymbol{\xi}) \in \tilde{X}$, rather then $\mathbf{x}(t) = \boldsymbol{\xi}(t), t \in [-L,0], \boldsymbol{\xi}(t) \in X$. Then the solution operator and infinitesimal generator are defined in the realm of $\tilde{X}$, differently from (2.12) and (2.13), see details in [11].

Another family of discretization approaches (used mainly for the spectrum estimation) consists in those based on the infinitesimal generator of the semigroup. The discrete form of (2.15) acquires the form

$$\frac{\mathrm{d}\boldsymbol{x}_t}{\mathrm{d}t} = \mathcal{A}\,\boldsymbol{x}_{T_s},\ t > 0$$

$$\boldsymbol{x}_0 = [\boldsymbol{\xi}(0), \boldsymbol{\xi}(-T_s), \ldots, \boldsymbol{\xi}(-(H_A - 1)T_s), \boldsymbol{\xi}(-H_A T_s)]^T \tag{2.143}$$

The Euler explicit approximation scheme together with the Trapezoidal rule and the quadratic approximation of the derivative can be found e.g. in [171]. Similar approaches were introduced in [5]. A R-K method was presented in [12], a comparison of that with LMS ones e.g. in [13]. A pseudospectral approach utilizing Lagrange interpolating polynomial and its derivative for backward differentiation was proposed in

[14]. The differentiation methods in the Hilbert space mentioned above together with convergence results were introduced in [15].

Notice that all the above mentioned methods consider retarded systems (with or without distributed delays) only. In the author's of this thesis opinion, the extension of the methods above to neutral TDS requires either to introduce a discrete state vector $\boldsymbol{x}_t \to \mathbf{x}_k = \left[\mathbf{x}_k, \mathbf{x}_{k-1}, \ldots, \mathbf{x}_{k-H_A+1}, \mathbf{x}_{k-H_A}, \ldots, \mathbf{x}_{k-H_A-H_N}\right]^T$ instead of (2.140), where H_N is the maximum delay in neutral terms, or to take (2.139) and (2.143) in a recursive form.

A rather different approach was presented in [56]. Briefly, the idea is based on the Taylor series expansion of $\mathbf{x}(t)$ in the vicinity of the operation point

$$\mathbf{x}(t+\Delta) = \mathbf{x}(t) + \Delta\frac{\mathrm{d}\mathbf{x}(t)}{\mathrm{d}t} + \frac{\Delta^2}{2!}\frac{\mathrm{d}^2\mathbf{x}(t)}{\mathrm{d}t^2} + \ldots \tag{2.144}$$

where Δ is a discretization step (e.g. the sampling period) and derivatives of state and input variables are calculated as derivations of (2.1), hence, for instance

$$\begin{aligned}\frac{\mathrm{d}^2\mathbf{x}(t)}{\mathrm{d}t^2} = \mathbf{A}_0\frac{\mathrm{d}\mathbf{x}(t)}{\mathrm{d}t} + \sum_{i=1}^{N_A}\mathbf{A}_i\frac{\mathbf{x}(t-\eta_i)}{\mathrm{d}t} + \mathbf{B}_0\frac{\mathrm{d}\mathbf{u}(t)}{\mathrm{d}t} + \sum_{i=1}^{N_B}\mathbf{B}_i\frac{\mathrm{d}\mathbf{u}(t-\eta_i)}{\mathrm{d}t} \\ + \int_0^L \mathbf{A}(\tau)\frac{\mathrm{d}\mathbf{x}(t-\tau)}{\mathrm{d}t}\mathrm{d}\tau + \int_0^L \mathbf{B}(\tau)\frac{\mathrm{d}\mathbf{u}(t-\tau)}{\mathrm{d}t}\mathrm{d}\tau\end{aligned} \tag{2.145}$$

By a backward substitution (2.1) into (2.145) and then the result into (2.144) and by the interpolation (2.134) and the approximation of distributed delays (2.135), the final form (2.139) is obtained (its autonomous part). Functional $\Phi(\mathbf{f}_k)$ is determined by the number of expansion elements in (2.144). The accuracy of the discretization increases with the number of elements; however, the more elements are taken the higher maximum delay value is. The use of the method to neutral TDS is questionable since it is not possible to obtain zero derivatives of state and input variables by recursion.

The delta transform, generally introduced in [98], was used for discretization and spectrum estimation, respectively, of neutral TDS e.g. in [171], [175], [204].

Let q be the shifting operator and δ the delta transform operator defined by

$$\delta = \frac{q-1}{T_s} = \frac{\exp(sT_s)-1}{T_s} \tag{2.146}$$

then

$$q = \exp(sT_s) = 1 + \delta T_s \tag{2.147}$$

The fundamental feature of the delta transform is that as $T_s \to 0$ the delta model of the system converges to its Laplace transform, i.e. $\gamma \to s$, where γ is the variable associated with operator δ; however, the discrete model does not. Then the model

$$\mathbf{X}(\delta) = I(\delta)\mathbf{F}(\delta) \tag{2.148}$$

instead of (2.139) can be considered - easily by substituting (2.148) into (2.139) - where $\mathbf{X}(\delta)$ is the δ-transform of $\mathbf{x}(t)$, $\mathbf{F}(\delta)$ stands for the transform of (2.137) and $I(\delta)$ means the discrete-time integrator, see [21], [204], satisfying

$$\lim_{T_s \to 0} I(\delta) = \frac{1}{\delta} \tag{2.149}$$

The delta transform of (2.141) and (2.142) reads

$$\delta \boldsymbol{X}(\delta) = \frac{\boldsymbol{\Phi} - \mathbf{I}}{T_s} \boldsymbol{X}(\delta) \tag{2.150}$$

where $\boldsymbol{X}(\delta)$ means transformed $\boldsymbol{x}_t$ and $\mathbf{I}$ is the unit matrix.

2.9.2 Input-output methods

In the literature, the task of the discretization of TDS in an input-output formulation is not as frequent as in the state-space case. However, let us mention here two possible ideas depending on the relative value of T_s with respect to the system dynamics and external signals.

In case of a short period, it is possible to use the δ-transform as a derivative estimation, as introduced in Subchapter 2.9.1. The idea rests on the introduction of variable γ associated with operator δ defined as

$$\gamma = \frac{z-1}{\alpha T_s z + (1-\alpha)T_s} \tag{2.151}$$

where z is the variable from the z-transform and $\alpha \in [0,1]$ represents a weighting parameter. The choice of α enables to obtain different first order models, such as forward ($\alpha = 0$), backward ($\alpha = 1$) or Tustin ($\alpha = 0.5$) one. The substitution $s \to \gamma$ in the transfer function system model results in a discrete-time model in z associated with the shifting operator *q*. However, this substitution is applied to *s*-powers expressing derivatives only, whereas delay exponential terms are subjected to a natural transformation

$$\exp(-\eta s) X(s) \hat{=} x(t-\eta) \tag{2.152}$$

followed by (linear) interpolation (2.134) and

$$z^{-k} X(z) \hat{=} x(t - kT_s) \tag{2.153}$$

The advantage of the input-output map approximation in applications is that there is not need to approximate distributed delays.

For a higher sampling period T_s, there is a possibility of a rational approximation in the general form

$$\exp(-s\tau) \approx \frac{p(-s\tau)}{p(s\tau)} \tag{2.154}$$

where e.g. the Padé approximation, Laguerre shift, Kautz shift, Fourier analysis-based method, etc., see [4], [80], [81], [114], [120], followed by the known equivalent z-transform formula

$$G_R(z) = (1 - z^{-1}) Z\left\{ L^{-1}\left\{ \frac{G_R(s)}{s} \right\} \right\} \tag{2.155}$$

Although (2.155) represents the *exact* discretization, controller transfer function $G_R(s)$ includes rational approximation, hence, there is an information loss problem about the dynamics.

It is suitable to filter the measured input signal due to sensors noise when controller realization, e.g. by using an averaging or the Butterworth filter of an appropriate order (with the maximally flat characteristics at low frequencies).

3 GOALS OF THE THESIS

The principal goal of this doctoral thesis is to utilize proposed algebraic control laws achieved through the general solutions of the Bézout identity in R_{MS} for systems with delays.

The work deals not only with theoretical aspects of the ring and algebraic controller design but also with the (quasi)finite spectrum assignment, (sub)optimal pole placement, TDS stability analysis, improved relay test identification for TDS and last but not least with problems of a practical application, represented by utilization of designed controllers on a circuit heating laboratory model.

Ergo, the main aims of the thesis can be summarized into the following points:

1. Description and classification of TDS, their stability issues, algebraic notions related to TDS and their control, general introduction of a relay feedback test and some tuning, robust analysis and discretization matters for these systems. Crucial parts are supported by an overview of the state of the art. This goal has been the issue of Chapter 2 of this thesis.
2. Analysis and description of linear time-invariant SISO TDS in R_{MS} ring and determination of the basic algebraic properties of this ring.
3. Formulation and development of algebraic approach to design of SISO continuous-time controllers in R_{MS} ring.
4. Derivation of stability conditions for a selected class of retarded quasipolynomials depending on a non-delay real parameter for the purpose of performing the coprime factorization and controller parameterization, and the derivation of the generalized Nyquist criterion for control system robust analysis.
5. Definition of a suboptimal and optimal pole placement for infinite-dimensional control systems and the implementation of advanced iterative algorithms for the solution of this task.

6. Design of a relay feedback experiment for identification of a simple TDS model of retarded type using advanced methods – the saturation relay, determination of more frequency characteristics points – in time and frequency domain.
7. Verification and implementation of proposed identification and control approaches in control of a laboratory circuit heating system followed by robust analysis of the solution and a simplification of final controllers.

4 ALGEBRAIC CONTROLLER DESIGN IN RMS

This, the most crucial, subsection of this thesis aims the novel definition of R_{MS} ring followed by all basic steps of algebraic controller design utilizing this ring. Some stability issues for selected retarded quasipolynomials are also discussed and the generalized Nyquist criterion for two feedback control system structures is simply derived.

4.1 R_{MS} ring

As mentioned in Subchapter 2.3.3, the original definition of the ring, [199], has some drawbacks. Therefore, it is necessary to revise the definition and propose a new, alternative, definition of the ring eliminating the above mentioned deficiencies.

4.1.1 Revision of the ring

First, the following simple example shows that the original definition does not constitute a ring

Example 4.1

Consider two elements of R_{MS}

$$T_1(s)=\frac{s}{s+2}, T_2(s)=\frac{(s+1)\exp(-s)}{s+2} \tag{4.1}$$

Yet, a sum of them

$$T(s)=T_1(s)+T_2(s)=\frac{s(1+\exp(-s))+\exp(-s)}{s+2}\notin R_{MS} \tag{4.2}$$

since the numerator is a neutral (even formally unstable) quasipolynomial, which is inconsistent with the original ring definition. ■

The above introduced example indicates that it is necessary to include neutral terms in the definition.

The second drawback comes from the requirement of stable denominator. The transfer function of a stable system with distributed delays has common numerator and

denominator root from the right half-plane; however, there is no reason to consider it as unstable in any sense, see Example 2.1. Rephrased, an element of the ring should include a removable singularity in $\mathbb{C}^+$ (but not poles). Analogously, spectral stabilizability can be viewed in the similar manner, see Example 2.3.

From these two examples, $H_\infty(\mathbb{C}^+)$ seems to be a suitable candidate for the ring definition (as for R_{PS} ring, see Subchapter 2.3.2). However, there are some troubles with neutral systems, as discussed in 2.4.1 (Example 2.4) and 2.4.2. Namely, although a formally unstable neutral TDS with a vertical strip of poles tending to the imaginary axis from left (for $\operatorname{Im} s_0 \to \infty$) can be BIBO (and hence $H_\infty(\mathbb{C}^+)$) stable, it does not permit the Bézout factorization, [75], [115]. Since formal stability is not given in input-output relation (transfer function), consider a rather more strict notion – strong stability – given by condition (2.25) instead. Formal stability is hence required; however, its testing by strong stability condition (2.25) could not be included in the ring definition since it may lead to strong instability during algebraic operations on ring elements.

The following short examples demonstrate and clarify the above ideas.

Example 4.2

Let be given three neutral delayed systems (plants) governed by transfer functions

$$G_1(s)=\frac{1}{s+s\exp(-s)+1}, G_2(s)=\frac{1}{(s+s\exp(-s)+1)(s+1)}, \\ G_3(s)=\frac{1}{(s+s\exp(-s)+1)(s+1)^4} \tag{4.3}$$

All the systems have poles located in $\mathbb{C}_0^-$, except for $\operatorname{Im} s_0 \to \infty$ where the asymptotic pole lies on the imaginary axis, see Fig. 4.1, where displayed poles (asterisks) are -0.4011, -0.0379 + 3.4264j, -0.0054 + 9.5293j, -0.0020 + 15.7713j, -0.0010 + 22.0365j, -0.0006 + 28.3096j, -0.0004 + 34.5864j, -0.0003 + 40.8652j, -0.0002 + 47.1451j.

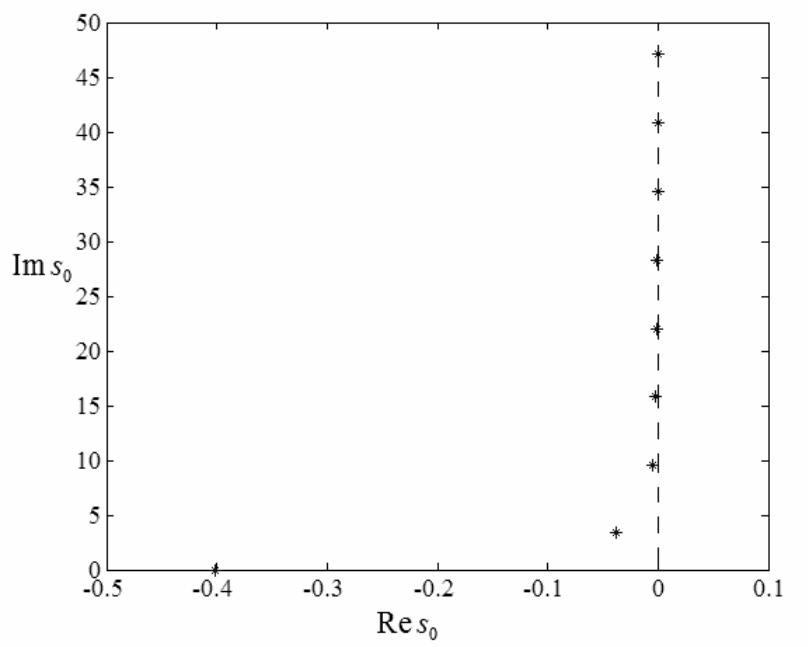

Fig. 4.1 Root loci of the rightmost poles of $G_1(s)$ from (4.3)

However, although there is no pole (except the asymptotic case) in $\mathbb{C}^+$, neutral systems (4.3) can not be considered as asymptotically stable since there is no positive α satisfying $\operatorname{Re} s_0 \le -\alpha$ for all s_0, see Subchapter 2.2.2. Moreover, these systems are neither strongly nor formally stable - use test (2.25) and any state-space realization followed by (2.23), or simply, the chain of poles reaches the imaginary axis. Nevertheless, other stability notions are more attractive. An easy test on $G_1(\mathrm{j}\omega)$, $G_2(\mathrm{j}\omega)$, $G_3(\mathrm{j}\omega)$ shows that $\|G_1\|_\infty = \infty$, $\|G_2\|_\infty = 2$, $\|G_3\|_\infty = 1$, hence $G_1 \notin H_\infty(\mathbb{C}^+)$, $G_2, G_3 \in H_\infty(\mathbb{C}^+)$. As proved in [115], G_1 and G_2 are not BIBO stable, yet G_3 is BIBO stable. This means that formal instability does not automatically implies H_∞ or BIBO instability which makes problems when decision about the inclusion of the system into an algebraic structure (or set). ■

Example 4.3

This example demonstrates the necessity of formal stability in the definition of R_{MS} ring, not only for elements of R_{MS} but also for their inversions.

Consider a coprime factorization in $H_\infty(\mathbb{C}^+)$ of system $G_2(s)$ from (4.3), i.e.

$$G(s)=\frac{\frac{1}{(s+2)^2}}{\frac{(s+s\exp(-s)+1)(s+1)}{(s+2)^2}}=\frac{B(s)}{A(s)} \tag{4.4}$$

More information about (Bézout) coprime factorization can be found in Subchapter 4.1.2. Notice that the factorization (4.4) is coprime yet not Bézout.

As stated above, the system $G(s)$ is formally unstable but from $H_\infty(\mathbb{C}^+)$, i.e. $B(s)/A(s)\in H_\infty(\mathbb{C}^+)$. However, one can verify that $1/A(s)\notin H_\infty(\mathbb{C}^+)$. This yields a mismatch in the ring definition since there is not an unambiguous answer whether $A(s)$ is invertible (a unit) or not. If both terms were not coprime, it would not pose a problem since such situations are natural also in R_{PS} ring. If $G(s)$ was formally stable, it would hold that $1/A(s)\in H_\infty(\mathbb{C}^+)$. As a conclusion, a set $H_\infty(\mathbb{C}^+)$ is not a sufficient candidate for R_{MS} ring. ■

Hence, there seem to be two possibilities for the ring definitions regarding formal stability. Either to include the requirement of formal stability of the quasipolynomial numerator in the ring definition and thus to exclude the existence of coprime factorization for formally unstable systems, or to take it into consideration in ring divisibility conditions (i.e. to admit a formally unstable numerator). Naturally, we decided to choose the latter option, since it is not possible to avoid a formal unstable numerator in ring elements as demonstrated in Example 4.1.

Example 4.4

The aim of this example is to show that strong stability could not be included in the ring definition; however, the necessity of formal stability has been already proved in Example 4.3.

Consider a formally and strongly stable element from $H_\infty(\mathbb{C}^+)$

$$T(s)=\frac{1}{(1+0.8\exp(-s))s+1} \tag{4.5}$$

Now make a multiplication

$$\begin{aligned} T_2(s)=T(s)T(s)&=\frac{1}{[(1+0.8\exp(-s))s+1]^2}\\ &=\frac{1}{(1+1.6\exp(-s)+0.64\exp(-2s))s^2+2(1+0.8\exp(-s))s+1} \end{aligned} \tag{4.6}$$

which is obviously strongly unstable, yet formally stable, since $T(s)$ and $T_2(s)$ have the same spectrum (except for poles multiplicity). Hence, this algebraic operation (multiplication) preserves formal yet not strong stability. Recall, however, that formal stability will be tested by verification of strong stability, so there is some kind of conservativeness. ■

The crucial part of this subchapter, the R_{MS} ring proposal, as a revisited and extended definition to the original one, follows.

Definition 4.1 (R_{MS} ring)

An element $T(s)$ of R_{MS} ring is represented by a ratio of two (quasi)polynomials $y(s)/x(s)$ where the denominator is a (quasi)polynomial of degree *n* and the numerator can be factorized as

$$y(s)=\tilde{y}(s)\exp(-\tau s) \tag{4.7}$$

where $\tilde{y}(s)$ is a (quasi)polynomial of degree *l* and $\tau \geq 0$. Note that the degree of a quasipolynomial means its highest *s*-power.

The element lies in the space $H_\infty(\mathbb{C}^+)$, i.e. it is analytic and bounded in $\mathbb{C}^+$, particularly, there is no pole s_0 such that $\mathrm{Re}\, s_0 \geq 0$ for a retarded denominator. Moreover, $T(s)$ is formally stable, i.e. there is no vertical strip of poles with $\mathrm{Re}\, s_0 \geq -\varepsilon, \varepsilon > 0$ for a neutral element. The strong stability condition (2.25) for (quasi)polynomial $x(s)$ is a

sufficient but not necessary condition guaranteeing that. If the term includes distributed delays, all roots of $x(s)$ in $\mathbb{C}^+$ are those of $y(s)$ (i.e. they are removable singularities).

In addition, the ratio is proper, i.e. $l \le n$. More generally, there exists a real number $R > 0$ for which holds that

$$\sup_{\mathrm{Re}\, s>0,\, |s|\ge R} |T(s)| < \infty \tag{4.8}$$

see [115]. ■

Notice that the properness condition (4.8) is not necessary in the definition since the H_∞ stability condition according to (2.27) implies (4.8).

4.1.2 Coprime factorization and the Bézout identity

A basic operation on the quasipolynomial transfer function of TDS is coprime factorization by which the transfer function is decomposed into a coprime (or relatively prime) pair of ring elements. Since the intention is to use coprime factors in the Bézout equation (2.68), the factorization should also be Bézout, i.e. there must exists a stabilizing solution of (2.68) satisfying (2.69).

When dealing with coprime factorization, the divisibility condition has to be stated.

Lemma 4.1 (Divisibility in R_{MS})

Any $A(s) \in R_{MS}$ divides $B(s) \in R_{MS}$ if and only if all unstable zeros (including $s \to \infty$) of $A(s)$ are those of $B(s)$, and moreover, the numerator of $A(s)$ is formally stable. ■

Note that zeros mean the roots of the whole term of the ring, not only those of the numerator.

Again, problems appear when dealing with neutral TDS or with those including distributed delays. An example of coprime, yet not Bézout, factorization of formally unstable neutral TDS was demonstrated in Example 2.4 and Example 4.3.

The following two examples demonstrate a typical coprime factorization over R_{MS} and a specific problem with distributed delays, respectively.

Example 4.5

The system is governed by the transfer function

$$G(s)=\frac{b(s)}{a(s)}=\frac{s+\exp(-s)}{s^2+(2+\exp(-s))s+1}\exp(-2s) \tag{4.9}$$

which is a stable retarded TDS. Coprime factorization of (4.9) over R_{MS} can be performed e.g. as follows

$$G(s)=\frac{\frac{b(s)}{m(s)}}{\frac{a(s)}{m(s)}}=\frac{\frac{(s+\exp(-s))\exp(-2s)}{m(s)}}{\frac{s^2+(2+\exp(-s))s+1}{m(s)}}=\frac{B(s)}{A(s)} \tag{4.10}$$

where $A(s)$, $B(s)\in R_{MS}$ and $m(s)$ is a stable (quasi)polynomial of degree 2. It is suitable to set $m(s)$ as a polynomial since it appears as a factor in the control feedback characteristic quasipolynomial, see Subchapters 4.2 - 4.4, 4.7. Its degree must equal 2, otherwise elements would not be proper or coprime. ■

Example 4.6

Consider a simple system with distributed delays with transfer function (2.16) and suggest a factorization

$$G(s)=\frac{1-\exp(1)\exp(-s)}{s-1}=\frac{\frac{1-\exp(1)\exp(-s)}{m(s)}}{\frac{s-1}{m(s)}}=\frac{B(s)}{A(s)} \tag{4.11}$$

In this case, the common denominator (quasi)polynomial $m(s)$ could not be stable since it would lead to non-coprime elements in R_{MS}. Indeed, let, for instance, $m(s)=s+1$, then there exists a term $T(s)\in R_{MS}$ that is a non-zero non-invertible common divisor of both $A(s), B(s)$ (which are then reducible), e.g.

$$A(s)=T(s)A_0(s)=\frac{s-1}{s+1}\frac{s+1}{s+1},\ B(s)=T(s)B_0(s)=\frac{s-1}{s+1}\frac{1-\exp(1)\exp(-s)}{s-1} \qquad (4.12)$$

The solution of this problem is read as follows: The common denominator $m(s)$ must include all common zeros s_0 of $a(s),b(s)$ with $\mathrm{Re}\, s_0 \geq 0$ (even asymptotic ones tending to the imaginary axis). Thus, the coprime factorization (4.11) should read

$$G(s)=\frac{1-\exp(1)\exp(-s)}{s-1}=\frac{\dfrac{1-\exp(1)\exp(-s)}{s-1}}{\dfrac{s-1}{s-1}}=\frac{B(s)}{A(s)} \qquad (4.13)$$

■

The notion of coprime factorization is closely related to the existence of a solution of the Bézout identity. As stated e.g. in Example 2.4, for formally unstable TDS such solution in $H_\infty(\mathbb{C}^+)$ (an thus not in R_{MS}) does not exist – we can obtain coprime yet not Bézout coprime factors.

If a pair $A(s),B(s)\in R_{MS}$ is Bézout coprime, it is possible to solve the Bézout identity (or to find the GCD) using the extended Euclidean algorithm, see Subchapter 2.3.1. Prior to the implementation of the extended Euclidean algorithm to R_{MS} ring, an ordering of ring elements has to be defined, so that a poset is obtained. Thus, define $P=(R_{MS},\preceq)$ as

a) $A(s)\underline{\prec} B(s)$ if and only if $A(s)\,|\,B(s)$.

b) $A(s)\equiv B(s)$ if and only if $A(s)\,|\,B(s)$ and $B(s)\,|\,A(s)$, or equivalently, $A(s)$ is associated with $B(s)$.

c) $A(s)$ is not related to $B(s)$ if and only if $A(s)\nmid B(s)$ and $B(s)\nmid A(s)$.

The procedure of finding the $\mathrm{GCD}(A(s),B(s))$ can be characterized as follows. Assume these three situations:

a) If $A(s)\equiv B(s)$, the GCD of both is simply either $A(s)$ or $B(s)$.

b) If $A(s) \succeq B(s)$, keep the following scheme

$$\left[\begin{array}{cc|c} 1 & 0 & A(s) \\ 0 & 1 & B(s) \end{array}\right] \sim \left[\begin{array}{cc|c} 1 & -\dfrac{A(s)}{B(s)} & 0 \\ 0 & 1 & B(s) \end{array}\right] \tag{4.14}$$

hence, $B(s)$ is the GCD of $A(s)$ and $B(s)$, according to (2.46). If $B(s) \succeq A(s)$, the procedure is analogous with $\mathrm{GCD}(A(s), B(s)) = A(s)$.

c) Let $A(s)$ and $B(s)$ be not related to each other. In this case, follow this scheme

$$\begin{aligned} &\left[\begin{array}{cc|c} 1 & 0 & A(s) \\ 0 & 1 & B(s) \end{array}\right] \sim \left[\begin{array}{cc|c} X(s) & 0 & A(s)X(s) \\ 0 & 1 & B(s) \end{array}\right] \\ &\sim \left[\begin{array}{cc|c} X(s) & Y(s) & A(s)X(s)+B(s)Y(s) \\ 0 & 1 & B(s) \end{array}\right] \sim \left[\begin{array}{cc|c} 0 & 1 & B(s) \\ X(s) & Y(s) & A(s)X(s)+B(s)Y(s) \end{array}\right] \\ &\sim \left[\begin{array}{cc|c} \dfrac{-B(s)X(s)}{A(s)X(s)+B(s)Y(s)} & \dfrac{A(s)X(s)}{A(s)X(s)+B(s)Y(s)} & 0 \\ X(s) & Y(s) & A(s)X(s)+B(s)Y(s) \end{array}\right] \end{aligned} \tag{4.15}$$

Here, the GCD of $A(s)$ and $B(s)$ equals $A(s)X(s)+B(s)Y(s)$. In scheme (4.15), it is supposed that there can be found quotients $X(s), Y(s)$ such that the element $A(s)X(s)+B(s)Y(s)$ divides $A(s), B(s)$. Since $A(s), B(s)$ are Bézout coprime, $A(s)X(s)+B(s)Y(s)$ must be a unit of the ring.

In other words, the objective is to find structures of $X(s), Y(s)$ and to set zeros and poles of $A(s)X(s)+B(s)Y(s)$ such that divisibility conditions as in Lemma 4.1 are satisfied or the element is invertible. This task can be troublesome; however, if formally unstable neutral TDS were avoided being included, every numerator/denominator quasipolynomial would have only a finite number of unstable zeros, which would make possible to find the $\mathrm{GCD}(A(s), B(s))$.

If the task is to solve the Bézout identity (2.68) itself instead of the $\mathrm{GCD}(A(s), B(s))$, one can use scheme (2.49) where $c = 1$. This yields these results, respectively

a) $P(s)=\frac{1}{A(s)}$, $Q(s)=0$ and/or $P(s)=0$, $Q(s)=\frac{1}{B(s)}$ (4.16)

b) $P(s)=\frac{1}{A(s)}$, $Q(s)=0$ or $P(s)=0$, $Q(s)=\frac{1}{B(s)}$ (4.17)

c) $P(s)=\frac{X(s)}{A(s)X(s)+B(s)Y(s)}$, $Q(s)=\frac{Y(s)}{A(s)X(s)+B(s)Y(s)}$ (4.18)

The following examples elucidate the whole procedure.

Example 4.7

Assume coprime factorization (4.13) and find $\mathrm{GCD}(A(s),B(s))$ first. Since $A(s)$ divides $B(s)$, it holds that $B(s)\succeq A(s)$, hence

$$\mathrm{GCD}(A(s),B(s))=A(s)=\frac{s-1}{s-1}=1 \tag{4.19}$$

according to (4.14).

The Bézout identity (2.68) then has the solution given by (4.17) as

$$P(s)=\frac{1}{A(s)}=1,\ Q(s)=0 \tag{4.20}$$

■

Example 4.8

Now let the factorization be given by (4.10) with $m(s)=(s+1)^2$. In this case, the both elements $A(s)$ and $B(s)$ are associated, thus $A(s)\equiv B(s)$ and scheme (4.15) can be used when solving $\mathrm{GCD}(A(s),B(s))$. This scheme yields e.g.

$$X(s)=Y(s)=1$$
$$\Rightarrow A(s)X(s)+B(s)Y(s)=\frac{s^2+(2+\exp(-s))s+1+(s+\exp(-s))\exp(-2s)}{(s+1)^2} \tag{4.21}$$
$$=\frac{s^2+(2+\exp(-s)+\exp(-2s)+\exp(-3s))s+1}{(s+1)^2}=\mathrm{GCD}(A(s),B(s))$$

where $X(s),Y(s)$ are chosen for the simplicity. Then the solution of the Bézout identity according to (4.18) reads

$$P(s)=Q(s)=\frac{(s+1)^2}{s^2+(2+\exp(-s)+\exp(-2s)+\exp(-3s))s+1} \tag{4.22}$$

In case of asymptotically stable systems, i.e. $A(s)$ is invertible (a unit), it is possible to use also a simple procedure when solving the Bézout identity

$$Q(s)=1\Rightarrow P(s)=\frac{1-B(s)}{A(s)} \tag{4.23}$$

By applying this rule to the example, the following solution is obtained

$$P(s)=\frac{(s+1)^2-(s+\exp(-s))\exp(-2s)}{s^2+(2+\exp(-s))s+1} \tag{4.24}$$

This scheme has some advantages, i.a. it enables that the reference-to-output transfer function to have only real poles if $m(s)$ is a polynomial, see Subchapter 4.3. The use of the Bézout identity for control feedback stabilization is introduced in Subchapter 4.2. ■

4.1.3 Basic properties of the ring

Follow now terms introduced in Subchapter 2.3.1 and try to match some of them with R_{MS} ring.

Lemma 4.2

A set R_{MS} introduced in Definition 4.1 constitutes a commutative ring. ■

Proof. A sketch of proof that R_{MS} meets ring conditions follows.

Clearly, R_{MS} is closed under addition with associativity and the neutral element $E=0$. The inverse element $B(s)\in R_{MS}$ under addition of $A(s)\in R_{MS}$ is simply $B(s)=-A(s)$. Since $A(s)+B(s)=B(s)+A(s)\in R_{MS}$, it is a commutative group.

The closure under multiplication with associativity is also evident since the numerator and denominator of any $A(s)\in R_{MS}$ are composed of quasipolynomial factors – retarded ones and formally stable neutral ones, respectively. Since the operation of multiplication is commutative, left and right distributivity hold as well. In case of distributed delays, it is not possible to obtain more unstable denominator zeros then numerator ones of any $A(s)\in R_{MS}$ under multiplication. The multiplicative identity element equals 1. □

Lemma 4.3

An element $A(s)\in R_{MS}$ is a unit (invertible element) if and only if $A(s)$ has zero relative order and has the (asymptotically and formally) stable numerator. ■

The proof of Lemma 4.3 is evident (e.g. the necessity can be proved by the negation of the right hand side of the lemma) with the aid of Lemma 4.1. Note that stable numerator means that is has only stable zeros in the appropriate meaning.

Lemma 4.4

An element $A(s)\in R_{MS}$ is irreducible if and only if its numerator is formally stable and

$$O_R + N_U \le 1 \tag{4.25}$$

where O_R is the relative order and N_U stands for the number of real zeros $s_{U,i}, i=1,2,...N_U$ or conjugate pairs $s_{U,i}, \bar{s}_{U,i}, i=1,2,...N_U$ with $\mathrm{Re}\, s_{U,i}\ge 0$ and $\mathrm{Re}\, \bar{s}_{U,i}\ge 0$ of $A(s)$, respectively. ■

Proof. Necessity. Consider the following three cases

a) $O_R=0$, $N_U=1$

b) $O_R = 1,\ N_U = 0$

c) $O_R \geq 2$

Use an indirect proof. First, let a) is not valid; hence, $O_R = 0,\ N_U > 1$. Consider a (quasi)polynomial $c(s)$ with only one unstable zero (or a pair of unstable zeros), say $c(s_{U,1}) = 0$ (or $c(s_{U,1}) = c(\bar{s}_{U,1}) = 0$) and an arbitrary stable (quasi)polynomial $b(s)$ of the same order (i.e. first or second one). Then

$$A(s) = \frac{a_{num}(s)}{a_{den}(s)} = \frac{a_{num}(s)b(s)}{a_{den}(s)c(s)} \frac{c(s)}{b(s)} = A_1(s)A_2(s) \tag{4.26}$$

where $A_1(s)$ and $A_2(s)$ are neither associated with $A(s)$ nor units.

Now, let b) is not valid, i.e. $O_R = 1,\ N_U > 0$, and assume a stable (quasi)polynomial $d(s)$ of the first order. Then follow the scheme

$$A(s) = \frac{a_{num}(s)}{a_{den}(s)} = \frac{a_{num}(s)d(s)}{a_{den}(s)} \frac{1}{d(s)} = A_1(s)A_2(s) \tag{4.27}$$

Again, $A_1(s)$ and $A_2(s)$ are neither associated with $A(s)$ nor units.

Finally, let c) holds. Then it is possible to write e.g. scheme (4.27).

Sufficiency. Consider the three cases introduced above again.

If a) holds and the numerator is formally stable (even asymptotically), scheme (4.26) fails, since $A_1(s)$ is a unit and $A_2(s)$ is associated with $A(s)$. Moreover, there is not possible to find another “reducible” scheme.

Similarly, if b) holds and is formally stable, $A_1(s)$ is a unit and $A_2(s)$ is associated with $A(s)$ in scheme (4.27); hence, $A(s)$ is irreducible. □

Lemma 4.5

R_{MS} ring does not constitute UFR. ■

Proof. Consider the following element of the ring

$$\frac{1-\exp(-\tau s)}{s} \tag{4.28}$$

Nonzero zeros of the numerator of (4.28) are

$$s_k = \frac{2k\pi}{\tau}\,\mathrm{j}, \bar{s}_k = -\frac{2k\pi}{\tau}\,\mathrm{j},\ k \in \mathbb{N} \tag{4.29}$$

Define polynomials

$$P_k(s) = (s - s_k)(s - \bar{s}_k) \tag{4.30}$$

Then the factorization

$$\begin{aligned} &\frac{1-\exp(-\tau s)}{s} = \frac{(1-\exp(-\tau s))(s+m_0)^2}{sP_1(s)} \frac{P_1(s)}{(s+m_0)^2} = \\ &= \frac{(1-\exp(-\tau s))(s+m_0)^4}{sP_1(s)P_2(s)} \frac{P_1(s)P_2(s)}{(s+m_0)^4} = \\ &\ldots \end{aligned} \tag{4.31}$$

where $m_0 > 0$ is infinite and thus the R_{MS} ring is not a UFR, and none of left-hand factors in (4.31) is irreducible and none of all factors is a unit. □

Lemma 4.6

R_{MS} is an integral domain. ■

Proof. Consider $A(s), B(s) \in R_{MS}$ where $A(s)$ is a unit. Let $A(s)B(s) = 0$ and multiply the whole equation by $1/A(s)$. It yields $B(s) = 0$ and we have a contradiction. □

Hence, Lemma 4.5 and Lemma 4.6 imply that R_{MS} is not UFD.

Lemma 4.7

R_{MS} does not constitute PID. ■

Proof. Simply, it holds that every PID is UFD. Since R_{MS} is not UFD according to Lemma 4.6, it is not PID. □

Lemma 4.8

R_{MS} does not constitute a Bézout domain. ■

Proof. It is sufficient to show that there exists a pair $A(s), B(s) \in R_{MS}$ which does not give a solution pair $Q(s), P(s) \in R_{MS}$ of (2.68). Indeed, as mentioned above several times, coprime factorization of formally unstable TDS does not have a stabilizing solution of the Bézout identity in $H_\infty(\mathbb{C}^+)$, i.e. condition (2.69) does not hold. Since $H_\infty(\mathbb{C}^+) \supset R_{MS}$, which is evident from Definition 4.1, such solution does not exist in R_{MS} as well. □

The decision whether R_{MS} is a Noetherian ring is not successfully solved. Typically, a ring is a Bézout domain yet not PID, i.e. there exists an infinitely generated ideal which is not principal. In such cases, the ring is not Noetherian, see e.g. ring $\mathcal{E}$ of pseudopolynomials or ring $\mathcal{H}$, see Subchapter 2.3.2.

4.2 Objectives in controller design

The aim of this section is to outline controller design based on the algebraic approach in the R_{MS} ring satisfying the closed loop stability in that sense that all transfer functions in the feedback are from R_{MS} and the characteristic quasipolynomial (or meromorphic function) is formally stable. Moreover, controller feasibility, reference tracking and load disturbance rejection are other basic control performance requirements to be satisfied.

The following subchapters present the whole controller design procedure for two various control schemes in details.

4.3 Derivation of controllers for 1DoF

Consider the simple negative feedback loop as in Fig. 2.1. External inputs, reference and load disturbance signals, respectively, have forms

$$W(s) = \frac{H_W(s)}{F_W(s)}, \quad D(s) = \frac{H_D(s)}{F_D(s)} \tag{4.32}$$

where $H_W(s),\ H_D(s),\ F_W(s),\ F_D(s) \in R_{MS}$. Basic general feedback transfer functions are introduced in (2.72).

The first step in controller design is the fulfillment of control system stability, here in R_{MS} sense.

4.3.1 Closed loop stabilization

A crucial theorem follows.

Theorem 4.1

Given a Bézout coprime pair $A(s), B(s) \in R_{MS}$ of a plant $G(s) = B(s)/A(s)$ the closed-loop system is R_{MS} stable if and only if there exist pairs $P(s), Q(s) \in R_{MS}$ of all proper (feasible) controllers $G_R(s) = Q(s)/P(s)$ satisfying the Bézout identity

$$A(s)P(s) + B(s)Q(s) = 1 \tag{4.33}$$

a particular stabilizing solution of which, say $P_0(s), Q_0(s)$, can be then parameterized as

$$\begin{aligned} P(s) &= P_0(s) \pm B(s)Z(s) \\ Q(s) &= Q_0(s) \mp A(s)Z(s) \end{aligned} \tag{4.34}$$

where $Z(s) \in R_{MS}$, $P_0(s) \mp B(s)Z(s) \neq 0$. ■

Proof. Follow basic steps of the proof of the analogous theorem for R_{PS} ring [167] or the original R_{MS} ring [199]. However, some details have to be modified and precised.

The proof has three steps (they can be considered as separate lemmas).

Step 1: If $G(s) = B(s)/A(s)$, $G_R(s) = Q(s)/P(s)$ are two Bézout coprime fractions in R_{MS}, then the feedback control system is stable (in R_{MS} sense) if and only if $1/C(s) \in R_{MS}$ where $C(s) = A(s)P(s) + B(s)Q(s)$.

Consider the following four transfer functions

$$\begin{aligned} \begin{bmatrix} U(s) \\ Y(s) \end{bmatrix} &= \frac{1}{1 + G(s)G_R(s)} \begin{bmatrix} 1 & G_R(s) \\ G(s) & G(s)G_R(s) \end{bmatrix} \begin{bmatrix} D(s) \\ W(s) \end{bmatrix} \\ &= \frac{1}{C(s)} \begin{bmatrix} A(s)P(s) & A(s)Q(s) \\ B(s)P(s) & B(s)Q(s) \end{bmatrix} \begin{bmatrix} D(s) \\ W(s) \end{bmatrix} \end{aligned} \tag{4.35}$$

The feedback system is stable if and only if the four transfer functions in (4.35) are from R_{MS}. Sufficiency is evident. To prove necessity, induce a contradiction: Let $1/C(s) \notin R_{MS}$ and there is a common zero z_0 with $\mathrm{Re}\, z_0 \geq 0$ (including asymptotic ones or infinity) of $A(s)P(s)$, $A(s)Q(s)$, $B(s)P(s)$, $B(s)Q(s)$ which is cancelled such that all transfer functions are stable. However, this case is impossible, either since both pairs $A(s), B(s)$ and $P(s), Q(s)$ are coprime or they are even Bézout coprime, i.e. (2.69) holds. As known e.g. from Example 4.3, a simple coprimeness can not be sufficient in some cases of neutral systems. Moreover, note that the definition of the ring and the divisibility rule do not allow situation that $1/C(s) \notin R_{MS}$ and functions in (4.35) are simultaneously from the ring.

Step 2: A controller $G_R(s)$ stabilizes $G(s)$ if and only if it has the form $G_R(s) = \tilde{Q}(s)/\tilde{P}(s)$ where $\tilde{P}(s), \tilde{Q}(s) \in R_{MS}$ is a solution pair of $A(s)\tilde{P}(s) + B(s)\tilde{Q}(s) = 1$.

Sufficiency: If the Bézout identity holds, $C(s) = 1$, and thus the feedback system is stable according to Step 1.

Necessity: If there exists a stabilizing controller $G_R(s) = Q(s)/P(s)$, then $C(s) = A(s)P(s) + B(s)Q(s)$ and $1/C(s) \in R_{MS}$, see Step 1. Clearly, the same controller

$$G_R(s) = \frac{\tilde{Q}(s)}{\tilde{P}(s)} = \frac{\dfrac{\tilde{Q}(s)}{C(s)}}{\dfrac{\tilde{P}(s)}{C(s)}} \tag{4.36}$$

satisfies the Bézout identity $A(s)\tilde{P}(s) + B(s)\tilde{Q}(s) = 1$.

Step 3: All stabilizing pairs $P(s), Q(s) \in R_{MS}$ of (4.33) are given by (4.34) where $P_0(s), Q_0(s)$ is a particular solution of the equation and $Z(s) \in R_{MS}$.

Inserting (4.34) into the Bézout identity (4.33) clearly yields the same formula structure. Conversely, it holds that $A(s)(P_0(s) - P(s)) = B(s)(Q(s) - Q_0(s))$. Since $A(s), B(s)$ are coprime, $A(s)$ is a factor of $Q(s) - Q_0(s)$, i.e. $A(s)Z(s) = Q(s) - Q_0(s)$ for some

$Z(s) \in R_{MS}$. Viceversa $B(s)$ is a factor of $P_0(s) - P(s)$, i.e. $B(s)Z(s) = P_0(s) - P(s)$. It is easy to prove that there is also possible to switch signs in (4.33). Hence, every R_{MS} stabilizing controller can be parameterized as in (4.34). □

Parameterization (4.34) is used to satisfy remaining control and performance requirements, such as reference tracking, disturbance rejection etc.

4.3.2 Reference tracking and load disturbance rejection

The task of this subsection is to find $Z(s) \in R_{MS}$ in (4.34) so that the reference signal is tracked and load disturbance is asymptotically attenuated. First, the both tasks are separated and analyzed; yet, finally, it is shown that they have to be solved together.

As first, consider the problem of reference tracking. The solution idea results from the form of $G_{WE}(s)$ defined in (2.72). Consider the limit

$$\lim_{t\to\infty} e_W(t) = \lim_{s\to 0} sE_W(s) = \lim_{s\to 0} sG_{WE}(s)W(s) = \lim_{s\to 0} sA(s)P(s)\frac{H_W(s)}{F_W(s)} \quad (4.37)$$

where $\cdot_W$ means that the signal is a response to the reference not influenced by other external inputs. Limit (4.37) reaches zero if $\lim_{s\to 0} E_W(s) < \infty$ and $E_W(s)$ is analytic and bounded in the closed right half-plane, i.e. $E_W(s) \in H_\infty(\mathbb{C}^+)$ and has no pole there (including an asymptotic case). If one wants to prevent the closed loop stability from the sensitivity to small delays, the denominator of $E_W(s)$ must be a (quasi)polynomial satisfying (2.25), in addition. Moreover, it must hold that $G_{WE}(s)$ is proper (or, equivalently, $E_W(s)$ is strictly proper) because of the feasibility (impulse free modes) of $e_W(t)$. This implies, in other words, that the reference tracking is fulfilled if $E_W(s) \in R_{MS}$.

Alternatively, from the algebraic point of view, $F_W(s)$ must divide the product $A(s)P(s)$ in R_{MS}. It means that one has to set all zeros of $P(s)$ (with corresponding multiplicities) in $\mathbb{C}^+$ as zeros of $F_W(s)$ - unless there are any already contained in $A(s)$. Recall that zeros mean zero points of a whole term in R_{MS} here, not only those of a quasipolynomial numerator.

As second, take a look at load disturbance attenuation, which is analyzed in a very similar way. Thus, the task is to find a suitable $Z(s) \in R_{MS}$ in (4.34) so that the load disturbance is asymptotically rejected. Assume the limit

$$\lim_{t\to\infty} y_D(t) = \lim_{s\to 0} sY_D(s) = \lim_{s\to 0} sG_{DY}(s)W(s) = \lim_{s\to 0} sB(s)P(s)\frac{H_D(s)}{F_D(s)} \tag{4.38}$$

using (2.72). The analogous analysis as in the previous subchapter yields the requirement

$$F_D(s) \mid (B(s)P(s)) \tag{4.39}$$

in R_{MS}. Since $B(s)$ is given, the task is to find a suitable form of $P(s)$ again.

Now, there are two various requirements on $P(s)$, i.e. $F_W(s) \mid (A(s)P(s))$ and $F_D(s) \mid (B(s)P(s))$, which can not be solved by a sequential utilization of (4.34). Indeed, if any $P(s)$ is found so that $F_W(s)$ divides $A(s)P(s)$, a subsequent use of parameterization (4.34) for (4.39) can invalidate the preceding divisibility. As a conclusion, the both conditions have to be considered together as

$$\mathrm{LCM}(F_W(s), F_D(s)) \mid \mathrm{GCD}(A(s), B(s))P(s) \tag{4.40}$$

which makes the general procedure more involved and it naturally carries some conservativeness (compared to the separate two conditions).

Introduce a constructive procedure in more details. As first, assume a set

$$\Omega_W = \{\sigma_{W,i} : F_W(\sigma_{W,i}) = 0, \mathrm{Re}\,\sigma_{W,i} \geq 0, i = 1,2,...,l_W\} \tag{4.41}$$

of zeros of $F_W(s)$ in $\mathbb{C}^+$ with their corresponding multiplicities $m_{W,i}, i = 1,2,...l_W$. Note that $m_W = 1$ means a single zero, $m_W = 2$ stands for a double one, etc. Let, in general, there be some zeros of $A(s)$ in $\mathbb{C}^+$ that are those of $F_W(s)$. Define now the set of indexes

$$\mathrm{I}_{A_w} = \{i : \sigma_{W,i} \in \Omega_W, A(\sigma_{W,i}) = 0\} \tag{4.42}$$

and the set of common zeros

$$\Omega_{A_W} = \{\sigma_{W,i} \in \Omega_W : i \in \mathrm{I}_{A_W}\} \subseteq \Omega_W \tag{4.43}$$

with multiplicities $m_{A_W,i}, i \in \mathrm{I}_{A_W}$ (in $A(s)$). For zeros in Ω_{A_W}, introduce multiplicity differences as $\Delta m_{WA_W,i} = \max\{m_{W,i} - m_{A_W,i}, 0\}$.

Now, let the multiplicities $m_{W,i}, i = 1,2,...l_W$ of zeros of Ω_W be updated to $\overline{m}_{W,i}, i = 1,2,...l_W$ as follows

$$\overline{m}_{W,i} = \begin{cases} \Delta m_{WA_W,i}, i \in \mathrm{I}_{A_W} \\ m_{W,i}, \quad i \notin \mathrm{I}_{A_W} \end{cases} \tag{4.44}$$

which takes zeros of $A(s)$ into consideration as well.

Analogously, a set

$$\Omega_D = \{\sigma_{D,i} : F_D(\sigma_{D,i}) = 0, \mathrm{Re}\,\sigma_{D,i} \geq 0, i = 1,2,...,l_D\} \tag{4.45}$$

is introduced. The corresponding multiplicities are $m_{D,i}, i = 1,2,...l_D$. Consider a set of common zeros of some zeros in $\mathbb{C}^+$ of $B(s)$ and $F_D(s)$ as

$$\Omega_{B_D} = \{\sigma_{D,i} \in \Omega_D : i \in \mathrm{I}_{B_D}\} \subseteq \Omega_D \tag{4.46}$$

where

$$\mathrm{I}_{B_D} = \{i : \sigma_{D,i} \in \Omega_D, B(\sigma_{D,i}) = 0\} \tag{4.47}$$

with multiplicities $m_{B_D,i}, i \in \mathrm{I}_{B_D}$ in $B(s)$ and introduce multiplicity differences $\Delta m_{DB_D,i} = \max\{m_{D,i} - m_{B_D,i}, 0\}$, $i \in \mathrm{I}_{B_D}$.

Again, update the multiplicities $m_{D,i}, i = 1,2,...l_D$ of zeros of Ω_D to $\overline{m}_{D,i}, i = 1,2,...l_D$ as follows

$$\overline{m}_{D,i} = \begin{cases} \Delta m_{DB_D,i}, i \in \mathrm{I}_{B_D} \\ m_{D,i}, \quad i \notin \mathrm{I}_{B_D} \end{cases} \tag{4.48}$$

Now, merge the both sets

$$\Omega_{WD} = \Omega_W \bigcup \Omega_D \tag{4.49}$$

and define the corresponding multiplicities as

$$m_{WD,i} = \begin{cases} \overline{m}_{W,i}, \sigma_{W,i} \in \Omega_W \setminus (\Omega_W \bigcap \Omega_D) \\ \overline{m}_{D,i}, \sigma_{D,i} \in \Omega_D \setminus (\Omega_W \bigcap \Omega_D) \\ \max\{\overline{m}_{W,i}, \overline{m}_{D,i}\}, \sigma_{\cdot,i} \in \Omega_W \bigcap \Omega_D \end{cases} \tag{4.50}$$

Let the overall number of zeros in Ω_{WD} be $|\Omega_{WD}| = l_{WD}$.

Assume a stabilizing particular solution given by a pair $P_0(s)$, $Q_0(s)$ and consider a factorization of a suitable parameterizing element $Z(s) \in R_{MS}$ as

$$Z(s) = Z_1(s) Z_2(s) \tag{4.51}$$

The structure of the first factor, $Z_1(s)$, is chosen so that the product $B(s)Z_1(s)$ has a suitable form, e.g. $P_0(s)$ and $B(s)Z_1(s)$ has the same denominator quasipolynomial, and it has no unknown parameters. Contrariwise, $Z_2(s)$ includes some selectable controller parameters which are to be placed properly. Let

$$Z_2(s) = \frac{z_{2,N}(s)}{z_{2,D}(s)} \tag{4.52}$$

where $z_{2,D}(s)$ has a simple and known form and $z_{2,N}(s)$ be a in a simple form again, say as a polynomial, with N selectable parameters $\alpha_1, \alpha_2, ...\alpha_N$

$$z_{2,N}(s) = z_{2,N}(s, \alpha_1, \alpha_2, ...\alpha_N) \tag{4.53}$$

The task is to determine the number N and to prescribe how to set all the unknown parameters. Hence, denote

$$P(s) = P_0(s) - B(s)Z_1(s)\frac{z_{2,N}(s, \alpha_1, \alpha_2, ...\alpha_N)}{z_{2,D}(s)} = \frac{p_N(s, \alpha_1, \alpha_2, ...\alpha_N)}{p_D(s)} \tag{4.54}$$

Define now the set of indexes

$$\mathrm{I}_{p_D} = \{i : \sigma_{WD,i} \in \Omega_{WD}, p_D(\sigma_{WD,i}) = 0\} \tag{4.55}$$

and the set of common zeros

$$\Omega_{p_D} = \left\{ \sigma_{WD,i} \in \Omega_{WD} : i \in \mathrm{I}_{p_D} \right\} \subseteq \Omega_{WD} \tag{4.56}$$

with corresponding multiplicities $m_{p_D,i}, i \in \mathrm{I}_{p_D}$ in $p_D(s)$.

Now, basically, all zeros of $F_W(s)$ and $F_D(s)$ in $\mathbb{C}^+$ must be placed as zeros of $P(s)$, unless they are included in $A(s)$ and $B(s)$, respectively. Again, update the zeros multiplicities in Ω_{WD} as follows

$$\overline{m}_{WD,i} = \begin{cases} m_{WD,i} + m_{p_D,i}, i = 1...l_{WD} \in \mathrm{I}_{p_D} \\ m_{WD,i}, \quad i = 1...l_{WD} \notin \mathrm{I}_{p_D} \end{cases} \tag{4.57}$$

The cumulative multiplicity is

$$M = \sum_{i=1}^{l_{WD}} \overline{m}_{WD,i} \tag{4.58}$$

The analysis above yields the requirement of the following setting equations for reference tracking and load disturbance rejection

$$\left[\frac{\mathrm{d}^{j-1}}{\mathrm{d}s^{j-1}} p_N\left(\sigma_{WD,i}, \alpha_1, \alpha_2, ...\alpha_N\right) \right]_{\sigma_{WD,i} \in \Omega_{WD}} = 0,\ i = 1...l_{WD},\ j = 1,2,...\overline{m}_{WD,i} \tag{4.59}$$

Zeros with $\overline{m}_{WD,i} \leq 0$ are naturally excluded from (4.59). If equations (4.59) are independent, the number of these equations is M, thus, finally, $N = M$.

4.4 Derivation of controllers for TFC

Analogously as for 1DoF control system, the controller design procedure is now proposed for the TFC structure, see Fig. 2.2. This control scheme brings two advantages. As first, it is possible to partially decouple and solve separately tasks of (asymptotic) reference tracking and load disturbance rejection. However, these problems are still partially connected. As second, it is possible to introduce new free control parameters which give additional degrees of freedom. Moreover, the control structure enables to obtain a finite number of poles for some feedback transfer functions, namely for reference-

to-output one, hence, the submethod proposed in Subchapter 4.4.4 is called the quasi-finite spectrum assignment.

4.4.1 Closed loop stabilization

Let both external inputs be considered as in (4.32). Crucial transfer functions for the TFC scheme are given by (2.73).

A statement analogous to Theorem 4.1 follows.

Theorem 4.2

Given a Bézout coprime pair $A(s), B(s) \in R_{MS}$ of a plant $G(s) = B(s)/A(s)$ the TFC system is R_{MS} stable if and only if there exist pairs $P(s), T(s) \in R_{MS}$ satisfying the Bézout identity

$$A(s)P(s) + B(s)T(s) = 1 \tag{4.60}$$

a particular stabilizing solution of which, say $P_0(s), T_0(s)$, can be then parameterized as

$$\begin{aligned} P(s) &= P_0(s) \pm B(s)Z(s) \\ T(s) &= T_0(s) \mp A(s)Z(s) \end{aligned} \tag{4.61}$$

where $Z(s) \in R_{MS}$, $P_0(s) \mp B(s)Z(s) \neq 0$ and $T(s) = Q(s) + R(s)$, i.e. pairs $P(s), Q(s) \in R_{MS}$ and $P(s), R(s) \in R_{MS}$ give rise to proper controllers $G_Q(s) = Q(s)/P(s)$ and $G_R(s) = R(s)/P(s)$, respectively. ■

A proof of Theorem 4.2 can be easily performed by substituting $T(s)$ into (4.33) instead of $Q(s)$ and taken into consideration transfer functions (2.73) instead of (2.72).

4.4.2 Solution decomposition

It holds that $T(s) = R(s) + Q(s)$, which indicates that the solution $T(s)$ of (4.60) and (4.61) has to be decomposed so that other requirements on $Q(s)$ and $R(s)$ are met.

Let

$$T(s)=\frac{t_N(s)}{t_D(s)}=\frac{s^n+\sum_{i=0}^{n}\sum_{j=1}^{k_i}t_{ij}s^i\exp(-\vartheta_{ij}s)}{t_D(s)} \tag{4.62}$$

Introduce a set of real selectable parameters $\gamma_{ij}, i=0,1,...n,\ j=1...k_i$ where n is the degree of $t_N(s)$, k_i expresses the number of non-zero (delay) terms for s^i, $N_T=1+\sum_{i=1}^{n}k_i$ is the number of all non-zero terms in $t_N(s)$, and set

$$\begin{aligned} R(s)&=\frac{\gamma_{n0}s^n+\sum_{i=0}^{n}\sum_{j=1}^{k_i}\gamma_{ij}t_{ij}s^i\exp(-\vartheta_{ij}s)}{t_D(s)}\\ Q(s)&=\frac{(1-\gamma_{n0})s^n+\sum_{i=0}^{n}\sum_{j=1}^{k_i}(1-\gamma_{ij})t_{ij}s^i\exp(-\vartheta_{ij}s)}{t_D(s)} \end{aligned} \tag{4.63}$$

Obviously, $T(s)=R(s)+Q(s)$.

4.4.3 Load disturbance rejection and reference tracking

Let disturbance rejection be investigated first. The load disturbance rejection condition can be derived similarly as for 1DoF structure as introduced in Subchapter 4.3.2. This task can be solved by a suitable selection of $Z(s)$ in (4.61). The crucial condition stems from $G_{DY}(s)$ defined in (2.73) which is formally identical with that introduced in (2.72). Hence, the limit (4.38) reaches zero if divisibility condition (4.39) holds.

The asymptotic reference tracking is a bit more involved then that for 1DoF structure. Consider the limit

$$\begin{aligned} \lim_{t\to\infty}e_W(t)&=\lim_{s\to0}sE_W(s)=\lim_{s\to0}sG_{WE}(s)W(s)\\ &=\lim_{s\to0}s[A(s)P(s)+B(s)Q(s)]\frac{H_W(s)}{F_W(s)} \end{aligned} \tag{4.64}$$

The limit reaches zero if $F_W(s)\,|\,(A(s)P(s))$ and, simultaneously, $F_W(s)\,|\,(B(s)Q(s))$. The former condition can be combined and satisfied analogously as for 1DoF; however, the latter one requires the use of decomposition (4.63). Therefore, in the following text, the

load disturbance rejection problem is worked out completely, whereas the reference tracking task is solved only partially and it will be fully established later.

Simply, one can follow equations from (4.41) to (4.59) exactly. As a result, $F_W(s)|(A(s)P(s))$ and $F_D(s)|(B(s)P(s))$ which ensures load disturbance rejection; however, to meet the requirement of asymptotic reference tracking, it is necessary to provide $F_W(s)|(B(s)Q(s))$ in addition. This task can be efficiently solved by decomposition (4.63). Note that the notation from equations (4.41) to (4.59) is adopted in the sequel.

To solve the task more precisely, recall first that $P(s)$ and $T(s)$ – after parameterization (4.61) – contain the number of N parameters α_i unambiguously determined by the number M of equations (4.59), and Ω_W stands for the set of zeros of $F_W(s)$ located in $\mathbb{C}^+$ with their corresponding multiplicities $m_{W,i}, i=1,2,...l_W$. Define the set of indexes

$$\mathrm{I}_{B_W} = \{i : \sigma_{W,i} \in \Omega_W, B(\sigma_{W,i}) = 0\} \tag{4.65}$$

and the set of corresponding zeros

$$\Omega_{B_W} = \{\sigma_{W,i} \in \Omega_W : i \in \mathrm{I}_{B_W}\} \subseteq \Omega_W \tag{4.66}$$

with multiplicities $m_{B_W,i}, i \in \mathrm{I}_{B_W}$ (in $B(s)$). For zeros in Ω_{B_W}, introduce multiplicity differences as $\Delta m_{WB_W,i} = \max\{m_{W,i} - m_{B_W,i}, 0\}$.

Now, let the multiplicities $m_{W,i}, i=1,2,...l_W$ of zeros of Ω_W be updated to $m_{WB,i}, i=1,2,...l_W$ as follows

$$m_{WB,i} = \begin{cases} \Delta m_{WB_W,i}, & i \in \mathrm{I}_{B_W} \\ m_{W,i}, & i \notin \mathrm{I}_{B_W} \end{cases} \tag{4.67}$$

Recall that the quasipolynomial numerator of $T(s)$, i.e. $t_N(s)$, can be generally decomposed by means the number N_T of (free) parameters γ_{ij}. To take the influence of the denominator $t_D(s)$ into consideration, let

$$\mathrm{I}_{t_D} = \left\{ i : \sigma_{W,i} \in \Omega_W, t_D\left(\sigma_{W,i}\right) = 0 \right\} \tag{4.68}$$

and

$$\Omega_{t_D} = \left\{ \sigma_{W,i} \in \Omega_W : i \in \mathrm{I}_{t_D} \right\} \subseteq \Omega_W \tag{4.69}$$

with corresponding multiplicities $m_{t_D,i}, i \in \mathrm{I}_{t_D}$ in $t_D(s)$.

Update the zeros multiplicities in Ω_W as follows

$$m_{WBt_D,i} = \begin{cases} m_{WB,i} + m_{t_D,i}, i = 1...l_W \in \mathrm{I}_{t_D} \\ m_{WB,i}, \quad i = 1...l_W \notin \mathrm{I}_{t_D} \end{cases} \tag{4.70}$$

Denote the cumulative multiplicity as

$$M_{WBt_D} = \sum_{i=1}^{l_W} m_{WBt_D,i} \tag{4.71}$$

Consider now the following three cases

1) If $N_T > M_{WBt_D}$, parameters γ_{ij} can be prescribed by the solution of

$$\left[\frac{\mathrm{d}^{j-1}}{\mathrm{ds}^{j-1}} t_N\left(\sigma_{W,i}, \boldsymbol{\gamma}\right) \right]_{\sigma_{W,i} \in \Omega_W} = 0,\ i = 1...l_W,\ j = 1,2,...m_{WBt_D,i} \tag{4.72}$$

where $\boldsymbol{\gamma} = \left[\gamma_{01},...\gamma_{0k_0}, \gamma_{11},...\gamma_{1k_1},...., \gamma_{n0},...\gamma_{nk_n} \right]^T$. In this case, there is a number of $\Delta N = N_T - M_{WBt_D}$ free independent parameters (i.e. the solution of (4.72) is ambiguous).

2) If $N_T = M_{WBt_D}$, the reference tracking can be satisfied by (4.72) as well; however, $\boldsymbol{\gamma}$ is determined unambiguously and there are no additional degrees of freedom.

3) If $N_T < M_{WBt_D}$, the number N_T of free parameters is not enough to solve (4.72), hence, other selectable parameters $\beta_i, i = 0...n_\beta$ have to be added, e.g. by a simple modification of $T(s)$ as follows

$$T_1(s) = T(s) \frac{s^{n_\beta} + \beta_{n_\beta - 1} s^{n_\beta - 1} + ... + \beta_1 s + \beta_0}{s^{n_\beta} + \beta_{n_\beta - 1} s^{n_\beta - 1} + ... + \beta_1 s + \beta_0} \tag{4.73}$$

where $n_\beta \geq -\Delta N$. Now $T_1(s)$ is recalculated such that a new vector $\bar{\gamma} = \left[\gamma, \beta_0, ... \beta_{n_\beta}\right]^T$ of free parameters is obtained and (4.72) can be solved, after the decomposition analogous to (4.63).

This adjustment can be also preformed when some additional degrees of freedom are required (in points 1 or 2).

4.4.4 Quasi-finite spectrum assignment

As mentioned above, the TFC structure can be used to perform quasi-finite spectrum assignment controller design in the sense that, at least, reference-to-output transfer function has a finite number of poles. It is easy to prove that asymptotically (and formally) stable systems naturally yield a finite spectrum feedback via procedures already described for the 1DoF and TFC structures.

To make it clear e.g. for TFC (the following procedure can be done analogously for 1DOF), consider that $a(s)$ in (4.10) has all zeros in $\mathbb{C}_0^-$ (including the asymptotic case) and $m(s)$ is a polynomial. Then $A(s) \in R_{MS}$ is a unit (invertible) and hence $A(s) \mid B(s)$, i.e. $B(s) \succeq A(s)$, which means $\mathrm{GCD}(A(s), B(s)) = A(s)$. In this case, the stabilizing Bézout equation (4.60) can be solved according to (4.23) as

$$T_0(s) = 1 \Rightarrow P_0(s) = \frac{1 - B(s)}{A(s)} = \frac{m(s) - b(s)}{a(s)} \tag{4.74}$$

If the parameterization (4.51) – (4.54) is adopted with $Z_1(s) = m(s)/a(s)$ and $Z_2(s) \in \mathbb{R}(s)$, the denominator $t_D(s)$ of $T(s)$ is a polynomial (or a real constant in most cases). Then $R(s)$ has a polynomial denominator, and since the reference-to-output transfer function reads $G_{WY}(s) = B(s)R(s)$, it has a finite number of poles. However, as it is obvious from (2.73), load disturbance transfers via infinite-dimensional subsystems and the numerator and denominator in $M(s)$ are quasipolynomials in general, hence a “full” finite spectrum assignment is not reached.

The main idea to satisfy the quasi-finite spectrum assignment for an unstable TDS using TFC stems from the consideration of the scheme in Fig. 2.2 as a simple feedback loop (i.e. 1DoF) with a pre-stabilizing inner loop, instead of a "direct" solution in R_{MS} described in Subchapters 4.4.1 - 4.4.3. Then the stable inner subsystem can be proceeded as it was introduced above.

The pre-stabilization is given by the solution of (4.33) which can be obtained by the extended Euclidean algorithm described for R_{MS} in Subchapter 4.1.2. The main trouble is how find $X(s), Y(s)$ in (4.15) such that $A(s)X(s)+B(s)Y(s)$ is a unit, i.e. the numerator quasipolynomial of the term is stable. Due to this reason, stability analyses of simple retarded quasipolynomials with respect to a real undelayed parameter have been made [125], [126]. The main results are the matter of the following subchapter.

4.5 Stability analysis of selected retarded quasipolynomials

Study now the stability of the following two selected simple retarded quasipolynomials by means of the argument principle (the Mikhaylov stability criterion) given by condition (2.36)

$$m_1(s) = s + a\exp(-\vartheta s) + kq \tag{4.75}$$

$$m_2(s) = s + a\exp(-\vartheta s) + kq\exp(-\tau s) \tag{4.76}$$

where $a \neq 0 \in \mathbb{R}$, k, ϑ, $\tau \in \mathbb{R}^+$ are fixed. The main goal is to find upper and lower bounds on the parameter $q \neq 0 \in \mathbb{R}$ such that quasipolynomials (4.75) and (4.76) have all zeros located in $\mathbb{C}_0^-$. Although the quasipolynomial (4.75) is a special case of (4.76), these analyses are made separately.

Consider quasipolynomial (4.75) first. The loop-shape-like procedure is based on the requirement that the appropriate Mikhaylov curve for $\omega \in [0,\infty)$ must have the overall argument change equal to $\pi/2$ (starting on the positive real axis).

Lemma 4.9

For $\omega = 0$, the imaginary part of the Mikhaylov curve of quasipolynomial (4.75) equals zero and it approaches infinity for $\omega \to \infty$. ■

Proof. Decompose $m_1(\mathrm{j}\omega)$ into real and imaginary parts as

$$\mathrm{Re}\{m_1(\mathrm{j}\omega)\} = a\cos(\vartheta\omega) + kq \tag{4.77}$$

$$\mathrm{Im}\{m_1(\mathrm{j}\omega)\} = \omega - a\sin(\vartheta\omega) \tag{4.78}$$

Obviously

$$\mathrm{Im}\{m_1(\mathrm{j}\omega)\}\big|_{\omega=0} = 0, \lim_{\omega\to\infty} \mathrm{Im}\{m_1(\mathrm{j}\omega)\} = \infty$$ □

Lemma 4.10

If (4.75) has all its zeros located in $\mathbb{C}_0^-$, the following inequality holds

$$q > \frac{-a}{k} \tag{4.79}$$

and thus the Mikhaylov curve starts on the positive real axis. ■

Proof. If (4.75) has all its zeros located in $\mathbb{C}_0^-$, the overall argument shift equals to $\pi/2$ according to (2.36). Moreover, Lemma 4.9 states that the imaginary part goes to infinity. These two requirements imply that for stable quasipolynomial is

$$\mathrm{Re}\{m_1(\mathrm{j}\omega)\}\big|_{\omega=0} > 0 \tag{4.80}$$

By application of (4.80) onto (4.77) yields the condition (4.79). □

Lemma 4.10 represents the necessary stability condition and the lower bound for *q*. The curve can either pass through the first or the fourth quadrant for an infinitesimally small $\omega = \Delta > 0$, which is clarified in the following simple lemma.

Lemma 4.11

A point on the Mikhaylov curve of (4.75) lies in the first quadrant for an infinitesimally small $\omega = \Delta > 0$ if and only if

$$a\vartheta \le 1 \tag{4.81}$$

This point lies in the fourth quadrant if and only if

$$a\vartheta > 1 \tag{4.82}$$

■

Proof. Necessity. If the point on the curve goes to the first quadrant for an infinitesimally small $\omega = \Delta > 0$, then the change of function $\mathrm{Im}\{m_1(\mathrm{j}\omega)\}$ in $\omega = 0$ is positive or this function is increasing in $\omega = \Delta$. It is known fact that this is satisfied if either

$$\frac{\mathrm{d}}{\mathrm{d}\omega}\mathrm{Im}\{m_1(\mathrm{j}\omega)\}\Big|_{\omega=0} > 0 \tag{4.83}$$

or there exists *even* $n \in \mathbb{N}$ such that

$$\frac{\mathrm{d}}{\mathrm{d}\omega}\mathrm{Im}\{m_1(\mathrm{j}\omega)\}\Big|_{\omega=0} = \ldots = \frac{\mathrm{d}^{n-1}}{\mathrm{d}\omega^{n-1}}\mathrm{Im}\{m_1(\mathrm{j}\omega)\}\Big|_{\omega=0} = 0, \frac{\mathrm{d}^{n}}{\mathrm{d}\omega^{n}}\mathrm{Im}\{m_1(\mathrm{j}\omega)\}\Big|_{\omega=0} > 0 \tag{4.84}$$

(i.e. there is a local minimum of $\mathrm{Im}\{m_1(\mathrm{j}\omega)\}$ in $\omega = 0$) or there is *odd* $n \ge 3 \in \mathbb{N}$ such that

$$\begin{aligned} &\frac{\mathrm{d}}{\mathrm{d}\omega}\mathrm{Im}\{m_1(\mathrm{j}\omega)\}\Big|_{\omega=0} = \ldots = \frac{\mathrm{d}^{n-1}}{\mathrm{d}\omega^{n-1}}\mathrm{Im}\{m_1(\mathrm{j}\omega)\}\Big|_{\omega=0} = 0, \frac{\mathrm{d}^{n}}{\mathrm{d}\omega^{n}}\mathrm{Im}\{m_1(\mathrm{j}\omega)\}\Big|_{\omega=0} \neq 0, \\ &\frac{\mathrm{d}}{\mathrm{d}\omega}\mathrm{Im}\{m_1(\mathrm{j}\omega)\}\Big|_{\omega=\Delta} > 0 \end{aligned} \tag{4.85}$$

(i.e. there is a point of inflexion of $\mathrm{Im}\{m_1(\mathrm{j}\omega)\}$ in $\omega = 0$; however, the function is increasing in $\omega = \Delta$).

Analyze the previous three conditions. First, relation (4.83) with respect to (4.78) reads

$$\frac{\mathrm{d}}{\mathrm{d}\omega}\mathrm{Im}\{m_1(\mathrm{j}\omega)\}\Big|_{\omega=0} = 1 - a\vartheta\cos(\vartheta\omega)\Big|_{\omega=0} = 1 - a\vartheta > 0 \tag{4.86}$$

which is satisfied for $a\vartheta < 1$.

Second, condition (4.84) can be taken into account if

$$\frac{\mathrm{d}}{\mathrm{d}\omega}\mathrm{Im}\{m_1(\mathrm{j}\omega)\}\Big|_{\omega=0} = 0 \Leftrightarrow a\vartheta = 1 \tag{4.87}$$

hence

$$\frac{\mathrm{d}^2}{\mathrm{d}\omega^2}\mathrm{Im}\{m_1(\mathrm{j}\omega)\}\Big|_{\substack{\omega=0\\ a\vartheta=1}} = 0,\ \frac{\mathrm{d}^3}{\mathrm{d}\omega^3}\mathrm{Im}\{m_1(\mathrm{j}\omega)\}\Big|_{\substack{\omega=0\\ a\vartheta=1}} > 0 \tag{4.88}$$

where the first non-zero *n*th derivation is odd, and thus (4.84) can not be satisfied for $a\vartheta = 1$; however, we can test (4.85). Indeed

$$\frac{\mathrm{d}}{\mathrm{d}\omega}\mathrm{Im}\{m_1(\mathrm{j}\omega)\}\Big|_{\substack{\omega=\Delta\\ a\vartheta=1}} > 0 \tag{4.89}$$

and thus function $\mathrm{Im}\{m_1(\mathrm{j}\omega)\}$ in $\omega = \Delta$ is increasing.

Similarly, one can easily verify that if the Mikhaylov plot pass through the fourth quadrant first, then function $\mathrm{Im}\{m_1(\mathrm{j}\omega)\}$ decreases in $\omega = 0$ when (4.82) holds .

Sufficiency. If conditions (4.81) or (4.82) are considered, particular derivations of $\mathrm{Im}\{m_1(\mathrm{j}\omega)\}$ can be calculated, which guarantee, according to (4.83) – (4.85), whether there is a tendency of the Mikhaylov curve to go to the first or the fourth quadrant, respectively. □

The meaning of Lemma 4.11 is demonstrated in Fig. 4.2

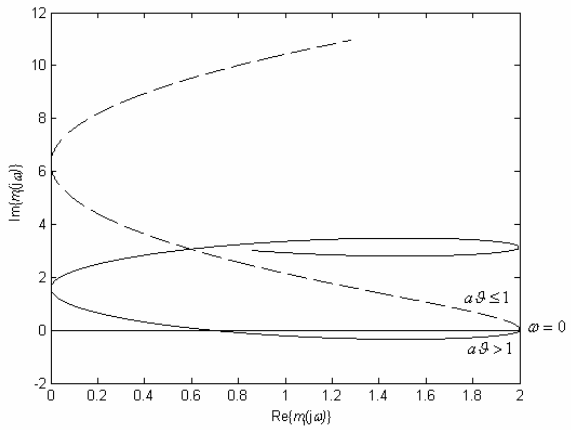

Fig. 4.2 Clarification of Lemma 4.11

Lemma 4.12

If the lower bound (4.79) holds and *a*, *k*, *q* are bounded, then $\mathrm{Re}\{m_1(\mathrm{j}\omega)\}$ is bounded for all $\omega > 0$. ■

Proof. Assume that $a > 0$. Then

$$-2a < -a + kq \le \mathrm{Re}\{m_1(\mathrm{j}\omega)\} = a\cos(\vartheta\omega) + kq \le a + kq \tag{4.90}$$

On the other hand, if $a < 0$

$$0 < a + kq \le \mathrm{Re}\{m_1(\mathrm{j}\omega)\} \le -a + kq < 2kq \tag{4.91}$$

where the left-hand sides of (4.90) and (4.91) and the right-hand one of (4.91) employ condition (4.79). The case when $a = 0$ can be discarded due to definition (4.75) of the quasipolynomial. □

The requirement of bounded parameters is natural with regard to their physical meaning as process quantities or controller gains.

Lemma 4.13

If (4.79) holds, there it exists an intersection of the Mikhaylov plot with the imaginary axis for some $\omega > 0$ if and only if

$$a > 0 \text{ and } |kq| \le a \tag{4.92}$$

■

Proof. Necessity. Show a contradiction, hence if $a < 0$ and (4.79) holds, then $0 < a + kq \le \mathrm{Re}\{m_1(\mathrm{j}\omega)\}$ according to Lemma 4.12 and thus there is no intersection with the imaginary axis.

Sufficiency. Consider $a > 0$. If $|kq| \le a$, there must exists $\omega > 0$ such that $a\cos(\vartheta\omega) = kq$, hence, $\mathrm{Re}\{m_1(\mathrm{j}\omega)\} = 0$. □

Searching of the stability upper bound will be made in two branches, so that conditions (4.81) and (4.82) are solved separately. The following theorem presents the necessary and sufficient stability condition for the former case.

Theorem 4.3

If (4.81) holds, then quasipolynomial (4.74) has all its zeros in $\mathbb{C}_0^-$ if and only if condition (4.79) is satisfied. ■

Proof. Necessity. See Lemma 4.10.

Sufficiency. Lemma 4.10 indicates that if (4.79) is satisfied, the Mikhaylov curve starts on the positive real axis for $\omega = 0$. According to Lemma 4.9 the imaginary part of the curve goes to infinity and Lemma 4.12 states that for bounded parameters, the curve is bounded in the real axis. Now for the stability it is sufficient to certify that for $a\vartheta \le 1$ the Mikhaylov plot does not leave either the first and the fourth quadrant, or the first and the second quadrant, since then the overall phase shift is $\pi/2$.

Indeed, Lemma 4.12 and Lemma 4.13 state that if $a < 0$, there is no intersection with the imaginary axis and thus the plot lies in the first and the fourth quadrant. Otherwise, if $0 < a \le 1/\vartheta$, an intersection with the imaginary axis can exist because of Lemma 4.13. Thus, it ought to be verified that there is no intersection with the real axis. Consider two cases:

1) If $\sin(\vartheta\omega) \ge 0,\ \omega > 0$, then

$$\mathrm{Im}\{m_1(\mathrm{j}\omega)\} = \omega - a\sin(\vartheta\omega) \ge \omega - \frac{\sin(\vartheta\omega)}{\vartheta} = \omega\left(1 - \frac{\sin(\vartheta\omega)}{\vartheta\omega}\right) > 0 \tag{4.93}$$

2) If $\sin(\vartheta\omega) < 0,\ \omega > 0$, we induce a contradiction. Hence, assume that there exists $\omega > 0$ such that $\sin(\vartheta\omega) < 0$ and $\mathrm{Im}\{m_1(\mathrm{j}\omega)\} = 0$. Then

$$a = \frac{\omega}{\sin(\vartheta\omega)} \tag{4.94}$$

which yields $\sin(\vartheta\omega) > 0$ and thus we have a contradiction. □

The both cases above in the second part of the proof of Theorem 4.3 are pictured in Fig. 4.3.

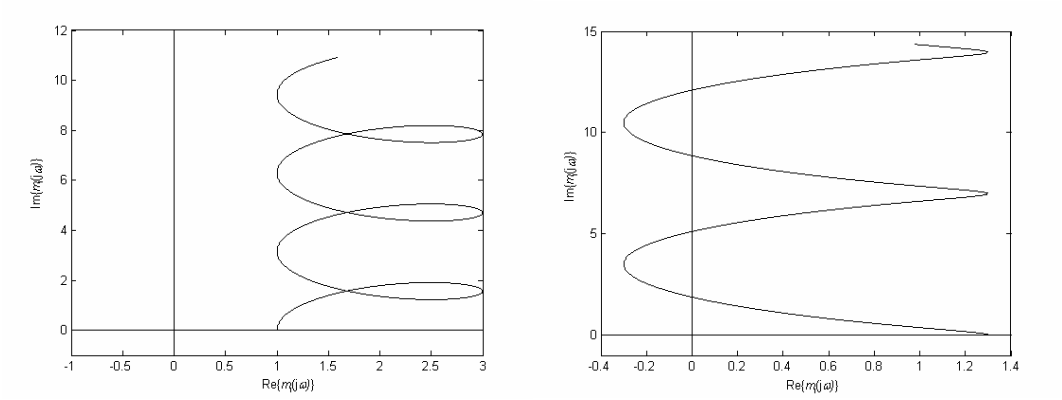

Fig. 4.3 For $a\vartheta \le 1$, the Mikhaylov plot of $m_1(s)$ must lie in the first and the fourth quadrant (left) or in the first and second quadrant (right)

Consider now the second case, i.e. $a\vartheta > 1$. The following result reinforces condition (4.79).

Definition 4.2

Let (4.79) holds. The *crossover frequency* ω_0 (for $m_1(s)$) is defined as

$$\omega_0 := \min\{\omega : \omega > 0, \operatorname{Im}\{m_1(\mathrm{j}\omega)\} = 0\} \tag{4.95}$$

for some $a \neq 0$, $\vartheta > 0$. In other words, it represents the least solution of (4.94). ■

The frequency is graphically displayed in Fig. 4.4.

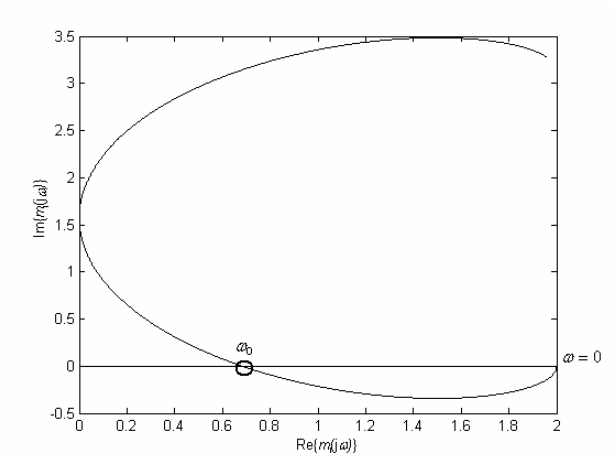

Fig. 4.4 Crossover frequency for $m_1(s)$

Theorem 4.4

If (4.82) holds, then quasipolynomial (4.75) has all its zeros located in $\mathbb{C}_0^-$ if and only if

$$q > \frac{-a\cos(\vartheta\omega_0)}{k} \tag{4.96}$$

Proof. Necessity. Lemma 4.9 and Lemma 4.10 state that the Mikhaylov curve for stable quasipolynomial (4.75) starts on the positive real axis. Condition (4.82) guaranties that the initial movement of the curve in the imaginary axis is negative, see Lemma 4.11. Thus, the curve has to pass through the fourth followed by the first quadrant. In other words, the first crossing with the real axis on the frequency $\omega_0 > 0$ has to satisfy

$$\begin{aligned} \mathrm{Im}\{m_1(\mathrm{j}\omega_0)\} &= \omega_0 - a\sin(\vartheta\omega_0) = 0 \\ \mathrm{Re}\{m_1(\mathrm{j}\omega_0)\} &= a\cos(\vartheta\omega_0) + kq > 0 \end{aligned} \tag{4.97}$$

which gives (4.96) directly.

Sufficiency. If (4.82) holds, then $a > 0$ and

$$q > \frac{-a\cos(\vartheta\omega_0)}{k} \geq \frac{-a}{k} \tag{4.98}$$

and thus the Mikhaylov curve for quasipolynomial (4.75) starts on the positive real axis according to Lemma 4.10 and the initial change of the curve in the imaginary axis is negative, see Lemma 4.11. Condition (4.96) then agrees with the fact that the curve crosses positive real axis first, as it is obvious from (4.77). Since the curve is bounded in the real part and the imaginary part goes to infinity (see Lemma 4.9 and Lemma 4.12), the overall phase shift is $\pi/2$ and thus the quasipolynomial $m_1(s)$ has all its zeros located in $\mathbb{C}_0^-$. □

Regarding $m_2(s)$ defined in (4.76), introduce formally particular lemmas first which are identical with some lemmas above.

Lemma 4.14

For $\omega = 0$, the imaginary part of the Mikhaylov curve of quasipolynomial (4.76) equals zero and it approaches infinity for $\omega \to \infty$. ■

Lemma 4.15

If (4.76) has all its zeros located in $\mathbb{C}_0^-$, (4.79) holds. ■

Proofs of Lemma 4.14 and Lemma 4.15 can be performed analogously as for Lemma 4.9 and Lemma 4.10, respectively. The following lemma is analogous to Lemma 4.11, yet let us build a proof for it.

Lemma 4.16

A point on the Mikhaylov curve of (4.76) lies in the first quadrant for an infinitesimally small $\omega = \Delta > 0$ if and only if

$$a\vartheta + kq\tau \le 1 \tag{4.99}$$

This point lies in the fourth quadrant if and only if

$$a\vartheta + kq\tau > 1 \tag{4.100}$$

■

Proof. Necessity. If the point goes to the first quadrant for an infinitesimally small $\omega = \Delta > 0$, one of conditions (4.83) – (4.85) holds for $m_2(s)$.

Relation (4.83) with respect to (4.76) reads

$$\frac{\mathrm{d}}{\mathrm{d}\omega}\mathrm{Im}\{m_2(\mathrm{j}\omega)\}\Big|_{\omega=0} = 1 - a\vartheta\cos(\vartheta\omega) - kq\tau\cos(\tau\omega)\Big|_{\omega=0} = 1 - a\vartheta - kq\tau > 0 \tag{4.101}$$

which gives $a\vartheta + kq\tau < 1$.

Condition (4.84) applied to (4.76) yields

$$\frac{\mathrm{d}}{\mathrm{d}\omega}\mathrm{Im}\{m_2(\mathrm{j}\omega)\}\Big|_{\omega=0} = 0 \Leftrightarrow a\vartheta + kq\tau = 1 \tag{4.102}$$

The second derivation is

$$\frac{\mathrm{d}^2}{\mathrm{d}\omega^2}\mathrm{Im}\{m_2(\mathrm{j}\omega)\}\Big|_{\omega=0} = a\vartheta^2\sin(\vartheta\omega) + kq\tau^2\sin(\tau\omega)\Big|_{\omega=0} = 0 \tag{4.103}$$

Generally, any *even n*-th derivation reads

$$\frac{\mathrm{d}^n}{\mathrm{d}\omega^n}\mathrm{Im}\{m_2(\mathrm{j}\omega)\} = (-1)^{\frac{n}{2}-1}\left(a\vartheta^n \sin(\vartheta\omega) + kq\tau^n \sin(\tau\omega)\right)$$
$$\Rightarrow \frac{\mathrm{d}^n}{\mathrm{d}\omega^n}\mathrm{Im}\{m_2(\mathrm{j}\omega)\}\Big|_{\omega=0} = 0 \tag{4.104}$$

This implies that (4.84) can not be satisfied.

Third, assume that there exists a non-zero *odd* *n*-th derivation, $n \geq 3$, in $\omega = 0$

$$\frac{\mathrm{d}^n}{\mathrm{d}\omega^n}\mathrm{Im}\{m_2(\mathrm{j}\omega)\}\Big|_{\omega=0} = (-1)^{\frac{n-3}{2}}\left(a\vartheta^n \cos(\vartheta\omega) + kq\tau^n \cos(\tau\omega)\right)\Big|_{\omega=0}$$
$$\overset{a\vartheta+kq\tau=1}{=} (-1)^{\frac{n-3}{2}}\left(a\vartheta^n \cos(\vartheta\omega) - (a\vartheta-1)\tau^{n-1}\cos(\tau\omega)\right)\Big|_{\omega=0} = (-1)^{\frac{n-3}{2}}\left(a\vartheta^n - (a\vartheta-1)\tau^{n-1}\right) \tag{4.105}$$

Test the latter condition in (4.85), obviously

$$\frac{\mathrm{d}}{\mathrm{d}\omega}\mathrm{Im}\{m_2(\mathrm{j}\omega)\}\Big|_{\substack{\omega=\Delta \\ a\vartheta+kq\tau=1}} = a\vartheta(\cos(\vartheta\Delta) - \cos(\tau\Delta)) + \cos(\tau\Delta) > 0 \tag{4.106}$$

since

$$\lim_{\Delta\to 0^+} \frac{\cos(\vartheta\Delta)}{\cos(\tau\Delta)} = 1 \tag{4.107}$$

Analogously, one can easily verify that if the Mikhaylov plot passes through the fourth quadrant first, then function $\mathrm{Im}\{m_2(\mathrm{j}\omega)\}$ decreases in $\omega = 0$ and (4.100) holds.

Sufficiency. Consider condition (4.99) and verify that it satisfies (4.83) or (4.85) for $m_2(s)$, respectively. In the same way, formula (4.100) gives rise to

$$\frac{\mathrm{d}}{\mathrm{d}\omega}\mathrm{Im}\{m_2(\mathrm{j}\omega)\}\Big|_{\omega=0} < 0 \tag{4.108}$$

which induces the initial tendency of the Mikhaylov plot to go to the fourth quadrant. □

Lemma 4.17

If *a*, *k*, *q* are bounded, then $\mathrm{Re}\{m_2(\mathrm{j}\omega)\}$ is bounded for all $\omega > 0$. ■

Proof. Assume the following four different condition.

1) If $a > 0$ and $kq > 0$, then

$$-a - kq \le \mathrm{Re}\{m_2(\mathrm{j}\omega)\} = a\cos(\vartheta\omega) + kq\cos(\tau\omega) \le a + kq \tag{4.109}$$

2) If $a > 0$ and $kq < 0$, then

$$-a + kq \le \mathrm{Re}\{m_2(\mathrm{j}\omega)\} \le a - kq \tag{4.110}$$

3) If $a < 0$ and $kq > 0$, then

$$a - kq \le \mathrm{Re}\{m_2(\mathrm{j}\omega)\} \le -a + kq \tag{4.111}$$

4) If $a < 0$ and $kq < 0$, then

$$a + kq \le \mathrm{Re}\{m_2(\mathrm{j}\omega)\} \le -a - kq \tag{4.112}$$

It is possible to summarize and unify results (4.109) – (4.112) as

$$-(|a| + |kq|) \le \mathrm{Re}\{m_2(\mathrm{j}\omega)\} \le |a| + |kq| \tag{4.113}$$

□

Proposition 4.1

If (4.79) and (4.99) are satisfied simultaneously, then

$$a(\vartheta - \tau) \le 1 \tag{4.114}$$

Proof. Obviously,

$$a(\vartheta - \tau) \overset{kq > -a}{<} a\vartheta + kq\tau \le 1 \tag{4.115}$$

□

The preceding proposition also expresses that for a quasipolynomial (4.76) with zeros in $\mathbb{C}_0^-$, when the corresponding Mikhaylov plot passes the first quadrant as first, the condition (4.115) holds.

Proposition 4.2

If the following inequality holds

$$a(\vartheta-\tau)>1 \tag{4.116}$$

then the corresponding Mikhaylov plot of a quasipolynomial (4.76) with zeros in $\mathbb{C}_0^-$ passes the fourth quadrant as first. ■

Proof. Lemma 4.15 states that (4.79) holds for a "stable" quasipolynomial (4.76). Then

$$1 < a(\vartheta-\tau) \overset{kq>-a}{<} a\vartheta + kq\tau \tag{4.117}$$

which induces that the Mikhaylov plot goes to the fourth quadrant as first, due to Lemma 4.16. □

Proposition 4.3

There always exists an intersection of the Mikhaylov curve of (4.76) with the imaginary axis. ■

Proof. The intersection exists if $\mathrm{Re}\{m_2(\mathrm{j}\omega)\}=0$, i.e.

$$a\cos(\vartheta\omega) = -kq\cos(\tau\omega) \tag{4.118}$$

for some $\omega>0$. Obviously, since $\vartheta>0$, $\tau>0$, there is $\omega>0$ satisfying relation (4.118). □

The upper stability bound will now be found via some unproven observations and a theorem.

Definition 4.3

Let (4.79) holds. A *crossover frequency* ω_0 for $m_2(s)$ is an element of the set

$$\Omega_0 := \{\omega : \omega>0, \mathrm{Re}\{m_2(\mathrm{j}\omega)\}=0, \mathrm{Im}\{m_2(\mathrm{j}\omega)\}=0\} \tag{4.119}$$

for some *crossover gain* q_0 and $a\neq 0, k, \tau, \vartheta>0$. ■

A crossover frequency, hence, has to satisfy simultaneously these two identities

$$\begin{aligned} &a\cos(\vartheta\omega_0)+kq_0\cos(\tau\omega_0)=0 \\ &\omega_0 - a\sin(\vartheta\omega_0)-kq_0\sin(\tau\omega_0)=0 \end{aligned} \tag{4.120}$$

Relations (4.120) can also be expressed by transcendental equation

$$\omega_0 \cos(\tau\omega_0) = a \sin((\vartheta - \tau)\omega_0) \tag{4.121}$$

Note that equation (4.121) is in the form suitable for utilization of numerical methods, i.e. some ratios of goniometric functions are not desirable for this purpose.

The crossover gain q_0 can be calculated from (4.120) as

$$q_0 = \frac{\omega_0 - a \sin(\vartheta\omega_0)}{k \sin(\tau\omega_0)} \tag{4.122}$$

Definition 4.4

Let (4.79) holds. The *critical frequency* ω_C is defined as

$$\omega_C := \min\left\{\omega : \omega \in \Omega_0, \underset{s=\omega j, \omega\in[0,\,\omega_C)}{\Delta \arg m_2(s) = 0}, \underset{s=\omega j, \omega\in[\omega_C,\,\infty)}{\Delta \arg m_2(s) = \frac{\pi}{2}}\right\} \tag{4.123}$$

for the corresponding *critical gain* q_C given by (4.122), where ω_C is placed instead of ω_0, and $a \neq 0, k, \tau, \vartheta > 0$. ■

Obviously, the critical frequency is the least crossover frequency for which the argument change is zero for $\omega \in [0, \omega_C)$ and consequently it equals $\pi/2$ for $\omega \in [\omega_C, \infty)$. The quasipolynomial is then on the "stability margin" for q_C, which has to satisfy the necessary condition (4.79). There can hence exist some crossover frequencies less then the critical one which do not mean the "stability margin".

The difference between the crossover and the critical frequency is clarified in Fig. 4.5. Whereas the left-hand side picture displays the critical frequency, the right-hand side position shows the crossover one only, because the phase shift of $m_2(j\omega)$ for $\omega \in [\omega_0, \infty)$ is $-7\pi/2$ and there is not another ω_0.

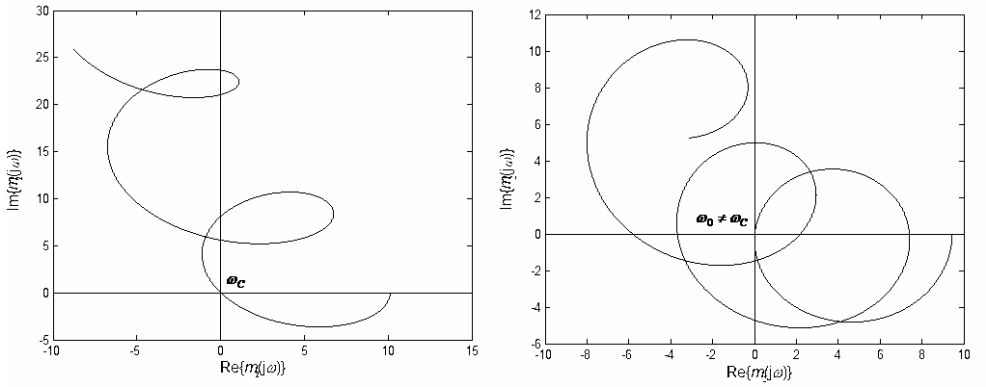

Fig. 4.5 The difference between ω_C (left) and $\omega_0 \neq \omega_C$ (right)

Observation 4.1

Let $q = q_C$, then the Mikhaylov plot of (4.76) circumscribes curves in the clockwise direction around the center of the rotation (like a "whirligig"). Moreover, if (4.99) holds, then the Mikhaylov plot initially moves to the first quadrant (as proved in Lemma 4.16) followed by the fourth quadrant for some frequencies $\omega > 0$. It means that although relation (4.99) quarantines that the plot tends to move to the first quadrant for $\omega = 0$, it immediately passes over the positive real axis to the fourth quadrant anyway. The situation is displayed in Fig. 4.6. ■

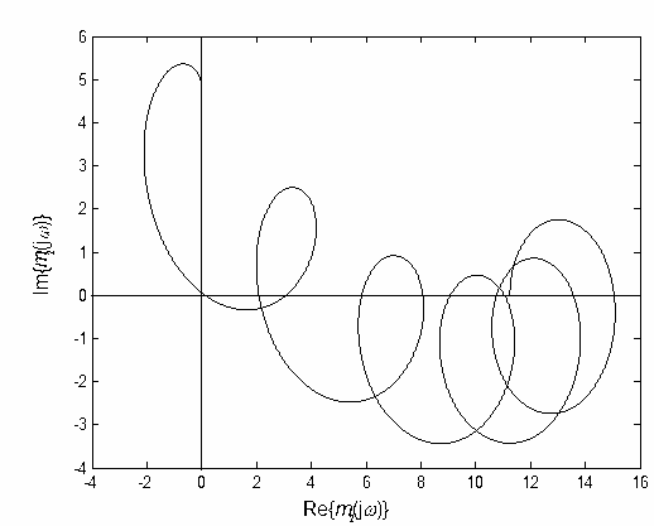

Fig. 4.6 Explanation of Observation 4.1

Remark 4.1

In [89], [90], a lemma which states that the spectrum of a general retarded quasipolynomial is continuous with respect to continuous changes of all its parameters is proved. This fact implies that the Mikhaylov plot of an appropriate quasipolynomial is continuous in both axes with respect to these parameters' changes, and viceversa. ■

Theorem 4.5

Consider the following five possibilities:

a) If $\sin(\tau\omega_C)=0$ and $\cos(\tau\omega_C)>0$, $\cos(\tau\omega_C)<0$, then quasipolynomial (4.76) has all its zeros in $\mathbb{C}_0^-$ if and only if

$$\max\left(\frac{-a\cos(\vartheta\omega_C)}{k\cos(\tau\omega_C)},\frac{-a}{k}\right)<q \tag{4.124}$$

$$\frac{-a}{k}<q<\frac{-a\cos(\vartheta\omega_C)}{k\cos(\tau\omega_C)} \tag{4.125}$$

respectively.

b) If $\cos(\tau\omega_C)=0$ and $\sin(\tau\omega_C)>0$, $\sin(\tau\omega_C)<0$, then quasipolynomial (4.76) has all its zeros in $\mathbb{C}_0^-$ if and only if

$$\frac{-a}{k}<q<\frac{\omega_C-a\sin(\vartheta\omega_C)}{k\sin(\tau\omega_C)} \tag{4.126}$$

$$\max\left(\frac{\omega_C-a\sin(\vartheta\omega_C)}{k\sin(\tau\omega_C)},\frac{-a}{k}\right)<q \tag{4.127}$$

c) If $\sin(\tau\omega_C)>0$ and $\cos(\tau\omega_C)<0$, $\sin(\tau\omega_C)<0$ and $\cos(\tau\omega_C)>0$, then quasipolynomial (4.76) has all its zeros in $\mathbb{C}_0^-$ if and only if (4.125) or (4.126), (4.124) or (4.127), hold, respectively.

d) If $\sin(\tau\omega_C)>0$ and $\cos(\tau\omega_C)>0$, then if

$$\left|a\vartheta\sin(\vartheta\omega_C)+kq_C\tau\sin(\tau\omega_C)\right|>\left|1-a\vartheta\cos(\vartheta\omega_C)-kq_C\tau\cos(\tau\omega_C)\right| \tag{4.128}$$

then quasipolynomial (4.76) has all its zeros in $\mathbb{C}_0^-$ if and only if (4.124) holds, otherwise the quasipolynomial has all its zeros in $\mathbb{C}_0^-$ if and only if (4.126) holds.

e) If $\sin(\tau\omega_C) < 0$ and $\cos(\tau\omega_C) < 0$, then if (4.128) holds, (4.76) has all its zeros in $\mathbb{C}_0^-$ if and only if (4.125) is satisfied. Otherwise, if condition (4.128) does not hold, the quasipolynomial is stable if and only if (4.127) holds.

Recall that ω_C is the critical frequency.

Proof. Necessity. For all the cases in the theorem, the Mikhaylov curve of a "stable" quasipolynomial (4.76) starts on the positive real axis, and thus the necessary condition (4.79) included in (4.124) - (4.127) holds, as proved in Lemma 4.15. Lemma 4.16 states condition (4.99) guaranties that the initial change of the Mikhaylov curve in the imaginary axis is positive. i.e. the curve tends to move to the first quadrant for $\omega = 0$; however, according to Observation 4.1, it immediately moves to the fourth quadrant. If (4.100) is satisfied, the curve passes through the fourth quadrant already for an infinitesimally small ω. The critical (marginal) case is characterized by ω_C and q_C where the curve crosses the origin of the complex plane and a small change of q would cause that the overall phase change would be $\pi/2$, see Remark 4.1. The limit "stable" case thus obviously means that $\mathrm{Re}\{m_2(\mathrm{j}\omega_C)\} > 0$ and $\mathrm{Im}\{m_2(\mathrm{j}\omega_C)\} > 0$ must hold simultaneously; here the following relations can be used

$$\mathrm{Re}\{m_2(\mathrm{j}\omega)\} = a\cos(\vartheta\omega) + kq\cos(\tau\omega) \tag{4.129}$$

$$\mathrm{Im}\{m_2(\mathrm{j}\omega)\} = \omega - a\sin(\vartheta\omega) - kq\sin(\tau\omega) \tag{4.130}$$

Consider case a) in the theorem and take $\cos(\tau\omega_C) > 0$. Since $\sin(\tau\omega_C) = 0$, we can not deal with (4.130), whereas (4.129) gives (4.124) immediately. Analogously, a case when $\cos(\tau\omega_C) < 0$ results in the right-hand side of (4.125).

If conditions b) hold, inequalities (4.126) and (4.127) are obtained from (4.130) in the similar way as in the previous paragraph.

In the case c), condition $\mathrm{Re}\{m_2(\mathrm{j}\omega_C)\}>0$ using (4.129) yields results (4.124) and (4.125) which are as the same as conditions (4.127) and (4.126), respectively, obtained from $\mathrm{Im}\{m_2(\mathrm{j}\omega_C)\}>0$ with (4.130).

The most involved cases in the theorem are d) and e) since conditions $\mathrm{Re}\{m_2(\mathrm{j}\omega_C)\}>0$ and $\mathrm{Im}\{m_2(\mathrm{j}\omega_C)\}>0$ collide here – one gives the upper limit for q whereas the second yields the lower one. To decide which of them is valid, one has to test the sensitivity of the Mikhaylov plot in the vicinity of $q=q_C$. If the infinitesimal change of the curve in the real axis is higher than that in the imaginary one, condition $\mathrm{Re}\{m_2(\mathrm{j}\omega_C)\}>0$ establishes the behavior of the curve near the origin. Contrariwise, if the plot shifts in the imaginary axis faster than in the real one, the stability is given by condition $\mathrm{Im}\{m_2(\mathrm{j}\omega_C)\}>0$ because it influences the Mikhaylov plot near the critical point more.

Hence, if

$$\left|\left[\frac{\mathrm{d}}{\mathrm{d}\omega}\mathrm{Re}\{m_2(\mathrm{j}\omega)\}\right]_{\omega=\omega_C}\right|>\left|\left[\frac{\mathrm{d}}{\mathrm{d}\omega}\mathrm{Im}\{m_2(\mathrm{j}\omega)\}\right]_{\omega=\omega_C}\right| \qquad (4.131)$$
$$\left|-a\vartheta\sin(\vartheta\omega_C)-kq_C\tau\sin(\tau\omega_C)\right|>\left|1-a\vartheta\cos(\vartheta\omega_C)-kq_C\tau\cos(\tau\omega_C)\right|$$

then (4.129) decides about the behavior of the Mikhaylov plot near the origin, which results in (4.124) for $\cos(\tau\omega_C)>0$ and in (4.125) for $\cos(\tau\omega_C)<0$, respectively.

Otherwise, if (4.131) does not hold, the imaginary part (4.130) of the quasipolynomial (4.76) dominates in the critical point, which gives (4.126) for $\sin(\tau\omega_C)>0$ and (4.127) for $\sin(\tau\omega_C)<0$.

Sufficiency. Bound (4.79) included in (4.124) - (4.127) guarantees that the Mikhaylov curve initiates on the positive real axis, see Lemma 4.15. Lemma 4.16 verifies that the curve reaches infinity in the imaginary axis for $\omega\to\infty$, and Lemma 4.17 states that it is bounded in the real axis. Moreover, if (4.99) holds, the Mikhaylov curve tends to move to the first quadrant and, consequently, to the fourth quadrant for $\omega=0$; otherwise, it moves to the fourth quadrant for $\omega=\Delta$ when (4.100) is satisfied. For the

quasipolynomial “stability”, expressed by the overall phase shift $\pi/2$, it is now sufficient to show that the curve does not encircle the origin of the complex plane in the clockwise direction.

Let the critical stability case be expressed by ω_C and q_C and consider case a) first. Since $\sin(\tau\omega_C)=0$, condition $\mathrm{Im}\{m_2(\mathrm{j}\omega_C)\}>0$ could not be guaranteed from (4.130) and $\mathrm{Im}\{m_2(\mathrm{j}\omega_C)\}=0$ remains for any q. However, inequalities (4.124) and (4.125) yield $\mathrm{Re}\{m_2(\mathrm{j}\omega_C)\}>0$ from (4.129) using $\cos(\tau\omega_C)>0$ and $\cos(\tau\omega_C)<0$, respectively, for a particular $q > q_C$ and $q < q_C$, respectively. Thus, it means that the real axis is crossed in the positive semi-axis first on the critical frequency and thus, with respect to Remark 4.1, the origin is encircled in the anti-clockwise direction with the overall phase shift $\pi/2$.

Second, assume the case b). Similarly as in the previous paragraph, $\cos(\tau\omega_C)=0$ gives $\mathrm{Re}\{m_2(\mathrm{j}\omega_C)\}=0$ for any q. Inequalities (4.126) and (4.127) together with $\sin(\tau\omega_C)>0$ and $\sin(\tau\omega_C)<0$, respectively, result in $\mathrm{Im}\{m(\mathrm{j}\omega_C)\}>0$, from (4.130). Thus, the overall phase shift is $\pi/2$ again.

In c), pairs of conditions (4.125) and (4.126), (4.124) and (4.127:), agree with $\mathrm{Re}\{m_2(\mathrm{j}\omega_C)\}>0$ and $\mathrm{Im}\{m_2(\mathrm{j}\omega_C)\}>0$ simultaneously for $\sin(\tau\omega_C)>0$ and $\cos(\tau\omega_C)<0$, $\sin(\tau\omega_C)<0$ and $\cos(\tau\omega_C)>0$, respectively, which implies the desired phase shift for the “stability”.

Condition (4.128) in d) and e) expresses the fact that the absolute value of a derivative of the Mikhaylov curve in the critical point is higher in the real than in the imaginary one. Thus, condition $\mathrm{Re}\{m_2(\mathrm{j}\omega_C)\}>0$ is stricter than $\mathrm{Im}\{m_2(\mathrm{j}\omega_C)\}>0$ when decision about the behavior of the plot in the vicinity of the origin for ω_C. Inequalities (4.124) and (4.125) correspond to $\mathrm{Re}\{m_2(\mathrm{j}\omega_C)\}>0$ for $\cos(\tau\omega_C)>0$ and $\cos(\tau\omega_C)<0$, respectively, which means that the critical point is not encircled.

In the contrary, if (4.128) does not hold, i.e. $\mathrm{Im}\{m_2(\mathrm{j}\omega_C)\}>0$ decides about the critical behavior, inequalities (4.126) and (4.127) correspond to $\mathrm{Im}\{m_2(\mathrm{j}\omega_C)\}>0$ for $\sin(\tau\omega_C)>0$ and $\sin(\tau\omega_C)<0$, respectively, which guarantees the stability again. □

Remark 4.2

Definition 4.4 and Theorem 4.5 suggest situations when the quasipolynomial stabilization by the suitable choice of q is not possible. These are two unpleasant possibilities:

1) If ω_C does not exist. Thus, although Ω_0 is non-empty set, it may not contain $\omega_0 = \omega_C$.

2) If q could not satisfy (4.125) or (4.126), i.e. if

$$\frac{\omega_C - a\sin(\vartheta\omega_C)}{k\sin(\tau\omega_C)} \le \frac{-a}{k} \tag{4.132}$$

or

$$\frac{-a\cos(\vartheta\omega_C)}{k\cos(\tau\omega_C)} \le \frac{-a}{k} \tag{4.133}$$

depending on the particular case from Theorem 4.5.

This case is, however, not very likable since the continuity of the Mikhaylov curve with respect to q supposes that there is a "stabilizing" q in the neighborhood of the marginal case $q = q_C$. ■

The following example demonstrates Remark 4.2.

Example 4.9

Consider quasipolynomial (4.76) with a = -5, $\tau = 0.2$, $\vartheta = 1$, k = 1, which gives the following set of crossover frequencies according to (4.119): $\Omega_0 = \{4.663, 7.855, 10.244, 23.562, 39.27, ...\}$, giving rise to crossover gains calculated from (4.122) as $q_0 \in$ {-0.4112, 12.855, 7.423, -18.562, 44.27,...}. One can verify by drawing the appropriate Mikhaylov plot that no $\omega_0 \in \Omega_0$ is the critical frequency. ■

Observation 4.2

Numerical experiments showed that if $\sin(\tau\omega_0) < 0$, then $\omega_0 \neq \omega_C$, which might render condition (4.127) useless. ■

Note that the investigated quasipolynomials were analyzed already e.g. in [7], [25]; however, different approaches were utilized in these papers.

4.6 Generalized Nyquist criterion for TDS

The Mikhaylov criterion is closely related to the Nyquist criterion for control feedback stability conditions. The both criteria are based on the argument principle which is a rather more involved compared to a finite-dimensional case due to the infinite spectrum of TDS and the existence of common roots in the transfer function numerator and denominator (because of distributed delays). In the following subchapters, the Nyquist criterion is revised for both retarded and neutral TDS and the question whether the notorious axiom about the number of unstable poles and the corresponding number of encirclements is answered. Moreover, the results are useful when testing robust stability and robust performance, particularly for the TFC structure.

4.6.1 1DoF control structure

As usual, the Nyquist criterion gives information about the closed-loop stability based on the knowledge of the overall phase shift (argument increment) of the open-loop transfer function $G_O(s)$ around the critical point -1.

Consider a simple control system as in Fig. 2.1 and notation $G(s)=b(s)/a(s)$, $G(s)=q(s)/p(s)$ where $a(s), b(s), q(s), p(s)$ are retarded quasipolynomials and $G(s)$ is strictly proper and $G_R(s)$ is proper. Then the corresponding closed loop reference-to-output (i.e. complementary sensitivity) transfer function reads

$$G_{WY}(s)=\frac{Y(s)}{W(s)}=\frac{G_R(s)G(s)}{1+G(s)G_R(s)}=\frac{G_0(s)}{1+G_0(s)}=\frac{\frac{q(s)b(s)}{p(s)a(s)}}{\frac{p(s)a(s)+q(s)b(s)}{p(s)a(s)}} \tag{4.134}$$

where the characteristic quasipolynomial $m(s)$ is

$$m(s)=p(s)a(s)+q(s)b(s) \tag{4.135}$$

Recall that in the case of input-output or internal distributed delays, zeros of (4.135) do not agree with poles of (4.134) since there are some common roots of $a(s), b(s)$ and/or those of $q(s), p(s)$ in $\mathbb{C}^+$.

Study now retarded and neutral systems with lumped delays only as first. Then, those with distributed delays will be included.

For retarded TDS without distributed delays we can formulate and prove the following theorem.

Theorem 4.6

Let the plant and the controller have transfer functions as in (4.134) without distributed delays and the control system be in a simple form as in Fig. 2.1. Let retarded quasipolynomials $a(s)$ and $p(s)$ have no root on the imaginary axis, i.e. $a(s) \neq 0, p(s) \neq 0$ for any $s = \mathrm{j}\omega$, $\omega \in \mathbb{R}$.

Then, if

$$\Delta \arg_{s=\mathrm{j}\omega, \omega \in [0,\infty)} p(s)a(s) = l\pi/2, l \in \mathbb{Z} \tag{4.136}$$

then the closed-loop system is asymptotically stable if

$$\Delta \arg_{s=\mathrm{j}\omega, \omega \in [0,\infty)} (1 + G_O(s)) = (n-l)\frac{\pi}{2} \tag{4.137}$$

where $n \in \mathbb{Z}$ is the highest s-power in the closed-loop characteristic quasipolynomial $m(s)$ as in (4.135) which equals the sum of the highest s-powers of $a(s)$ and $p(s)$. ■

Proof. The highest s-power, n, of $m(s) = p(s)a(s) + q(s)b(s)$ equals that of $p(s)a(s)$ due to the properness. If

$$\Delta \arg_{s=\mathrm{j}\omega, \omega \in [0,\infty)} m(s) = n\pi/2 \tag{4.138}$$

then the closed-loop system is asymptotically stable according to (2.36) (i.e. its characteristic quasipolynomial has all zeros in $\mathbb{C}_0^-$), and, simultaneously, since retarded quasipolynomials are analytic functions, it holds that

$$\underset{s=j\omega,\omega\in[0,\infty)}{\Delta\arg} m(s)/(a(s)p(s)) = n\pi/2 - l\pi/2 \tag{4.139}$$

Moreover, from (4.134) it is obvious that

$$\underset{s=j\omega,\omega\in[0,\infty)}{\Delta\arg} m(s)/(a(s)p(s)) = \underset{s=j\omega,\omega\in[0,\infty)}{\Delta\arg} (1+G_O(s)) \tag{4.140}$$

and the proof is finished. □

Thus, to test the closed-loop asymptotic stability, one can figure the Nyquist plot of $G_O(s)$ and count its overall number of encirclements around the critical point -1, or more precisely, the overall phase shift of the curve around the point.

Now, the natural question is whether the notorious precept about the number of unstable poles of $G_O(s)$ (as for delay-free systems) can be used. The answer is the following modification of Theorem 4.6.

Theorem 4.7

Let the prerequisities for Theorem 4.6 hold.

Then, the closed-loop system is asymptotically stable if

$$\underset{s=j\omega,\omega\in[0,\infty)}{\Delta\arg} (1+G_O(s)) = N_U\pi \tag{4.141}$$

where N_U is the number of poles of $G_O(s)$ in $\mathbb{C}^+$. ■

Proof. Assume results from Theorem 4.6. If there in no pure complex conjugate pair of poles of $G_O(s)$ (i.e. roots of $a(s)p(s)$), all its unstable poles have positive real parts, the number of which is given by (2.35). If notations (4.136) and (4.137) are taken into account, one can write

$$N_U = \frac{(n-l)}{2} \Rightarrow l = n - 2N_U \tag{4.142}$$

Substitution (4.142) into (4.137) yields (4.141), finally. □

If the plant or the controller is of a neutral type, the Nyquist criterion satisfying both the asymptotic and strong stability can be easily formulated in the light formulas

(2.37) and (2.38) and the knowledge of relation between strong and formal stability and the number of unstable quasipolynomial zeros, described in Subchapter 2.2.

Theorem 4.8

Let the plant and the controller have transfer functions as in (4.134) with lumped delays only and let the control system be of the scheme as in Fig. 2.1. Let neutral quasipolynomials $a(s)$ and $p(s)$ have no root on the imaginary axis, i.e. $a(s) \neq 0$, $p(s) \neq 0$ for any imaginary $s = \mathrm{j}\omega$, $\omega \in \mathbb{R}$, and define the denominator of $G_O(s)$ as

$$m_{ap}(s) = p(s)a(s) = s^n + \sum_{i=0}^{n} \sum_{j=1}^{h_{ap,i}} m_{ap,ij} s^i \exp(-s\eta_{ij}) \tag{4.143}$$

for which (2.25) holds.

Then, if

$$\underset{s=\omega\mathrm{j},\omega\in[0,\infty)}{\Delta \arg} m_{ap}(s) \in (l\pi/2 - \Phi_{ap}, l\pi/2 + \Phi_{ap}) \tag{4.144}$$

where

$$\Phi_{ap} = \arcsin\left(\sum_{j=1}^{h_{ap,n}} |m_{ap,nj}| \right) \tag{4.145}$$

then the closed-loop system is asymptotically stable if (4.137) holds true. Note that n is the highest s-power in the closed-loop characteristic quasipolynomial $m(s)$ as in (4.137), which equals the highest s-power of the $G_O(s)$ denominator $m_{ap}(s)$. ■

Proof. If the quasipolynomial is formally stable, i.e. it has only a finite number of zeros located in $\mathbb{C}^+$, the number of such unstable zeros is given by formula (2.35). Condition (2.25) ensures i.a. that the argument change Φ in (2.38) is finite (see proof of Theorem 1 in [208]), more precisely, $\Phi \in (0, \pi/2)$. If (2.25) does not hold true, the quasipolynomial is not strongly stable, yet it can be formally stable. Thus, (2.25) is a sufficient condition for formal stability of the neutral quasipolynomial and it implies that (2.35) can be utilized for the relation between the "main" part of the argument change (divisible by $\pi/2$ and ignoring Φ) and the number of unstable roots.

Follow now the proof of Theorem 4.6. If

$$\underset{s=j\omega,\omega\in[0,\infty)}{\Delta\arg}\, m(s)\in\left(n\pi/2-\Phi, n\pi/2+\Phi\right),\ \Phi=\arcsin\left(\sum_{j=1}^{h_n}\left|m_{nj}\right|\right) \tag{4.146}$$

then the closed-loop system is asymptotically and strongly stable according to (2.37) and (2.38). Since $\deg m(s)=\deg m_{ap}(s)=n$, $\Phi=\Phi_{ap}$, and (4.145) ensures the strong stability of both $m(s)$, $m_{ap}(s)$. Because of the fact that neutral quasipolynomials are analytic functions, it holds using (4.134) that

$$\begin{aligned}\underset{s=j\omega,\omega\in[0,\infty)}{\Delta\arg}\, m(s)/m_{ap}(s)&=n\pi/2\pm\Phi-l\pi/2\mp\Phi_{ap}=(n-l)\frac{\pi}{2}\\&=\underset{s=j\omega,\omega\in[0,\infty)}{\Delta\arg}\left(1+G_0(s)\right)\end{aligned} \tag{4.147}$$

□

As was mentioned, since strong stability condition (2.25) ensures that the number of unstable zeros of a neutral quasipolynomial is finite, the relation between the main part of the overall argument shift (that divisible by $\pi/2$) and the number of unstable zeros is given by (2.35). If we use this fact on (4.147) and $m_{ap}(s)$, one can easily prove that (4.141) from Theorem 4.7 holds also for formally stable neutral systems with lumped delays.

In the case of input-output distributed delays, there are some zeros of $a(s)$ in $\mathbb{C}^+$ that are those of $b(s)$. Let us study the stability of the characteristic meromorphic function first. Hence

$$M(s)=\det[s\mathbf{I}-\mathbf{A}(s)]=\frac{m_n(s)}{m_d(s)} \tag{4.148}$$

where $m_n(s)$ is a (retarded or neutral) quasipolynomial of degree n_m and $m_d(s)$ is a polynomial of a degree d_m with N_{um} zeros in $\mathbb{C}^+$ which are those of $m_n(s)$. Then the following theorem can be formulated.

Theorem 4.9

Consider the meromorphic function $M(s)$ as in (4.148) where $m_n(s) \neq 0,\ m_d(s) \neq 0$ for any imaginary $s = \mathrm{j}\omega,\ \omega \in \mathbb{R}$. Then

a) If $m_n(s)$ is a retarded quasipolynomial, $M(s)$ has no zero in $\mathbb{C}^+$ if and only if

$$\Delta \arg_{s=\mathrm{j}\omega,\omega\in[0,\infty)} M(s) = \frac{(n_m - d_m)\pi}{2} \tag{4.149}$$

b) If $m_n(s)$ is a neutral quasipolynomial satisfying (2.25), $M(s)$ has no zero in $\mathbb{C}^+$ and it is strongly stable if and only if

$$\frac{(n_m - d_m)\pi}{2} - \Phi_m \leq \Delta \arg_{s=\mathrm{j}\omega,\omega\in[0,\infty)} M(s) \leq \frac{(n_m - d_m)\pi}{2} + \Phi_m \tag{4.150}$$

where

$$\begin{aligned} \Phi_m &= \arcsin\left(\sum_{j=1}^{h_{n_m}} \left| m_{n,nj} \right| \right) \\ m_n(s) &= s^{n_m} + \sum_{i=0}^{n_m} \sum_{j=1}^{h_i} m_{n,ij} s^i \exp\left(-s\eta_{ij}\right) \end{aligned} \tag{4.151}$$

■

Proof. Let us make a proof of the case a). The second part of the proof can be done analogously using the fact that $m_n(s)$ is strongly stable and (2.35) can be taken into account.

Assume two cases. First, let (quasi)polynomials $m_n(s)$, $m_d(s)$ have all their zeros located in $\mathbb{C}_0^-$. Since both functions are analytic, from (2.36) it holds that

$$\Delta \arg_{\omega\in[0,\infty)} M(\mathrm{j}\omega) = \Delta \arg_{\omega\in[0,\infty)} m_n(\mathrm{j}\omega) - \Delta \arg_{\omega\in[0,\infty)} m_d(\mathrm{j}\omega) = (n_m - d_m)\frac{\pi}{2} \tag{4.152}$$

Second, let all N_{um} zeros of $m_d(s)$ in are those of $m_n(s)$ and there is no other one in $m_n(s)$. From (2.35) we have

$$\Delta \arg_{\omega\in[0,\infty)} m_n(\mathrm{j}\omega) = (n_m - 2N_{um})\frac{\pi}{2}, \Delta \arg_{\omega\in[0,\infty)} m_d(\mathrm{j}\omega) = (d_m - 2N_{um})\frac{\pi}{2} \tag{4.153}$$

which gives (4.149) and (4.152) again.

The inverse can be proved analogously (by steps in reverse order). □

Consider now a feedback system as in Fig. 2.1 with a plant affected by distributed delays.

Theorem 4.10

Let the plant and the controller have transfer functions as in (4.134) with distributed delays (and possibly lumped ones) and let the control system be of the scheme as in Fig. 2.1. Let quasipolynomials $a(s)$ and $p(s)$ have no root on the imaginary axis, i.e. $a(s) \neq 0, p(s) \neq 0$ for any $s = \mathrm{j}\omega$, $\omega \in \mathbb{R}$, and define the denominator $m_{ap}(s)$ of $G_O(s)$ as in (4.143). Then

a) If $m_{ap}(s)$ is a retarded quasipolynomial with

$$\Delta \arg_{s=\mathrm{j}\omega,\omega\in[0,\infty)} m_{ap}(s) = l\pi/2 \tag{4.154}$$

then the closed-loop system is asymptotically stable if

$$\Delta \arg_{s=\mathrm{j}\omega,\omega\in[0,\infty)} (1+G_O(s)) = (n-l-2\overline{N}_u)\frac{\pi}{2} = \overline{N}_{u,ap}\pi \tag{4.155}$$

holds where *n* is the highest *s*-power in $m_{ap}(s)$, $\overline{N}_u$ is the number of common zeros of the numerator and denominator of $G_O(s)$ in $\mathbb{C}^+$ and $\overline{N}_{u,ap}$ stands for the number of unstable zeros of $m_{ap}(s)$ which are not included in the numerator of $G_O(s)$.

b) If $m_{ap}(s)$ is a neutral quasipolynomial with (4.144) and (4.145) satisfying (2.25), then the closed-loop system is asymptotically and strongly stable if (4.155) holds.■

Proof. Consider a general case for retarded TDS. Formulation b) of Theorem 4.10 can be proved in a similar way.

Let the numerator and denominator (i.e. $m_{ap}(s)$) of $G_O(s)$ have exactly $\overline{N}_u$ common zeros in $\mathbb{C}^+$. From (4.134) it arises that these roots are zeros of $m(s)$ as well, hence, they are not the system poles since are canceled just by $m_{ap}(s)$.

Thus, the number $N_{u,ap}$ of all "unstable zeros" of $m_{ap}(s)$ is given by (2.35) as

$$\begin{aligned} N_{u,ap} &= \overline{N}_u + \overline{N}_{u,ap} = \left(\frac{n}{2} - \frac{\Delta \arg \underset{s=j\omega,\omega\in[0,\infty)}{} m_{ap}(s)}{\pi} \right) \\ &\Rightarrow \Delta \arg \underset{s=j\omega,\omega\in[0,\infty)}{} m_{ap}(s) = \left(n - 2\left(\overline{N}_u + \overline{N}_{u,ap}\right)\right)\frac{\pi}{2} \end{aligned} \tag{4.156}$$

and those of $m(s)$ as

$$\overline{N}_u = \left(\frac{n}{2} - \frac{\Delta \arg \underset{s=j\omega,\omega\in[0,\infty)}{} m(s)}{\pi} \right) \Rightarrow \Delta \arg \underset{s=j\omega,\omega\in[0,\infty)}{} m(s) = \left(n - 2\overline{N}_u\right)\frac{\pi}{2} \tag{4.157}$$

From (4.134), (4.135), (4.154), (4.156) and (4.157) we finally have

$$\begin{aligned} &\Delta \arg \underset{s=j\omega,\omega\in[0,\infty)}{} m(s)/m_{ap}(s) = \Delta \arg \underset{s=j\omega,\omega\in[0,\infty)}{} \left(1 + G_0(s)\right) \\ &= \Delta \arg \underset{s=j\omega,\omega\in[0,\infty)}{} m(s) - \Delta \arg \underset{s=j\omega,\omega\in[0,\infty)}{} m_{ap}(s) = \left(n - l - 2\overline{N}_u\right)\frac{\pi}{2} = \overline{N}_{u,ap}\pi \end{aligned} \tag{4.158}$$

□

Clearly, Theorem 4.7 holds true as well. Examples of the usage of criteria above can be found in [127].

4.6.2 TFC control structure

Regarding the TFC control structure as in Fig. 2.2., there are more possibilities how to define the criterion since it depends on how the feedback is viewed. Consider the following two possibilities

$$G_{WY}(s) = \frac{Y(s)}{W(s)} = \frac{G_R(s)G(s)}{1 + G(s)\left(G_R(s) + G_Q(s)\right)}, G_O(s) = G(s)\left(G_R(s) + G_Q(s)\right) \tag{4.159}$$

$$G_{WY}(s)=\frac{Y(s)}{W(s)}=\frac{\dfrac{G(s)}{1+G(s)G_Q(s)}G_R(s)}{1+\dfrac{G(s)}{1+G(s)G_Q(s)}G_R(s)},G_O(s)=\frac{G(s)}{1+G(s)G_Q(s)}G_R(s) \qquad (4.160)$$

The former form, i.e. (4.159), respects perturbations of the plant and the sum of controllers' transfer functions. Contrariwise, the letter form, i.e. (4.160), is quite natural in the sense of 1DoF structure since the left-hand side factor in $G_O(s)$ represents the inner feedback loop.

For the further text, structure (4.159) is taken into account because separate perturbations of the plant and both controllers are more natural in practice than separate perturbations of the outer controller and the whole inner feedback loop as in (4.160).

Now theorems from the preceding subsection can be used directly by substituting $G_O(s)=G(s)\left(G_R(s)+G_Q(s)\right)$ instead of $G_O(s)=G(s)G_R(s)$. However, the notions of robust stability and robust performance are much more involved that in 1DoF case, as presented in Subchapter 7.6.

4.7 Examples

Several examples demonstrating the controller design procedure introduced in Subchapters 4.3 and 4.4 are presented in this subchapter.

4.7.1 Stable system

Example 4.10

Consider a stable TDS giving rise to the transfer function

$$G(s)=\frac{b\exp(-\tau s)}{s+a\exp(-\vartheta s)}=\frac{\dfrac{b\exp(-\tau s)}{s+m_0}}{\dfrac{s+a\exp(-\vartheta s)}{s+m_0}}=\frac{\dfrac{b(s)}{m(s)}}{\dfrac{a(s)}{m(s)}}=\frac{B(s)}{A(s)} \qquad (4.161)$$

$$b,\tau,\vartheta,m_0>0;\ A(s),B(s)\in R_{MS}$$

where the stability condition reads

$$a\vartheta\in(0,\pi/2) \tag{4.162}$$

see e.g. [47], [199]. Clearly, $A(s)$, $B(s)$ are coprime.

Let both external signals be stepwise functions, i.e.

$$W(s)=\frac{H_W(s)}{F_W(s)}=\frac{\frac{w_0}{m_w(s)}}{\frac{s}{m_w(s)}},\ D(s)=\frac{H_D(s)}{F_D(s)}=\frac{\frac{d_0}{m_d(s)}}{\frac{s}{m_d(s)}} \tag{4.163}$$

where $m_w(s), m_d(s)$ are suitable "stable" (quasi)polynomials of the first order, e.g. for the simplicity, let $m_w(s)=m_d(s)=s+m_0$ again. Consider 1DoF control structure.

A particular stabilizing solution provides the Bézout identity (4.33) as

$$\frac{s+a\exp(-\vartheta s)}{s+m_0}P_0(s)+\frac{b\exp(-\tau s)}{s+m_0}Q_0(s)=1 \tag{4.164}$$

For $Q_0(s)=1$, one gets

$$P_0(s)=\frac{s+m_0-b\exp(-\tau s)}{s+a\exp(-\vartheta s)} \tag{4.165}$$

Alternatively, the generalized Euclidean algorithm can be used.

Parameterization (4.34) reads

$$\begin{aligned}P(s)&=\frac{s+m_0-b\exp(-\tau s)}{s+a\exp(-\vartheta s)}-\frac{b\exp(-\tau s)}{s+m_0}Z(s)\\ Q(s)&=1+\frac{s+a\exp(-\vartheta s)}{s+m_0}Z(s)\end{aligned} \tag{4.166}$$

For reference tracking and disturbance rejection, it is necessary to choose $Z(s)$, so that $F_W(s)|(A(s)P(s))$ and $F_D(s)|(B(s)P(s))$. Equivalently, the numerator of $P(s)$ must contain at least one zero root. To obtain $P(s)$ in a simple form, let

$$Z(s)=\left(\frac{m_0}{b}-1\right)\frac{s+m_0}{s+a\exp(-\vartheta s)} \tag{4.167}$$

see (4.51) – (4.54), which give

$$P(s)=\frac{s+m_0(1-\exp(-\tau s))}{s+a\exp(-\vartheta s)},\ Q=\frac{m_0}{b} \tag{4.168}$$

The controller transfer function hence reads

$$G_R(s)=\frac{Q(s)}{P(s)}=\frac{m_0(s+a\exp(-\vartheta s))}{b(s+m_0(1-\exp(-\tau s)))} \tag{4.169}$$

The controller is of the so-called anisochronic type (i.e. with internal delays), which is obvious from its MATLAB/Simulink structure, see Fig. 4.7

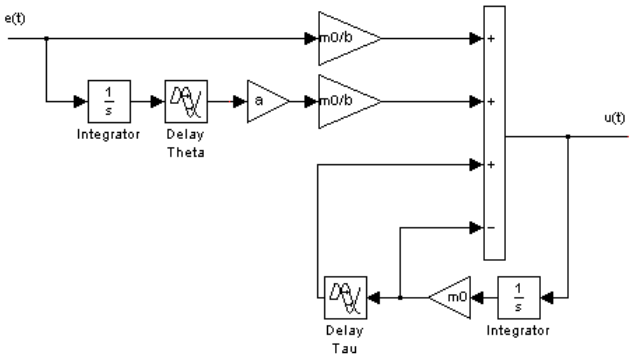

Fig. 4.7 MATLAB/Simulink scheme of controller (4.169)

Note that it is naturally possible to take $m(s)$ as a quasipolynomial instead of polynomial; however, this option would make a controller more complicated. The importance of $m(s)$ reveals from the closed loop transfer function

$$G_{WY}(s)=\frac{Y(s)}{W(s)}=\frac{m_0\exp(-\tau s)}{s+m_0} \tag{4.170}$$

The obtained control structure can be easily compared with the well-known Smith predictor structure (Fig. 4.8), see e.g. in [121].

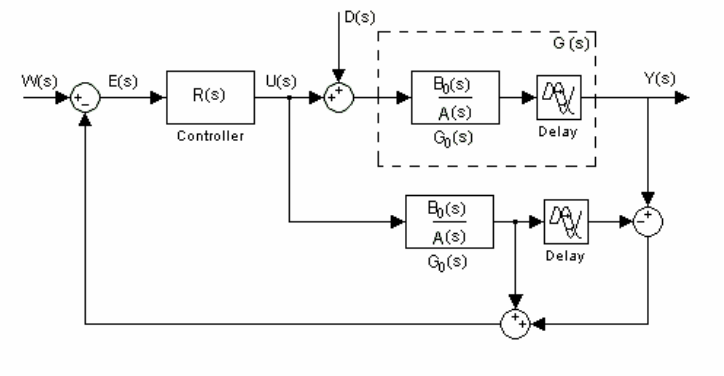

Fig. 4.8 Smith predictor structure

If the model is exact, it holds that

$$R(s)=\frac{G_R(s)}{1-G_R(s)G_0(s)(1-\exp(-\tau s))} \tag{4.171}$$

which gives

$$R(s)=\frac{m_0}{b}\frac{s+a\exp(-\vartheta s)}{s} \tag{4.172}$$

Hence, $R(s)$ represents a generalized (delayed) PI controller in the Smith structure.■

4.7.2 Integration system

The following example was thoroughly studied in (Pekař and Prokop, 2008b). Only the basic and selected results are presented here.

Example 4.11

Let an integral plant be described by the transfer function

$$G(s)=\frac{b}{s}\exp(-\tau s)=\frac{\frac{b\exp(-\tau s)}{m(s)}}{\frac{s}{m(s)}}=\frac{B(s)}{A(s)},\ A(s),B(s)\in R_{MS} \tag{4.173}$$

where $m(s)$ is an appropriate stable quasipolynomial of degree one. Consider TFC control system as in Fig. 2.2 and external inputs let be form the class of stepwise functions as in (4.163).

Present now the "direct" controller design according to (4.60) – (4.73).

Stabilizing Bézout identity reads

$$\frac{s}{m(s)}P_0(s)+\frac{b\exp(-\tau s)}{m(s)}T_0(s)=1 \tag{4.174}$$

Without loss of generality, let $T_0 = \alpha \in \mathbb{R}$ and $P_0(s)=P_0 = 1$, and the remaining task is to find a suitable stable quasipolynomial $m(s)$. Hence, (4.174) results in

$$\alpha=\frac{m(s)-s}{b\exp(-\tau s)} \tag{4.175}$$

The claim is α to be real; therefore the simplest $m(s)$ has to be of the form

$$m(s)=s+\alpha b\exp(-\tau s) \tag{4.176}$$

Stability condition (4.162) yields

$$0<\alpha<\frac{\pi}{2b\tau} \tag{4.177}$$

The convenient option of $Z(s)$ in the parameterization (4.61) enables to find the solution of (4.60), so that requirements of reference tracking and load disturbance rejection are accomplished. To solve reference tracking, if the reference signal is considered as a stepwise function (4.163), the numerator of $Q(s)$ must have the "derivative" pattern (the zero root of $F_W(s)$ is not included in $B(s)$); however, there is not placed any condition on $P(s)$, since the zero root is already included in $A(s)$. Nevertheless, the load disturbance rejection condition $F_D(s)|(B(s)P(s))$ requires $P(s)$ containing the zero root.

There are more possibilities how to choose $Z(s)$. For instance, $Z(s)=\alpha$ gives

$$P(s)=\frac{s}{s+\alpha b\exp(-\tau s)} \tag{4.178}$$

$$T(s)=\frac{\alpha(2s+\alpha b\exp(-\tau s))}{s+\alpha b\exp(-\tau s)}=\frac{\gamma 2\alpha s+\alpha^2 b\exp(-\tau s)}{s+\alpha b\exp(-\tau s)}+\frac{(1-\gamma)2\alpha s}{s+\alpha b\exp(-\tau s)} \qquad (4.179)$$
$$=R(s)+Q(s)$$

$$G_R(s)=\frac{R(s)}{P(s)}=\frac{\gamma 2\alpha s+b\alpha^2\exp(-\tau s)}{s},\ G_Q(s)=\frac{Q(s)}{P(s)}=(1-\gamma)2\alpha \qquad (4.180)$$

where $\gamma\in[0,1]$. Whereas an alternative option

$$Z(s)=\frac{s+\alpha b\exp(-\tau s)}{s+m_0}\frac{m_0}{b} \qquad (4.181)$$

where $m_0>0$, which agrees with philosophy of (4.51) – (4.54), yields

$$P(s)=\frac{s+m_0(1-\exp(-\tau s))}{s+m_0}$$
$$T(s)=\frac{(\alpha b+m_0)s+\alpha b}{b(s+m_0)}=\frac{\gamma\left(\alpha+\frac{m_0}{b}\right)s+\alpha}{s+m_0}+\frac{(1-\gamma)\left(\alpha+\frac{m_0}{b}\right)s}{s+m_0} \qquad (4.182)$$
$$=R(s)+Q(s)$$

$$G_R(s)=\frac{R(s)}{P(s)}=\frac{\gamma\left(\alpha+\frac{m_0}{b}\right)s+\alpha}{s+m_0(1-\exp(-\tau s))},\ G_Q(s)=\frac{Q(s)}{P(s)}=\frac{(1-\gamma)\left(\alpha+\frac{m_0}{b}\right)s}{s+m_0(1-\exp(-\tau s))} \qquad (4.183)$$

In both cases, there is a number $\Delta N=1$ of free parameters, i.e. γ, which can be tuned suitably (implicitly, $\gamma_{01}=1$, see (4.63)).

Characteristic quasipolynomial are

$$m(s)=(s+\alpha b\exp(-\tau s))^2$$
$$m(s)=(s+\alpha b\exp(-\tau s))(s+m_0) \qquad (4.184)$$

respectively. The quasi-optimal tuning guaranteeing multiple dominant real zeros (i.e. the "leftmost" possible real system poles) of the factor $m_1(s)=s+\alpha b\exp(-\tau s)$ is satisfied if

$$\alpha_{opt}=\frac{1}{b\tau e} \qquad (4.185)$$

see details in [118], [122].

Simulation comparative results for controllers (4.180) and (4.183) follow. As a comparative strategy, LQ polynomial method minimizing the functional - Integrated Squared Error (ISE) criterion -

$$J_{\mathrm{ISE}} = \int_0^{\infty} \left[e^2(t) + \varphi u^2(t) \right] \mathrm{d}t \tag{4.186}$$

is used, see e.g. [32]. This method utilizes a rational approximation of delay terms in the plant model, namely, the first order Padé approximation. We test also results of another - Integrated Squared Time Error (ISTE) – criterion

$$J_{\mathrm{ISTE}} = \int_0^{\infty} t \left[e^2(t) + \varphi u^2(t) \right] \mathrm{d}t \tag{4.187}$$

as a benchmark.

Let $b = 1$, $\tau = 5$. The reference signal is $w(t) = 1$ for $0 \le t < 100$ and $w(t) = 2$ for $100 \le t \le 300$. The step input disturbance $d(t) = -0.1$ enters at time $t = 200$; hence, the process of restoration of zero control error due to the input disturbance influences ISTE criterion significantly. The quasi-optimal tuning (4.185) gives $\alpha = 0.0736$ with dominant poles $\sigma_{1,2,3} = -0.2$, For the comparison, assume other two settings: $\alpha = 0.0835$ with $\sigma_{4,5} = -0.18 \pm 0.1\mathrm{j}$, and $\alpha = 0.125$ with $\sigma_{6,7} = -0.13 \pm 0.2\mathrm{j}$. Let $m_0 = 0.4$ in (4.183) and set e.g. $\gamma = 0.75$. Figs. 4.9 – 4.11 display the simulation responses and Tabs. 4.1 – 4.3 provides the corresponding values of J_{ISE} and J_{ISTE} with $\varphi = 500$.

Tab. 4.1 ISE and ISTE criteria values for $b = 1$, $\tau = 5$, $\gamma = 0.75$, $\varphi = 500$ using controllers (4.180)

α	J_{ISE}	J_{ISTE}
0.0736	22.21	765.6
0.0835	22.307	736.061
0.125	24.933	746.489

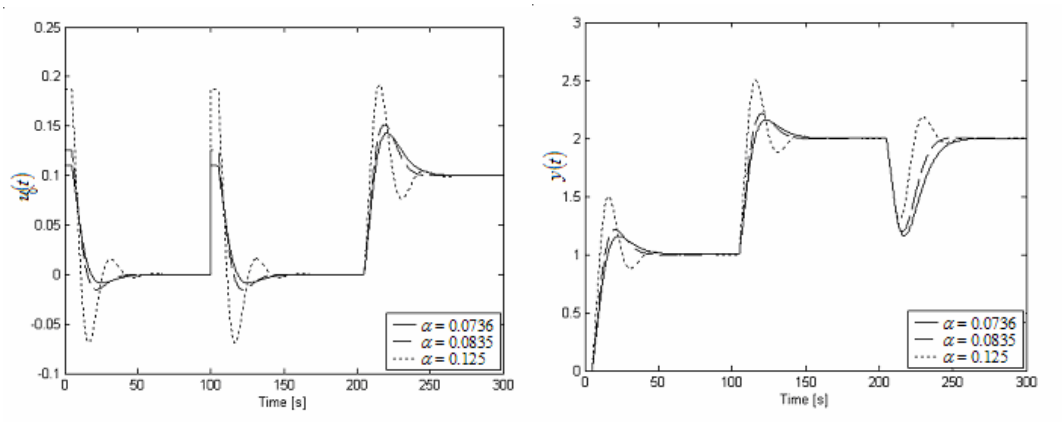

Fig. 4.9 Simulation control responses of $u_0(t)$ *(left) and* $y(t)$ *(right) for* $b=1$, $\tau=5$, $\gamma=0.75$ *using controllers (4.180)*

Tab. 4.2 ISE and ISTE criteria values for $b=1$, $\tau=5$, $\gamma=0.75$, $m_0=0.4$, $\varphi=500$ *using controllers (4.183)*

α	J_{ISE}	J_{ISTE}
0.0736	20.671	1448.2
0.0835	18.42	1153.8
0.125	19.679	913.7

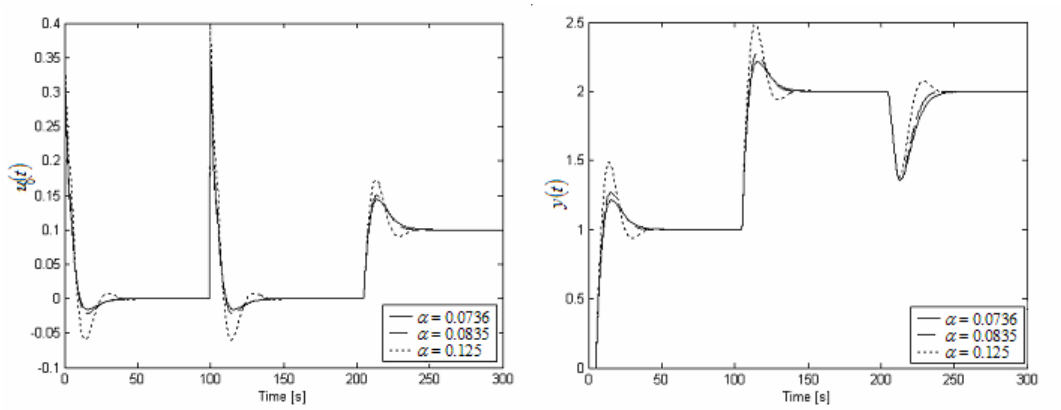

Fig. 4.10 Simulation control responses of $u_0(t)$ *(left) and* $y(t)$ *(right) for* $b=1$, $\tau=5$, $\gamma=0.75$, $m_0=0.4$, $\varphi=500$ *using controllers (4.183)*

Tab. 4.3 ISE and ISTE criteria values for $b=1$, $\tau=5$, $\gamma_1=\gamma_2=0.75$, $m_0=0.4$, $\varphi=500$ *using polynomial approach with optimal LQ controllers*

φ	J_{ISE}	J_{ISTE}
200	88.582	1062.2
500	38.879	812.107
900	26.652	789.973

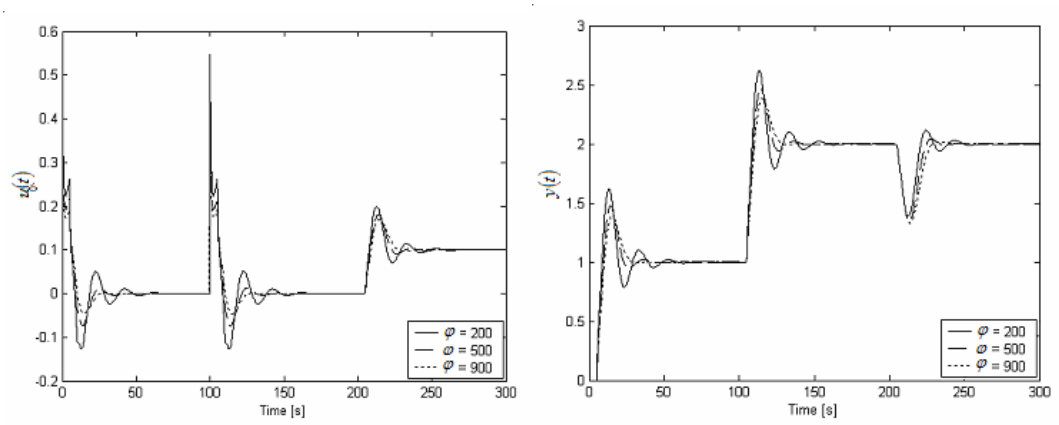

Fig. 4.11 Simulation control responses of $u_0(t)$ *(left) and* $y(t)$ *(right) for* $b=1$, $\tau=5$, $\gamma_1=\gamma_2=0.75$, $m_0=0.4$, *using polynomial approach with optimal LQ controllers*

Note that meaning of $\gamma_1=\gamma_2$ is analogous to γ. As can be seen, the both controllers (4.180) and (4.183) give comparable results where the higher values of α yield higher overshoots yet with a better damping factor. Obviously, controllers designed in R_{MS} provide even better results compared to the optimal LQ polynomial method.

Now, design controllers by a quasi-finite spectrum assignment methodology described in Subsection 4.4.4. Consider the pre-stabilizing proportional controller

$$G_Q(s)=G_Q=\alpha\in\mathbb{R} \tag{4.188}$$

then the transfer function of the inner pre-stabilized feedback loop is

$$G_0(s)=\frac{b\exp(-\tau s)}{s+\alpha b\exp(-\tau s)} \tag{4.189}$$

see Fig. 4.12, where $0<\alpha<\pi/(2\tau b)$ according to (4.177).

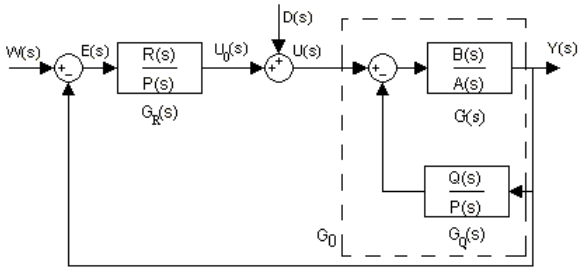

Fig. 4.12 Reconfigured TFC control system structure

Stable system $G_0(s)$ is considered as a controlled one in 1DoF structure in the sequel. Hence, e.g.

$$G_0(s)=\frac{\dfrac{b\exp(-\tau s)}{s+m_0}}{\dfrac{s+\alpha b\exp(-\tau s)}{s+m_0}} \tag{4.190}$$

and the stabilizing Bézout identity reads

$$\frac{s+\alpha b\exp(-\tau s)}{s+m_0}P_0(s)+\frac{b\exp(-\tau s)}{s+m_0}R_0(s)=1 \tag{4.191}$$

whose particular solution e.g. reads

$$R_0(s)=1,\ P_0(s)=\frac{s+m_0-b\exp(-\tau s)}{s+\alpha b\exp(-\tau s)} \tag{4.192}$$

Let

$$Z(s)=\frac{\left(\dfrac{m_0}{b}-1\right)(s+m_0)}{s+\alpha b\exp(-\tau s)} \tag{4.193}$$

in the parameterization (4.34) according to the principle (4.51) – (4.53) satisfying load disturbance rejection and reference tracking giving rise to

$$G_R(s)=\frac{R(s)}{P(s)}=\frac{\dfrac{m_0}{b}}{\dfrac{s+m_0(1-\exp(-\tau s))}{s+\alpha b\exp(-\tau s)}}=\frac{m_0}{b}\frac{s+\alpha b\exp(-\tau s)}{s+m_0(1-\exp(-\tau s))} \tag{4.194}$$

Set $\alpha=0.0736$, $\alpha=0.0835$, $\alpha=0.125$, respectively, and $m_0=0.4$ again. The corresponding simulation control responses and values of J_{ISE}, J_{ISTE}, are displayed in Tab. 4.4 and Fig. 4.13, respectively.

Tab. 4.4 ISE and ISTE criteria values for $b=1$, $\tau=5$, $m_0=0.4$, $\varphi=500$ using controllers (4.188) and (4.194)

α	J_{ISE}	J_{ISTE}
0.0736	28.617	959.431
0.0835	28.353	725.04
0.125	28.229	702.907

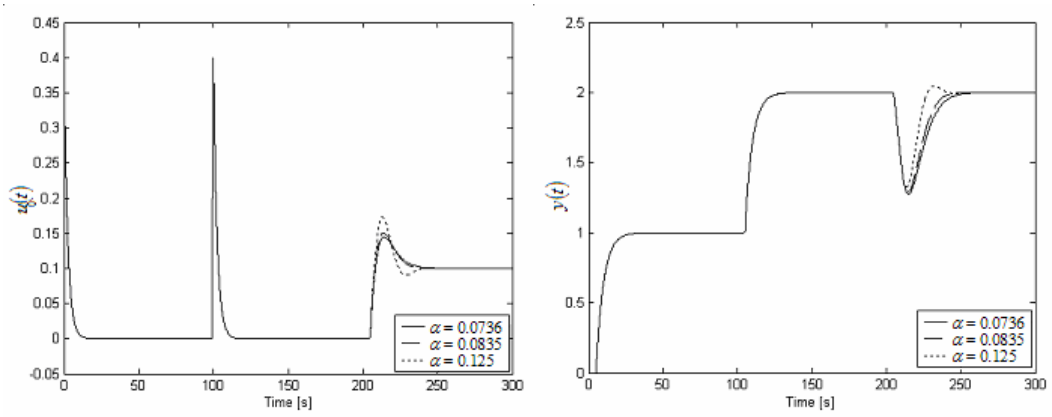

Fig. 4.13 Simulation control responses of $u_0(t)$ (left) and $y(t)$ (right) for $b=1$, $\tau=5$, $m_0=0.4$ using controllers (4.188) and (4.194)

Clearly, the objective values of J_{ISE} and J_{ISTE} are close to the ones introduced in Tabs. 4.1 – 4.3, yet subjectively, the simulation responses seem better mainly due to the aperiodical reference-to-output response. However, reactions to the disturbance is periodical again because of zeros right from the poles of the corresponding transfer functions. This can be clear from the following transfer functions.

$$G_{WY}(s)=\frac{Y(s)}{W(s)}=\frac{m_0\exp(-\tau s)}{s+m_0},\ G_{DY}(s)=\frac{D(s)}{W(s)}=\frac{s+m_0(1-\exp(-\tau s))}{s+m_0} \qquad (4.195)$$

A disadvantage of the methodology is that there are no free "weighting" parameters in the controller. ■

4.7.3 Unstable system

Example 4.12

Consider a plant described by model (4.161), yet with $a\vartheta\notin(0,\pi/2)$, i.e. the controlled system is purely (asymptotically) unstable. Let both external signals be stepwise functions again and assume 1DoF control structure, for the simplicity. Study now solutions for two different setting of the common quasipolynomial $m(s)$.

As first, let the claim be that the particular stabilizing solution of (4.33) is a real number, say again $Q_0(s)=\alpha$, $P_0(s)=1$. Analogously to (4.174) – (4.176), it leads to

$$m(s)=s+a\exp(-\vartheta s)+\alpha b\exp(-\tau s) \qquad (4.196)$$

Here, results of Theorem 4.5 can be utilized. Parameterization setting

$$Z(s)=\frac{m_0}{b}\frac{s+a\exp(-\vartheta s)+\alpha b\exp(-\tau s)}{s+m_0} \qquad (4.197)$$

where $m_0>0$ is a free parameter, gives

$$Q(s)=\frac{(m_0+\alpha b)s+m_0(\alpha b+a\exp(-\vartheta s))}{b(s+m_0)},\ P(s)=\frac{s+m_0(1-\exp(-\tau s))}{s+m_0} \qquad (4.198)$$

and hence

$$G_R(s)=\frac{Q(s)}{P(s)}=\frac{1}{b}\frac{(m_0+\alpha b)s+m_0(\alpha b+a\exp(-\vartheta s))}{s+m_0(1-\exp(-\tau s))} \qquad (4.199)$$

The reference-to-output transfer function reads

$$G_{WY}(s)=\frac{Y(s)}{W(s)}=\frac{s+(m_0+\alpha b)+m_0(\alpha b+a\exp(-\vartheta s))}{(s+m_0)(s+a\exp(-\vartheta s)+\alpha b\exp(-\tau s))}\exp(-\tau s) \qquad (4.200)$$

As second, try to take customary option $m(s)=s+m_0$. However, stabilizing solution (4.165) can not be used now since $A(s)$ is not invertible in R_{MS}. Thus, the generalized Euclidean algorithm (4.15) and (4.18) is a suitable tool for the solution of (4.164). This scheme results in

$$Q_0(s)=\frac{y_0(s+m_0)}{y_0 b\exp(-\tau s)+s+a\exp(-\vartheta s)},\ P_0(s)=\frac{s+m_0}{y_0 b\exp(-\tau s)+s+a\exp(-\vartheta s)} \tag{4.201}$$

where a simple choice $X(s)=1, Y(s)=y_0\in\mathbb{R}$ has been used in (4.15). Naturally, it is supposed that the denominator quasipolynomial in (4.201) has all its zeros in $\mathbb{C}_0^-$.

Let

$$Z(s)=\frac{m_0}{b}\frac{s+m_0}{s+a\exp(-\vartheta s)+y_0 b\exp(-\tau s)} \tag{4.202}$$

which agrees with the idea of (4.51) – (4.53), then

$$Q(s)=\frac{(m_0+y_0 b)s+m_0(\alpha b+a\exp(-\vartheta s))}{y_0 b\exp(-\tau s)+s+a\exp(-\vartheta s)},\ P(s)=\frac{s+m_0(1-\exp(-\tau s))}{y_0 b\exp(-\tau s)+s+a\exp(-\vartheta s)} \tag{4.203}$$

which yields the controller (4.199) with y_0 instead of α. Nevertheless, the generalized Euclidean algorithm enables to use other (different) $X(s), Y(s)$ than was used above, to get more complex controller structure or to satisfy that $Q_0(s), P_0(s)\in R_{MS}$. ■

4.7.4 Non-stepwise reference and/or disturbance

The following two examples are focused on the demonstration of controller design for non-stepwise external input(s). To provide the reader with a deep insight, the notation of Subsections 4.3 and 4.4 is adopted.

Example 4.13

Consider the stable plant (4.161), yet with a linearwise reference signal and a stepwise input disturbance, hence

$$W(s)=\frac{H_W(s)}{F_W(s)}=\frac{\dfrac{w_0}{m_w(s)}}{\dfrac{s^2}{m_w(s)}},\ D(s)=\frac{H_D(s)}{F_D(s)}=\frac{\dfrac{d_0}{m_d(s)}}{\dfrac{s}{m_d(s)}} \tag{4.204}$$

where $m_W(s)$ and $m_D(s)$ are arbitrary "stable" (retarded) (quasi)polynomials of degree two and one, respectively, and $H_W(s)$, $H_D(s)$, $F_W(s)$, $F_D(s)\in R_{MS}$.

Let TFC structure be utilized here.

Stabilization formula (4.60) for the choice $T_0=1$ yields $P_0(s)$ as in (4.165). Parameterization (4.61) is given by (4.66), yet with $T(s)$ instead of $Q(s)$. Analyze now the number of free parameters in $Z(s)$ by following (4.41) etc., thus, $\Omega_W=\{0\}$, $m_{W,1}=2$, $\mathrm{I}_{A_W}=\varnothing, \Omega_{A_W}=\varnothing$, then $\overline{m}_{W,1}=m_{W,1}$. Moreover, $\Omega_D=\{0\}, m_{D,1}=1, \mathrm{I}_{B_D}=\varnothing, \Omega_{B_D}=\varnothing$, $\overline{m}_{D,1}=m_{D,1}$. This gives $\Omega_{WD}=\{0\}$ with $m_{WD,1}=2$. Since $\mathrm{I}_{p_D}=\varnothing, \Omega_{p_D}=\varnothing$, then $\overline{m}_{WD,1}=m_{WD,1}=2$. It means that it is necessary to place one double zero root into $p_N(s)$, i.e. $M=N=2$, $p_N(s)=p_N(s,\alpha_1,\alpha_2)$. Sign $\beta_0=\alpha_1, \beta_1=\alpha_2$. To obtain $P(s)$ in a relatively simple form, let

$$Z(s)=\frac{s+m_0}{s+a\exp(-\vartheta s)}\frac{\beta_1 s+\beta_0}{s+m_1} \tag{4.205}$$

where $m_1>0$, then

$$P(s)=\frac{s^2+(m_0+m_1)s+b(\beta_1-1)s\exp(-\tau s)+m_0m_1+b(m_1-\beta_0)}{(s+a\exp(-\vartheta s))(s+m_1)} \tag{4.206}$$

According to (4.59), one has to solve the following set of algebraic equations for reference tracking and disturbance rejection

$$\begin{aligned}&\left[s^2+(m_0+m_1)s+b(\beta_1-1)s\exp(-\tau s)+m_0m_1+b(m_1-\beta_0)\right]_{s=0}=0\\&\frac{\mathrm{d}}{\mathrm{d}s}\left[s^2+(m_0+m_1)s+b(\beta_1-1)s\exp(-\tau s)+m_0m_1+b(m_1-\beta_0)\right]_{s=0}=0\end{aligned} \tag{4.207}$$

The solution of these equations gives

$$\beta_0 = b^{-1}m_1(b-m_0), \beta_1 = b^{-1}(b-m_0-m_1(1+\tau m_0)) \tag{4.208}$$

From (4.61) and (4.205), $T(s)$ reads

$$T(s) = \frac{(1-\beta_1)s + m_1 - \beta_0}{s+m_1} \tag{4.209}$$

For reference tracking, it is necessary to o the decomposition (4.63) so that $F_W(s) \mid (B(s)Q(s))$. Follow the procedure starting from (4.65). Hence, for instance,

$$\begin{aligned} T(s) &= \frac{\gamma_1(1-\beta_1)s + \gamma_0(m_1-\beta_0)}{s+m_1} + \frac{(1-\gamma_1)(1-\beta_1)s + (1-\gamma_0)(m_1-\beta_0)}{s+m_1} \\ &= R(s) + Q(s) \end{aligned} \tag{4.210}$$

Because of $\mathrm{I}_{B_w} = \varnothing, \Omega_{B_w} = \varnothing$, then $m_{WB,1} = 2$ for a zero root; and similarly $\mathrm{I}_{t_D} = \Omega_{t_D} = \varnothing$, hence $m_{WBt_D,1} = M_{WBt_D} = 2$. The number N_T of (free) parameters is also 2 (i.e. γ_0, γ_1), therefore these parameters can be determined unambiguously by the solution of

$$\begin{aligned} &[(1-\gamma_1)(1-\beta_1)s + (1-\gamma_0)(m_1-\beta_0)]_{s=0} = 0 \\ &\frac{\mathrm{d}}{\mathrm{d}s}[(1-\gamma_1)(1-\beta_1)s + (1-\gamma_0)(m_1-\beta_0)]_{s=0} = 0 \end{aligned} \tag{4.211}$$

The only solution is trivial, i.e. $\gamma_1 = \gamma_0 = 1$, yielding $Q(s) = 0, R(s) = T(s)$, which means that a simple feedback loop (1DoF) is obtained with the controller

$$G_R(s) = \frac{R(s)}{P(s)} = \frac{(s + a\exp(-\vartheta s))((1-\beta_1)s + (m_1-\beta_0))}{s^2 + (m_0+m_1)s + b(\beta_1-1)s\exp(-\tau s) + m_0m_1 + b(m_1-\beta_0)} \tag{4.212}$$

To overcome this dull result, try to take $Z(s)$ with more free parameters, say $N = 3$, to get some degrees of freedom, i.e.

$$\begin{aligned} &Z(s) = \frac{s+m_0}{s+a\exp(-\vartheta s)} \frac{\beta_2 s^2 + \beta_1 s + \beta_0}{(s+m_1)(s+m_2)} \\ &m_1, m_2 > 0 \end{aligned} \tag{4.213}$$

The reader can verify that after some calculations it is obtained

$$\beta_0 = b^{-1}m_1m_2(b-m_0),\ \beta_1 = b^{-1}\left(b(m_1+m_2)-m_1m_2-m_0(m_1+m_2+\tau m_1m_2)\right)$$
$$\beta_2 - \text{ arbitrary},\ \gamma_2 - \text{arbitrary},\ \gamma_1 = 0,\ \gamma_0 = 0 \tag{4.214}$$

where $N_T = 3$. We obtained two degrees of freedom β_2, γ_2, whereas the rest must be set as in (4.214). Final (a rather complex) controllers' structures are given by transfer functions

$$G_R(s) = \frac{R(s)}{P(s)} = \frac{(s+a\exp(-\vartheta s))\left((1-\gamma_2)(1-\beta_2)s^2+(m_1+m_2-\beta_1)s+(m_1m_2-\beta_0)\right)}{(s+m_0-b\exp(-\tau s))(s+m_1)(s+m_2)+b\exp(-\tau s)(\beta_2 s^2+\beta_1 s+\beta_0)}$$
$$G_Q(s) = \frac{Q(s)}{P(s)} = \frac{(s+a\exp(-\vartheta s))\gamma_2(1-\beta_2)s^2}{(s+m_0-b\exp(-\tau s))(s+m_1)(s+m_2)+b\exp(-\tau s)(\beta_2 s^2+\beta_1 s+\beta_0)} \tag{4.215}$$

Suppose a plant model in the form (4.161) with $a = b = 6.5\cdot 10^{-2}, \tau = 15.3,\ \ \vartheta = 6.7$, see [207]. A comparison of both results, i.e. (4.212) and (4.215), for the particular case, is displayed in Fig. 4.14, where $m_0 = m_1 = m_2 = 5\cdot 10^{-2}$, $\beta_2 = \gamma_2 = 0.5$.

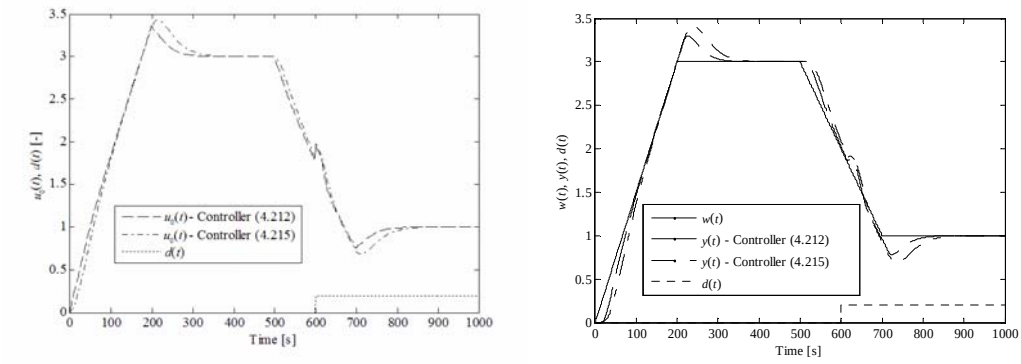

Fig. 4.14 Simulation control responses of $u_0(t)$ (left) and $y(t), w(t)$ (right) for $a = b = 6.5\cdot 10^{-2}$, $\tau = 15.3$, $\vartheta = 6.7$ using controllers (4.212) and (4.215)

Note that inversed values of m_0, m_1, m_2 appear as closed loop systems poles. Apparently, controller (4.212) offers faster control response in the example; however, two degrees of freedom can be used to tune the controller (4.215).

Alternatively, as another possibility, one can use $Z(s)$ as in (4.205) followed by

$$T(s)=\frac{(1-\beta_1)s+m_1-\beta_0}{s+m_1}\frac{s+\gamma}{s+\gamma} \tag{4.216}$$

with $\gamma>0$ as another semi-limited tuning parameter. ■

Example 4.14

Again, let the controlled plant be described by (4.161) with a stepwise reference signal and a harmonic load disturbance, which gives rise to

$$W(s)=\frac{H_W(s)}{F_W(s)}=\frac{\frac{w_0}{m_w(s)}}{\frac{s}{m_w(s)}},\ D(s)=\frac{H_D(s)}{F_D(s)}=\frac{\frac{d_0}{m_d(s)}}{\frac{s^2+\omega^2}{m_d(s)}} \tag{4.217}$$

where $m_w(s)$ and $m_d(s)$ are arbitrary stable retarded (quasi)polynomials of degree one and two, respectively. Consider the use of 1DoF control system. Follow the steps introduced in Subsection 4.3 using the notation utilized therein.

Stabilizing particular solution agrees with (4.165). It holds that $\Omega_W=\{0\}$, $m_{W,1}=1$, $\mathrm{I}_{A_w}=\varnothing, \Omega_{A_w}=\varnothing$, then $\overline{m}_{W,1}=m_{W,1}$. However, $\Omega_D=\{\omega\mathrm{j},-\omega\mathrm{j}\}$, $m_{D,1}=m_{D,2}=1$, $\mathrm{I}_{B_D}=\varnothing$, $\Omega_{B_D}=\varnothing$, $\overline{m}_{D,1}=m_{D,1}$. This gives $\Omega_{WD}=\{0,\omega\mathrm{j},-\omega\mathrm{j}\}$ with updated values of multiplicities $m_{WD,1}=m_{WD,2}=m_{WD,3}=1$. Since $\mathrm{I}_{p_D}=\varnothing, \Omega_{p_D}=\varnothing$, then $\overline{m}_{WD,i}=m_{WD,i}$, $i=1,2,3$. It means that it is necessary to place three single roots into $p_N(s)$ (or a real root and a complex conjugate pair of roots). Hence, it is possible to take e.g.

$$Z(s)=\frac{s+m_0}{s+a\exp(-\vartheta s)}\frac{\beta_2 s^2+\beta_1 s+\beta_0}{(s+m_1)(s+m_2)} \tag{4.218}$$

where $m_1, m_2>0$ are restricted parameters. Then

$$\begin{aligned}P(s)&=\frac{p_N(s)}{p_D(s)}\\&=\frac{(s+m_0-b\exp(-\tau s))(s+m_1)(s+m_2)-b(\beta_2 s^2+\beta_1 s+\beta_0)\exp(-\tau s)}{(s+a\exp(-\vartheta s))(s+m_1)(s+m_2)}\end{aligned} \tag{4.219}$$

The remaining parameters $\beta_0, \beta_1, \beta_2 \in \mathbb{R}$ are calculated from these three conditions

$$[p_N(s,\beta_0,\beta_1,\beta_2)]_{s=0}=0,\ [p_N(s,\beta_0,\beta_1,\beta_2)]_{s=\omega j}=0,[p_N(s,\beta_0,\beta_1,\beta_2)]_{s=-\omega j}=0 \tag{4.220}$$

which are coincident with

$$\begin{aligned}&[p_N(s,\beta_0,\beta_1,\beta_2)]_{s=0}=0\\&[\mathrm{Re}\{p_N(s,\beta_0,\beta_1,\beta_2)\}]_{s=\omega j}=0,[\mathrm{Im}\{p_N(s,\beta_0,\beta_1,\beta_2)\}]_{s=\omega j}=0\end{aligned} \tag{4.221}$$

The solution of (4.220) or (4.221) is rather complex which is the reason why it is not displayed here. Notice that $p_N(s)$ does not contain ϑ and thus the solution is independent on this delay.

The final controller structure reads

$$G_R(s)=\frac{q_3s^3+s^2(q_2+\exp(-\vartheta s)q_{2D})+s(q_1+\exp(-\vartheta s)q_{1D})+\exp(-\vartheta s)q_{0D}}{s^3+s^2(p_2+\exp(-\tau s)p_{2D})+s(p_1+\exp(-\tau s)p_{1D})+p_0+\exp(-\tau s)p_{0D}} \tag{4.222}$$

where

$$\begin{aligned}&q_3=1+\beta_2,\ q_2=m_1+m_2+\beta_1,\ q_{2D}=aq_3,\ q_1=m_1m_2+\beta_0,\ q_{1D}=aq_2,\\&q_{0D}=aq_1,\ p_2=m_0+m_1+m_2,\ p_{2D}=-b(1+\beta_2),\ p_1=m_2(m_0+m_1)+m_0m_1,\\&p_{1D}=-b(\beta_1+m_1+m_2),\ p_0=m_0m_1m_2,\ p_{0D}=-b(\beta_0+m_1m_2)\end{aligned} \tag{4.223}$$

As can be seen, the final controller has a complicated structure.

If the plant parameters are given as in Example 4.13, $d(t)=\sin(0.1t)$ and $m_0=m_1=0.1$, $m_2=0.05$, then $\beta_2=1.432$, $\beta_1=-0.495$, $\beta_0=-2.2\cdot10^{-3}$. Simulation results are displayed are in Fig. 4.15.

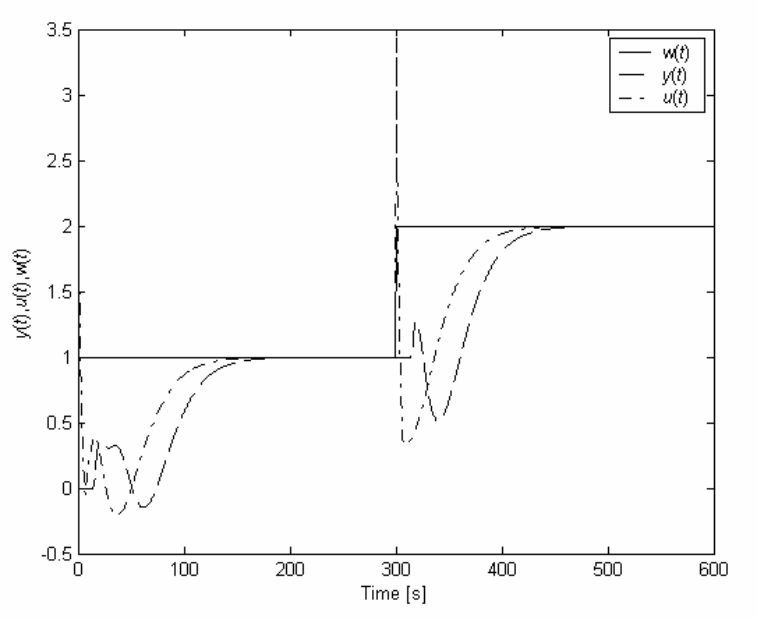

Fig. 4.15 Simulation control responses for $a = b = 6.5 \cdot 10^{-2}$, $\tau = 15.3$, $\vartheta = 6.7$ *using controller (4.222)*

5 TUNING OF ANISOCHRONIC CONTROLLERS

Final controllers obtained by the algebraic methodology described above contain free (selectable) real parameters which ought to be set appropriately. A sub-optimal controller tuning idea based on the desired or ultimate position of the rightmost feedback poles is the topic of this chapter. Its presentation is supported by a concise description of two numerical (iterative) optimization algorithms.

5.1 Estimation of a step response overshoot

The tuning algorithm stems from the dependence of the maximum relative step response overshoot and the relative time-to-overshoot on the position of poles and zeros of a finite-dimensional model. It is usable in the case of infinite-dimensional reference-to-output transfer function. The methodology will be demonstrated on a second order model.

Hence, let the prescribed (desired) closed-loop model be

$$G_{WY,m}(s) = \frac{b_1 s + b_0}{s^2 + a_1 s + a_0} = k \frac{s - z_1}{(s - s_1)(s - \bar{s}_1)} \tag{5.1}$$

where $k, b_1, b_0, a_1, a_0 \neq 0 \in \mathbb{R}$ are model parameters $z_1 \in \mathbb{R}_0^-$ stands for a model zero and $s_1 \in \mathbb{C}_0^-$ is a model stable pole where $\bar{s}_1$ expresses its complex conjugate. To obtain the unit static gain of $G_{WY,m}(s)$ it must hold that

$$\frac{b_0}{a_0} = 1, k = -\frac{|s_1|^2}{z_1} \tag{5.2}$$

Sign $s_1 = \alpha + \mathrm{j}\omega, \alpha < 0, \omega \geq 0$ and calculate the impulse function $g_{WY,m}(t)$ of $G_{WY,m}(s)$ using the Matlab function *ilaplace* as

$$g_{WY,m}(t) = k \exp(\alpha t)\left[\cos(\omega t) - \frac{z_1 - \alpha}{\omega}\sin(\omega t)\right] \tag{5.3}$$

Since $i_{WY,m}(t) = \dot{h}_{WY,m}(t)$, where $h_{WY,m}(t)$ is the step response function, the necessary condition for the existence of a step response overshoot at time t_O is

$$i_{WY,m}(t_O)=0, t_O>0 \tag{5.4}$$

The condition (5.4) yields these two solutions: either $t_O \to -\infty$ (which is trivial) or

$$t_O=\frac{1}{\omega}\arccos\left(\pm\frac{|\alpha-z_1|}{\sqrt{(\alpha-z_1)^2+\omega^2}}\right)=\frac{1}{\omega}\arctan\left(\frac{\omega}{-\alpha+z_1}\right) \tag{5.5}$$

when considering $\arccos(\cdot),\arctan(\cdot)\in[0,\pi], \omega>0$. Obviously, (5.5) has infinitely many solutions. If $\alpha<0, z_1<0$, the maximum overshoot occurs at time

$$t_{\max}=\min(t_O) \tag{5.6}$$

One can further calculate the step response function $h_{WY,m}(t)$ as

$$h_{WY,m}(t)=\frac{k}{|s_1|^2}\left[\exp(\alpha t)\left(z_1\cos(\omega t)-\frac{z_1\alpha-|s_1|^2}{\omega}\sin(\omega t)\right)-z_1\right] \tag{5.7}$$

Define now the maximum relative overshoot as

$$\Delta h_{WY,m,\max}:=\frac{h_{WY,m}(t_{\max})-h_{WY,m}(\infty)}{h_{WY,m}(\infty)} \tag{5.8}$$

see Fig. 5.1.

Using definition (5.8) one can obtain

$$\Delta h_{WY,m,\max}=\left[\exp(\alpha t)\left(\frac{-z_1\omega\cos(\omega t)+\left(z_1\alpha-|s_1|^2\right)\sin(\omega t)}{z_1\omega}\right)\right]_{t=t_{\max}} \tag{5.9}$$

Obviously, $\Delta h_{WY,m,\max}$ is a function of three parameters, i.e. z_1,α,ω, which is not suitable for a general formulation of the maximal overshoot. Hence, let us introduce new parameters ξ_α,ξ_z as

$$\xi_\alpha=-\frac{\alpha}{\omega},\ \xi_z=-\frac{z_1}{\omega} \tag{5.10}$$

which give rise from (5.5), (5.6) and (5.9) to

$$\Delta h_{WY,m,\max} = \frac{1}{\xi_z}\exp\left(-\xi_\alpha t_{\max,norm}\right)\left(-\xi_z\cos\left(t_{\max,norm}\right)+\left(\xi_\alpha^2+1-\xi_\alpha\xi_z\right)\sin\left(t_{\max,norm}\right)\right)$$

$$t_{\max,norm} = \omega t_{\max} = \min\left(\arccos\left(\pm\frac{|\xi_\alpha-\xi_z|}{\sqrt{(\xi_\alpha-\xi_z)^2+1}}\right)\right) = \min\left(\arctan\left(\frac{1}{\xi_\alpha-\xi_z}\right)\right)$$

(5.11)

where $t_{\max,norm}$ represents the normalized maximum-overshoot time.

We can successfully use Matlab to display function $\Delta h_{WY,m,\max}(\xi_\alpha,\xi_z)$ and $t_{\max,norm}(\xi_\alpha,\xi_z)$ graphically, for suitable ranges of ξ_α,ξ_z as can be seen from Fig. 5.2 – Fig. 5.6.

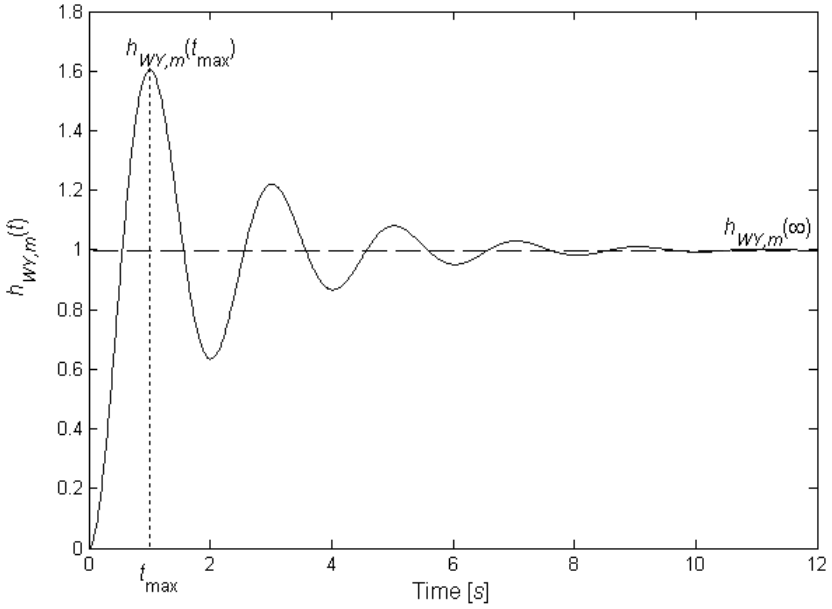

Fig. 5.1 Reference-to-output step response characteristics and the maximum overshoot

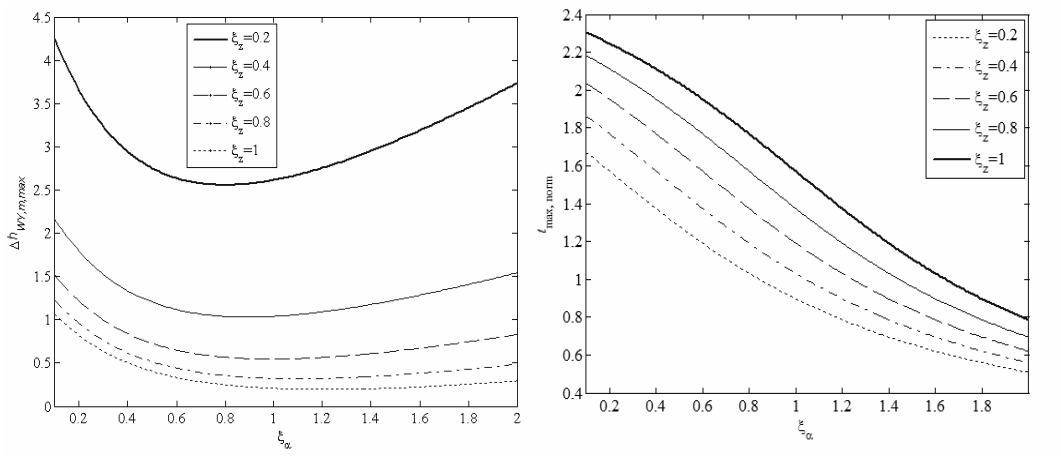

Fig. 5.2 Maximum overshoots $\Delta h_{WY,m,\max}(\xi_\alpha,\xi_z)$ *(left) and normalized maximum-overshoot times* $t_{\max,norm}(\xi_\alpha,\xi_z)$ *(right) for* $\xi_\alpha=[0.1,2],\ \xi_z=\{0.2,0.4,0.6,0.8,1\}$

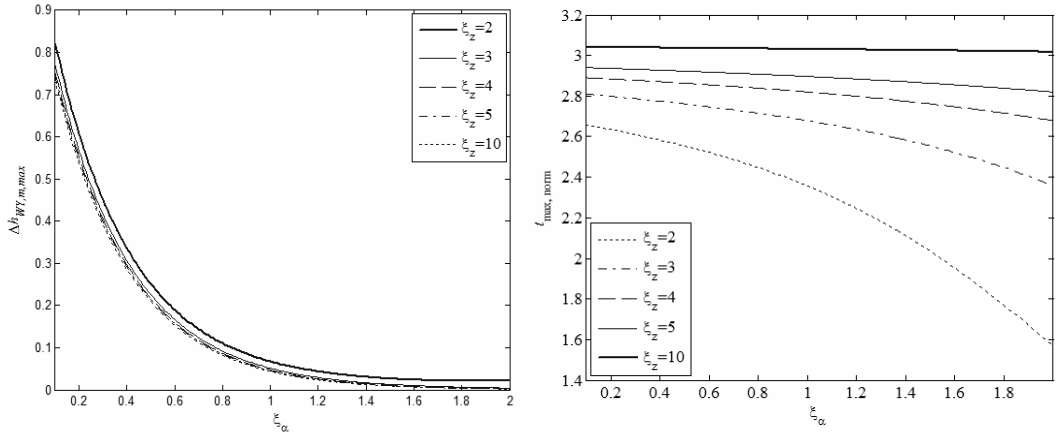

Fig. 5.3 Maximum overshoots $\Delta h_{WY,m,\max}(\xi_\alpha,\xi_z)$ *(left) and normalized maximum-overshoot times* $t_{\max,norm}(\xi_\alpha,\xi_z)$ *(right) for* $\xi_\alpha=[0.1,2],\ \xi_z=\{2,3,4,5,10\}$

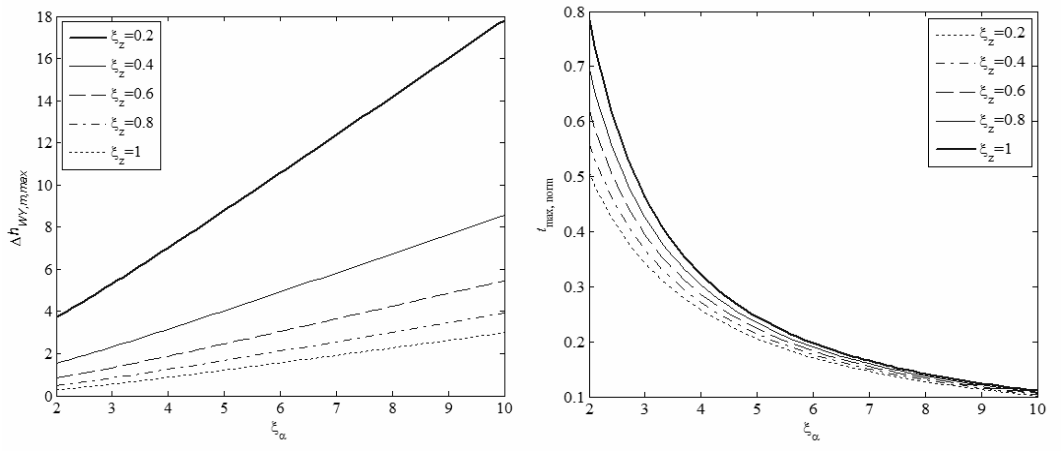

Fig. 5.4 Maximum overshoots $\Delta h_{WY,m,\max}(\xi_\alpha,\xi_z)$ *(left) and normalized maximum-overshoot times* $t_{\max,norm}(\xi_\alpha,\xi_z)$ *(right) for* $\xi_\alpha=[2,10],\ \xi_z=\{0.2,0.4,0.6,0.8,1\}$

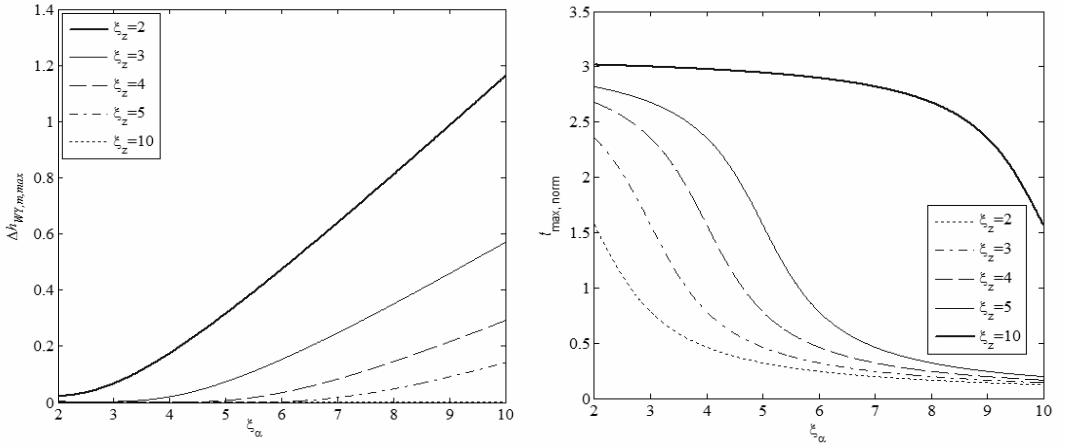

Fig. 5.5 Maximum overshoots $\Delta h_{WY,m,\max}(\xi_\alpha,\xi_z)$ *(left) and normalized maximal-overshoot times* $t_{\max,norm}(\xi_\alpha,\xi_z)$ *(right) for* $\xi_\alpha=[2,10],\ \xi_z=\{2,3,4,5,10\}$

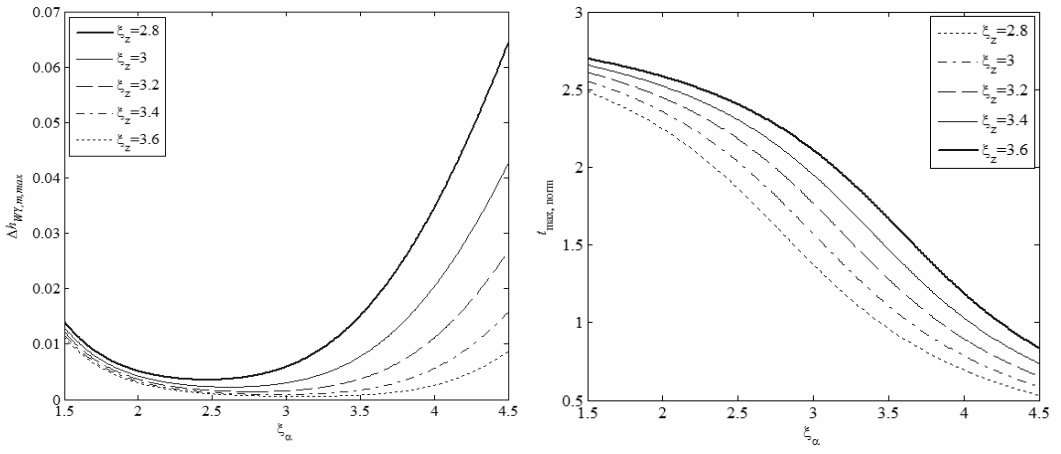

Fig. 5.6 Maximum overshoots $\Delta h_{WY,m,\max}(\xi_\alpha,\xi_z)$ *(left) and normalized maximal-overshoot times* $t_{\max,norm}(\xi_\alpha,\xi_z)$ *(right) for* $\xi_\alpha=[1.5,4.5]$, $\xi_z=\{2.8,3,3.2,3.4,3.6\}$ *- A detailed view on "small" overshoots*

The procedure of searching suitable prescribed poles can be done e.g. as in the following way. A user requires $\Delta h_{WY,m,\max}=0.03$ (i.e. the maximal overshoot equals 3 %), $\xi_\alpha=4$ (i.e. "the quarter dumping") and $t_{\max}=5\,\mathrm{s}$. Fig. 5.6 gives approximately $\xi_z=2.9$ which yields $t_{\max,norm}\approx 1.2$. These two values together with (5.10) and (5.11) result in $s_1=-0.96+0.24\,\mathrm{j}$, $z_1=-0.7$.

5.2 Continuous pole placement for desired overshoot

The idea now is to gradually shift the rightmost (dominant) poles of the infinite-dimensional reference-to-output transfer function to the prescribed positions found by the procedure introduced in the preceding subchapter.

The algorithm, called the Pole-Placement Shifting based controller tuning Algorithm (PPSA), is based on the QCSA described in Subchapter 2.6.3. The submethod based on [90] is utilized below; however, the PPSA can be easily modified to the use of the calculations by Vyhlídal [171]. Moreover, only retarded TDS are considered in Algorithm 5.1 – the

extension to neutral systems can be made by analogously to Algorithm 2.1 and remarks about neutral TDS introduced in Subchapter 2.6.3.

Algorithm 5.1

Input: Closed-loop reference-to-output transfer function $G_{WY}(s)$ with the number of *r* parameters in the set $\mathbf{K} = \mathbf{K}_{num} \cup \mathbf{K}_{den}$, where $\mathbf{K}_{num}$ is its subset of r_{num} parameters in the numerator, whereas $\mathbf{K}_{den}$ means the subset with the number of r_{den} parameters in the denominator. Let $r_{nd} = |\mathbf{K}_{num} \setminus (\mathbf{K}_{num} \bigcap \mathbf{K}_{den})| = |\mathbf{K}_{nd}|$.

Step 1: Choose a simple model of a stable finite-dimensional system with the unit static gain in the form of the transfer function $G_{WY,m}(s)$ with a numerator of degree $n_{num} \le r_{nd}$ and the denominator of degree $n_{den} \le r_{den}$. Calculate step response maximum overshoots of the model for a suitable range of its n_{num} zeros and n_{den} poles (including their multiplicities).

Step 2: Prescribe all poles of the model with respect to the calculated maximum overshoot (and the maximal overshoot time). If the poles are dominant (i.e. the rightmost), the procedure is finished. Otherwise do following steps.

Step 3: Initialize the counter of currently shifted poles as $n_{sp} = n_{den}$. Shift the rightmost poles to the prescribed locations successively using the QCSA. If necessary, increase n_{sp}. If $n_{den} < n_{sp} \le r_{den}$, try to move the rest of dominant (rightmost) poles to the left, again e.g. using the QCSA.

Step 4: If all prescribed poles are dominant, the procedure is finished. Otherwise, select a suitable cost function reflecting the distance of dominant poles from prescribed positions and distances of spectral abscissas of both, prescribed and dominant poles. Minimize the cost function.

Step 5: Do Steps 2-4 for prescribed zeros, where it holds for the number n_{sz} of currently shifted zeros that $n_{num} \le n_{sz} \le r_{nd}$, to update the values of $\mathbf{K}_{nd}$.

Output: The vector of controller parameters $\mathbf{K}$ and the positions of the rightmost poles. ■

Some remarks on the algorithm follow. First of all, the presented version of the PPSA prefers the positions of feedback poles at the expense of zeros. Once the set $\mathbf{K}_{den}$ is found, these values are fixed in the numerator and $\mathbf{K}_{nd}$ is to be found subsequently. Alternatively, it is possible to "merge" the shifting of zeros and poles, which may, however, lead to problems when reaching control system stability because of the "weight" put on zeros.

In case of multiple shifted poles, it is convenient to consider them as two (or more) close single poles.

The rightmost shifted pole (zero) goes toward the rightmost prescribed pole etc. Problem appears e.g. when a complex conjugate pair ought to be shifted to a real position, and viceversa. In both cases, a complex pair must be perceived as two separate poles.

Since the shifting comes to pass not only in the real axis, formula (2.95) can not be used in general. The following approximation ought to be used instead

$$\Delta\mathbf{K} \approx \mathrm{Re}\left\{\mathbf{S}^{+}\Delta\boldsymbol{\sigma}\right\} \tag{5.12}$$

or try to utilize

$$\mathrm{Re}\{\Delta\sigma_i\} = \mathrm{Re}\left\{\frac{\Delta\sigma_i}{\Delta K_j}\right\}\Delta K_j, \mathrm{Im}\{\Delta\sigma_i\} = \mathrm{Im}\left\{\frac{\Delta\sigma_i}{\Delta K_j}\right\}\Delta K_j \tag{5.13}$$

in the sensitivity matrix for real ΔK_j.

The number $n_{sp} \in [n_{den}, r_{den}]$ or $n_{sz} \in [n_{nun}, r_{nd}]$ is incremented whenever the approaching starts to fail for any pole or zero, respectively.

The optimization of the cost function from Step 4 can be done using several methods. Two advanced iterative algorithms are described in the following two subchapters. They can be useful for the spectral abscissa minimization introduced in Subchapter 2.6.4 as well, see e.g. [133].

5.3 Self-Organizing Migration Algorithm

The Self-Organizing Migration Algorithm (SOMA) is ranked among evolution algorithms, more precisely genetic algorithms, dealing with populations similarly as differential evolution does, see e.g. [192]. The algorithm is based on vector operations over the space of feasible solutions (parameters) in which the population is defined. In the SOMA, every single generation, in which a new population is generated, is called a migration round. Population specimens cooperate while searching the best solution (the minimum of the cost function) and, simultaneously, each of them tries to be a leader. They move to each other and the searching is finished when all specimens are localized on a small area.

The method converges very fast; however, the number of function evaluations within iteration can be very high - depending on the number of specimens and step length when moving on the hyperspace.

The main steps of the basic algorithm strategy called “All to One” can be formulated as follows.

Algorithm 5.2

Input: Objective function $\Phi(\mathbf{K})$.

Step 1: Set control and termination parameters. Generate a population based on a selected prototypal specimen.

Step 2: Find the best specimen (leader), i.e. that with the minimal function value.

Step 3: Move all other specimens towards the leader and evaluate their function values in each step.

Step 4: Select the new population and test the minimal divergence of the population. If it succeeds, stop. Otherwise, go to Step 2.

Output: The leader and its function value. ■

Look at these steps in more details. A population described below in a separate subsection must be generated based on a prototypal specimen. This specimen is a vector of

controller (free) parameters $\mathbf{K}$ which can be found e.g. by the quasi-continuous poles shifting algorithm.

Specific control and termination parameters, which have to be set before the rest of the algorithm starts, are explained in this subchapter. Two parameters, the initial radius (*Rad*) and the size of the population (*PopSize*), control the construction of an initial population based on the prototypal specimen. *Rad* > 0 should be chosen high enough to cover the range of all acceptable parameters. *PopSize* > 0 means the number of specimens in the population – the higher value yields a higher chance to find a global minimum yet the computational time increases.

The moving of specimens on the hyperspace of searched parameters is given by four control parameters: *PathLength*, *Step*, *PRT* and $\mathbf{v}_{PRT}$. *PathLength* should be within the interval $[1.1, 5]$ and it expresses the length of the path when approaching the leader. For instance, *PathLength* = 1 means that the specimen stops its moving exactly at the position of the leader. The value of $Step \in [0.11, PathLength]$ represents the sampling of the path. E.g. a pair of settings *PathLength* = 1 and *Step* = 0.2 agrees with that the specimen makes five steps until it reaches the leader. $PRT \in [0,1]$ enables to calculate the perturbation vector $\mathbf{v}_{PRT}$ which indicates whether the active specimen moves to the leader directly or not. $\mathbf{v}_{PRT}$ is defined as

$$\begin{aligned} &\mathbf{v}_{PRT} = [v_{PRT,1}, v_{PRT,2}, \ldots, v_{PRT,r}]^T \in \{0,1\}^r \\ &v_{PRT,j} = 1 \qquad \text{if } rnd_j < PRT \\ &v_{PRT,j} = 0 \qquad \text{else} \\ &j = 1,2,\ldots,r \end{aligned} \tag{5.14}$$

where $rnd_j \in [0,1]$ is a randomly generated number for each coordinate of a specimen. The perturbation vector enters stochasticity to the specimens moving.

There are two termination parameters in the algorithm: *M*, *MinDiv*. The value of *M* means the maximal number of migration rounds defined by the user, and *MinDiv* expresses the selected minimal diversity, i.e. the algorithm running is terminated if

$$\max_j \Phi(\mathbf{K}_{i,j}) - \min_j \Phi(\mathbf{K}_{i,j}) < MinDiv \tag{5.15}$$

where a subscript *i* means the current iteration (migration round) and *j* denotes the *j*th specimen in the current population.

As mentioned above, population $P = \{\mathbf{K}_1, \mathbf{K}_2, ..., \mathbf{K}_{PopSize}\}$ has to be generated based on a prototypal specimen controlled by parameters *Rad* and *PopSize*. Let $\mathbf{K}_1$ be the prototypal specimen, then other specimens can generated as

$$\mathbf{K}_j = \mathbf{K}_1 + Rad[rnd_1, rnd_2, ..., rnd_r]^T,\ j = 2,3,..., PopSize \tag{5.16}$$

where $rnd_i \in [-1,1], i = 1,2,..., r$, is a random number. Each specimen in the population is then evaluated by the cost function.

Once the population is generated (or generally after every migration round in the *i*th iteration) the best valued specimen, so called leader, $\mathbf{K}_{i,L}$, which is determined as

$$\mathbf{K}_{i,L} = \arg\min_j \Phi(\mathbf{K}_{i,j}),\ j = 1,2,..., PopSize \tag{5.17}$$

All other specimens are then moved towards the leader during the migration round. The movement randomness is given by $\mathbf{v}_{PRT}$. Although the authors of the SOMA suggest to calculate $\mathbf{v}_{PRT}$ only once in migration round for every specimen, we try to do this in every step of the moving to the leader. Hence, the path is given by

$$\begin{aligned} &\mathbf{K}_{i,j,k} = \mathbf{K}_{i,j,0} + Step[(k-1)(\mathbf{K}_{i,L} - \mathbf{K}_{i,j,0}) + \mathrm{diag}(\mathbf{v}_{PRT})(\mathbf{K}_{i,L} - \mathbf{K}_{i,j,0})] \\ &j = 1,2,...PopSize \neq L; k = 1,2,..., \mathrm{round}(PathLength / Step) \end{aligned} \tag{5.18}$$

where $\mathrm{diag}(\mathbf{v}_{PRT})$ means the diagonal square matrix with elements of $\mathbf{v}_{PRT}$ on the main diagonal and *k* is the *k*-th step in the path of the *j*th specimen in the current population (in *i*th iteration).

The role of $\mathbf{v}_{PRT}$ is evident, for instance, if $\mathbf{v}_{PRT} = [1,1,...,1]^T$, the active specimen goes to the leader directly without “zig-zag” moves.

For every specimen of the population in a migration round, the cost function (i.e. value of the specimen) is calculated in every single step during the moving towards the leader. If the current position is better then the actual best, it becomes the best now. Hence, the new position of an active specimen for the next migration round is given by the best position of the specimen from all steps of moving towards the leader within the current migration round, i.e.

$$\mathbf{K}_{i+1,j} = \arg\min_{k} \Phi\left(\mathbf{K}_{i,j,k}\right), k = 0,1,..., \text{round}\left(PathLength / Step\right) \tag{5.19}$$

These specimens then generate the new population for the next migration round (iteration).

5.4 Nelder-Mead iterative optimization algorithm

The Nelder-Mead (NM) algorithm belonging to the class of comparative (direct search) algorithms, also called irregular simplex search algorithm, was originally published in [105]. This easy-to-use method does not require derivatives of the objective function and thus it is suitable for non-smooth functions. It is very popular and can be implemented in many different ways.

The method typically requires only one or two function evaluations per iteration, which is useful especially in applications where each function evaluation is time-consuming. On the other hand, the algorithm can fail since the convergence for non-smooth or discontinuous functions have not been proved yet [152]. It can also require an enormous amount of iterations to obtain a significant improvement in function value.

Consider a nonlinear objective function $\mathbf{K} \in \mathbb{R} \rightarrow \Phi\left(\mathbf{K}\right) \in \mathbb{R}^r$ to be minimized. The basic steps of the general algorithm can be done as follows.

Algorithm 5.3

Input: Objective function $\Phi\left(\mathbf{K}\right)$.

Step 1: Construct the initial working simplex *S*, set transformation and termination parameters.

Step 2: Calculate the termination test information. If the test is satisfied, stop the algorithm.

Step 3: Order simplex vertices as the worst, second worst and the best one.

Step 4: Calculate the central point and reflex the worst vertex. If the reflection is successful, accept the reflected point in the new working simplex and go to Step 3.

Step 5: Try to use contraction or expansion. If this succeeds, the accepted point becomes the new vertex; otherwise, shrink the simplex towards the best vertex. Go to Step 3.

Output: The best vertex and its function value. ■

Let us describe each step of the algorithm in more details. A simplex S in $\mathbb{R}^r$ is a convex hull of $r+1$ vertices $\mathbf{K}_1,\mathbf{K}_2,...,\mathbf{K}_{r+1} \in \mathbb{R}^r$

$$S = \text{conv}\{\mathbf{K}_1,\mathbf{K}_2,...,\mathbf{K}_{r+1}\} \tag{5.20}$$

The initial (non-degenerate) simplex can be constructed either as a regular or as a right-angled simplex. The latter is easier to handle as

$$\mathbf{K}_j = \mathbf{K}_1 + h_j \mathbf{e}_j,\ j = 2,...,r+1 \tag{5.21}$$

where $\mathbf{K}_1$ is a "starting" point, h_j stands for a stepsize and $\mathbf{e}_j$ is a unit (Euclidean) vector in $\mathbb{R}^r$.

During the minimization, the simplex changes in its size and shape as well. The algorithm terminates when either the simplex is sufficiently small or the function values at the vertices are close to each other or the number of iterations reaches the prescribed number. Usually some of these three conditions are combined together and the procedure ends when at least one of the conditions becomes true. We use the limit number of iterations, say *ni*. Moreover, for discontinuous functions, the termination test has to include the information of the simplex size [152] whereas the function values test is useless. Let ε_S is the limit simplex size defined by the user, and then the termination test related to the simplex size can be formulated as

$$\sum_{i=2}^{r+1} \left\| \mathbf{K}_i - \mathbf{K}_1 \right\| < \varepsilon_S \tag{5.22}$$

Determine the best ($\mathbf{K}_{min}$), second worst ($\mathbf{K}_s$) and the worst vertex ($\mathbf{K}_{max}$) as

$$\Phi_{min} = \min_i \Phi(\mathbf{K}_i), \Phi_{max} = \max_i \Phi(\mathbf{K}_i), \Phi_s = \max_{i \neq max} \Phi(\mathbf{K}_i) \tag{5.23}$$

The central point can be imagined as the "mean" coordinate of all vertices except the worst one, i.e.

$$\mathbf{K}_c = \frac{1}{r} \sum_{\substack{i=1 \\ i \neq max}}^{r} \mathbf{K}_i \tag{5.24}$$

The calculation of the new simplex then continues by reflecting $\mathbf{K}_{max}$ over $\mathbf{K}_c$ to a new position $\mathbf{K}_{ref}$ according to the formula

$$\mathbf{K}_{ref} = \mathbf{K}_c + \alpha(\mathbf{K}_c - \mathbf{K}_{max}) \tag{5.25}$$

where $\alpha > 0$ is a reflection control parameter, usually $\alpha = 1$.

If it holds that $\mathbf{K}_{min} \leq \mathbf{K}_{ref} < \mathbf{K}_s$, the iteration is finished and $\mathbf{K}_{ref}$ becomes a new simplex point instead of $\mathbf{K}_{max}$.

If the reflection does not succeed, one has to perform expansion or contraction, depending on the value of $\Phi(\mathbf{K}_{ref})$ relation to $\Phi(\mathbf{K}_{min})$, $\Phi(\mathbf{K}_s)$ and $\Phi(\mathbf{K}_{max})$. Hence, if $\Phi(\mathbf{K}_{ref}) < \Phi(\mathbf{K}_{min})$, i.e. the reflected point is the best one, the expansion point is computed as follows

$$\mathbf{K}_{exp} = \mathbf{K}_c + \beta(\mathbf{K}_{ref} - \mathbf{K}_c) \tag{5.26}$$

where $\beta > 1$ is an expansion control parameter, usually $\beta = 2$. There are more ways how to construct the new working simplex; however, to avoid premature termination of iterations for non-smooth functions, see [147], $\mathbf{K}_{exp}$ becomes the new simplex vertex if $\Phi(\mathbf{K}_{exp}) < \Phi(\mathbf{K}_{min})$. Otherwise, $\mathbf{K}_{ref}$ is accepted.

There are two types of contractions; first, if $\Phi(\mathbf{K}_s) \leq \Phi(\mathbf{K}_{ref}) < \Phi(\mathbf{K}_{max})$, compute the contracted point as

$$\mathbf{K}_{con} = \mathbf{K}_c + \gamma\left(\mathbf{K}_{ref} - \mathbf{K}_c\right) \tag{5.27}$$

where $0 < \gamma < 1$ is a contraction control parameter mostly set as $\gamma = 0.5$. If $\Phi\left(\mathbf{K}_{con}\right) < \Phi\left(\mathbf{K}_{ref}\right)$, $\mathbf{K}_{con}$ becomes a vertex in the new working simplex; otherwise, shrinkage has to be made. On the contrary, if $\Phi\left(\mathbf{K}_{ref}\right) \geq \Phi\left(\mathbf{K}_{max}\right)$, i.e. $\mathbf{K}_{ref}$ is the worst point, one ought to perform contraction according to

$$\mathbf{K}_{con} = \mathbf{K}_c + \gamma\left(\mathbf{K}_{max} - \mathbf{K}_c\right) \tag{5.28}$$

If it holds that $\Phi\left(\mathbf{K}_{con}\right) < \Phi\left(\mathbf{K}_{max}\right)$, accept $\mathbf{K}_{con}$; otherwise, perform shrinkage.

In the case that expansion or contraction fails, one has to shrink the current simplex towards the best vertex $\mathbf{K}_{min}$. This operation is given by the formula

$$\mathbf{K}_i = \mathbf{K}_{min} + \delta\left(\mathbf{K}_i - \mathbf{K}_{min}\right), i = 1,2,...,r+1 \neq min \tag{5.29}$$

Experiences with the algorithm show that shrink transformations almost never happen in practice [152]. A non-shrink iteration of the algorithm is fast, since only one or two function values are computed.

5.5 Study case: A skater on the swaying bow

The presented example demonstrates the algebraic controller desing in the R_{MS} ring for an unstable retarded TDS plant followed by the tuning process and setting according to the PPSA and the spectral abscissa optimization via some iterative algorithms. The aim is to test and verify tuning approaches primarily, thus, the 1DoF control structure is utilized here instead of TFC which would give a better controller structure (i.e. quasi-finite spectrum assignment).

Consider an unstable system as in Fig. 5.7 expressing the roller skater a controlled swaying bow. In [202] it has been stated that the transfer function of the system reads

$$G(s) = \frac{Y(s)}{U(s)} = \frac{b\exp\left(-\left(\tau + \vartheta\right)s\right)}{s^2\left(s^2 - a\exp\left(-\upsilon s\right)\right)} \tag{5.30}$$

where $y(t)$ is the skater's deviation from the bow symmetry axis, $u(t)$ expresses the slope angle of a bow caused by force *P*, delays τ, ϑ means the skater's and servo latencies, respectively, and *b*, *a* are real parameters. Skater controls the servo driving by remote signals into servo electronics. As presented in the literature, let b = 0.2, a = 1, $\tau = 0.3$ s, $\vartheta = 0.1$ s.

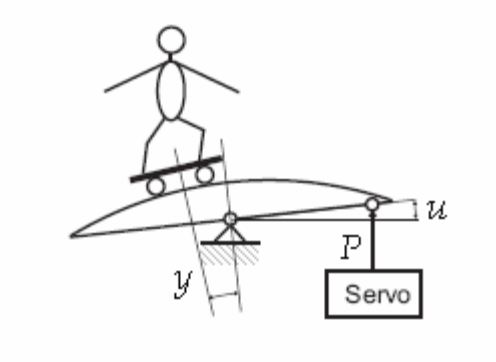

Fig. 5.7 Roller skater on a controlled swaying bow

5.5.1 Controller structure design

First of all, factorize the plant transfer function as

$$G(s) = \frac{B(s)}{A(s)} = \frac{\dfrac{b\exp(-(\tau+\vartheta)s)}{(s+m_0)^4}}{\dfrac{s^2(s^2 - a\exp(-\vartheta s))}{(s+m_0)^4}},\ A(s), B(s) \in \mathbf{R}_{MS} \tag{5.31}$$

where $m_0 > 0$ is a selectable real parameter. Consider the reference and load disturbance in the form of stepwise functions, hence their Laplace forms are respectively

$$W(s) = \frac{H_W(s)}{F_W(s)} = \frac{\dfrac{w_0}{m_W(s)}}{\dfrac{s}{m_W(s)}},\ D(s) = \frac{H_D(s)}{F_D(s)} = \frac{\dfrac{d_0}{m_D(s)}}{\dfrac{s}{m_D(s)}} \tag{5.32}$$

where w_0, $d_0 \in$ R, $m_W(s)$ and $m_W(s)$ are arbitrary stable (retarded) (quasi)polynomials of degree one and $H_W(s), H_D(s), F_W(s), F_D(s) \in R_{MS}$.

Stabilization formula (4.33) using the generalized Euclidean algorithm yields e.g.

$$Q_0(s) = \frac{\left(q_3 s^3 + q_2 s^2 + q_1 s + q_0\right)(s+m_0)^4}{s^2\left(s^2 - a\exp(-\vartheta s)\right)\left(s^3 + p_2 s^2 + p_1 s + p_0\right) + b\exp\left(-(\tau+\vartheta)s\right)\left(q_3 s^3 + q_2 s^2 + q_1 s + q_0\right)}$$

$$P_0(s) = \frac{\left(s^3 + p_2 s^2 + p_1 s + p_0\right)(s+m_0)^4}{s^2\left(s^2 - a\exp(-\vartheta s)\right)\left(s^3 + p_2 s^2 + p_1 s + p_0\right) + b\exp\left(-(\tau+\vartheta)s\right)\left(q_3 s^3 + q_2 s^2 + q_1 s + q_0\right)} \tag{5.33}$$

where p_2, p_1, p_0, q_3, q_2, q_1, $q_0 \in \mathbb{R}$ are free parameters. Notice that numerical experiments shown that a smaller number of parameters could not satisfy denominator stability.

In order to satisfy tasks of stepwise reference tracking and load disturbance rejection, parameterization (4.34) can be used so that both, $F_W(s)$ and $F_D(s)$, divide $P(s)$; hence, the numerator of $P(s)$ satisfies $P(0)=0$. To make $P(s)$ as simple as possible, choose

$$Z(s) = \frac{z_0(s+m_0)^4}{s^2\left(s^2 - a\exp(-\vartheta s)\right)\left(s^3 + p_2 s^2 + p_1 s + p_0\right) + b\exp\left(-(\tau+\vartheta)s\right)\left(q_3 s^3 + q_2 s^2 + q_1 s + q_0\right)} \tag{5.34}$$

where $z_0 \in \mathbb{R}$ is a selectable parameter. Both divisibility conditions are satisfied if

$$z_0 = \frac{-p_0 m_0^4}{b} \tag{5.35}$$

This results in the final anisochronic controller transfer function

$$G_R(s) = \frac{Q(s)}{P(s)} = \frac{b\left(q_3 s^3 + q_2 s^2 + q_1 s + q_0\right)(s+m_0)^4 + p_0 m_0^4 s^2\left(s^2 - a\exp(-\vartheta s)\right)}{b\left[\left(s^3 + p_2 s^2 + p_1 s + p_0\right)(s+m_0)^4 - p_0 m_0^4\exp\left(-(\tau+\vartheta)s\right)\right]} \tag{5.36}$$

The reference-to-output transfer function reads

$$G_{WY}(s)=\frac{1}{(s+m_0)^4}$$
$$\frac{b\left[b\left(q_3s^3+q_2s^2+q_1s+q_0\right)(s+m_0)^4+p_0m_0^4s^2\left(s^2-a\exp(-\vartheta s)\right)\right]\exp(-(\tau+\vartheta)s)}{s^2\left(s^2-a\exp(-\vartheta s)\right)\left(s^3+p_2s^2+p_1s+p_0\right)+b\exp(-(\tau+\vartheta)s)\left(q_3s^3+q_2s^2+q_1s+q_0\right)} \tag{5.37}$$

which gives rise to the characteristic quasipolynomial

$$m(s)=(s+m_0)^4$$
$$\left[s^2\left(s^2-a\exp(-\vartheta s)\right)\left(s^3+p_2s^2+p_1s+p_0\right)+b\exp(-(\tau+\vartheta)s)\left(q_3s^3+q_2s^2+q_1s+q_0\right)\right] \tag{5.38}$$

Obviously, there are two factors in (5.38), a polynomial and a quasipolynomial one. Since the spectral assignment for the polynomial factor is trivial, the goal is to set up dominant roots or minimize the spectral abscissa, respectively, of the quasipolynomial factor with seven unknown parameters. To cancel the impact of the quadruple real pole $s_1=-m_0$, it must hold that $m_0>>-\alpha(\mathbf{K})$.

5.5.2 Desired maximum overshoot

Follow now the methodology introduced in Subchapter 5.2. Clearly, $r=r_{den}=7$, $r_{num}=5$, $r_{nd}=0$, $\mathbf{K}=[q_3,q_2,q_1,q_0,p_2,p_1,p_0]^T$ and consider $G_{WY,m}(s)$ according to (5.1).

Now, there are two possibilities – either set zero exactly to obtain constrained controller parameter (then r_{den} = 6) or to deal with the numerator and denominator of (5.37) together – we decided to utilize the former one first (version 1). Generally, one can obtain from (5.37)

$$p_0=-\frac{b(z_1+m_0)^4\left(q_3z_1^3+q_2z_1^2+q_1z_1+q_0\right)}{m_0^4z_1^2\left(z_1^2-a\exp(-\vartheta z_1)\right)} \tag{5.39}$$

Choose $\Delta h_{WY,m,\max}=0.5$, $\xi_\alpha=0.5$ and $t_{\max}=10$ s. From Fig. 5.2 we have $\xi_z=0.9$, $t_{\max,norm}\approx 2$ which gives $\omega=0.2, z_1=-0.18, \alpha=-0.1$. Then take e.g. $m_0=5$. Inserting plant parameters in (5.39) yields

$$p_0 = 5.4078\left(q_0 - 0.18q_1 + 0.0324q_2 - 0.005832q_3\right) \tag{5.40}$$

The particular quasipolynomial which roots are being set, thus, reads

$$\begin{aligned} m_1(s) = {} & s^2\left(s^2 - \exp(-0.1s)\right) \\ & \left(s^3 + p_2 s^2 + p_1 s + 5.4078\left(q_0 - 0.18q_1 + 0.0324q_2 - 0.005832q_3\right)\right) \\ & + 0.2\exp(-0.4s)\left(q_3 s^3 + q_2 s^2 + q_1 s + q_0\right) \end{aligned} \tag{5.41}$$

Initial direct pole placement results in controller parameters as

$$\mathbf{K}_0 = \left[1.1014, 0.9852, -0.0113, 0.0171, 1.113, 0.7, 0.2411\right]^T \tag{5.42}$$

which gives the rightmost spectrum of poles

$$\Omega_{p,0} = \left\{0.8959, 0.1445, -0.1 \pm 0.2\,\mathrm{j}, -0.5201 \pm 0.5029\,\mathrm{j}, -1.0114\right\} \tag{5.43}$$

and zeros

$$\Omega_{z,0} = \left\{-0.1373 \pm 0.1536\,\mathrm{j}, -0.18, -1.0822, -2.3507 \pm 0.8.4523\,\mathrm{j}\right\} \tag{5.44}$$

Hence, the prescribed poles and zeros are not dominant ones. The process of the PPSA is described by the evolution of controller parameters, the spectral abscissa (i.e. the real part of the rightmost pole pair $\sigma_1, \overline{\sigma}_1$) and the distance of the dominant pole from the prescribed one $\left|\sigma_1 - s_1\right|$, as can be seen in Fig. 5.8 – Fig. 5.9, respectively. Note that p_0 is related to shifted parameters according to (5.40).

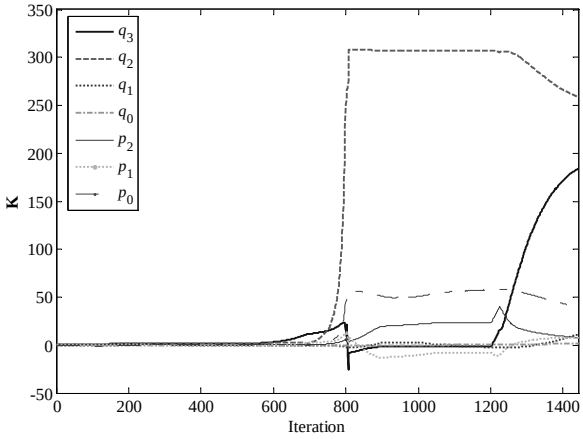

Fig. 5.8 Evolution of **K** *using the PPSA – version 1*

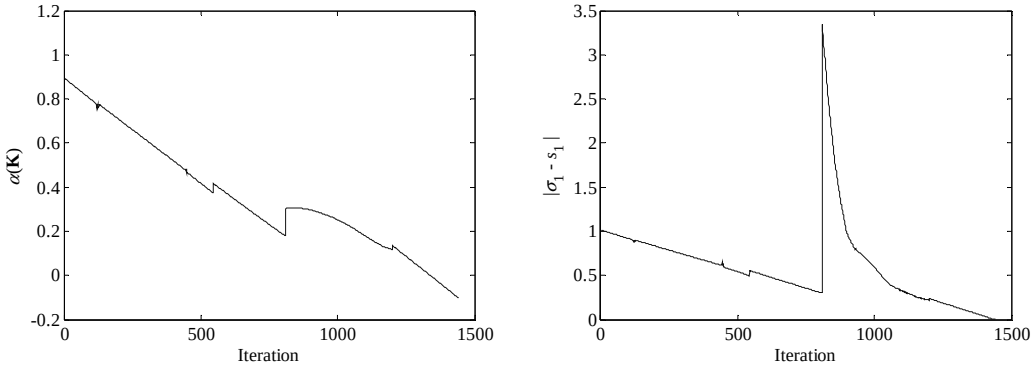

Fig. 5.9 Evolution of $\alpha(\mathbf{K})$ *(left) and* $|\sigma_1 - s_1|$ *(right) using the PPSA – version 1*

The rightmost pole reaches the vicinity of the desired position in the iteration number i = 1440. The peak in Fig. 5.9 (left) is caused by a bifurcation of a double real root to a complex conjugate pair. The final controller parameters from the PPSA (version 1) are the following

$$\mathbf{K}_{1440} = [183.566, 259.076, 11.083, 2.0754, 0.0171, 7.8427, 8.0865, 40.039]^T \quad (5.45)$$

giving rise to the spectrum (poles)

$$\Omega_{p,1440} = \{-0.0999 \pm 0.1989\,\mathrm{j}, -0.1449 \pm 0.7574\,\mathrm{j}, -0.298 \pm 1.4563\,\mathrm{j}\} \quad (5.46)$$

and zeros

$$\Omega_{z,1440} = \{0.0091 \pm 0.1817\,\mathrm{j}, -0.18, -0.9768, -2.4832 \pm 8.5435\,\mathrm{j}\} \quad (5.47)$$

In order to improve this result, an optimization procedure minimizing the objective (cost) function

$$\Phi(\mathbf{K}) = |\sigma_1 - s_1| + \lambda \alpha_r(\mathbf{K}) \quad (5.48)$$

has been performed where σ_1 is a pole from the dominant pair in (5.46), s_1 stands for a pole from the prescribed pair of poles, $\alpha_r(\mathbf{K})$ means the spectral abscissa of the rest of poles except the dominant pair and λ represents a weighting parameter (here $\lambda = 0.01$ has been chosen). The optimization results via the SOMA are then the following

$$\mathbf{K}_{1440,opt} = [185.202, 259.114, 11.253, 2.0971, 7.7535, 7.9451, 39.946]^T$$
$$\boldsymbol{\Omega}_{p,1440,opt} = \{-0.0999 \pm 0.2\,\mathrm{j}, -0.1712 \pm 0.7565\,\mathrm{j}, -0.2609 \pm 1.4552\,\mathrm{j}\} \quad (5.49)$$
$$\boldsymbol{\Omega}_{z,1440,opt} = \{0.0093 \pm 0.1822\,\mathrm{j}, -0.18, -0.9787, -2.4821 \pm 8.5423\,\mathrm{j}\}$$

Unfortunately, the prescribed zero is not the dominant one in both cases; therefore, the obtained results are useless since their dynamic characteristics (e.g. the step responses) are far from the desired one.

As a second (version 2), simultaneous shifting of poles and zeros of (5.37) to the desired positions has been performed. It must hold that $n_{den} + n_{num} \le n_s \le r_{den} + r_{nd}$, where n_s means the cumulative number of shifted (controlled) zeros and poles, here.

The initial setting of $\mathbf{K}_0$ and the corresponding spectra of poles and zeros are given by (5.42) – (5.44). The process of evolution of $\mathbf{K}$ is depicted in Fig. 5.10.

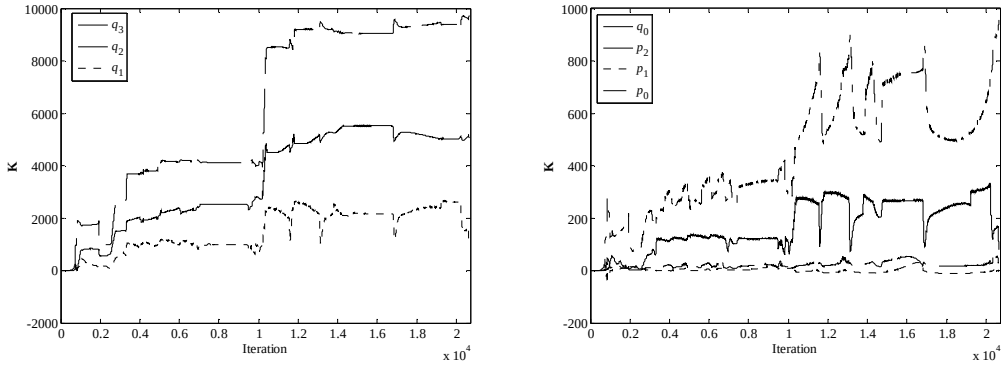

Fig. 5.10 Evolution of **K** *using the PPSA – version 2*

The final parameters' values using the PPSA (version 2) are

$$\mathbf{K}_{20636} = [5051.788, 9734.946, 1046.105, 78.9573, 32.3117, 1.7838, 954.866]^T \quad (5.50)$$

Evolutions of $\alpha_P(\mathbf{K})$ and $\alpha_Z(\mathbf{K})$ of poles and zeros, respectively are presented in Fig. 5.11, and the distance of the dominant pole, σ_1, from the prescribed one $|\sigma_1 - s_1|$ and that of the dominant zero, ζ_1, from the prescribed one $|\zeta_1 - z_1|$ can be seen in Fig. 5.12.

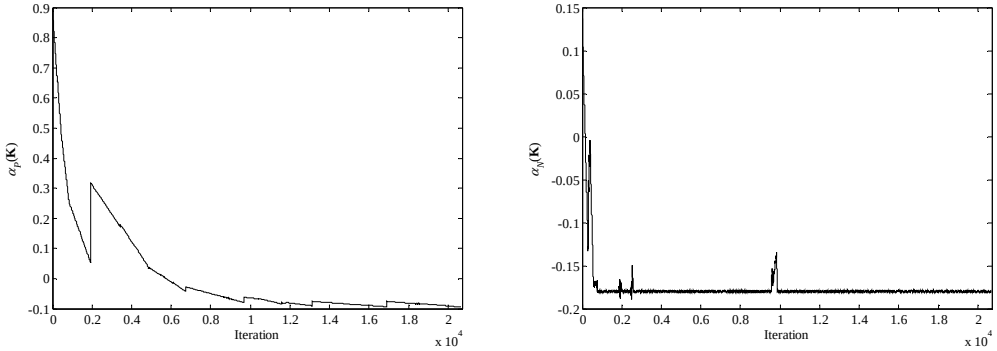

Fig. 5.11 Evolution of $|\sigma_1 - s_1|$ *(left)* $|\zeta_1 - z_1|$ *(right) using the PPSA – version 2*

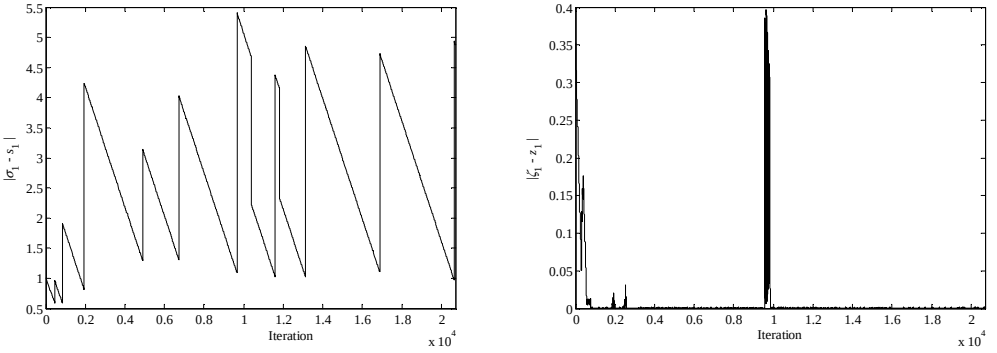

Fig. 5.12 Evolution of $\alpha_P(\mathbf{K})$ *(left)* $\alpha_N(\mathbf{K})$ *(right) using the PPSA – version 2*

Obviously, we tried to keep the rightmost zero as close to the prescribed one as possible, while to shift the rightmost pole. However, the distance is cyclically changed so that there is not possible to get closer without exceeding values of controller parameters.

The obtained spectra read

$$\mathbf{\Omega}_{p,20636} = \{-0.0945 \pm 1.1778\,\mathrm{j}, -0.1168 \pm 0.0697\,\mathrm{j}, -0.118 \pm 5.0275\,\mathrm{j}\} \tag{5.51}$$

$$\mathbf{\Omega}_{z,20636} = \{-0.1804, -0.22 \pm 0.1187\,\mathrm{j}, -0.7546, -2.7809 \pm 8.2997\,\mathrm{j}\} \tag{5.52}$$

Similarly as for version 1, the objective function

$$\Phi(\mathbf{K}) = |\sigma_1 - s_1| + |\zeta_1 - z_1| + \lambda_1 \alpha_{r,p}(\mathbf{K}) + \lambda_2 \alpha_{r,z}(\mathbf{K}) \tag{5.53}$$

using the SOMA is minimized, where $\alpha_{r,p}(\mathbf{K})$ means the spectral abscissa of the rest of poles except the dominant pair, $\alpha_{r,z}(\mathbf{K})$ has the same meaning yet for zeros and $\lambda_1 = \lambda_2 = 0.01$. The results are then the following

$$\begin{aligned}
&\mathbf{K}_{20636,opt} = [5235.169, 9829.219, 1060.87, 78.2405, 30.9684, 1.763, 947.517]^T \\
&\Omega_{p,20636,opt} = \{-0.1158 \pm 0.0674\mathrm{j}, -0.1161 \pm 5.1163\mathrm{j}, -0.1211 \pm 1.2103\mathrm{j}\} \\
&\Omega_{z,1440,opt} = \{-0.1801, -0.2247 \pm 0.1032\mathrm{j}, -0.7607, -2.817 \pm 8.1939\mathrm{j}\}
\end{aligned} \tag{5.54}$$

The comparison of step responses of the original model having the desired location of poles and zeros with four results using the PPSA and the SOMA is presented in Fig. 5.13.

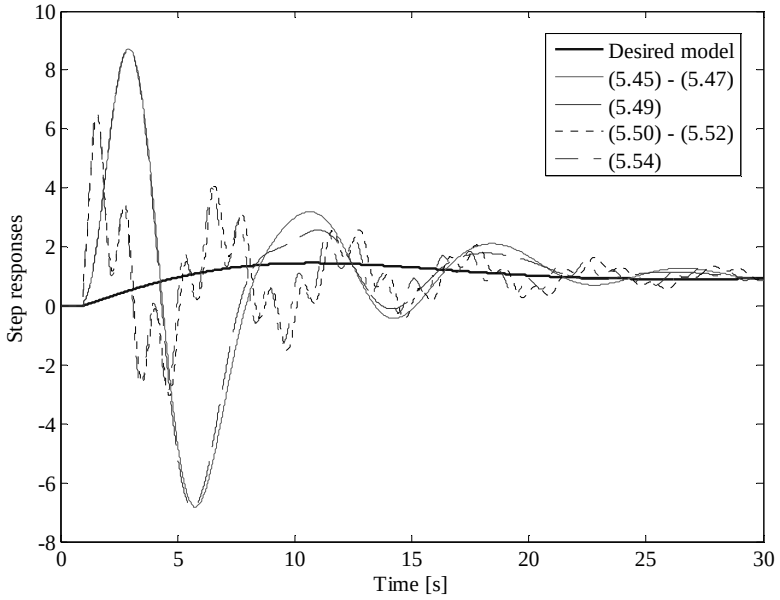

Fig. 5.13 Step responses comparison of results of the PPSA

It is apparent that the desired model has not been reached, nevertheless it can be stated that version 2 has given better results and the optimization (SOMA) procedure has slightly improved poles and zeros distribution. This example hence also demonstrated that it is not always possible to meet the prescribed rightmost poles and zeros due to the complexity of the spectrum of TDS and delayed control feedbacks.

5.5.3 Spectral abscissa minimization

Assume controller (5.36) and the characteristic quasipolynomial $m(s)$ as in (5.38), and formulate now the following minimization problem

$$\begin{aligned}\mathbf{K}_{opt} &= [p_2, p_1, p_0, q_3, q_2, q_1, q_0]^T_{opt} = \arg\min_{\mathbf{K}} \alpha(\mathbf{K}) \\ &= \arg\min_{\mathbf{K}} \{\mathrm{Re}\, s_i : [m(s)]_{s=s_i} = 0\}\end{aligned} \tag{5.55}$$

instead of shifting poleas nad zeros to the prescribed positions.

Four optimization algorithms and techniques are benchmarked and verified, namely, the QCSA (see Subsection 2.6.3), the EGSA [166], the SOMA (Subsection 5.3) and the NM algorithm (Subsection 5.4).

Let the minimization starts by the QCSA from the point $\mathbf{K}_0 = [1,1,1,1,1,1,1]^T$ defined in (5.55). This initial setting gives rise to the spectrum Ω_0 (system poles s_i are from the region with $\mathrm{Re}\, s_i > -2$)

$$\Omega_0 = \{0.849185, 0.477189, 1, 1, -0.604644, -0.820218, -1\} \tag{5.56}$$

Obviously, the feedback system is unstable with $\alpha(\mathbf{K}) = 0.849185$. The QCSA is capable to move some controlled poles to the left. Unlike the original paper [90], the number of controller poles is not increased gradually here, however, this quantity is changed depending on poles locations. More precisely, whenever the dominant root of (5.38) (or a bunch of dominant roots) secedes from the rest of the spectrum and the number of currently controlled roots is higher then the number of seceded ones, the number of controlled roots decreases so that only of seceded roots are controlled.

The evolution of system poles is displayed in Fig. 5.14 where the controlled ones are in bold lines. Notice that in an iterations range approximately of *i* = 600-1750, there is a huge number of bifurcations of a complex pair of roots or that a double real root into a pair of single real roots, and viceversa. This yields many changes in the number of controlled roots. Whenever a root remains uncontrolled, it eventually reaches the

controlled rightmost bunch of roots. A detailed view on the iterations range of i = 600-1750 is in Fig. 5.15.

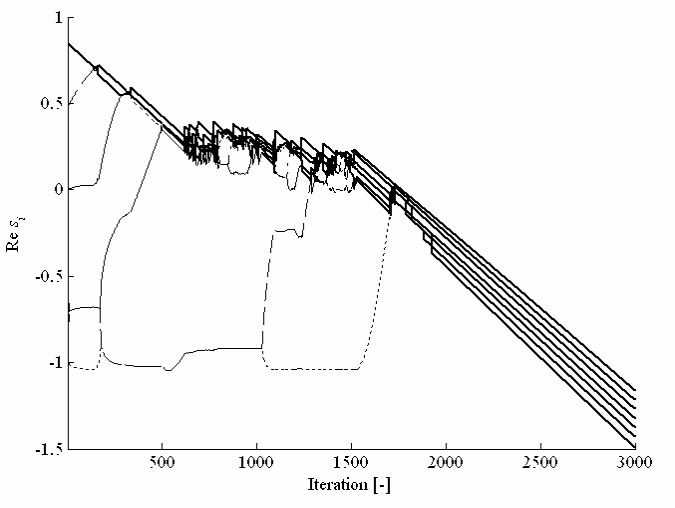

Fig. 5.14 Evolution of real parts of the rightmost roots of (5.38) using the QCSA

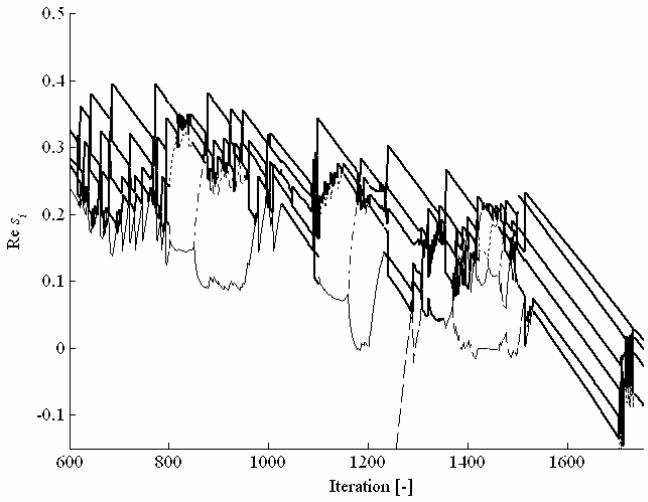

Fig. 5.15 A detailed view on Fig. 5.14 for the iterations range of i = 600-1750

The overall development of $\mathbf{K}$ can be seen in Fig. 5.16 (left); however, due to the noticeable rise in values for i > 1700, the detailed view on the iterations range of 1-1700 is in depicted Fig. 5.16 (right).

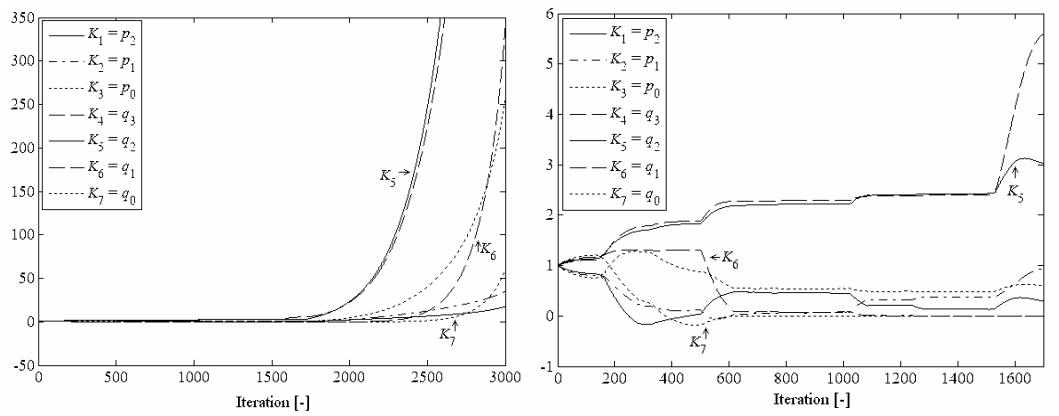

Fig. 5.16 Evolution of $\mathbf{K}$ *for (5.38) and (5.55) using the QCSA*

From Fig. 5.14 it is obvious that the procedure can adjust the spectral abscissa such that $\alpha(\mathbf{K}) < -1.5$ and it seems that this improvement may continue long. The comparison of the three remaining methods together with the evolution of $\mathbf{K}$ for i = 1-3000 has been presented in [133]. In the cited literature, it has been stated that the NM algorithm gives a fast (≈ 8 s per iteration on Intel Core2 Duo CPU E8500@3.16 GHz, 4BG RAM) and noticeable cost function improvement qualitatively comparable with the SOMA which is a rather slower (1 iteration step of SOMA lasts 70 iterations of the NM). However, the QCSA is approximately as fast as the NM and it has provided much better decline of the cost function. On the contrary, the EGSA has not brought a significant improvement (i.e. a sufficient decreasing) of $\alpha(\mathbf{K})$. Moreover, the method is eight times more time consumptive then the NM, since it requires (in the worse case) $l+1+k\cdot(l+1)=(l+1)(k+1)$ spectrum calculations per iteration, where l is the number of points where the gradient is estimated and k stands for the maximum number of discrete steps when searching the suitable gradient length, see details in **Chyba! Nenalezen zdroj odkazů.**. To sum up, it has seemed that the three remaining algorithms can serve for searching the local minimum rather then the global optimum when solving the spectral abscissa of TDS.

However, later we found out that the improvement is limited by trying to perform a new test consisting in continuation of iterations via the QCSA. Results for the iteration range $i \in [3000, 3520]$ can be seen in Fig. 5.17.

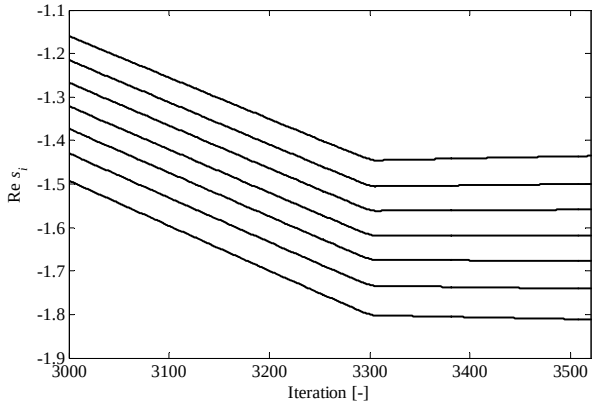

Fig. 5.17 Evolution of real parts of the rightmost roots of (5.38) using the QCSA within the iteration range $i \in [3000, 3520]$

It is clear that the improvement of the spectral abscissa terminates at $i = 3305$. The values of **K** and the corresponding spectrum (its dominant part, more precisely) in this iteration step read

$$\mathbf{K}_{3305} = [469418.2, 640264.2, 10560107, 8222650, \\ 106523133, 26247749, 5617613]^T \tag{5.57}$$

$$\Omega_{3305} = \{-1.4454, -1.5056, -1.5617, -1.6187, -1.6745, -1.7345, -1.802\} \tag{5.58}$$

The NM algorithm yields the development of $\alpha(\mathbf{K})$ as in Fig. 5.18

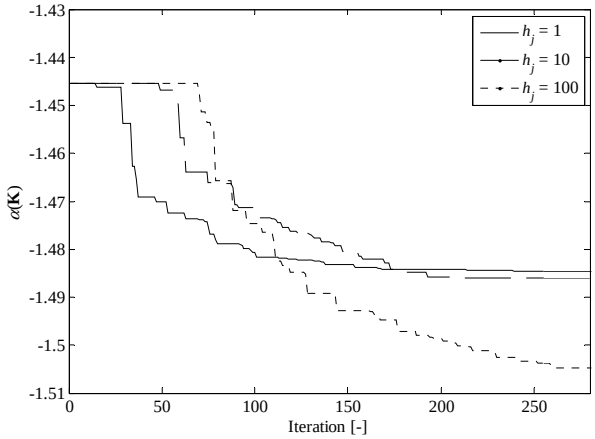

Fig. 5.18 Evolution of $\alpha(\mathbf{K})$ *using the NM for* h_j *= {1, 10, 100} from i = 3305*

As can be seen from (5.57), values of **K** are very high and unusable in practice. However, we try to test the remaining algorithms starting in this local minimum, i.e. from $i = 3305$. Fig. 5.18 indicates that a longer initial simplex edge results in a slower but much better minimization since it brings more possibilities how to escape from the local minimum and prevents the premature termination due to the simplex size. It is substantial that the local minimum from the QCSA has been improved by the NM.

The EGSA gives results displayed in Fig. 5.19. where $\Delta\lambda$ means the discretization step when searching a suitable gradient length.

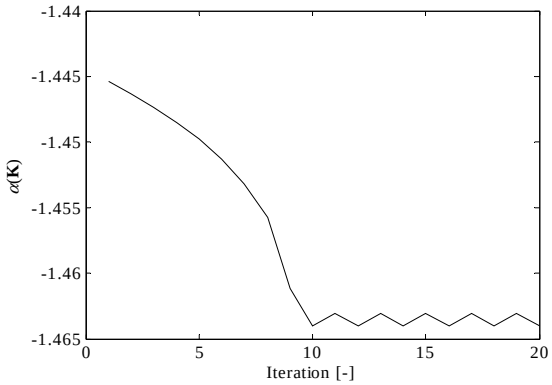

Fig. 5.19 Evolution of $\alpha(\mathbf{K})$ using the EGSA for $\Delta\lambda = 10^{-5}$ from i = 3305

It is questionable whether the result can be improved by decreasing of the sampling radius for numerical estimation of the steepest descent direction, ρ, or that of $\Delta\lambda$; however, in [133] we observed that a variation in $\Delta\lambda$ within one order does not bring a satisfactory result. Contrariwise, a lower value of ρ results in a higher gradient norm, which implies numerical difficulties.

Finally, the development of $\alpha(\mathbf{K})$ using the SOMA for two different initial population radii, *Rad*, is shown in Fig. 5.20. A higher value of *Rad* enables to scan the parameters space more effectively resulting in a faster decrease of $\alpha(\mathbf{K})$. The result is almost comparable with the NM method, yet, the iteration process is much slower compared to this classical optimization method. Meanwhile the NM has approximately 2 or 3 spectrum calculations per iteration, the SOMA requires

$\text{round}\left(\left(PopSize-1\right)\cdot PathLength/Step\right)$ enumerations. This fact is clear from Fig. 5.21 where the best results from all the three methods are compared in the time range.

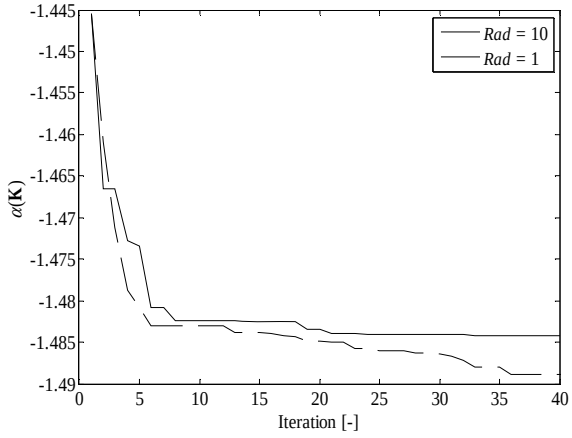

Fig. 5.20 Evolution of $\alpha(\mathbf{K})$ using the SOMA for $Rad=\{1,10\}$ from i = 3305

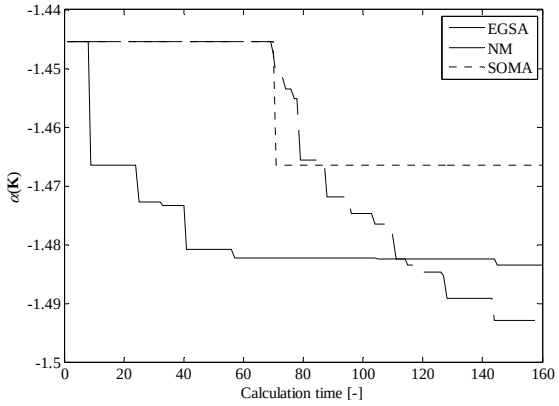

Fig. 5.21 Evolution of $\alpha(\mathbf{K})$ using the NM (d_j = 100), EGSA ($\Delta\lambda=10^{-5}$) and SOMA (Rad = 10) in the calculation time range starting from i = 3305

To sum up, the best result with the minimal value of $\alpha(\mathbf{K})$ obtained by the NM gives the following position of the rightmost poles

$$\Omega_{3305,NM}=\{-1.5108\pm0.0168\text{j},-1.5108\pm0.0168\text{j},-1.7197\pm0.1459\text{j},-1.8804\} \quad (5.59)$$

The corresponding values of **K** do not differ significantly from (5.57). Simulated control responses are not displayed here due to the numerical problems with simulation program (caused by high values of controller parameters).

6 RELAY FEEDBACK IDENTIFICATION TEST

Low order modelling constitutes one of possible principles how to deal with modelling and, consequently, control of high order systems [171], [207]. This chapter aims anisochronic low order modelling and identification of a plant by means of relay-feedback test, see Subchapter 2.8. A rather more complex plant model is utilized compared to the references above and, moreover, a novel, simple and intuitive, time-domain assembling of identification equations of type (2.127) is presented [123].

In particular, consider a plant model

$$G_m(s) = \frac{b_0 \exp(-\tau s)}{s + a_0 + a_1(-\vartheta s)} \tag{6.1}$$

and the task is to find conditional equations for identification of model parameters by means of a relay feedback test with an on-off and saturation relay. There five unknown real parameters in the model, i.e. $b_0, a_0, a_1, \tau, \vartheta$; however, two of them can be estimated not from the knowledge of the ultimate gain and frequency. Namely, the static gain $k = b_0 / a_1$ can be calculated from (2.126) and the value of input-output delay τ can be estimated from Fig. 2.10. Hence, in the first step, a biased on-off relay with hysteresis is used to estimate these two parameters. Then, a simple (symmetrical) on-off relay and/or a saturation relay can be utilized to calculate the remaining parameters from (2.127) and the use of an artificial delay τ^+, see Subchapter 2.8.4. Four conditional equation can be obtained from (2.127) by doing this, therefore one may improve the estimation of k or τ.

6.1 Frequency-domain solution

Consider a symmetrical on-off relay first. Conditions (2.127) with respect to (2.125) read

$$f_{11} := \frac{b_0}{\sqrt{(a_0 + a_1 \cos(\vartheta\omega_u))^2 + (\omega_u - a_1 \sin(\vartheta\omega_u))^2}} \frac{4B}{\pi A} - 1 = 0 \tag{6.2}$$

$$f_{12} := -\arctan\frac{\omega_u - a_1\sin(\vartheta\omega_u)}{a_0 - a_1\cos(\vartheta\omega_u)} - \tau\omega_u + \pi = 0 \tag{6.3}$$

In addition, the use of an artificial delay element τ^+ (characterized by a phase leg ϕ_D on the ultimate frequency $\tilde{\omega}_u$) yields

$$f_{13} := \frac{b_0}{\sqrt{(a_0 + a_1\cos(\vartheta\tilde{\omega}_u))^2 + (\omega_u - a_1\sin(\vartheta\tilde{\omega}_u))^2}}\frac{4B}{\pi\tilde{A}} - 1 = 0 \tag{6.4}$$

$$f_{14} := -\arctan\frac{\tilde{\omega}_u - a_1\sin(\vartheta\tilde{\omega}_u)}{a_0 - a_1\cos(\vartheta\tilde{\omega}_u)} - \tau\tilde{\omega}_u - \phi_D + \pi = 0 \tag{6.5}$$

where $\tilde{A}$ means the amplitude of $y(t)$ under the additional delay.

Analogously, for the saturation relay governed by (2.128), it holds

$$f_{21} := \frac{b_0}{\sqrt{(a_0 + a_1\cos(\vartheta\omega_u))^2 + (\omega_u - a_1\sin(\vartheta\omega_u))^2}}\frac{2B}{\pi\bar{A}}\left(\arcsin\left(\frac{\bar{A}}{A}\right) + \frac{\bar{A}}{A}\sqrt{1-\left(\frac{\bar{A}}{A}\right)^2}\right) - 1 = 0 \tag{6.6}$$

$$f_{22} := f_{12} = 0 \tag{6.7}$$

and

$$f_{23} := \frac{b_0}{\sqrt{(a_0 + a_1\cos(\vartheta\tilde{\omega}_u))^2 + (\tilde{\omega}_u - a_1\sin(\vartheta\tilde{\omega}_u))^2}}\frac{2B}{\pi\tilde{\bar{A}}}\left(\arcsin\left(\frac{\tilde{\bar{A}}}{\tilde{A}}\right) + \frac{\tilde{\bar{A}}}{\tilde{A}}\sqrt{1-\left(\frac{\tilde{\bar{A}}}{\tilde{A}}\right)^2}\right) - 1 = 0 \tag{6.8}$$

$$f_{24} := f_{14} = 0 \tag{6.9}$$

6.2 Time-domain solution

This subsection offers an alternative assembling of the identification nonlinear algebraic equations.

The simple idea stems from the fact that rectangular waves on a plant input can be approximated by (or viewed as) sinus waves using linearization (2.125) or (2.128). Hence, using on-off relay, the approximating input sinus signal is

$$u(t) = \frac{4B}{\pi}\sin(t\omega_u) \tag{6.10}$$

Note that in case of biased relay where $B^+ \approx B^-$, one can take $B = 0.5(B^+ + B^-)$. Since the ideal relay does not evoke a phase shift, a plant output has a phase shift $-\pi$, in other words, a plant output is given by

$$y(t) = -A\sin(t\omega_u) \tag{6.11}$$

Model transfer function agrees with the FDE

$$y'(t) + a_0 y(t) + a_1 y(t-\vartheta) = b_0 u(t-\tau) \tag{6.12}$$

thus (6.12) with respect to (6.10) and (6.11) reads

$$-A(\omega_u \cos(t\omega_u) + a_0 \sin(t\omega_u) + a_1 \sin((t-\vartheta)\omega_u)) = b_0 \frac{4B}{\pi}\sin((t-\tau)\omega_u) \tag{6.13}$$

Now placing the appropriate time values into (6.13), relations for the unknown model parameters can be derived. Since one point on the Nyquist curve can determine the values of two unknown parameters, two particular arguments can be chosen.

First, let $t = \omega_u^{-1}(2k\pi)$, $k \in \mathbb{Z}_0^+$, and k be chosen so that $t > \max\{\tau, \vartheta\}$ and the limit cycle is stable (settled). Then (6.13) gives

$$f_{31} := A(-\omega_u + a_1 \sin(\vartheta\omega_u)) + b_0 \frac{4B}{\pi}\sin(\tau\omega_u) = 0 \tag{6.14}$$

As second, let $t = \omega_u^{-1}((0.5 + 2k)\pi)$, $k \in \mathbb{Z}_0^+$, then

$$f_{32} := -A(a_0 + a_1 \cos(\vartheta\omega_u)) - b_0 \frac{4B}{\pi}\cos(\tau\omega_u) = 0 \tag{6.15}$$

The use of an additional delay element gives rise to the following FDE

$$
\begin{aligned}
&-\tilde{A}(\tilde{\omega}_u \cos(t\tilde{\omega}_u + \phi_D) + a_0 \sin(t\tilde{\omega}_u + \phi_D) + a_1 \sin((t-\vartheta)\tilde{\omega}_u + \phi_D)) \\
&= b_0 \frac{4B}{\pi} \sin((t-\tau)\tilde{\omega}_u)
\end{aligned}
\tag{6.16}
$$

instead of (6.13). Inserting $t = \omega_u^{-1}(2k\pi - \phi_D)$ and $t = \omega_u^{-1}((0.5+2k)\pi - \phi_D)$ into (6.16) gives

$$
f_{33} := \tilde{A}(-\tilde{\omega}_u + a_1 \sin(\vartheta\tilde{\omega}_u)) + b_0 \frac{4B}{\pi} \sin(\tau\tilde{\omega}_u + \phi_D) = 0 \tag{6.17}
$$

and

$$
f_{34} := -\tilde{A}(a_0 + a_1 \cos(\vartheta\tilde{\omega}_u)) - b_0 \frac{4B}{\pi} \cos(\tau\tilde{\omega}_u + \phi_D) = 0 \tag{6.18}
$$

respectively.

The application of the saturation relay leads analogously to the following conditions

$$
f_{41} := -\omega_u + a_1 \sin(\vartheta\omega_u) + b_0 \frac{2B}{\pi\bar{\bar{A}}} \left(\arcsin\left(\frac{\bar{A}}{A}\right) + \frac{\bar{A}}{A}\sqrt{1-\left(\frac{\bar{A}}{A}\right)^2} \right) \sin(\tau\omega_u) = 0 \tag{6.19}
$$

$$
f_{42} := a_0 + a_1 \cos(\vartheta\omega_u) + b_0 \frac{2B}{\pi\bar{\bar{A}}} \left(\arcsin\left(\frac{\bar{A}}{A}\right) + \frac{\bar{A}}{A}\sqrt{1-\left(\frac{\bar{A}}{A}\right)^2} \right) \cos(\tau\omega_u) = 0 \tag{6.20}
$$

$$
f_{43} := -\tilde{\omega}_u + a_1 \sin(\vartheta\tilde{\omega}_u) + b_0 \frac{2B}{\pi\tilde{\bar{\bar{A}}}} \left(\arcsin\left(\frac{\tilde{\bar{\bar{A}}}}{\tilde{A}}\right) + \frac{\tilde{\bar{\bar{A}}}}{\tilde{A}}\sqrt{1-\left(\frac{\tilde{\bar{\bar{A}}}}{\tilde{A}}\right)^2} \right) \sin(\tau\tilde{\omega}_u + \phi_D) = 0 \tag{6.21}
$$

$$
f_{44} := a_0 + a_1 \cos(\vartheta\tilde{\omega}_u) + b_0 \frac{2B}{\pi\tilde{\bar{\bar{A}}}} \left(\arcsin\left(\frac{\tilde{\bar{\bar{A}}}}{\tilde{A}}\right) + \frac{\tilde{\bar{\bar{A}}}}{\tilde{A}}\sqrt{1-\left(\frac{\tilde{\bar{\bar{A}}}}{\tilde{A}}\right)^2} \right) \cos(\tau\tilde{\omega}_u + \phi_D) = 0 \tag{6.22}
$$

7 REAL PLANT APPLICATION EXAMPLE

A complex theoretical and practical example comprising mathematical modelling and identification of a laboratory heating plant with internal delays, controller design in R_{MS} for the obtained model, relay feedback identification test for a simplified model, controller tuning, robust analysis, discretization and real-time verification follows and finalizes this dissertation thesis.

7.1 Description of a laboratory heating circuit system

The plant to be mathematically modelled and control in this section was assembled at the Faculty of Applied Informatics of Tomas Bata University in Zlín in order to verify several control algorithms for systems with delays. Originally, it was intended to control input-output delays only; however, as it is shown below, the plant contains internal delays as well, and thus it is suitable also for testing control approaches for TDS. The plant dynamics is based on the principle of heat transferring from a source through a piping system using a heat transferring media to a heat-consuming appliance. External appearance of the plant and a schematic sketch of the model are shown in Fig. 7.1 [34].

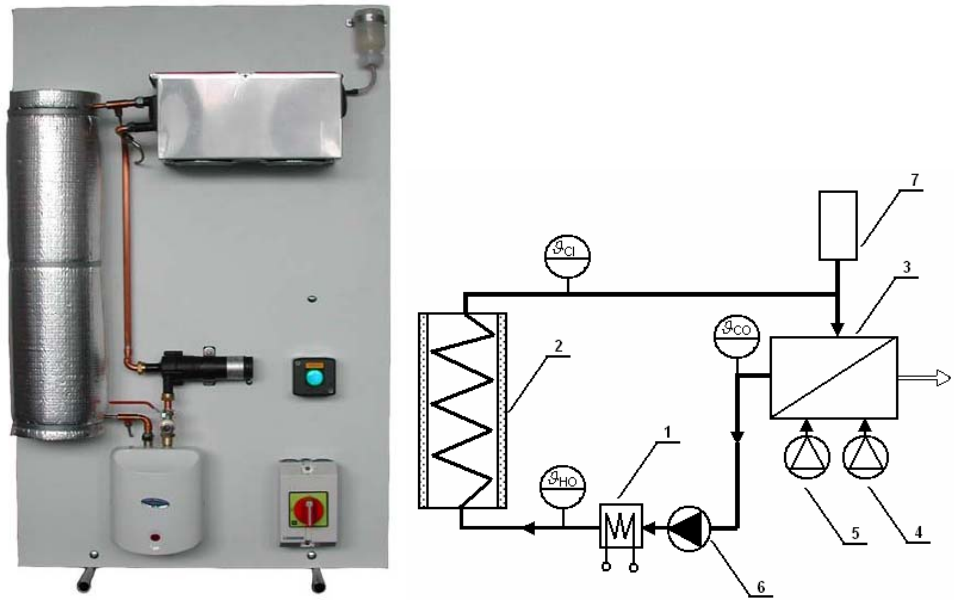

Fig. 7.1 A photo (left) and a scheme (right) of a laboratory heating model

Let us describe the plant according to a schematic sketch depicted in Fig. 7.1. The heat transferring fluid (namely distilled water) is transported using a continuously controllable DC pump {6} into a flow heater {1} with maximum power of 750 W. The temperature of a fluid at the heater output is measured by a platinum thermometer giving value of ϑ_{HO}. Warmed liquid then goes through a 15 meters long insulated coiled pipeline {2} which causes the significant delay in the system. The air-water heat exchanger (cooler) {3} with two cooling fans {4, 5} represents a heat-consuming appliance. The speed of the first fan can be continuously adjusted, whereas the second one is of an on/off type. Input and output temperatures of the cooler are measured again by platinum thermometers giving ϑ_{CI} and ϑ_{CO}, respectively. The expansion tank {7} compensates for the expansion effect of the water.

This small scale model can represent the dynamics of real heating systems, e.g. a cooling circuit system in cars, heating systems in buildings, etc. The laboratory model is connected to a standard PC (Intel Core2 Duo CPU E8500 @ 3.16 GHz, 4BG RAM) via serial bus RS232 and a portable data acquisition unit. All tasks relating to the monitoring and control of the plant are served by software running in Matlab 7.11 (R2010b) environment.

Recently, the computer has been equipped with the data acquisition card AD622 and Real-Time Toolbox for Matlab, which offers higher user and programming comfort [68].

7.2 Model of a laboratory heating circuit system

In this subsection, a possible mathematical model of the plant is proposed [128]. Obviously, an accurate mathematical model of the plant would be rather complicated due to the existence of components causing distributed delays in the system. However, the aim is not to find an exact description of the model, but a sufficiently simple mathematical model which can be used for the verification of control algorithms.

The methodology is based on comprehension of all significant delays and latencies in the model which is built in two steps: First, models of separate functional parts of the

plant are found; secondly, the separate models are combined by means of their common physical quantities.

Let us introduce notation for process quantities first:

c [J·kg^{-1}·K^{-1}] – the specific heat capacity of water

$\dot{m}(t)$ [kg·s^{-1}] – the mass flow rate of water

M_H [kg] – the overall mass of water in the heater

M_C [kg] – the overall mass of water in the cooler

M_P [kg] – the overall mass of water in the pipeline

$\vartheta_{HO}(t)$ [°C] – output temperature of the heater

$\vartheta_{CI}(t)$ [°C] – input temperature of the cooler

$\vartheta_{CO}(t)$ [°C] – output temperature of the cooler

$\vartheta_{HI}(t)$ [°C] – input temperature of the heater

ϑ_A [°C] – ambient temperature

$P(t)$ [W] – the power of the heater

τ_H [s] – the delay of a water flow through the heater

τ_{HC} [s] – the delay of a water flow between the heater and the cooler

τ_C [s] – the delay of a water flow through the cooler

τ_{KC} [s] – the delay between a control signal to the cooling fan and the output temperature of the cooler

τ_{CH} [s] – the delay of a water flow between the cooler and the heater

$u_P(t)$ [V] – a voltage input to the pump

$u_C(t)$ [V] – a voltage input to the cooling fan

$K_H(t)$ [W·K^{-1}] – the overall heat transmission coefficient of heater wastage energy

$K_C(t)$ [W·K^{-1}] – the overall heat transmission coefficient of the cooler

K_P [W·K^{-1}] – the overall heat transmission coefficient of the long pipeline

h_0, h_1, h_2, h_3, h_4, h_5 – weighting coefficients for the estimation of the overall heat transmission coefficient of the heater

c_0 [W·K^{-1}], c_1[W·K^{-1}·V^{-1}], c_2 – weighting coefficients for the estimation of the overall heat transmission coefficient of the cooler

p_0 [m^3·s^{-1}], p_1 [V], p_2 – weighting coefficients for the estimation of the mass flow rate of water

7.2.1 Analysis of the model plant dynamics

Let model the heater first. The energy balance equation is used for the description of the heater

$$\begin{aligned} cM_H \frac{\mathrm{d}\vartheta_{HO}(t)}{\mathrm{d}t} &= P(t-0.5\tau_H) + c\dot{m}(t)\left[\vartheta_{HI}(t-\tau_H) - \vartheta_{HO}(t)\right] \\ &\quad - K_H(t)\left[\frac{\vartheta_{HO}(t)+\vartheta_{HI}(t-\tau_H)}{2} - \vartheta_A\right] \end{aligned} \tag{7.1}$$

where the arithmetical mean temperature difference is taken for heat losses and a heating body is assumed to perform heat energy in the middle of the heater. Input temperature, $\vartheta_{HI}(t)$, is estimated by "the nearest" measured one, $\vartheta_{CO}(t)$, as

$$\vartheta_{HI}(t) = \vartheta_{CO}(t-\tau_{CH}) \tag{7.2}$$

due to the fact that the fluid transport between the cooler output and the heater input is fast enough so that these two temperatures almost do not differ, except for a time delay. The overall heat transmission coefficient of the heater, $K_H(t)$, is numerically approximated by the relation

$$K_H(t) = \frac{h_0 P^2(t) + h_1 \dot{m}^2(t) + h_2 P(t)\dot{m}(t) + h_3}{h_4 P(t) + h_5 \dot{m}(t)} \tag{7.3}$$

Regarding to the model of a coiled insulated pipeline, a transportation delay in the piping has a decisive influence on the behavior of the system. Consider the energy balance equation again where heat losses are supposed to be linear along the pipeline

$$cM_P \frac{\mathrm{d}\vartheta_{CI}(t)}{\mathrm{d}t} = c\dot{m}(t)\left[\vartheta_{HO}(t-\tau_{HC}) - \vartheta_{CI}(t)\right] - K_P\left[\frac{\vartheta_{CI}(t)+\vartheta_{HO}(t-\tau_{HC})}{2} - \vartheta_A\right] \qquad (7.4)$$

Notice that input and output temperatures are not considered in the same time since the thermal effect of the water inlet affects the outlet after some dead time. Heat transmitting coefficient is considered as a low valued constant, thanks to the very good isolation.

The mass of the piping is neglected in the model due to the fact that the specific heat capacity of the material of the pipeline (copper ≈ 385 $\mathrm{J{\cdot}kg^{-1}{\cdot}K^{-1}}$) is much smaller than that of water (≈ 4180 $\mathrm{J{\cdot}kg^{-1}{\cdot}K^{-1}}$), and because of the fact that the mass of used copper is lower than that of the fluid (water) inside the piping.

Time delays in the air-water exchanger are of a distributed nature, thus they have not an important role in system behaviour. On the other hand, the cooler significantly affects water temperature because of its high heat transmission coefficient supported by fans. The energy balance equation reads

$$cM_C \frac{\mathrm{d}\vartheta_{CO}(t)}{\mathrm{d}t} = c\dot{m}(t)\left[\vartheta_{CI}(t-\tau_C) - \vartheta_{CO}(t)\right] - K_C(t)\left[\frac{\vartheta_{CO}(t)+\vartheta_{CI}(t-\tau_C)}{2} - \vartheta_A\right] \qquad (7.5)$$

The dynamics of the air part of the cooler is much faster in comparison with the water one, thus this dynamics is neglected. The heat transmission coefficient, $K_C(t)$, is attempted to be approximated by a quadratic function

$$K_C(t) = c_2 u_C^2(t-\tau_{KC}) + c_1 u_C(t-\tau_{KC}) + c_0 \qquad (7.6)$$

Changes in the fan speed affect $K_C(t)$. Notice that there is a delay between the control input voltage to the continuously controllable cooling fan, $u_C(t)$, and a change of $K_C(t)$, in the model. There is no attempt to use models of all electrical and electronic equipments (e.g. the fan motor), and thus coefficients c_0, c_1, c_2 are determined experimentally.

Dealing with the pump - the influence of the voltage input to the pump, $u_P(t)$, upon the mass flow rate of water, $\dot{m}(t)$, can be described by a static characteristic

$$\dot{m}(t) = p_0[u_P(t) + p_1]^{p_2} \tag{7.7}$$

see [85]. The pump dynamics is omitted comparing to the whole process dynamics. Changes of process delays caused by the change of $\dot{m}(t)$ are neglected as well, in order to avoid a rather complicated mathematical description of the plant dynamics, although these changes influence process delays significantly.

7.2.2 Linearization of the model in the vicinity of the operation point

From the modelling above, a nonlinear MIMO model of the plant is obtained. Measured temperatures $\vartheta_{HO}(t)$, $\vartheta_{CI}(t)$, $\vartheta_{CO}(t)$ are taken as system outputs, whereas analog input voltages $u_P(t)$, $u_C(t)$ and the power $P(t)$ are considered as system inputs. To obtain a linearized model, the first two terms of the Taylor series expansion at an operation point are used.

Equations (7.1) - (7.3) and (7.7) give

$$\begin{aligned}\Delta\frac{\mathrm{d}\vartheta_{HO}(t)}{\mathrm{d}t} \approx{}& A_1\Delta u_P(t) + \frac{1}{cM_H}\Delta P(t-0.5\tau_H) + A_2\Delta P(t) + A_3\Delta\vartheta_{HO}(t)\\ &+ A_4\Delta\vartheta_{CO}(t-\tau_H-\tau_{CH})\end{aligned} \tag{7.8}$$

where

$$\begin{aligned}A_1 = \frac{\partial}{\partial u_P(t)}\frac{\mathrm{d}\vartheta_{HO}(t)}{\mathrm{d}t}\bigg|_0 = {}& \frac{p_0 p_2 (u_{P0}+p_1)^{p_2-1}}{M_H}\Big[\vartheta_{HI0} - \vartheta_{HO0} + (0.5\vartheta_{HI0} + 0.5\vartheta_{HO0} - \vartheta_A)\\ &\left(\frac{-h_1h_5p_0^2(u_{P0}+p_1)^{2p_2}}{c\left[h_5p_0(u_{P0}+p_1)^{p_2}+h_4P_0\right]^2} + \frac{-2h_1h_4P_0p_0(u_{P0}+p_1)^{p_2}}{c\left[h_5p_0(u_{P0}+p_1)^{p_2}+h_4P_0\right]^2}\right.\\ &\left.+\frac{(h_0h_5-h_2h_4)P_0^2 - h_3h_5}{c\left[h_5p_0(u_{P0}+p_1)^{p_2}+h_4P_0\right]^2}\right)\Big]\end{aligned} \tag{7.9}$$

$$A_2 = \frac{\partial}{\partial P(t)} \frac{\mathrm{d}\,\vartheta_{HO}(t)}{\mathrm{d}t}\bigg|_0 = \Big[\vartheta_{HI0} - \vartheta_{HO0} + \left(0.5\vartheta_{HI0} + 0.5\vartheta_{HO0} - \vartheta_A\right) + \frac{\left(h_1 h_4 - h_2 h_5\right) p_0^2 \left(u_{P0} + p_1\right)^{2p_2}}{cM_H \left[h_5 p_0 \left(u_{P0} + p_1\right)^{p_2} + h_4 P_0\right]^2} + \frac{-2h_0 h_5 P_0 p_0 \left(u_{P0} + p_1\right)^{p_2} - h_0 h_4 P_0^2 + h_3 h_4}{cM_H \left[h_5 p_0 \left(u_{P0} + p_1\right)^{p_2} + h_4 P_0\right]^2}\Big] \tag{7.10}$$

$$A_3 = \frac{\partial}{\partial\, \vartheta_{HO}(t)} \frac{\mathrm{d}\,\vartheta_{HO}(t)}{\mathrm{d}t}\bigg|_0 = -\frac{1}{M_H}\Big[p_0 \left(u_{P0} + p_1\right)^{p_2} + \frac{h_1 p_0^2 \left(u_{P0} + p_1\right)^{2p_2} + h_2 P_0 p_0 \left(u_{P0} + p_1\right)^{p_2}}{2c\left[h_5 p_0 \left(u_{P0} + p_1\right)^{p_2} + h_4 P_0\right]^2} + \frac{h_0 P_0^2 + h_3}{2c\left[h_5 p_0 \left(u_{P0} + p_1\right)^{p_2} + h_4 P_0\right]^2}\Big] \tag{7.11}$$

$$A_4 = \frac{\partial}{\partial\, \vartheta_{CO}(t - \tau_H - \tau_{CH})} \frac{\mathrm{d}\,\vartheta_{HO}(t)}{\mathrm{d}t}\bigg|_0 = \frac{1}{M_H}\Big[p_0 \left(u_{P0} + p_1\right)^{p_2} - \frac{h_1 p_0^2 \left(u_{P0} + p_1\right)^{2p_2}}{2c\left[h_5 p_0 \left(u_{P0} + p_1\right)^{p_2} + h_4 P_0\right]^2} + \frac{h_2 P_0 p_0 \left(u_{P0} + p_1\right)^{p_2} + h_0 P_0^2 + h_3}{2c\left[h_5 p_0 \left(u_{P0} + p_1\right)^{p_2} + h_4 P_0\right]^2}\Big] \tag{7.12}$$

Additional index $(\cdot)_0$ denotes the appropriate quantity value in the steady state (an operation point) and symbol Δ stands for a deviation from an operation point.

From (7.4) and (7.7) it is obtained

$$\Delta \frac{\mathrm{d}\,\vartheta_{CI}(t)}{\mathrm{d}t} = A_5 \Delta u_P(t) + A_6 \Delta \vartheta_{HO}(t - \tau_{HC}) + A_7 \Delta \vartheta_{CI}(t) \tag{7.13}$$

with

$$A_5 = \frac{\partial}{\partial u_P(t)} \frac{\mathrm{d}\,\vartheta_{CI}(t)}{\mathrm{d}t}\bigg|_0 = \frac{p_2 p_0 \left(u_{P0} + p_1\right)^{p_2 - 1} \left(\vartheta_{HO0} - \vartheta_{CI0}\right)}{M_P} \tag{7.14}$$

$$A_6 = \frac{\partial}{\partial\, \vartheta_{HO}(t - \tau_H)} \frac{\mathrm{d}\,\vartheta_{CI}(t)}{\mathrm{d}t}\bigg|_0 = \frac{1}{cM_P}\left[cp_0 \left(u_{P0} + p_1\right)^{p_2} - 0.5K_P\right] \tag{7.15}$$

$$A_7 = \frac{\mathrm{d}}{\mathrm{d}\,\vartheta_{CI}(t)} \frac{\mathrm{d}\,\vartheta_{CI}(t)}{\mathrm{d}t}\bigg|_0 = -\frac{1}{cM_P}\left[cp_0 \left(u_{P0} + p_1\right)^{p_2} + 0.5K_P\right] \tag{7.16}$$

Linearization of (7.5) - (7.7) gives

$$\Delta\frac{\mathrm{d}\vartheta_{CO}(t)}{\mathrm{d}t} = A_8\Delta u_P(t) + A_9\Delta u_C(t-\tau_{KC}) + A_{10}\Delta\vartheta_{CO}(t) + A_{11}\Delta\vartheta_{CI}(t-\tau_C) \tag{7.17}$$

$$A_8 = \frac{\partial}{\partial u_P(t)}\frac{\mathrm{d}\vartheta_{C0}(t)}{\mathrm{d}t}\bigg|_0 = \frac{p_2 p_0 (u_{P0}+p_1)^{p_2-1}(\vartheta_{CI0}-\vartheta_{CO0})}{M_C} \tag{7.18}$$

$$\begin{aligned} A_9 &= \frac{\partial}{\partial u_C(t-\tau_{KC})}\frac{\mathrm{d}\vartheta_{C0}(t)}{\mathrm{d}t}\bigg|_0 \\ &= -\frac{(2c_2u_{C0}+c_1)p_2 p_0 (u_{P0}+p_1)^{p_2-1}}{cM_C}(0.5\vartheta_{CI0}+0.5\vartheta_{CO0}-\vartheta_A) \end{aligned} \tag{7.19}$$

$$A_{10} = \frac{\partial}{\partial\vartheta_{CO}(t)}\frac{\mathrm{d}\vartheta_{CO}(t)}{\mathrm{d}t}\bigg|_0 = -\frac{1}{cM_P}\left[2cp_0(u_{P0}+p_1)^{p_2} + c_2u_{C0}^2 + c_1u_{C0} + c_0\right] \tag{7.20}$$

$$A_{11} = \frac{\partial}{\partial\vartheta_{CO}(t-\tau_C)}\frac{\mathrm{d}\vartheta_{CO}(t)}{\mathrm{d}t}\bigg|_0 = \frac{1}{cM_P}\left[2cp_0(u_{P0}+p_1)^{p_2} - c_2u_{C0}^2 + c_1u_{C0} + c_0\right] \tag{7.21}$$

A linearized state space model in an operation point then reads

$$\begin{aligned} \begin{bmatrix} \frac{d}{dt}\Delta\vartheta_{HO}(t) \\ \frac{d}{dt}\Delta\vartheta_{CI}(t) \\ \frac{d}{dt}\Delta\vartheta_{CO}(t) \end{bmatrix} &= \begin{bmatrix} A_3 & 0 & 0 \\ 0 & A_7 & 0 \\ 0 & 0 & A_{10} \end{bmatrix}\begin{bmatrix} \Delta\vartheta_{HO}(t) \\ \Delta\vartheta_{CI}(t) \\ \Delta\vartheta_{CO}(t) \end{bmatrix} + \begin{bmatrix} 0 & 0 & A_4 \\ 0 & 0 & 0 \\ 0 & 0 & 0 \end{bmatrix}\begin{bmatrix} \Delta\vartheta_{HO}(t-\tau_{CH}-\tau_H) \\ \Delta\vartheta_{CI}(t-\tau_{CH}-\tau_H) \\ \Delta\vartheta_{CO}(t-\tau_{CH}-\tau_H) \end{bmatrix} \\ &+ \begin{bmatrix} 0 & 0 & 0 \\ A_6 & 0 & 0 \\ 0 & 0 & 0 \end{bmatrix}\begin{bmatrix} \Delta\vartheta_{HO}(t-\tau_H) \\ \Delta\vartheta_{CI}(t-\tau_H) \\ \Delta\vartheta_{CO}(t-\tau_H) \end{bmatrix} + \begin{bmatrix} 0 & 0 & 0 \\ 0 & 0 & 0 \\ 0 & A_{11} & 0 \end{bmatrix}\begin{bmatrix} \Delta\vartheta_{HO}(t-\tau_C) \\ \Delta\vartheta_{CI}(t-\tau_C) \\ \Delta\vartheta_{CO}(t-\tau_C) \end{bmatrix} \\ &+ \begin{bmatrix} A_1 & 0 & A_2 \\ A_5 & 0 & 0 \\ A_8 & 0 & 0 \end{bmatrix}\begin{bmatrix} \Delta u_P(t) \\ \Delta u_C(t) \\ \Delta P(t) \end{bmatrix} + \begin{bmatrix} 0 & 0 & \frac{1}{cM_H} \\ 0 & 0 & 0 \\ 0 & 0 & 0 \end{bmatrix}\begin{bmatrix} \Delta u_P(t-0.5\tau_H) \\ \Delta u_C(t-0.5\tau_H) \\ \Delta P(t-0.5\tau_H) \end{bmatrix} \\ &+ \begin{bmatrix} 0 & 0 & 0 \\ 0 & 0 & 0 \\ 0 & A_9 & 0 \end{bmatrix}\begin{bmatrix} \Delta u_P(t-\tau_{KC}) \\ \Delta u_C(t-\tau_{KC}) \\ \Delta P(t-\tau_{KC}) \end{bmatrix} \end{aligned} \tag{7.22}$$

$$\begin{bmatrix} \Delta\vartheta_{HO}(t) \\ \Delta\vartheta_{CI}(t) \\ \Delta\vartheta_{CO}(t) \end{bmatrix} = \begin{bmatrix} 1 & 0 & 0 \\ 0 & 1 & 0 \\ 0 & 0 & 1 \end{bmatrix} \begin{bmatrix} \Delta\vartheta_{HO}(t) \\ \Delta\vartheta_{CI}(t) \\ \Delta\vartheta_{CO}(t) \end{bmatrix} \tag{7.23}$$

Symbol Δ for the linearized model is omitted hereinafter. Assuming zero initial conditions (i.e. a steady state in the operation point), the Laplace transform of (7.22) is given by

$$\begin{bmatrix} \Theta_{HO}(s) \\ \Theta_{CI}(s) \\ \Theta_{CO}(s) \end{bmatrix} s = \begin{bmatrix} A_3 & 0 & A_4 \exp(-(\tau_{CH}+\tau_H)s) \\ A_6 \exp(-\tau_H s) & A_7 & 0 \\ 0 & A_{11}\exp(-\tau_C s) & A_{10} \end{bmatrix} \begin{bmatrix} \Theta_{HO}(s) \\ \Theta_{CI}(s) \\ \Theta_{CO}(s) \end{bmatrix} + \begin{bmatrix} A_1 & 0 & A_2 \dfrac{\exp(-0.5\tau_H s)}{cM_H} \\ A_5 & 0 & 0 \\ A_8 & A_9 \exp(-\tau_{KC} s) & 0 \end{bmatrix} \begin{bmatrix} U_P(s) \\ U_C(s) \\ P(s) \end{bmatrix} \tag{7.24}$$

where the capital letters stand for transformed variables denoted with corresponding lower case letters. The transfer matrix of the model thus reads

$$\begin{bmatrix} \Theta_{HO}(s) \\ \Theta_{CI}(s) \\ \Theta_{CO}(s) \end{bmatrix} = \begin{bmatrix} G_{11}(s) & G_{12}(s) & G_{13}(s) \\ G_{21}(s) & G_{22}(s) & G_{23}(s) \\ G_{31}(s) & G_{32}(s) & G_{33}(s) \end{bmatrix} \begin{bmatrix} U_P(s) \\ U_C(s) \\ P(s) \end{bmatrix} = \frac{1}{A(s)} \begin{bmatrix} B_{11}(s) & B_{12}(s) & B_{13}(s) \\ B_{21}(s) & B_{22}(s) & B_{23}(s) \\ B_{31}(s) & B_{32}(s) & B_{33}(s) \end{bmatrix} \begin{bmatrix} U_P(s) \\ U_C(s) \\ P(s) \end{bmatrix} \tag{7.25}$$

where

$$\begin{aligned} B_{11}(s) &= \beta_{11,2}s^2 + \beta_{11,1}s + \beta_{11,1D}s\exp(-\tau_{11,1D}s) + \beta_{11,0} + \beta_{11,0D1}\exp(-\tau_{11,0D1}s) \\ &\quad + \beta_{11,0D2}\exp(-\tau_{11,0D2}s) \\ B_{12}(s) &= (\beta_{12,1}s + \beta_{12,0})\exp(-\tau_{12}s) \\ B_{13}(s) &= \beta_{13,2}s^2 + \beta_{13,2D}s^2\exp(-\tau_{13}s) + \beta_{13,1}s + \beta_{13,1D}s\exp(-\tau_{13}s) + \beta_{13,0}s \\ &\quad + \beta_{13,0D}s\exp(-\tau_{13}s) \end{aligned} \tag{7.26}$$

$$
\begin{aligned}
&B_{21}(s)=\beta_{21,2}s^2+\beta_{21,1}s+\beta_{21,1D}s\exp(-\tau_{21,1D}s)+\beta_{21,0}+\beta_{21,0D1}\exp(-\tau_{21,0D1}s)\\
&+\beta_{21,0D2}\exp(-\tau_{21,0D2}s)\\
&B_{22}(s)=\beta_{22,0}\exp(-\tau_{22}s)\\
&B_{23}(s)=\left[\beta_{23,1}s+\beta_{23,1D}s\exp(-\tau_{23,1D}s)+\beta_{23,0}+\beta_{23,0D}\exp(-\tau_{23,0D}s)\right]\exp(-\tau_{23}s)
\end{aligned}
\tag{7.27}
$$

$$
\begin{aligned}
&B_{31}(s)=\beta_{31,2}s^2+\beta_{31,1}s+\beta_{31,1D}s\exp(-\tau_{31,1D}s)+\beta_{31,0}+\beta_{31,0D1}\exp(-\tau_{31,0D1}s)\\
&\qquad+\beta_{31,0D2}\exp(-\tau_{31,0D2}s)\\
&B_{32}(s)=\left(\beta_{32,2}s^2+\beta_{32,1D}s+\beta_{32,0}\right)\exp(-\tau_{32}s)\\
&B_{33}(s)=\left[\beta_{33,0D}\exp(-\tau_{33,0}s)+\beta_{33,0}\right]\exp(-\tau_{33}s)
\end{aligned}
\tag{7.28}
$$

$$
A(s)=s^3+\alpha_2s^2+\alpha_1s+\alpha_0+\alpha_{0D}\exp(-\tau_{0D}s) \tag{7.29}
$$

with

$$
\begin{aligned}
&\beta_{11,2}=A_1,\ \beta_{11,1}=-A_1(A_7+A_{10}),\ \beta_{11,1D}=A_4A_8,\beta_{11,0}=A_1A_7A_{10},\\
&\beta_{11,0D1}=-A_4A_7A_8,\beta_{11,0D2}=A_4A_5A_{11},\tau_{11,1D}=\tau_{11,0D1}=\tau_{CH}+\tau_H,\\
&\tau_{11,0D2}=\tau_C+\tau_{CH}+\tau_H\\
&\beta_{12,1}=A_4A_9,\ \beta_{12,0}=-A_4A_7A_9,\ \tau_{12}=\tau_{KC}+\tau_{CH}+\tau_H\\
&\beta_{13,2}=A_2,\ \beta_{13,2D}=\frac{1}{cM_H},\ \beta_{13,1}=-A_2(A_7+A_{10}),\ \beta_{13,1D}=-\frac{1}{cM_H}(A_7+A_{10}),\\
&\beta_{13,0}=A_2A_7A_{10},\beta_{13,0D}=\frac{1}{cM_H}A_7A_{10},\tau_{13}=0.5\tau_H
\end{aligned}
\tag{7.30}
$$

$$
\begin{aligned}
&\beta_{21,2}=A_5,\ \beta_{21,1}=-A_5(A_3+A_{10}),\ \beta_{21,1D}=A_1A_6,\beta_{21,0}=A_3A_5A_{10},\\
&\beta_{21,0D1}=-A_1A_6A_{10},\ \beta_{21,0D2}=A_4A_6A_8,\ \tau_{21,1D}=\tau_{21,0D1}=\tau_{HC},\\
&\tau_{21,0D2}=\tau_{CH}+\tau_H+\tau_{HC}\\
&\beta_{22,0}=A_4A_6A_9,\ \tau_{22}=\tau_{KC}+\tau_{CH}+\tau_H+\tau_{HC}\\
&\beta_{23,1}=A_2A_6,\ \beta_{23,1D}=A_6\frac{1}{cM_H},\ \beta_{23,0}=-A_2A_6A_{10},\beta_{23,0D}=-A_6A_{10}\frac{1}{cM_H},\\
&\tau_{23}=\tau_{HC},\ \tau_{23,1D}=\tau_{23,0D}=0.5\tau_H
\end{aligned}
\tag{7.31}
$$

$$
\begin{aligned}
&\beta_{31,2}=A_8,\ \beta_{31,1}=-A_8(A_3+A_7),\ \beta_{31,1D}=A_5A_{11},\beta_{31,0}=A_3A_7A_8,\\
&\beta_{31,0D1}=-A_3A_5A_{11},\beta_{31,0D2}=A_1A_6A_{11},\ \tau_{21,1D}=\tau_{31,0D1}=\tau_C,\tau_{31,0D2}=\tau_{HC}+\tau_C\\
&\beta_{32,2}=A_9,\ \beta_{32,1}=-A_9(A_3+A_7),\ \beta_{32,0}=A_3A_7A_9,\ \tau_{32}=\tau_{KC}\\
&\beta_{33,0D}=A_6A_{11}\frac{1}{cM_H},\ \beta_{33,0}=A_2A_6A_{11},\ \tau_{33,0}=0.5\tau_H,\ \tau_{33}=\tau_{HC}+\tau_C
\end{aligned}
\tag{7.32}
$$

$$\alpha_2 = -(A_3 + A_7 + A_{10}),\ \alpha_1 = A_3A_7 + A_3A_{10} + A_7A_{10},\ \alpha_0 = -A_3A_7A_{10},$$
$$\alpha_{0D} = -A_4A_6A_{11}, \tau_{0D} = \tau_H + \tau_{HC} + \tau_C + \tau_{CH} \tag{7.33}$$

7.2.3 Parameters identification

Prior to solving the task of the estimation of model parameters, let us display how unconventional the step response of the system is. Consider the step change of $P(t)$ resulting in changes of system output temperatures, as it is pictured in Fig. 7.2. An interesting feature of the step response is the existence of "stairs" ("quasi" steady states) in the plot.

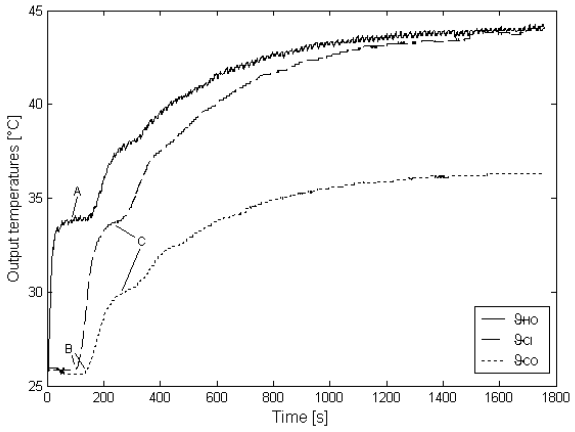

Fig. 7.2 Heater power step change responses

The existence of these multiple "quasi" steady states can be explained as follows: Temperature of water at the heater output, $\vartheta_{HO}(t)$, increases until the energy inlet and outlet of the heater equal. In the meanwhile, the "hot" water flow goes through the long pipe to the cooler, and, after some dead-time, τ_{HC}, it affects input, $\vartheta_{CI}(t)$, and output, $\vartheta_{CO}(t)$, temperatures of the cooler. At this time, the heater input temperature remains constant, because the water flow has not gone a round yet, and $\vartheta_{CO}(t)$ becomes constant. Then "cold" water goes back to the heater and closes a circuit. Again, the closed loop dead time between the cooler output and cooler input, $\tau = \tau_{CH} + \tau_H + \tau_{HC}$, is long enough so that $\vartheta_{CI}(t)$ and $\vartheta_{C0}(t)$ become almost constant.

There were made no attempts to determinate measure the mass flow rate of water by measuring of the diameter of the pipeline, the water-flow velocity, etc. Steady state data in Tab. 7.1 can be used for evaluation of $\dot{m}(t)$ by taking into account the fact that more than one steady state can usually be found in a step response of the system.

Tab. 7.1 Measurements of steady-state temperatures for $u_C = 3\,\mathrm{V}$

u_P [V]	P [W]	ϑ_{HO0} [°C]	ϑ_{CI0} [°C]	ϑ_{CO0} [°C]	ϑ_A [°C]
4	225	38.1	38.0	31.3	22
4	225	41.8	41.5	35.1	26
5	225	39.4	39.3	32.9	25
5	225	40.9	40.7	34.5	27
6	225	39.5	39.3	32.9	25.5
6	225	38.0	37.9	33.0	23.5
4	300	43.5	43.2	34.9	25
4	300	42.6	42.5	33.7	23
5	300	41.9	41.8	33.3	22.5
5	300	44.1	43.8	36.0	25
6	300	43.3	42.8	35.2	24
6	300	43.4	43.1	35.3	24
4	375	48.1	47.9	37.1	24
4	375	47.8	47.3	36.8	23.5
5	375	48.8	48.5	38.7	25.5
5	375	49.9	49.7	40.0	26
6	375	48.2	47.8	38.3	23
6	375	49.1	48.9	39.5	26.5
4	400	51.2	50.9	37.7	24
5	400	52.2	52.0	39.9	24
6	400	49.9	49.8	38.2	23

The steady state of (7.1) reads

$$0 = P_0 + c\dot{m}_0\left[\vartheta_{HI0} - \vartheta_{HO0}\right] - K_{H0}\left[\frac{\vartheta_{HO0} + \vartheta_{HI0}}{2} - \vartheta_A\right] \tag{7.34}$$

i.e. the derivative is assumed identically zero. There are two unknown static parameters in (7.34), $\dot{m}_0$ and K_{H0}, for a particular setting of inputs. Mass flow rate, $\dot{m}(t)$, as a function of $u_P(t)$ influences mainly system delays, whereas $K_H(t)$ given by (7.3) impresses a

"height" of the "first" steady state of $\vartheta_{HO}(t)$, see Fig. 7.2 (A). Tab. 7.2 contains the "first" steady state values of temperatures $\vartheta_{HO}(t)$ and $\vartheta_{HI}(t) = \vartheta_{CO}(t - \tau_{CH})$. These data together with data from Tab. 7.1 enable to estimate $\dot{m}_0$ and K_{H0} for a particular setting of input values by inserting these data into (7.34), thus, we have two independent equations (7.34) for a particular setting of inputs. The final values of $\dot{m}_0$ and K_{H0} are taken as the arithmetical mean of all calculated values from these tables for a particular (same) setting. There can be then estimated unknown parameters of $\dot{m}_0$ and K_{H0} in (7.3) and (7.7), from these values.

Tab. 7.2 Measurements of "quasi" steady-state temperatures for $u_C = 3\,\mathrm{V}$

u_P [V]	P [W]	ϑ_{HO0} [°C]	ϑ_{CI0} [°C]	ϑ_{CO0} [°C]	ϑ_A [°C]
4	225	28.8	21.7	22	22
4	225	33.0	26.1	26	26
5	225	31.2	24.7	25	25
5	225	33.8	26.9	27	27
6	225	31.8	25.6	25.5	25.5
6	225	29.6	23.1	23.5	23.5
4	300	33.9	24.5	25	25
4	300	30.7	21.7	23	23
5	300	33.9	25.4	25.5	22.5
5	300	33.9	25.1	25	25
6	300	32.1	23.6	24	24
6	300	32.7	24.1	24	24
4	375	35.5	24.1	24	24
4	375	35.3	23.6	23.5	23.5
5	375	36.4	25.2	25.5	25.5
5	375	36.7	25.7	26	26
6	375	29.2	22.9	23	23
6	375	32.8	26.5	26.5	26.5
4	400	38.2	23.5	24	24
5	400	38.9	25.2	24	24
6	400	36.3	23.3	23	23

Hence, equation (7.7) together with data in Tabs. 7.1 - 7.2 results in $\dot{m}_0$ as in Tab. 7.3, and K_{H0} as in Tab. 7.4 where the water density was chosen as $\rho = 993$ kg·m^{-3}, and c = 4180 J·kg^{-1}·K^{-1}.

Tab. 7.3 Measured relation $\dot{m}_0(u_P)$

u_P [V]	3	4	5	6
$\dot{m}_0$ [m^3·10^{-4}]	69.8	76.1	80.9	83.0

Tab. 7.4 Measured relation $K_{H0}(u_P, P)$ *[W·K^{-1}]*

u_P [V] / P[W]	4	5	6
225	1.07	1.37	1.40
300	1.59	1.54	1.24
375	1.46	2.14	2.04
400	2.31	2.76	2.63

The evaluation of these data with respect to (7.3) and (7.7) results in the following numeric estimation (made in MS Excel Solver): h_0 = 8.4925, h_1 = -0.0017, h_2 = -14999, h_3 = -12998, h_4 = 1507.988, h_5 = 77.766; $p_0 = 5.077 \cdot 10^{-3}$, p_1 = 0.266, p_2 = 0.274. A graphical comparisons of measured and calculated data are in Fig.7.3 and Fig.7.4.

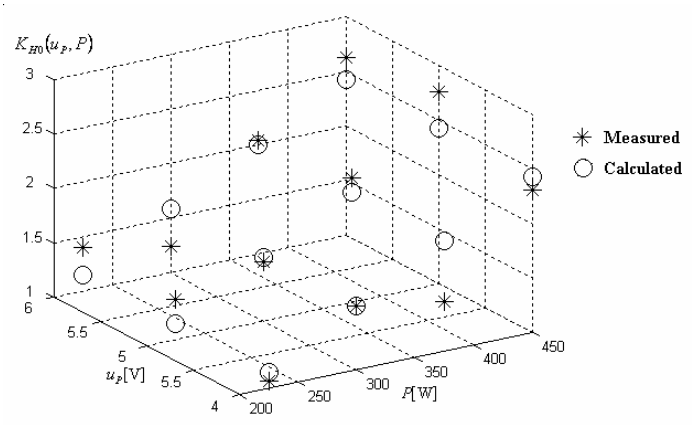

Fig. 7.3 Comparison of measured and calculated K_{H0}

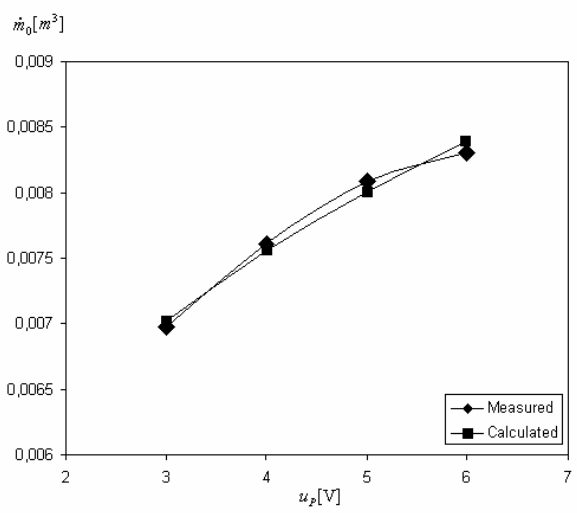

Fig. 7.4 Comparison of measured and calculated $\dot{m}_0$

One can see that $K_{H0}(u_P, P)$ is nearly not depended on the setting of u_P and thus a linear relation $K_{H0}(P)$ could be enough to take. The important disadvantage of these estimations is the fact that the results are strongly sensitive to the measurement of the ambient air temperature.

Data in Tab. 7.1 together with the static equation obtained from (7.4) can be also used for the evaluation of the (constant) heat transmission coefficient K_P which characterizes especially a "height" of the "quasi" steady state of $\vartheta_{CI}(t)$, see Fig. 7.2 (C). From (7.4) we have

$$0 = c\dot{m}_0[\vartheta_{HO0} - \vartheta_{CI0}] - K_P\left[\frac{\vartheta_{CI0} + \vartheta_{HO0}}{2} - \vartheta_A\right] \tag{7.35}$$

The final value of K_P is taken as the arithmetical mean again as $K_P = 0.39$ W·K^{-1}. Obviously, the pipeline is insulated very well and this coefficient does not affect the system dynamics significantly. The measurement is sensitive to ϑ_A again, and the A/D converter resolution (cca 0.1 °C) disables to find a more accurate value of K_P. Moreover, the effect of secondary heating (due to the material of the pipeline) makes a measurement of ϑ_{HO0} and ϑ_{CI0} more difficult.

As for the estimation of K_{C0}, steady state yields (7.5) of the form

$$0 = c\dot{m}_0\left[\vartheta_{CI0} - \vartheta_{CO0}\right] - K_{C0}\left[\frac{\vartheta_{CO0} + \vartheta_{CI0}}{2} - \vartheta_A\right] \tag{7.36}$$

This equation together with data in Tab. 7.5 gives the estimation of K_{C0}, which characterizes especially a "height" of the "quasi" steady state of $\vartheta_{CO}(t)$, see Fig. 7.2 (C), for a particular setting of u_C, similarly as it was proceeded above.

Tab. 7.5 Measurements of steady-state temperatures for various u_C, $P = 300\,\mathrm{W}$, $u_P = 5\,\mathrm{V}$

u_C [V]	ϑ_{HO0} [°C]	ϑ_{CI0} [°C]	ϑ_{CO0} [°C]	ϑ_A [°C]
1	48.1	47.9	40.0	24
1	45.3	45.0	36.2	21.5
1	46.5	46.3	38.2	25
2	43.3	42.9	34.7	22.5
2	43.3	42.8	34.9	23.5
2	44.5	44.3	35.8	23
4	39.8	39.3	30.0	20.5
4	42.3	42.2	32.7	23
4	43.1	42.8	34.5	25.5
5	39.6	39.3	31.0	21
5	39.9	39.6	31.6	22
5	40.9	40.6	32.3	24
6	40.6	40.5	32.2	23
6	41.1	40.9	32.6	24.5
6	38.6	38.4	30.2	21

Note that temperature values for $u_C = 3$ V are omitted in Tab. 7.5 since they can be obtained from Tab. 7.2.

The arithmetical mean of particular measured values of K_{C0} results in relations as in Tab. 7.6.

Tab. 7.6 Measured relation $K_{C0}(u_C)$

u_C [V]	K_{C0} [W·K^{-1}]
1	14.2
2	16.9
3	18.2
4	19.5
5	21
6	21.4

By means of the numerical optimization (MS Excel) one can obtain coefficients of (7.6) as

$$c_0 = 11.8,\ c_1 = 2.755,\ c_2 = -0.19 \tag{7.37}$$

A graphical comparison of measured and calculated $K_{C0}(u_C)$ is in Fig. 7.5.

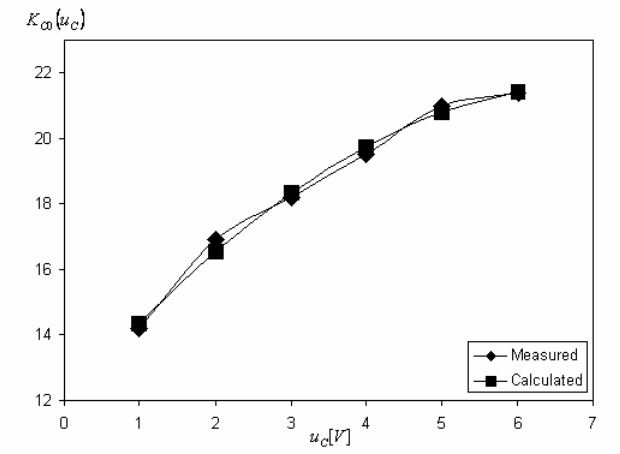

Fig. 7.5 Comparison of measured and calculated K_{C0}

All the above presented data enable to draw up the static characteristics of the studied model. Static relations between u_P and all output temperatures, for P = 300 W, $u_C = 3\,\mathrm{V}$, $\vartheta_A = 24\,^{\circ}\mathrm{C}$, are displayed in Fig. 7.6

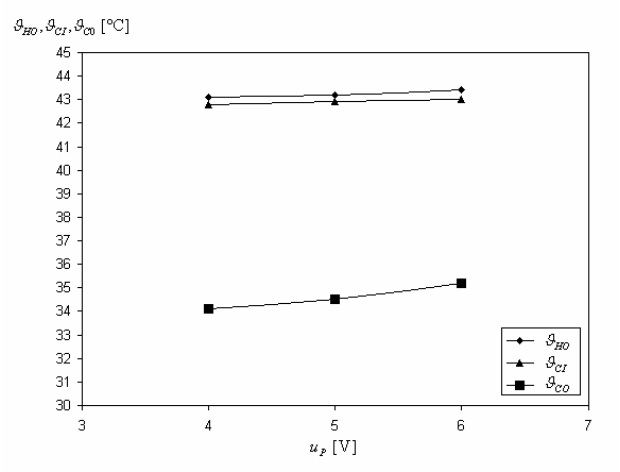

Fig. 7.6 Static characteristics $\vartheta_{HO}(u_P)$, $\vartheta_{CI}(u_P)$, $\vartheta_{CO}(u_P)$, *for P = 300 W,* $u_C = 3\,\mathrm{V}$, $\vartheta_A = 24\,^{\circ}\mathrm{C}$

Static characteristics $\vartheta_{HO}(u_C)$, $\vartheta_{CI}(u_C)$, $\vartheta_{CO}(u_C)$ are presented in Fig. 7.7 , for *P* = 300 W, $u_P = 5\,\mathrm{V}$, $\vartheta_A = 24\,^{\circ}\mathrm{C}$, and relations $\vartheta_{HO}(P)$, $\vartheta_{CI}(P)$, $\vartheta_{CO}(P)$ are depicted in Fig. 7.8, for $u_P = 5\mathrm{V}$, $u_C = 3\,\mathrm{V}$, $\vartheta_A = 24\,^{\circ}\mathrm{C}$.

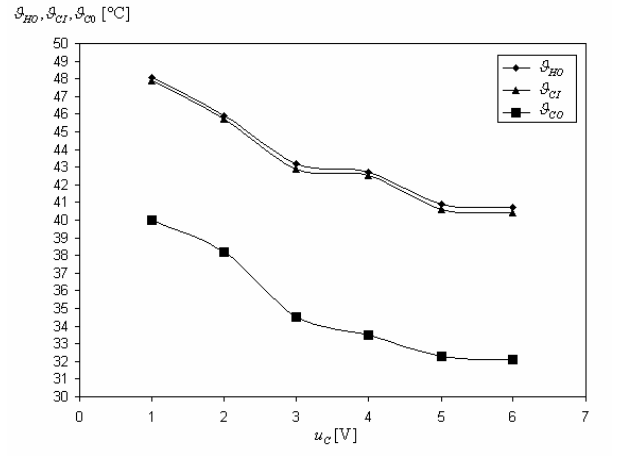

Fig. 7.7 Static characteristics $\vartheta_{HO}(u_C)$, $\vartheta_{CI}(u_C)$, $\vartheta_{CO}(u_C)$, *for P = 300 W,* $u_P = 5\,\mathrm{V}$, $\vartheta_A = 24\,^{\circ}\mathrm{C}$

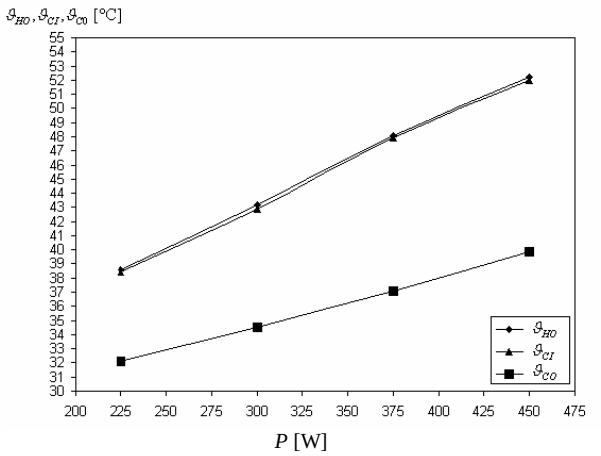

Fig. 7.8 Static characteristics $\vartheta_{HO}(P)$, $\vartheta_{CI}(P)$, $\vartheta_{CO}(P)$, *for* $u_P = 5\text{V}$, $u_C = 3\text{V}$, $\vartheta_A = 24°\text{C}$

The figures indicate a very good linearity of the model.

Delays can be estimated graphically from dynamic data (step responses) for appropriate system input changes; see Fig. 7.2 (B). The delay of the control action of the heat exchanger (cooler), τ_{KC}, was obtained from the cooling curve (not displayed here). Results are dependent on the particular mass flow rate; as it can be seen from Tab. 7.7.

Tab. 7.7 Measured delays as functions of u_P

u_P [V]	2	3	4	5	6
τ_H [s]	3	3	3	3	3
τ_{HC} [s]	125	125	120	110	105
τ_C [s]	24	23	22	21	20
τ_{KC} [s]	14	13	12	12	11
τ_{CH} [s]	10	10	9	9	8

Since the model does not reflect the influence of $u_P(t)$ upon the delays, arithmetical mean values were taken in the final (i.e. for $u_P = 4\text{V}$). Delay in the heater, τ_H, is short enough so that it can be omitted in the model, if one wants to.

$$\tau_H = 3\text{s},\ \tau_{HC} = 110\text{s}, \tau_C = 22\text{s},\ \tau_{KC} = 12\text{s},\ \tau_{CH} = 9\text{s} \tag{7.38}$$

Overall masses of water in the heater, the cooler and in the long pipeline were estimated graphically and numerically from dynamic characteristics, so that measured and calculated model give a good agreement. They influence mainly "slopes" of the steepest ascents in the particular step responses. For example, M_H influences the initial slope of the step response of $P(t)$ to $\vartheta_{HO}(t)$ mainly. An initial estimation had been made by graphical comparison of (model) simulated and measured responses

Final results obtained by the evaluation of the least mean squares criterion are the following

$$M_H = 0.08\,\text{kg},\ M_P = 0.22\ \text{kg},\ M_C = 0.27\ \text{kg} \tag{7.39}$$

The final comparison of measured step responses and the calculated ones is depicted in Fig. 7.9.

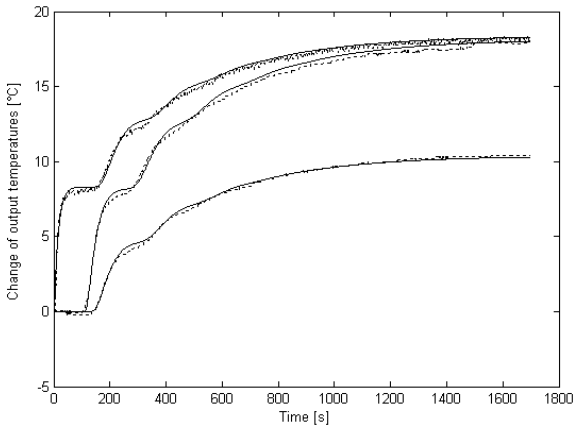

Fig. 7.9 Comparison of measured (dotted) and calculated (solid) step responses for the settings $u_P = 5\,\text{V}$, $u_C = 3\,\text{V}$, $\Delta P = 300\,\text{W}$, *on/off fan is on*

7.3 Design of a controller for the plant in R_{MS}

The derivation of two different controllers' structures for the heating plant described above using the algebraic approach in R_{MS} for various external inputs and feedback loops is the subject matter of this subsection. Because of the plant is MIMO, only one manipulated input and one measured output are chosen while the rest serve for

defining of the operation point. Namely, the intention is to control $\vartheta_{CO}(t)$ by means of $P(t)$. From model (7.25), (7.32) and (7.33), it can be obtained

$$G(s)=\frac{\Theta_{CO}(s)}{P(s)}=\frac{(\beta_{33,0D}\exp(-\tau_{33,0}s)+\beta_{33,0})\exp(-\tau_{33}s)}{s^3+\alpha_2 s^2+\alpha_1 s+\alpha_0+\alpha_{0D}\exp(-\tau_{0D}s)}$$
$$=\frac{(b_{0D}\exp(-\tau_0 s)+b_0)\exp(-\tau s)}{s^3+a_2 s^2+a_1 s+a_0+a_{0D}\exp(-\vartheta s)} \tag{7.40}$$

Let $P(t)$ be relabeled to $P_H(t)$ to avoid the confusion with the controller denominator.

7.3.1 1DoF control structure

Consider the 1DoF control system as in Fig. 2.1 and let the external inputs be from the class of stepwise functions (4.204) with $m_w(s)=m_d(s)=s+m_0$, $m_0>0$, for the simplicity. Utitlize now the methodology described in Subsection 4.3.

The plant transfer function can be factorized as

$$G(s)=\frac{\dfrac{(b_{0D}\exp(-\tau_0 s)+b_0)\exp(-\tau s)}{m(s)}}{\dfrac{s^3+a_2 s^2+a_1 s+a_0+a_{0D}\exp(-\vartheta s)}{m(s)}}=\frac{B(s)}{A(s)} \tag{7.41}$$

where $m(s)$ is a stable (quasi)polynomial of degree three, for instance, $m(s)=(s+m_0)^3$, again for the simplicity. Naturally, there are other possibilities how to select $m(s)$, e.g. as $m(s)=s^3+m_2 s^2+m_1 s+m_0$, which would bring more degrees of freedom (free selectable controller parameters).

The primary aim is to stabilize the control feedback loop using (4.33). If $Q_0(s)=1$, the following particular stabilizing solution is obtained

$$P_0(s)=\frac{(s+m_0)^3-(b_{0D}\exp(-\tau_0 s)+b_0)\exp(-\tau s)}{s^3+a_2 s^2+a_1 s+a_0+a_{0D}\exp(-\vartheta s)} \tag{7.42}$$

For reference tracking and disturbance rejection, condition (4.40), i.e. $F_W(s) \mid (A(s)P(s)) \wedge F_D(s) \mid (B(s)P(s))$. Equivalently, $P(s)$ must include at least one zero root which can be expressed by the condition

$$P(0) = 0 \tag{7.43}$$

Thus, try to choose the following structure

$$Z(s) = \frac{(s+m_0)^3}{s^3 + a_2 s^2 + a_1 s + a_0 + a_{0D}\exp(-\vartheta s)} Z_0 \tag{7.44}$$

where $Z_0 \in \mathbb{R}$, to obtain $P(s)$ in an arbitrarily simple form. Condition (7.43) results in

$$Z_0 = \frac{m_0^3}{b_{0D} + b_0} - 1 \tag{7.45}$$

Finally, the controller structure is given by inserting (7.45), (7.44) and (7.42) into (4.34) as

$$G_R(s) = \frac{m_0^3\left(s^3 + a_2 s^2 + a_1 s + a_0 + a_{0D}\exp(-\vartheta s)\right)}{(b_{0D} + b_0)(s+m_0)^3 - m_0^3(b_{0D}\exp(-\tau_0 s) + b_0)\exp(-\tau s)} \tag{7.46}$$

The controller contains only one selectable (free) parameter m_0 and it has anisochronic structure including internal delays; however, it is simply realizable by integrators and delay elements, see the MATLAB/Simulink scheme as in Fig. 7.10. The value of m_0 is going to be chosen according to the robust analysis, see Subsections 7.6 and 7.7.

7.3.2 TFC control structure

The TFC control system (Fig. 2.2) is utilized in this subsection to determine the controller law for different external inputs via the methodology described in Subsection 4.4.

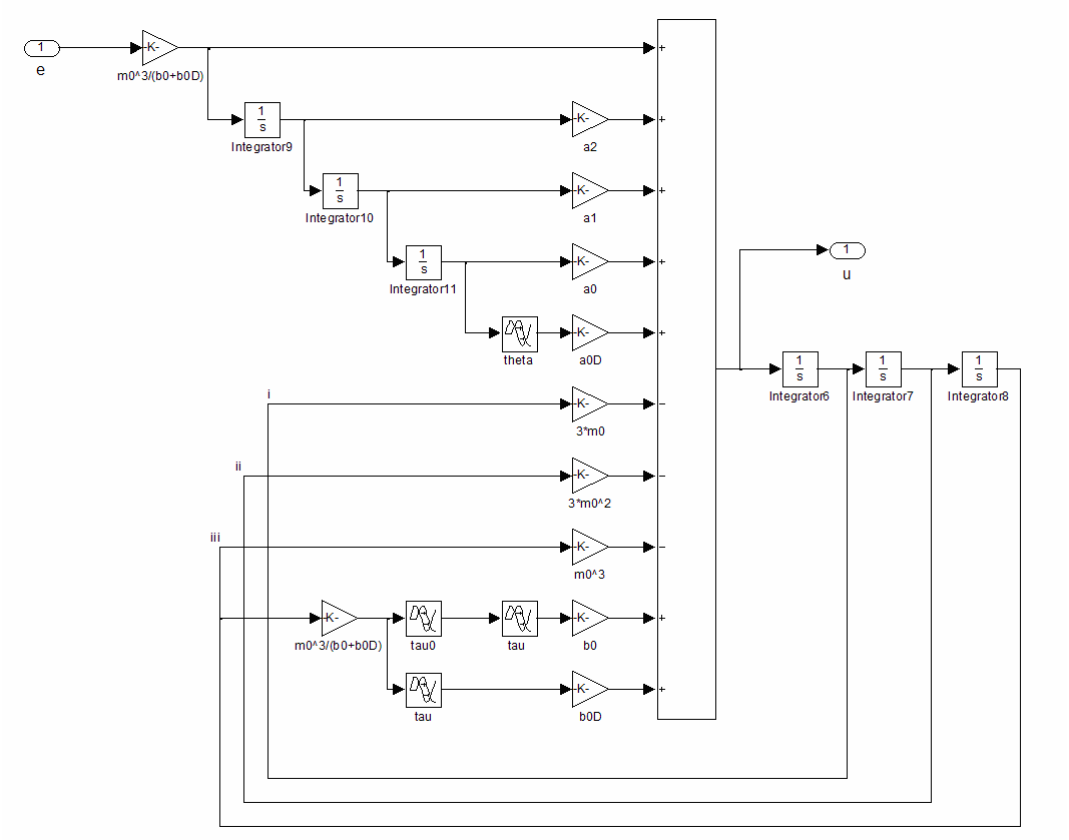

Fig. 7.10 MATLAB/Simulink scheme of controller (7.46)

Let the external inputs be described by (4.204), i.e. the reference is from the set of linearwise functions, whereas the disturbance has a stepwise character. Plant coprime factorization is given by (7.41).

Closed-loop stabilization according to (4.60) yields e.g.

$$T_0 = 1,\ P_0(s) = \frac{(s+m_0)^3 - (b_{0D}\exp(-\tau_0 s) + b_0)\exp(-\vartheta s)}{s^3 + a_2 s^2 + a_1 s + a_0 + a_{0D}\exp(-\vartheta s)} \tag{7.47}$$

which is equivalent to (7.42). Since it must hold that $F_W(s) \mid (A(s)P(s)) \wedge F_D(s) \mid (B(s)P(s))$ giving rise to two conditional equations (4.59) for $P(s)$, select $Z(s)$ with two free real parameters z_0, z_1 as

$$Z(s)=\frac{(s+m_0)^3}{s^3+a_2s^2+a_1s+a_0+a_{0D}\exp(-\vartheta s)}\frac{z_1s+z_0}{s+m_0} \tag{7.48}$$

Then the numerator of $P(s)$ reads

$$p_N(s,z_0,z_1)=(s+m_0)^4-(b_{0D}\exp(-\tau_0 s)+b_0)\exp(-\varpi s)((1+z_1)s+m_0+z_0) \tag{7.49}$$

Conditional equations

$$p_N(0,z_0,z_1)=0,\left[\frac{\mathrm{d}}{\mathrm{d}s}p_N(s,z_0,z_1)\right]_{s=0}=0 \tag{7.50}$$

result in

$$z_0=m_0\left(\frac{m_0^3}{b_0+b_{0D}}-1\right),z_1=\frac{-(b_0+b_{0D})\left(b_0+b_{0D}-m_0^3(m_0\tau+4)\right)+b_{0D}m_0^4\tau_0}{(b_0+b_{0D})^2} \tag{7.51}$$

and consequently

$$\begin{aligned}
P(s)&=\frac{p_4s^4+p_3s^3+p_2s^2+p_1(s)s+p_0(s)}{(b_0+b_{0D})^2(s^3+a_2s^2+a_1s+a_0+a_{0D}\exp(-\vartheta s))(s+m_0)}\\
T(s)&=\frac{m_0^3}{(b_0+b_{0D})^2}\frac{t_1s+t_0}{s+m_0}\\
p_4&=(b_0+b_{0D})^2,\ p_3=4m_0(b_0+b_{0D})^2,\ p_2=6m_0^2(b_0+b_{0D})^2,\\
p_1(s)&=m_0^3\\
&\quad\left(4(b_0+b_{0D})^2-(b_0+b_{0D}\exp(-\tau_0 s))(b_0(m_0\tau+4)+b_{0D}(m_0(\tau+\tau_0)+4))\exp(-\varpi s)\right)\\
p_0(s)&=m_0^4(b_0+b_{0D})(b_0(1-\exp(-\varpi s))+b_{0D}(1-\exp(-(\tau+\tau_0)s)))\\
t_1&=b_0(m_0\tau+4)+b_{0D}(m_0(\tau+\tau_0)+4)\\
t_0&=m_0(b_0+b_{0D})
\end{aligned} \tag{7.52}$$

Decomposition (4.63) must be done so that $F_W(s)|(B(s)Q(s))$; however, as $T(s)$ in (7.52) is of the first order numerator polynomial, it is not possible to meet the requirement. Nevertheless, one can make the following extension

$$T(s)=\frac{m_0^3}{(b_0+b_{0D})^2}\frac{t_1s+t_0}{s+m_0}\frac{s+m_1}{s+m_1}=\frac{m_0^3}{(b_0+b_{0D})^2}\frac{t_1s^2+(t_1m_1+t_0)s+t_0m_1}{(s+m_0)(s+m_1)},m_1>0 \tag{7.53}$$

and the decomposition obviosly reads

$$Q(s)=\frac{m_0^3}{(b_0+b_{0D})^2}\frac{(1-\gamma)t_1 s^2}{(s+m_0)(s+m_1)}$$
$$R(s)=\frac{m_0^3}{(b_0+b_{0D})^2}\frac{\gamma t_1 s^2+(t_1 m_1+t_0)s+t_0 m_1}{(s+m_0)(s+m_1)},0\le\gamma\le 1 \tag{7.54}$$

To sum up, the controllers' transfer functions are

$$G_Q(s)=m_0^3\frac{(s^3+a_2 s^2+a_1 s+a_0+a_{0D}\exp(-\vartheta s))(1-\gamma)t_1 s^2}{(p_4 s^4+p_3 s^3+p_2 s^2+p_1(s)s+p_0(s))(s+m_1)}$$
$$G_R(s)=m_0^3 \tag{7.55}$$
$$\frac{(s^3+a_2 s^2+a_1 s+a_0+a_{0D}\exp(-\vartheta s))(\gamma t_1 s^2+(t_1 m_1+t_0)s+t_0 m_1)}{(p_4 s^4+p_3 s^3+p_2 s^2+p_1(s)s+p_0(s))(s+m_1)}$$

In this case, there are two real selectable controller parameters. A simple suboptimal tuning idea is presented in Subsection 7.7.

7.4 Relay feedback identification test

We attempted to simplify model (7.40) by the use of the relay-feedback experiment, see Subchapter 2.8 and Chapter 6, and to compare control responses using the original mathematical model and that obtained from the relay test. Hence, consider model (6.1) and try to identify its parameters. Three different set of algebraic equations (6.6) – (6.9), (6.19) – (6.22) and (2.131) – (2.133), respectively, were solved by means of

a) the well-known Levenberg-Marquardt (LM) method (which is close to the Gauss-Newton one), see e.g. [78],

b) the NM algorithm, see Subchapter 5.4, and

c) the MS Excel Solver.

Note that for the operating point

$$\lfloor u_p, u_c, P_H, \vartheta_{HO}, \vartheta_{CI}, \vartheta_{CO}, \vartheta_A \rfloor = [5\,\mathrm{V}, 3\,\mathrm{V}, 300\,\mathrm{W}, 44.1\,^\circ\mathrm{C}, 43.8\,^\circ\mathrm{C}, 36\,^\circ\mathrm{C}, 24\,^\circ\mathrm{C}] \tag{7.56}$$

the parameters in (7.40) are the following

$$b_{0D} = 2.334 \cdot 10^{-6}, b_0 = -2.146 \cdot 10^{-7}, a_2 = 0.1767, a_1 = 0.009,$$
$$a_0 = 1.413 \cdot 10^{-4}, a_{0D} = -7.624 \cdot 10^{-5}, \tau_0 = 1.5, \tau = 131, \vartheta = 143 \quad (7.57)$$

Look at simulation results via several techniques in more details.

7.4.1 Frequency-domain solution

The relay test was performed with a biased on-off relay, $B^+ = 220, B^- = 180[\mathrm{W}]$, first, to get the estimation of the static gain according to (2.126) and that of the ultimate gain as in (2.125) for a saturation relay test. The results were the following: $A_1 = 1.9975[^\circ C]$, $T_{u,1} = 364.8[s]$, which gives $k_{u,1} = 127.48 = k_{\min}$, $k = b_0 / (a_0 + a_1) = 0.0325$. Dead time was estimated according to Fig. 2.10 as $\tau = 136.7$. Then we tried to perform the saturation-relay test with $k_{u,2} = 1.4k_{\min}$; however, the restoration of limit cycles took a long time and there was an obvious margin in the setting of the saturation relay. Thus, the option $k_{u,2} = 1.1k_{\min} = 140.23 \Rightarrow \overline{A}_2 = 1.426$ resulted in $T_{u,2} = 373.4$, $A_2 = 1.9245$. These results enable to estimate two model parameters.

Hence, introduce an artificial delay element with $\tau^+ = 5\pi / (12\omega_u)$ $= 5/24T_{u,2} = 77.8$. Again, the procedure started with a (symmetrical) on-off relay $B = 200$ yielding $\tilde{A}_1 = 3.1, \tilde{T}_{u,1} = 555.3, \tilde{k}_{u,1} = \tilde{k}_{\min} = 82.14$. Since $\tilde{k}_{u,2} = 1.1\tilde{k}_{\min}$ did not cause limit cycles, $\tilde{k}_{u,2} = 1.4\tilde{k}_{\min} = 115 \Rightarrow \overline{\tilde{A}}_2 = 1.7391$ were taken for the saturation-relay test which gave $\tilde{A}_2 = 2.52, \tilde{T}_{u,2} = 597.8$.

Solutions of the set (6.6) – (6.9) via various techniques are introduced in Tab. 7.8. The static gain value $k = 0.0325$ is fixed and the initial parameters estimation reads $a_0 = a_1 = 0.5 / T_{u,2} = 0.013$, $\tau = \vartheta = 136.7$.

Note that NM algorithm and the MS Excel Solver minimize the sum of squares of the left-hand sides of (6.6) – (6.9), which agrees with error e in the table.

Tab. 7.8 Frequency-domain solution with saturation relay and artificial delay

	LM method	NM method	Excel Solver
a_0	$1.751567 \cdot 10^{-2}$	$9.9301645 \cdot 10^{-3}$	$4.422509 \cdot 10^{-2}$
a_1	$-9.08719 \cdot 10^{-3}$	$-3.9951297 \cdot 10^{-3}$	$-2.4479 \cdot 10^{-2}$
τ	102.83	159.83	140.92
ϑ	131.49	130.75	155.2
e	$1.27 \cdot 10^{-2}$	$3.25 \cdot 10^{-20}$	$8.06 \cdot 10^{-4}$

7.4.2 Time-domain solution

Simulation experiment results from the preceding subchapter can be used for alternative, time-domain, solution of the relay identification problem given by the set (6.19) – (6. 22). Again, the results are summed up in Tab. 7.9.

Tab. 7.9 Time-domain solution with saturation relay and artificial delay

	LM method	NM method	Excel Solver
a_0	$9.9301645 \cdot 10^{-3}$	$9.9301645 \cdot 10^{-3}$	$9.9301645 \cdot 10^{-3}$
a_1	$-3.9951297 \cdot 10^{-3}$	$-3.9951297 \cdot 10^{-3}$	$-3.9951297 \cdot 10^{-3}$
τ	159.83	159.83	159.83
ϑ	130.75	130.75	130.75
e	$1.82 \cdot 10^{-13}$	$3.38 \cdot 10^{-25}$	$2.11 \cdot 10^{-21}$

Obviously, the three computational techniques provide (almost) the same results identical with that obtained by the frequency-domain solution via NM algorithm.

7.4.3 Use of relay transient

Finally, try to use the relay transient introduced in Subsection 2.8.5. Limit cycles from the experiment with on-off relay were utilized. Exponential decaying function was chosen as $\exp(-0.01t)$, the sampling period for the DTFT was set to $T_0 = 0.1$ and the final time was taken as $t_f = 2000$. These values give rise to discrete frequencies $\omega_l = l0.0031, l \in \mathbb{N}$ on which the DTFT is calculated and, subsequently, model parameters are estimated according to (2.131) – (2.133).

For $l=1$, $\overline{U}(\mathrm{j}\omega_1)=-1.1139\cdot10^4+3.3348\cdot10^2\,\mathrm{j}$, $\overline{Y}(\mathrm{j}\omega_1)=20.97+16\mathrm{j}$ and $\overline{Y}(\mathrm{j}\omega_1)/\overline{U}(\mathrm{j}\omega_1)=(1.924-1.379\mathrm{j})\cdot10^{-3}$.

For $l=3$, $\overline{U}(\mathrm{j}\omega_3)=-1.285243\cdot10^4+2.52541\cdot10^3\,\mathrm{j}$, $\overline{Y}(\mathrm{j}\omega_3)=11.208+25.188\mathrm{j}$ and $\overline{Y}(\mathrm{j}\omega_3)/\overline{U}(\mathrm{j}\omega_3)=(-1.8087-0.49819\mathrm{j})\cdot10^{-3}$.

Inserting these values into (2.132) for model (6.1), optimization techniques yield results introduced in Tab. 7.10.

Tab. 7.10 Solution by the use of the relay transient

	LM method	NM method	Excel Solver
a_0	$3.06598277\cdot10^{-2}$	$3.06598277\cdot10^{-2}$	$7.410418\cdot10^{-3}$
a_1	$-1.7487959\cdot10^{-2}$	$-1.7487959\cdot10^{-2}$	$-2.607269\cdot10^{-3}$
τ	143.42	143.42	136.7
ϑ	158.08	158.08	136.69
e	$3.19\cdot10^{-14}$	$1.59\cdot10^{-15}$	$1.29\cdot10^{-8}$

Thus, LM and NM techniques provided comparable results.

7.4.4 Comparison of the results

To sum up the relay experiment, results from Tabs. 7.8 – 7.10 are compared via step responses and Nyquist plots of original and approximating models. Concurrently, ISE and ISTE criteria – analogous to (4.186) and (4.187) with $\varphi=0$ – are calculated for step responses for the time range $t\in[0,2000]$ with the step $\Delta t=0.1$, and Nyquist plots are assessed using the criterion

$$J_{Nyq}=\sum_{\omega_i}\left|G(\omega_i)-\overline{G}(\omega_i)\right| \tag{7.58}$$

where G is the original model (7.40), $\overline{G}$ means the approximating one (6.1) and ω_i are discrete frequencies, here $\omega\in[0,0.1]$ with $\Delta\omega=\omega_i-\omega_{i-1}=10^{-4}$.

Figs. 7.11 and 7.12 provide a graphical comparison, whereas Tab. 7.11 gives criterial results.

Results from Tabs. 7.8 – 7.10 are labelled as follows:

a) “Result 1” – NM from Tab. 7.8, all results from Tab. 7.9.

b) “Result 2” – LM from Tab. 7.8

c) “Result 3” – Excel Solver from Tab. 7.8

d) “Result 4” – LM and NM from Tab. 7.10

e) “Result 5” – Excel Solver from Tab. 7.10

As can be seen from Tab. 7.11, the use of the relay transient solved by the LM and NM methods gives the best result. Especially, the Nyquist curves of the original model and the approximating one obtained by this way almost coincide for low frequencies (up to the ultimate frequency). The time-domain solution and the NM technique, generally, provide good approximation as well.

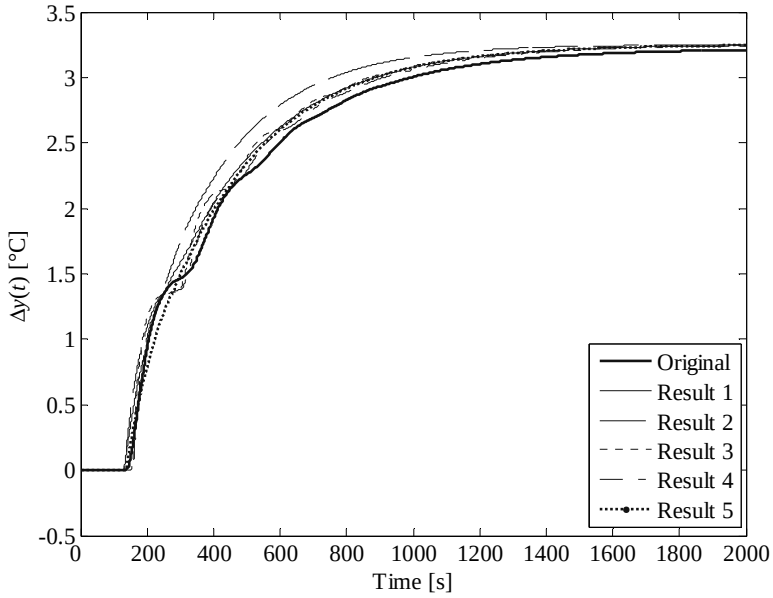

Fig. 7.11 Step responses of the original model (7.40) vs. approximating models (6.1) via relay-feedback test

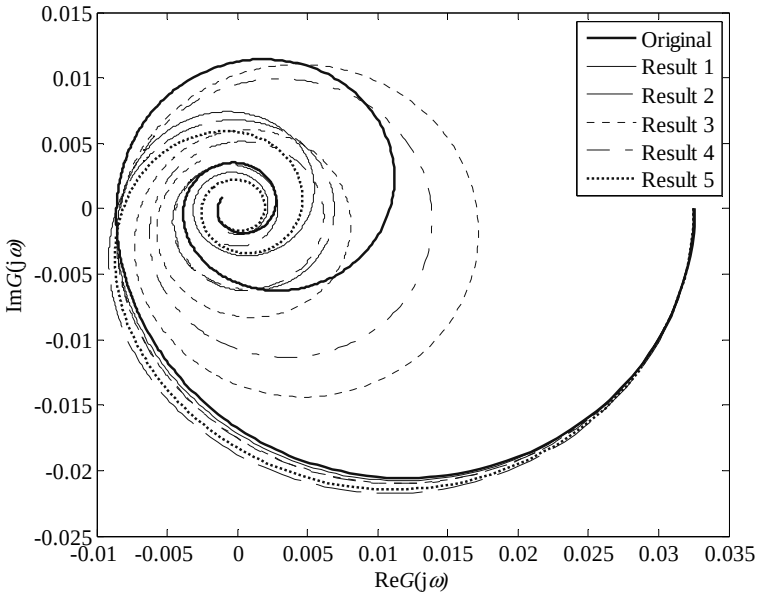

Fig. 7.12 Nyquist plots of the original model (7.40) vs. approximating models (6.1) via relay-feedback test

Tab. 7.11 Comparison of relay experiment results

Result	J_{ISE}	J_{ISTE}	J_{Nyq}
Result 1	1.363	845.2	3.227
Result 2	6.304	3704	4.475
Result 3	1.795	1063.4	4.472
Result 4	0.607	450.2	2.835
Result 5	1.015	713.7	2.852

7.4.5 Design of controllers in R_{MS} for the relay-identified model

Without superfluous details, let us present controllers derived for model (6.1), analogously to the procedure introduced in Subsections 7.3.1 and 7.3.2. The reader is referred therein for details.

For the 1DoF controller structure with stepwise inputs, i.e. reference and load disturbance, the final controller can be obtained e.g. as

$$\overline{G}_R(s)=\frac{m_0}{b_0}\frac{s+a_0+a_1\exp(-\vartheta s)}{s+m_0(1-\exp(-\tau s))},m_0>0 \tag{7.59}$$

If the TFC control system is considered and it is supposed that the reference signal is linearwise and load disturbance is from the class of stepwise functions, the eventual controllers' transfer functions read

$$\begin{aligned}
&\overline{G}_Q(s)=\frac{m_0}{b_0}\frac{(s+a_0+a_1\exp(-\vartheta s))(m_0\tau+2)(1-\gamma)s^2}{(s^2+m_0(2-(m_0\tau+2)\exp(-\tau s))s+m_0^2(1-\exp(-\tau s)))(s+m_1)}\\
&\overline{G}_R(s)=\frac{m_0}{b_0}\frac{(s+a_0+a_1\exp(-\vartheta s))((m_0\tau+2)\gamma s^2+(m_1(m_0\tau+2)+m_0)s+m_0m_1)}{(s^2+m_0(2-(m_0\tau+2)\exp(-\tau s))s+m_0^2(1-\exp(-\tau s)))(s+m_1)}\\
&m_0,m_1>0,\gamma\in[0,1]
\end{aligned} \tag{7.60}$$

Recall that another coprime factorization of the plant model, particular solution of the Bézout identity or choice of the form of parameterization term $Z(s)$ can lead to a different controller.

7.5 Controllers simplification

As can be seen from (7.46), (7.55), (7.59) and (7.60), the obtained controller structures are a rather complex. Thus, for the engineering practice, it would be desirable to simplify them, namely, to reach a finite-dimensional approximation of the control law.

In recent decades a huge number of papers and works have been focused on model reduction or rational approximation of TDS, see e.g. [4], [80], [81]. A fair overview of some methods and approaches has been published in [114]. An overwhelming majority of these methods, however, deals with input-output delays only ignoring internal or state delays on the left-hand side of differential equations, i.e. those transfer functions with exponential terms in the denominator. Moreover, the obtained controller structures would be of a very high order, as it is presented in [120] for some particular cases.

Hence, in this subchapter, two possible simple (intuitive) methods for a low-order finite-dimensional approximation of anisochronic controllers are suggested and, consequently, applied to original controllers (7.46) and (7.55).

Namely, consider a proportional-integral-derivative controller governed by the transfer function(s)

$$\overline{G}_R(s)=\frac{\overline{R}(s)}{\overline{P}(s)}=\frac{\overline{r}_2 s^2+\overline{r}_1 s+\overline{r}_0}{s(s+\overline{p}_0)},\ \overline{G}_Q(s)=\frac{\overline{Q}(s)}{\overline{P}(s)}=\frac{\overline{q}_2 s^2+\overline{q}_1 s+\overline{q}_0}{s(s+\overline{p}_0)} \tag{7.61}$$

and a proportional controller

$$\overline{\overline{G}}_Q(s)=\frac{\overline{\overline{Q}}(s)}{\overline{\overline{P}}(s)}=\overline{\overline{q}}_0 \tag{7.62}$$

as approximating models.

7.5.1 Using dominant poles and zeros

Intuitively, it is possible to preserve dominant (right-most) controller zeros and poles and asymptotic controller behavior, i.e. the slope of a step response direction at infinity for an integral controller and/or an initial point of a step response for a derivative one. This task can be defined as to find $\{s_1,s_2\}$, $\{z_{Q1},z_{Q2}\}$, $\{z_{R1},z_{R2}\}\in\mathbb{R}^2$ such that

$$\{s_1,s_2\}:=\left\{\begin{array}{l} s_i,s_j:\operatorname{Re}s_i\geq\operatorname{Re}s_j\geq\operatorname{Re}s_l, i\neq j\neq l,\\ P(s_i)=P(s_j)=P(s_l)=\overline{P}(s_i)=\overline{P}(s_j)=\overline{P}(s_l)=0\end{array}\right\} \tag{7.63}$$

$$\{z_{Q1},z_{Q2}\}:=\left\{\begin{array}{l} z_i,z_j:\operatorname{Re}z_i\geq\operatorname{Re}z_j\geq\operatorname{Re}z_l, i\neq j\neq l,\\ Q(z_i)=Q(z_j)=Q(z_l)=\overline{Q}(z_i)=\overline{Q}(z_j)=\overline{Q}(z_l)=0\end{array}\right\} \tag{7.64}$$

$$\{z_{R1},z_{R2}\}:=\left\{\begin{array}{l} z_i,z_j:\operatorname{Re}z_i\geq\operatorname{Re}z_j\geq\operatorname{Re}z_l, i\neq j\neq l,\\ R(z_i)=R(z_j)=R(z_l)=\overline{R}(z_i)=\overline{R}(z_j)=\overline{R}(z_l)=0\end{array}\right\} \tag{7.65}$$

and to satisfy the following conditions

$$\begin{array}{l}\lim_{s\to 0}s^k G_{\cdot}(s)=\lim_{s\to 0}s^k\overline{G}_{\cdot}(s)=\pm\infty, k=0,1,...\\ \lim_{s\to 0}s^{k+1}G_{\cdot}(s)=\lim_{s\to 0}s^{k+1}\overline{G}_{\cdot}(s)\neq\pm\infty\end{array} \tag{7.66}$$

for controllers with integral behavior (or for those tracking or rejecting harmonic signals) and

$$\lim_{s\to\infty} G_{\cdot}(s) = \lim_{s\to\infty} \overline{G}_{\cdot}(s) \tag{7.67}$$

for derivative-like controllers. The lower index "$_{\cdot}$" means either R or Q.

The application of the procedure to the original controllers (7.46) and (7.55) with a selected m_0 is introduced in Subsection 7.7.

7.5.2 Using the Padé approximation

The transfer function rationalization via the Padé approximation is usually performed in such a way that the approximation is applied to exponential terms only. This technique leads to high-order approximation models. A different approach, used here, rests in the approximation of the whole transfer function based on the Taylor (Maclaurin) series expansion of the approximated and approximating model and matching of some (low-degree) coefficients, which agrees with conditions

$$\begin{aligned} &\left[G_{\cdot}(s)\right]_{s=0} = \left[\overline{G}_{\cdot}(s)\right]_{s=0}, \left[\frac{\mathrm{d}}{\mathrm{d}s} G_{\cdot}(s)\right]_{s=0} = \left[\frac{\mathrm{d}}{\mathrm{d}s} \overline{G}_{\cdot}(s)\right]_{s=0}, \\ &\left[\frac{\mathrm{d}^2}{\mathrm{d}s^2} G_{\cdot}(s)\right]_{s=0} = \left[\frac{\mathrm{d}^2}{\mathrm{d}s^2} \overline{G}_{\cdot}(s)\right]_{s=0}, \ldots, \left[\frac{\mathrm{d}^{k-1}}{\mathrm{d}s^{k-1}} G_{\cdot}(s)\right]_{s=0} = \left[\frac{\mathrm{d}^{k-1}}{\mathrm{d}s^{k-1}} \overline{G}_{\cdot}(s)\right]_{s=0} \end{aligned} \tag{7.68}$$

Notice that it is possible to calculate identities (7.68) at a different point from $s = 0$, e.g. in the neighborhood of a frequency where a good approximation is desired. If any of derivatives does not exist, substitute $G_{\cdot}(s)$ by $1/G_{\cdot}(s)$, which is the case of controllers derived above as well. The value of k (usually) equals the number of approximating model parameters.

For this method, we can derive particular conditional equations for approximated models (7.46) and (7.55) and the approximating ones (7.61) and (7.62) directly. However, these algebraic equations are rather complex; therefore, they are not displayed in this thesis. Particular values of parameters in (7.61) and (7.62) are calculated in Subsection 7.7. Some notes to the general calculation follows.

Consider controller (7.46) first. Since $G_R(0) \to \infty$, the derivatives in (7.68) are calculated for $1/G_R(s)$ and model (7.61) is chosen. Moreover, condition $[1/G_R(s)]_{s=0} = [1/\overline{G}_R(s)]_{s=0}$ leads to identity $0 = 0$ directly, which implies no useful result. Therefore, let $k = 4$ rather than $k = 3$.

As second, controller $G_Q(s)$ in (7.55) has no pole at zero, hence, $k = 1$ and model (7.62) is considered here. Finally, $G_R(s)$ owns a double zero pole and $[1/G_R(s)]_{s=0} = [1/\overline{G}_R(s)]_{s=0} \Rightarrow 0 = 0$ again, therefore take $k = 4$ and model (7.61).

7.6 Robust analysis of controllers

Now let us analyze the robustness, i.e. robust stability and performance, of the designed controllers for various settings of selectable controller parameters. To demonstrate the procedure introduced in Subchapter 2.7, consider original controllers (7.46) and (7.55) only – controllers designed for a relay-test based model, i.e. (7.59) and (7.60) and approximating controllers (7.61) can be assessed analogously.

First, it is necessary to determine the family of plant transfer functions which is obtained by variations within the ranges of selected model parameters. We have selected three parameters the values of which are affected by measurements uncertainties or ambient conditions, namely, K_C, K_P and ϑ_A. Intervals for K_C and K_P have been chosen on the basis of two identification measurements, see [128], [162], and ϑ_A has been selected according to room temperature variations during the year. Hence, the intervals are the following

$$K_P \in [0.1, 0.5], K_C \in [15, 22], \vartheta_A \in [16, 30] \tag{7.69}$$

The set of Bode plots $|G(\mathrm{j}\omega)/G_0(\mathrm{j}\omega) - 1|$ for all eight combinations of margin values in (7.69) is depicted in Fig. 7.13. This set was covered by a plot expressing $|W_M(\mathrm{j}\omega)|$ given by the transfer function (7.70).

$$W_M(s) = 0.36 \frac{(200s+1)(10s+1)}{(340s+1)(15s+1)} = \frac{720s^2 + 75.6s + 0.36}{5100s^2 + 355s + 1} \tag{7.70}$$

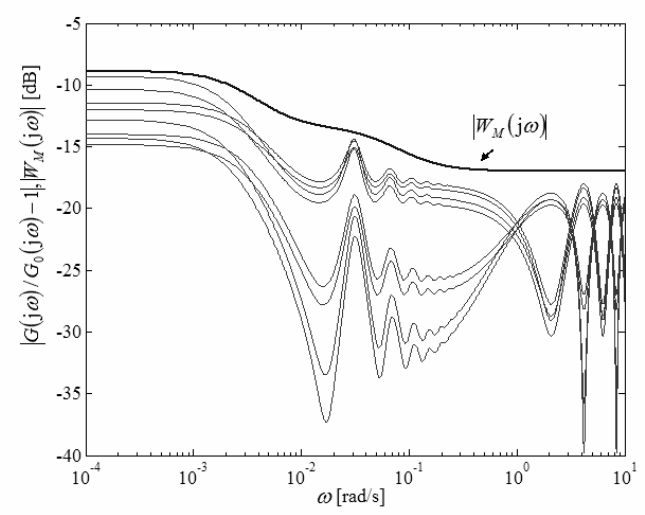

Fig. 7.13 Determination of $|W_M(j\omega)|$

Consider now the 1DoF and TFC control systems separatelly.

7.6.1 1DoF control structure

Theoretical background for robust analysis of the 1DoF control system has been presented in Subchapter 2.7. Verification of the robust stability criterion (2.116) for several settings of m_0 is displayed in Fig. 7.14.

The weighting function $|W_P(j\omega)|$ has been chosen so that the nominal performance condition (2.115) holds for a selected range of m_0, as

$$1/W_P(s) = 900\frac{s(40s+1)}{(350s+1)(90s+1)} = \frac{36000s^2+900s}{31500s^2+440s+1} \tag{7.71}$$

see Fig. 7.15.

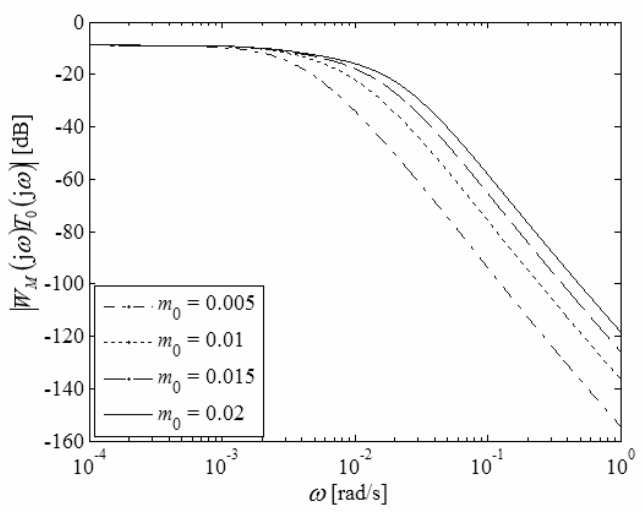

Fig. 7.14 Robust stability verification for 1DoF

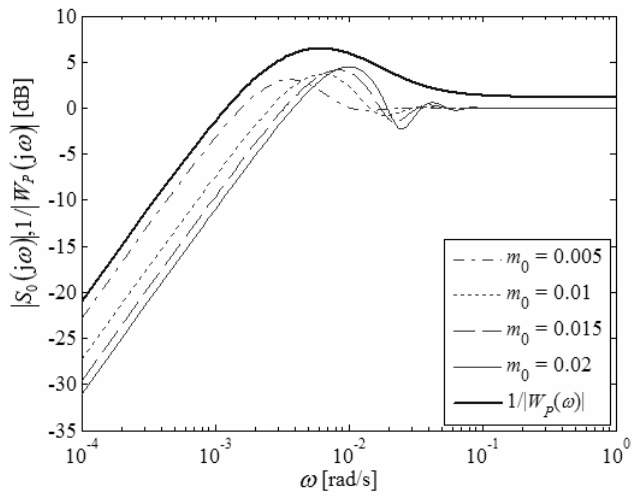

Fig. 7.15 Nominal performance – determination of $|W_P(j\omega)|$ for 1DoF

Obviously, the decreasing of m_0 would lead to poor nominal performance at lower frequencies, whereas its increasing would cause the same effect at middle frequencies.

Finally, test the robust performance condition (2.119) with $W_M(s)$ and $W_P(s)$ given by (7.70) and (7.71), respectively, as it is depicted in Fig. 7.16. The results indicate that for $m_0 = 0.005$ and $m_0 = 0.02$ the feedback system has poor robust performance.

Hence, the eventual range $m_0 \in [0.008, 0.012]$ has been chosen for controller tuning, simulations and real experiments.

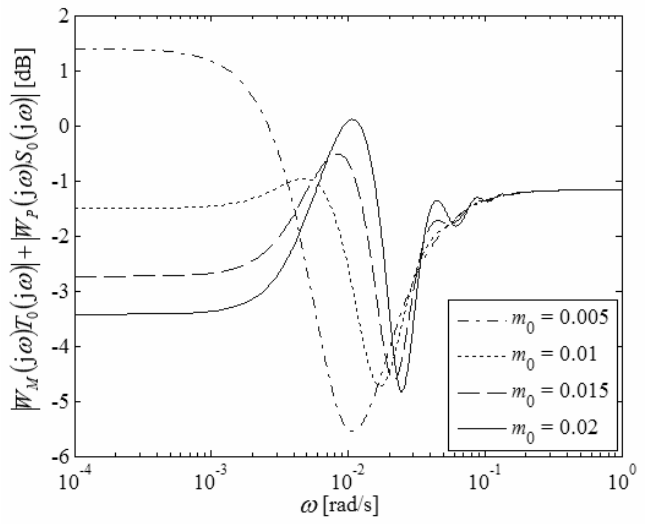

Fig. 7.16 Robust performance test for 1DoF

7.6.2 TFC control structure

As was mentioned e.g. in Subchapter 2.7.3, robust stability and robust performance conditions (2.116) and (2.119) hold for the 1DoF control structure; however, other structures require the derivation of specific conditions. While making effort to do this, it is possible to use principles demonstrated in Figs. 2.5 and 2.6, condition (2.118) and the Nyquist criterion the basis of which is formulated in (4.159). Let us introduce theorems about robust stability and robust performance for the TFC control system.

Theorem 7.1

If the open loop $L_0(s) = G_O(s)$ is stable, the TFC control system is robustly stable if and only if

$$\left\| W_M(j\omega) T_0(j\omega) \left(1 + \frac{G_Q(j\omega)}{G_R(j\omega)} \right) \right\|_\infty < 1 \tag{7.72}$$

■

Proof. Robust stability principle based on the Nyquist criterion (see Theorem 4.10), graphically expressed in Fig. 2.5 and analytically formulated in (2.117), with respect to (4.159) reads

$$\begin{aligned}&\left\|\frac{W_M(\mathrm{j}\omega)L_0(\mathrm{j}\omega)}{1+L_0(\mathrm{j}\omega)}\right\|_\infty<1\Leftrightarrow\left|W_M(\mathrm{j}\omega)L_0(\mathrm{j}\omega)\right|<\left|L_0(\mathrm{j}\omega)-(-1)\right|,\forall\omega\\&L_0(\mathrm{j}\omega)=G_O(\mathrm{j}\omega)=G(\mathrm{j}\omega)\left(G_R(\mathrm{j}\omega)+G_Q(\mathrm{j}\omega)\right)\end{aligned}\tag{7.73}$$

Since

$$\begin{aligned}&T_0(s)=G_{WY}(s)=\frac{L_0(s)-G(s)G_Q(s)}{1+L_0(s)}=\frac{G(s)G_R(s)}{1+L_0(s)}\\&\Rightarrow\frac{L_0(s)}{1+L_0(s)}=T_0(s)\left(1+\frac{G_Q(s)}{G_R(s)}\right)\end{aligned}\tag{7.74}$$

condition (7.73) can be written as

$$\left\|W_M(\mathrm{j}\omega)T_0(\mathrm{j}\omega)\left(1+\frac{G_Q(\mathrm{j}\omega)}{G_R(\mathrm{j}\omega)}\right)\right\|_\infty<1\tag{7.75}$$

□

The obtained result corresponds with (2.116) since $G_Q(s)=0$ for the 1DoF system.

A theorem dealing with robust performance follows.

Theorem 7.2

If the open loop $L_0(s)=G_O(s)$ is stable, the TFC control system meets robust performance if and only if

$$\left\|W_M(\mathrm{j}\omega)T_0(\mathrm{j}\omega)\left(1+\frac{G_Q(\mathrm{j}\omega)}{G_R(\mathrm{j}\omega)}\right)\right|+\left|W_P(\mathrm{j}\omega)\left(S_0(\mathrm{j}\omega)+W_M(\mathrm{j}\omega)T_0(\mathrm{j}\omega)\frac{G_Q(\mathrm{j}\omega)}{G_R(\mathrm{j}\omega)}\right)\right\|_\infty<1\tag{7.76}$$

■

Proof. The requirement of robust performance is satisfied if (2.118) holds. Follow the sketch of proof of (2.119) for the 1DoF control system in (2.120) – (2.122) analogously.

Because of

$$S_0(s)=G_{WE}(s)=1-T_0(s)=\frac{1+G(s)G_Q(s)}{1+L_0(s)}=\frac{1+L_0(s)-G(s)G_R(s)}{1+L_0(s)} \tag{7.77}$$

the right-hand side condition in (2.118) reads

$$\begin{aligned}
&\left|W_P(\mathrm{j}\omega)S(\mathrm{j}\omega)\right|<1,\forall\omega\\
&\Leftrightarrow\left|W_P(\mathrm{j}\omega)\frac{1+L_0(\mathrm{j}\omega)(1+\Delta(\mathrm{j}\omega)W_M(\mathrm{j}\omega))-G_0(\mathrm{j}\omega)G_R(\mathrm{j}\omega)(1+\Delta(\mathrm{j}\omega)W_M(\mathrm{j}\omega))}{1+L_0(\mathrm{j}\omega)(1+\Delta(\mathrm{j}\omega)W_M(\mathrm{j}\omega))}\right|<1,\forall\omega\\
&\Leftrightarrow\left|W_P(\mathrm{j}\omega)\frac{1+G_0(\mathrm{j}\omega)G_Q(\mathrm{j}\omega)(1+\Delta(\mathrm{j}\omega)W_M(\mathrm{j}\omega))}{1+L_0(\mathrm{j}\omega)(1+\Delta(\mathrm{j}\omega)W_M(\mathrm{j}\omega))}\right|<1,\forall\omega\\
&\Leftrightarrow\left|W_P(\mathrm{j}\omega)\frac{\frac{1+G_0(\mathrm{j}\omega)G_Q(\mathrm{j}\omega)}{1+L_0(\mathrm{j}\omega)}+\frac{G_0(\mathrm{j}\omega)G_Q(\mathrm{j}\omega)\Delta(\mathrm{j}\omega)W_M(\mathrm{j}\omega)}{1+L_0(\mathrm{j}\omega)}}{1+\frac{L_0(\mathrm{j}\omega)\Delta(\mathrm{j}\omega)W_M(\mathrm{j}\omega)}{1+L_0(\mathrm{j}\omega)}}\right|<1,\forall\omega
\end{aligned} \tag{7.78}$$

Using (7.74) and (7.77) it holds that

$$\left|W_P(\mathrm{j}\omega)\frac{S_0(\mathrm{j}\omega)+T_0(\mathrm{j}\omega)\frac{G_Q(\mathrm{j}\omega)}{G_R(\mathrm{j}\omega)}\Delta(\mathrm{j}\omega)W_M(\mathrm{j}\omega)}{1+\Delta(\mathrm{j}\omega)W_M(\mathrm{j}\omega)T_0(\mathrm{j}\omega)\left(1+\frac{G_Q(\mathrm{j}\omega)}{G_R(\mathrm{j}\omega)}\right)}\right|<1,\forall\omega \tag{7.79}$$

The worst case is

$$\max\left|W_P(\mathrm{j}\omega)S(\mathrm{j}\omega)\right|=W_P(\mathrm{j}\omega)\frac{\left|S_0(\mathrm{j}\omega)+W_M(\mathrm{j}\omega)T_0(\mathrm{j}\omega)\frac{G_Q(\mathrm{j}\omega)}{G_R(\mathrm{j}\omega)}\right|}{1-\left|W_M(\mathrm{j}\omega)T_0(\mathrm{j}\omega)\left(1+\frac{G_Q(\mathrm{j}\omega)}{G_R(\mathrm{j}\omega)}\right)\right|} \tag{7.80}$$

Finally, by applying (2.118) and (7.72) on (7.80), condition (7.76) is obtained. □

Again, if $G_Q(s) \to 0$, condition (7.76) convergates to (2.119) – for 1DoF.

Robust stability criterion (7.72) test for several settings of m_0 is displayed in Fig. 7.17, whereas our calculations show that neither m_1 nor γ affect the robust stability condition.

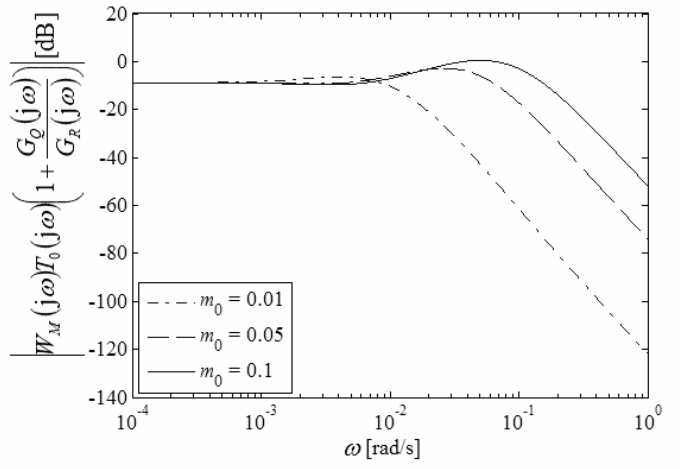

Fig. 7.17 Robust stability verification for TFC

Obviously, the higher the value of m_0 is, the worse robust stability is at middle frequencies. Here, the criterion is satisfied for approximately $m_0 \in [0, 0.09]$.

The weighting function $|W_P(j\omega)|$, has been chosen so that the nominal performance condition (2.115) holds for a selected ranges of m_0, m_1, γ again. Plots of $|S_0(j\omega)|$ for particular values of controller coefficients are presented in two bunches of figures titled as Fig. 7.18 and Fig. 7.19 and a cumulative graph with the desired curve of $1/|W_P(j\omega)|$ is displayed in Fig. 7.20. As can be seen from the figures, higher values of m_0 improves nominal performance at low frequencies but make it worse at middle ones. The same statement holds for m_1, whereas higher values of γ slightly worsen this feature at all frequencies.

The transfer function of $1/|W_P(j\omega)|$ has been chosen as

$$1/W_P(s)=9\cdot10^5\frac{s^2(1.5s+1)}{(1000s+1)(80s+1)(10s+1)}=9\cdot10^5\frac{1.5s^3+s^2}{8\cdot10^5s^3+9.08\cdot10^4s^2+1090s+1} \tag{7.81}$$

Finally, let us verify robust performance given by the criterion (7.76) for the calculated value of $|W_M(\mathrm{j}\omega)|$ as in (7.70) and the selected form of $|W_P(\mathrm{j}\omega)|$ introduced in (7.81). The set of results is provided in Fig. 7.21.

The figures can be analyzes as follows: The higher m_0 is, the higher the peak frequency is, yet, the peak value is improved only for a limited range of m_0. Higher values of m_1 tend to improve robust performance at lower frequencies where the peak is shifted to the right, whereas they deteriorate the feature at middle frequencies where the peak moves to the left. Finally, γ has the same effect on robust performance (the peak value) as m_1; however, its higher values yield the peak frequency lower at lower frequencies and higher at middle frequencies.

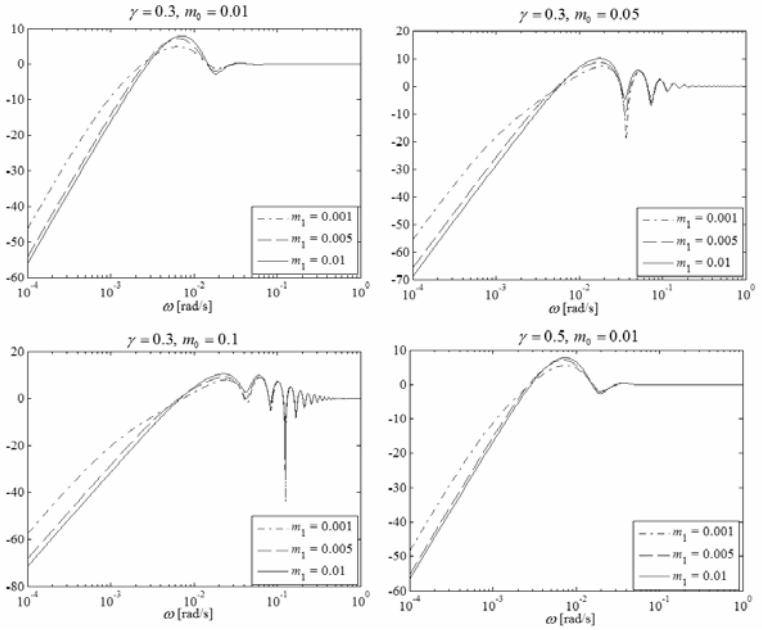

Fig. 7.18 Nominal performance $|S_0(\mathrm{j}\omega)|$ [dB] *for various* m_0, m_1, γ *for TFC – part 1*

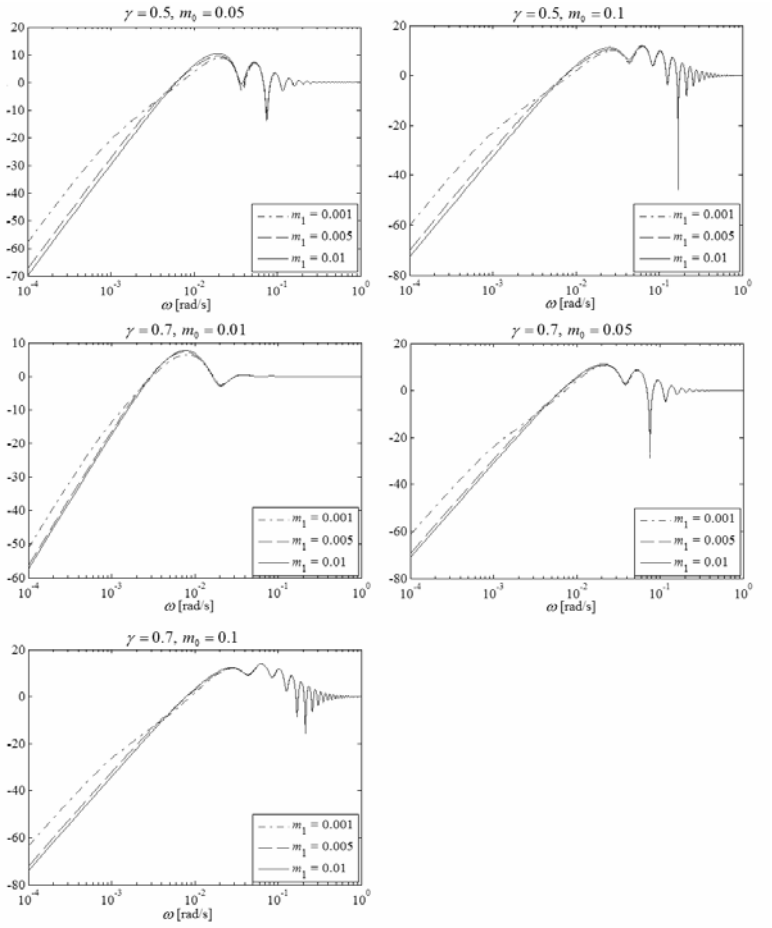

Fig. 7.19 Nominal performance $|S_0(\mathrm{j}\omega)|$ [dB] *for various* m_0, m_1, γ *for TFC – part 2*

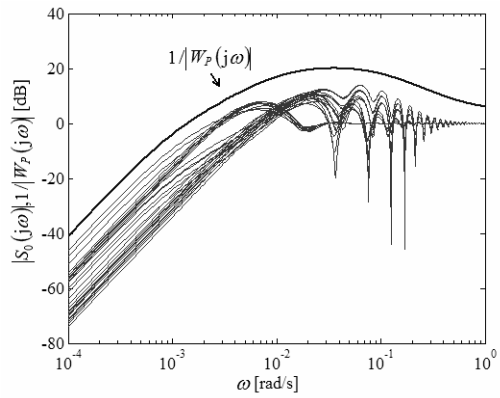

Fig. 7.20 Nominal performance – determination of $|W_P(\mathrm{j}\omega)|$ *for TFC*

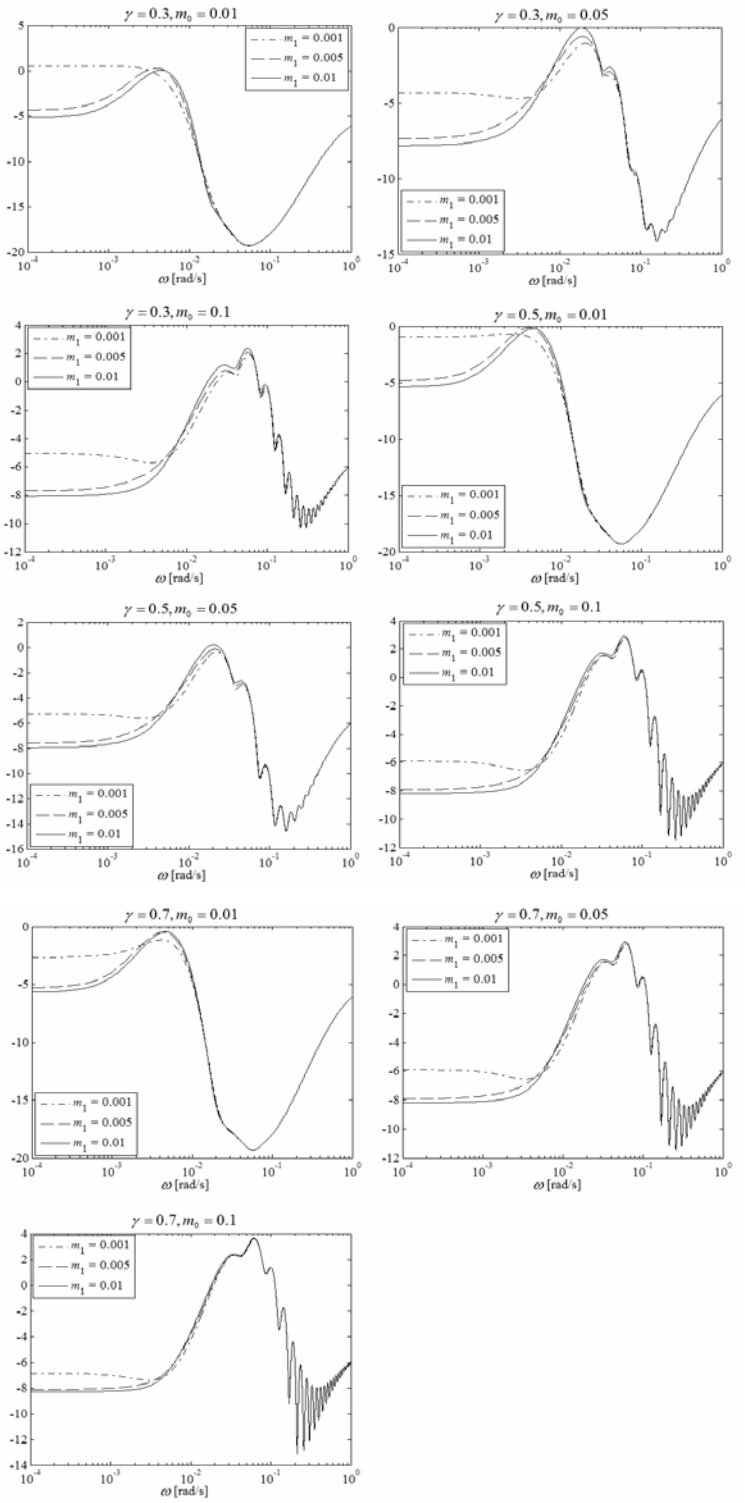

Fig. 7.21 Robust performance test (7.76) for TFC

The decision about the criterion (7.76) is clearly presented in Tab. 7.12. It is evident from the table that robust performance is satisfied only for a narrow range (domain) of controllers' parameters. As a solution of this problem, it is possible to set $|W_P(\mathrm{j}\omega)|$ more conservatively.

Tab. 7.12 Robust performance fulfillment for TFC – yes (Y), no(N)

m_0 \ γ	m_1	0.3	0.5	0.8
0.01	0.001	N	Y	Y
	0.005	N	Y	Y
	0.01	N	Y	Y
0.05	0.001	Y	Y	N
	0.005	Y	Y	N
	0.01	Y	N	N
0.1	0.001	N	N	N
	0.005	N	N	N
	0.01	N	N	N

7.7 Controllers tuning and simulation experiments

This subchapter strives to select suitable free controllers' parameters, i.e. the value of m_0 for the 1DoF control system represented by controller (7.46) and the triplet m_0, m_1, γ for the TFC structure with controllers (7.55), with respect to robust analysis results. Controllers derived in Subchapter 7.4.5 for relay-test plant models are then tested via MATLAB/Simulink experiments. Moreover, simplified controllers' structures according to Subchapter 7.5 are then calculated and benchmarked as well.

Let us consider the 1DoF structure first. Since the reference-to-output transfer function reads a relatively simple form

$$G_{WY}(s) = \frac{m_0^3\left(b_{0D}\exp(-\tau_0 s) + b_0\right)\exp(-\tau s)}{\left(b_{0D} + b_0\right)\left(s + m_0\right)^3} \tag{7.82}$$

and m_0 impacts the triple real pole, we decided to choose the value of the parameter by simulations only. Note that robust analysis yields the required restriction $m_0 \in [0.008, 0.012]$.

Control responses are displayed in Fig. 7.22 where $\Delta u_0(t) = \Delta P_H(t)$ and $\Delta y(t) = \Delta \vartheta_{CO}(t)$ denote the difference of a corresponding quantity from the operating point (7.56).

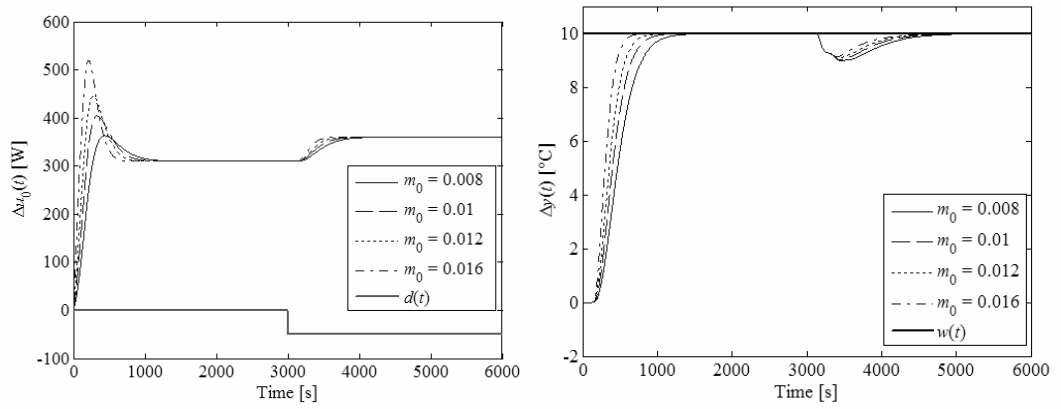

Fig. 7.22 Simulation control responses of $u_0(t)$ (left) and $y(t)$ (right) for 1DoF structure) with controller (7.46)

As it results from the figures, higher values of m_0 lead to faster yet higher control actions; namely, $m_0 > 0.012$ yields $\Delta u_{0,\max} > 450\,\mathrm{W}$ which is not physically acceptable since $P_{H,\max} = 750\,\mathrm{W}$ while operation point reads $P_{H,0} = 300\,\mathrm{W}$. Real time steering, for these cases, would claim the use of anti-windup control action calculations. Hence, it seems that $m_0 = 0.012$ is a convenient option, which confirms Tab. 7.13 incorporating values of the ISE and ISTE criteria, according to (4.186) and (4.187), respectively, with $\varphi = 10$. Apparently, the value of $m_0 = 0.012$ provides the best criteria values for the selected range of discrete values of m_0. Another choice of φ, naturally, would lead to a possibly different criteria grades.

Tab. 7.13 ISE and ISTE criteria values for controller (7.46) with $\varphi = 10$

m_0	J_{ISE}	J_{ISTE}
0.008	$4.3583 \cdot 10^4$	$4.3583 \cdot 10^7$
0.01	$4.0582 \cdot 10^4$	$9.1137 \cdot 10^6$
0.012	$3.9875 \cdot 10^4$	$8.2889 \cdot 10^6$
0.016	$4.2634 \cdot 10^4$	$1.0483 \cdot 10^7$

In the case of the TFC control structure, $G_{WY}(s)$ is rather more complex

$$G_{WY}(s)=\frac{m_0^3}{(b_0+b_{0D})^2}\frac{(b_{0D}\exp(-\tau_0 s)+b_0)(\gamma t_1 s^2+(t_1 m_1+t_0)s+t_0 m_1)}{(s+m_0)^4(s+m_1)}\exp(-\tau s) \quad (7.83)$$

We tried to adopt the following idea: It is well known that a stable system with real poles p_i inflicts an overshoots if there exist a zero (or zeros) z of $G_{WY}(s)$ with

$$\mathrm{Re}\, z > p_{\max} \quad (7.84)$$

where $p_{\max}=\{p_i : p_j \le p_i, \forall i \ne j\}$, see e.g. [87]. Hence, the intent is to find the triplet m_0, m_1, γ such that (7.84) does not hold, or the value of

$$\delta = \mathrm{Re}\, z - p_{\max} \quad (7.85)$$

or that of

$$\rho = |p_{\max} / \mathrm{Re}\, z|, \mathrm{Re}\, z < 0 \quad (7.86)$$

is minimal. Since zeros $z_{1,k}=1.5912 \pm k4.1888\mathrm{j}, k \in \mathbb{Z}$ of the factor $b_{0D}\exp(-\tau_0 s)+b_0$ can not be influenced, the aim is to affect zeros of the second factor in the numerator within ranges $m_0 \in [0.01, 0.1]$, $m_1 \in [0.001, 0.01]$, $\gamma \in \{0.25, 0.5, 0.75\}$. It has been found numerically that (7.84) holds true for all the ranges. Optimal values are given in Tab. 7.14.

Tab. 7.14 Values of δ and ρ according to (7.85) and (7.86), respectively

γ	δ	ρ	$m_{0,opt}$	$m_{1,opt}$
0.25	$4.6929\cdot10^{-5}$	1.0492	0.1	0.001
0.5	$8.5692\cdot10^{-5}$	1.0937	0.1	0.001
0.75	$1.1864\cdot10^{-4}$	1.1346	0.1	0.001

The results in Tab 7.14 can be interpreted in such a way that both criteria are improved if low values of γ and m_1 and a high value of m_0 are selected. Graphical results for $\gamma = 0.25$ are presented in Fig. 7.23 which indicates that there is a higher sensitivity of this issue to changes in m_1 rather then m_0 except for a domain $m_0 \to 0$.

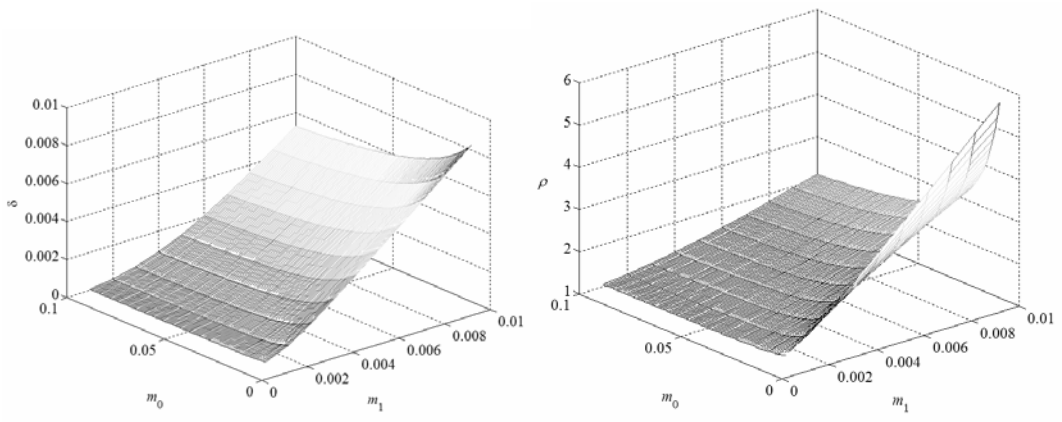

Fig. 7.23 Values of δ and ρ according to (7.85) and (7.86), respectively, for $\lambda = 0.25$

Simulation control responses for controllers (7.55) with $m_0 \in \{0.02, 0.03\}$, $m_1 \in \{0.003, 0.007\}$, $\gamma \in \{0.4, 0.8\}$ are displayed in Figs. 7.24 and 7.25. Note that higher values of m_0 have not been benchmarked because of numerical instability of MATLAB/Simulink calculations.

Results from the figures confirm the analysis above only partially. Detailed view on overshoots of $\Delta y(t)$ for a linear to constant change of $w(t)$, a response to $d(t)$ and step change in $w(t)$, respectively, are presented in bunches of figures labeled as Fig. 7.26 and Fig. 7.27.

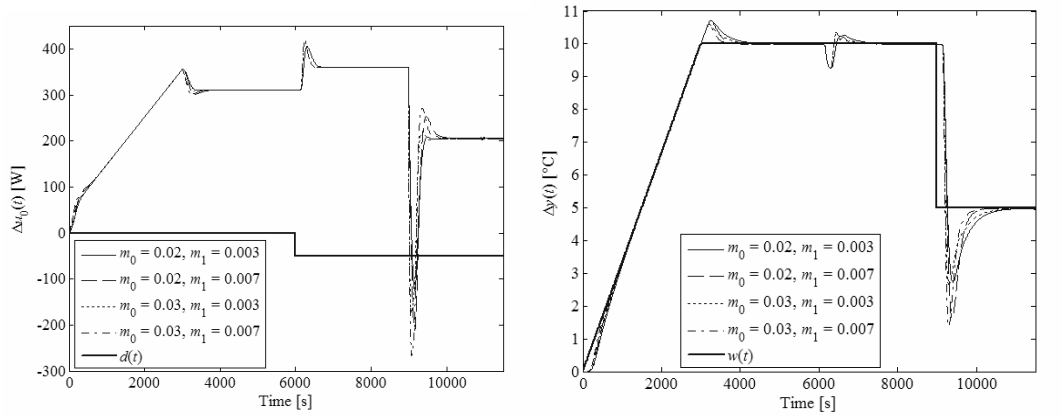

Fig. 7.24 Simulation control responses of $\Delta u_0(t)$ (left) and $\Delta y(t)$ (right) for the TFC structure with controllers (7.55) - $\gamma \in 0.4$

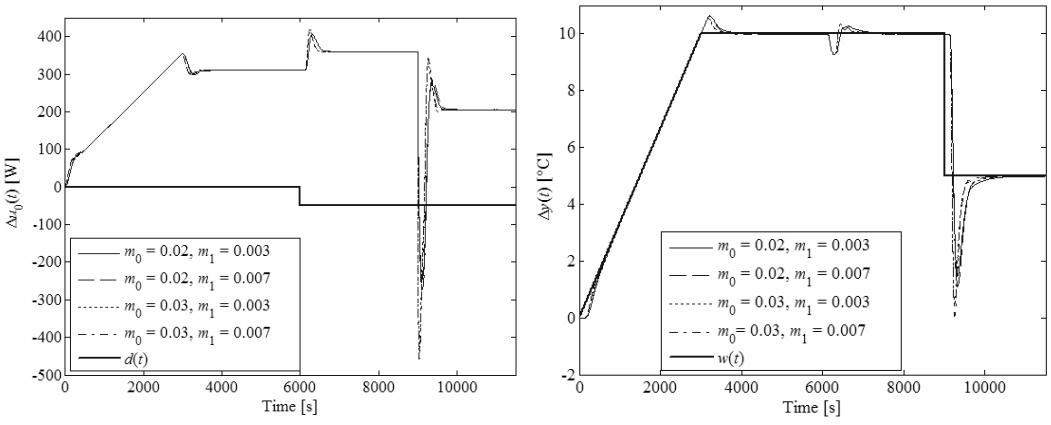

Fig. 7.25 Simulation control responses of $\Delta u_0(t)$ (left) and $\Delta y(t)$ (right) for the TFC structure with controllers (7.55) - $\gamma \in 0.8$

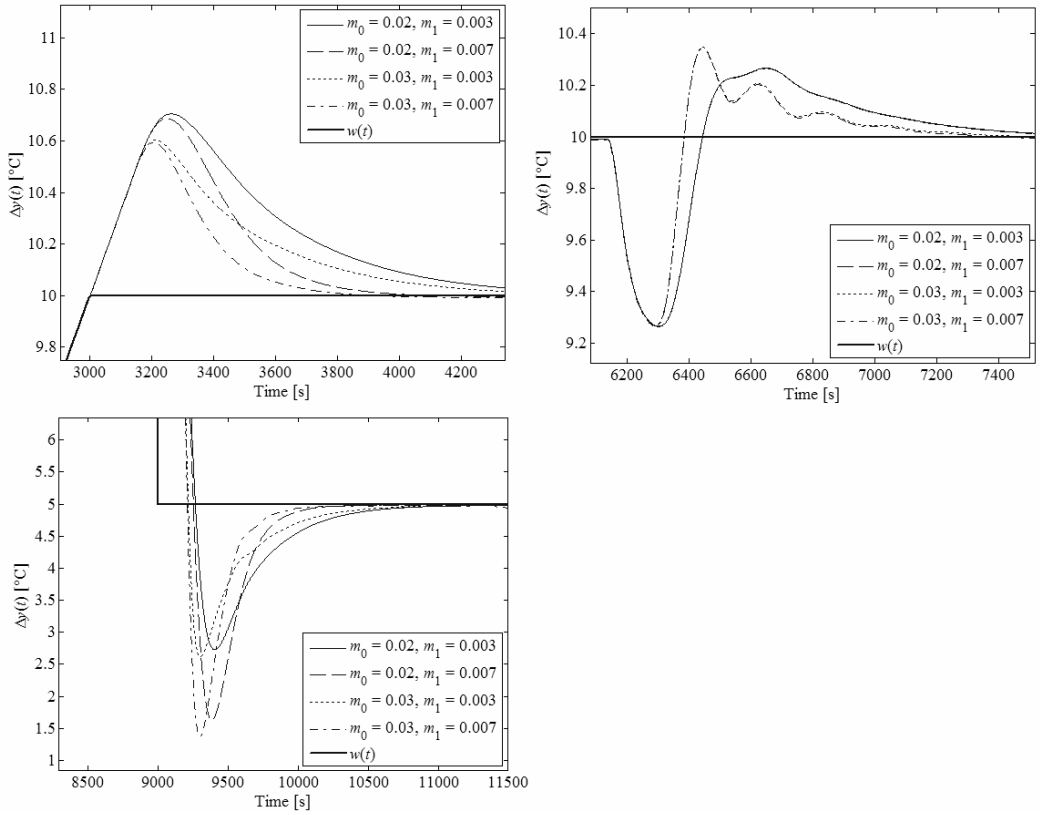

Fig. 7.26 A detailed view on overshoots of $\Delta y(t)$ from Fig. 7.24

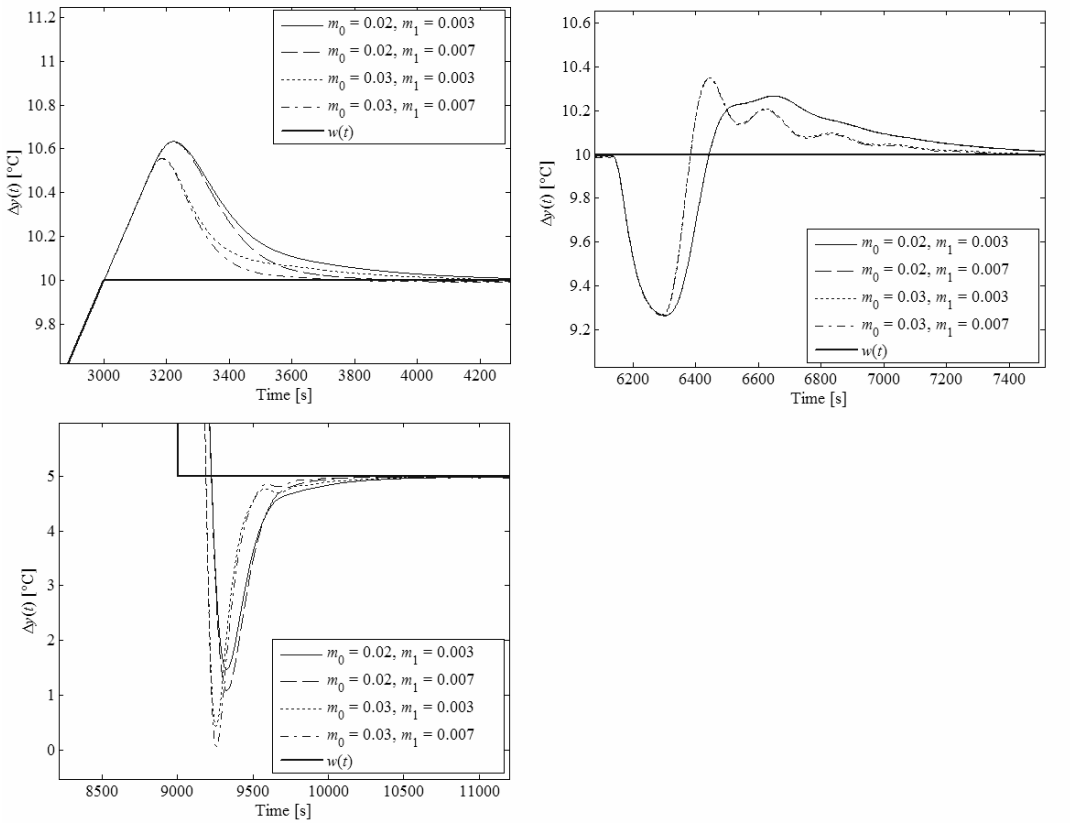

Fig. 7.27 A detailed view on overshoots of $\Delta y(t)$ from Fig. 7.25

Figures above indicate that a higher value of m_0 tends to reduce the initial overshoot in $\Delta y(t)$, yet blows the two rest overshoots (undershoots) up. Parameter m_1 has almost the same impact; however, it does not influence the reaction to load disturbance. Finally, the rising of γ results in a slightly reduction of the initial overshoot and a conspicuous undershoot while step-step changing of $w(t)$. It also decreases the sensitivity of the responses to changes of the rest two parameters.

The effect of coefficients to $\Delta u(t)$ must be taken into account as well. Similarly as for the 1DoF structure, some controller parameters' values are physically unacceptable, namely, the option $\gamma = 0.8$ yields control action $\Delta u_{0,\min} < -300$ W, i.e. $P_{H,\min} < 0$ W.

Taking into account the robust analysis, the quasi-optimal (overshoot) reduction idea and the simulation results above, we decided to set: $m_0 = 0.02, m_1 = 0.005, \gamma = 0.4$.

Now the task is to perform and benchmark controllers (7.59) and (7.60) derived for a simplified (yet infinite-dimensional) plant model (7.40), parameters of which are identified via the relay-feedback test, namely, using the relay transient given in Tab. 7.10. Robust analysis is omitted here since the aim is to demonstrate the usability of simplified controllers instead of their thorough analysis.

For the 1DoF control system with controller (7.59), the selected value $m_0 = 0.012$ can not be chosen because of a very high control action. We finally chose $m_0 = 0.005$, see Fig. 7.28. A comparison with the use of the original controller (7.46) is presented in the figure as well.

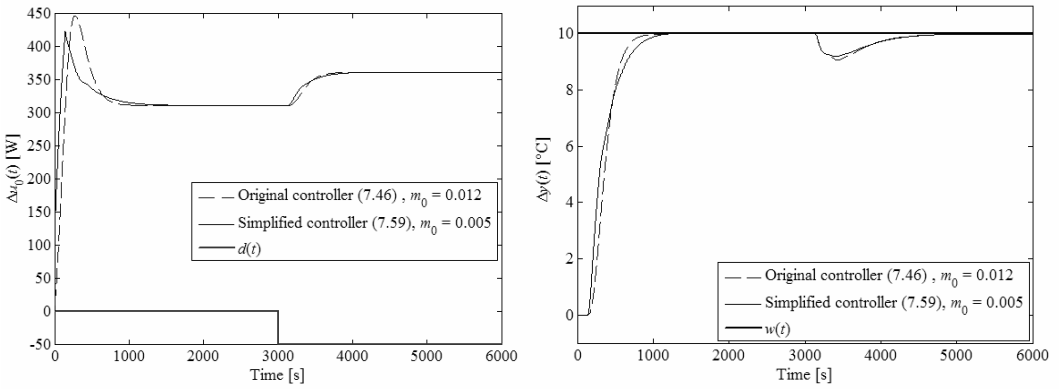

Fig. 7.28 Simulation control responses of $\Delta u_0(t)$ (left) and $\Delta y(t)$ (right) for the 1DoF structure with controllers (7.46) vs. (7.59)

Regarding the TFC structure with controllers (7.60), the following controllers' parameters values have been selected $m_0 = 0.01,\ m_1 = 0.005, \gamma = 0.4$. The original setting $m_0 = 0.02$ could not be used because of numerical instability of the MATLAB/Simulink experiment. Simulation results can be seen in Fig 7.29.

Both cases, i.e. 1DoF and TFC one, validate the usability and efficiency of controllers (7.59) and (7.60), respectively. Their structures are rather simpler compared to the original ones, i.e. (7.46) and (7.55), yet they provides comparable and satisfactory control responses.

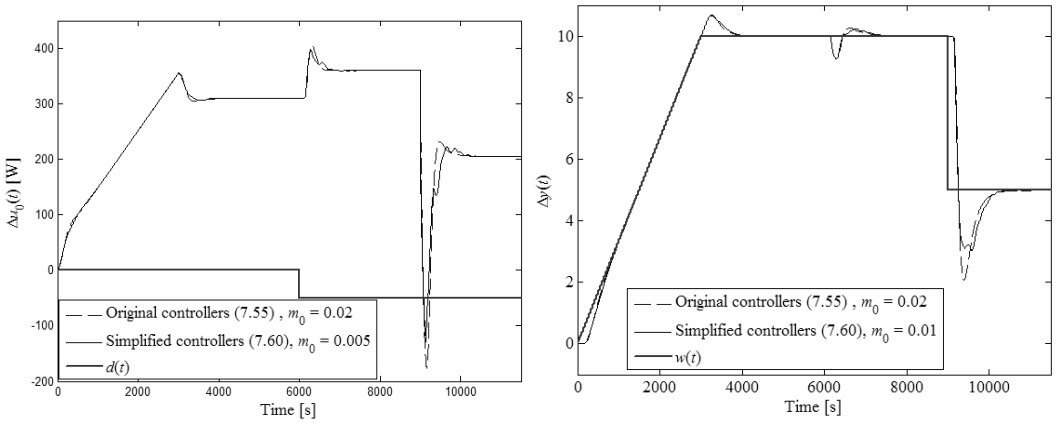

Fig. 7.29 Simulation control responses of $\Delta u_0(t)$ (left) and $\Delta y(t)$ (right) for the TFC structure with controllers (7.55) vs. (7.60) - $m_1 = 0.005, \gamma = 0.4$

Finally, follow now Subchapter 7.5 to benchmark finite-dimensional controllers (7.61) and (7.62). The use of dominant poles and zeros proposed in Subchapter 7.5.1 makes structure (7.61) for the 1DoF structure impossible, since the rightmost controller zeros are

$$\{z_{R1}, z_{R2}, z_{R3}\} = \{-2.97619 \cdot 10^{-3}, -6.43535 \cdot 10^{-3} \pm 3.077622 \cdot 10^{-2}\,\mathrm{j}\} \tag{7.87}$$

Hence, consider a more general approximating linear finite-dimensional controller structure

$$\overline{G}_R(s) = \frac{\overline{r}_3 s^3 + \overline{r}_2 s^2 + \overline{r}_1 s + \overline{r}_0}{s\left(s^2 + \overline{p}_1 s + \overline{p}_0\right)} \tag{7.88}$$

rather then (7.61). Because of

$$\{s_1, s_2, s_3\} = \{0, -6.74644 \cdot 10^{-3} \pm 2.346829 \cdot 10^{-2}\,\mathrm{j}\}, \lim_{s \to 0} sG_R(s) = 0.10978 \tag{7.89}$$

the approximating controller reads

$$\overline{G}_R(s) = \frac{22.2481 s^3 + 0.35256 s^2 + 2.2846 \cdot 10^{-2} s + 6.546 \cdot 10^{-5}}{s\left(s^2 + 1.3493 \cdot 10^{-2} s + 5.96275 \cdot 10^{-4}\right)} \tag{7.90}$$

However, this controller causes a very high control action, as can be seen in Fig. 7.30, therefore, a reduced controller gain as $\overline{G}_{R2}(s) = 0.75\overline{G}_R(s)$ has been set eventually.

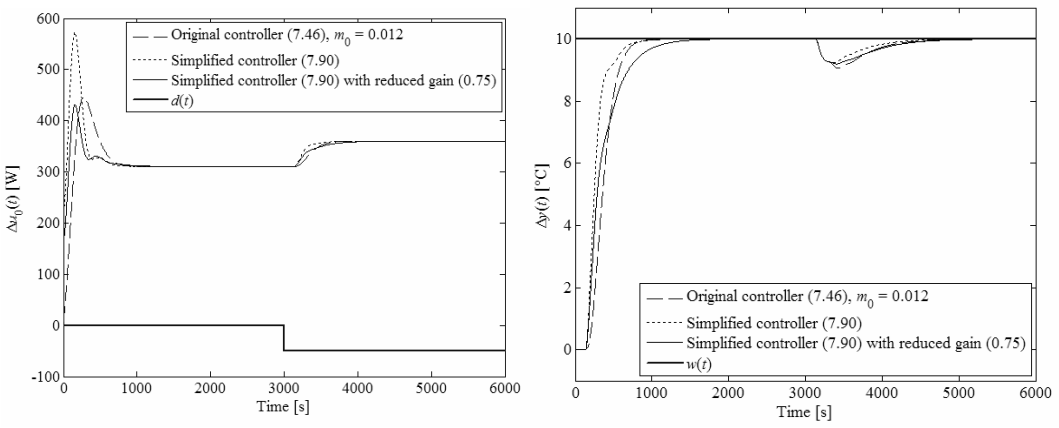

Fig. 7.30 Simulation control responses of $\Delta u_0(t)$ (left) and $\Delta y(t)$ (right) for 1DoF structure with controllers (7.46) vs. (7.90)

Regarding the TFC case, $G_Q(s)$ can be approximated by a proportional model (7.62) where the identity $\lim_{s\to 0} G_Q(s) = \lim_{s\to 0} \overline{\overline{G}}_Q(s)$ is taken as an objective, hence

$$\overline{\overline{G}}_Q(s) = \overline{\overline{G}}_Q = 24.6114 \tag{7.91}$$

Dominant poles and zeros of $G_R(s)$ in (7.55) are the following

$$\begin{aligned} \{s_1, s_2, s_3\} &= \{0, 0, -1.5421755\cdot 10^{-4} \pm 2.917941\cdot 10^{-2}\,\mathrm{j}\} \\ \{z_{R1}, z_{R2}, z_{R3}, z_{R4}\} &= \left\{ \begin{matrix} -2.0971272\cdot 10^{-3}, -2.9761945\cdot 10^{-3}, \\ -6.43535\cdot 10^{-3} \pm 3.077622\cdot 10^{-2}\,\mathrm{j} \end{matrix} \right\} \end{aligned} \tag{7.92}$$

which implies that model (7.61) can be used here as

$$\overline{G}_R(s) = \frac{98.7822 s^2 + 0.50115395 s + 6.16545\cdot 10^{-4}}{s^2} \tag{7.93}$$

where the condition $\lim_{s\to 0} s^2 G_R(s) = \lim_{s\to 0} s^2 \overline{G}_R(s) = 6.16545\cdot 10^{-4}$ is considered in addition.

However, control process with controllers (7.91) and (7.93) is unstable (and hence not displayed here); therefore, we have changed controllers‘ gains as $\overline{\overline{G}}_{Q2} = 0.5\overline{\overline{G}}_Q$, $\overline{G}_{R2}(s) = 0.5\overline{G}_R(s)$ - the corresponding control responses are depicted in Fig. 7.31.

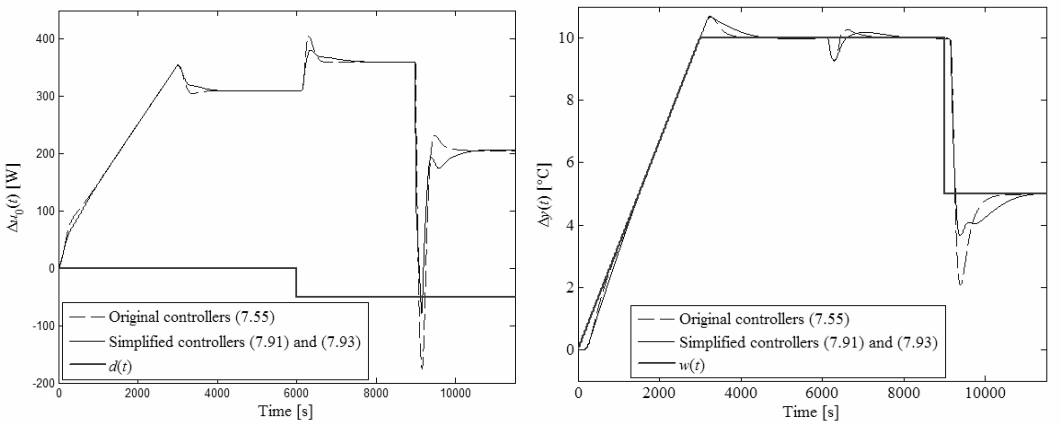

Fig. 7.31 Simulation control responses of $\Delta u_0(t)$ (left) and $\Delta y(t)$ (right) for the TFC structure with controllers (7.55) vs. (7.91) and (7.93)

As for the relay-based model, approximating controllers derived on the basis of a requirement of equality of controllers' poles and zeros provide satisfactory control responses that are a bit slower then the ones obtained by the algebraic approach in the R_{MS} ring, yet with reduced overshoots. Nevertheless, controllers' gains had to be adjusted.

The method presented in Subchapter 7.5.2, i.e. the use of the Padé approximation, gives the following approximation of controllers (7.46) and (7.55) by models (7.61) and (7.62)

$$\overline{G}_R(s) = \frac{-36.873s^2 + 0.871844s + 2.91172 \cdot 10^{-3}}{s\left(s + 3.59065 \cdot 10^{-2}\right)} \tag{7.94}$$

for the 1DoF structure and

$$\begin{aligned} \overline{G}_R(s) &= \frac{47.2676s^2 + 0.416887s + 6.16545 \cdot 10^{-4}}{s^2} \\ \overline{G}_Q(s) &= 24.6114 \end{aligned} \tag{7.95}$$

for the TFC system, respectively. The corresponding simulation control responses are pictured in Figs. 7.32 and 7.33, respectively.

Obviously, this type of approximation provides a very good result closely matching the original control responses curves without changing of controllers' settings. Its disadvantage can be viewed in rather complex calculations of (7.68).

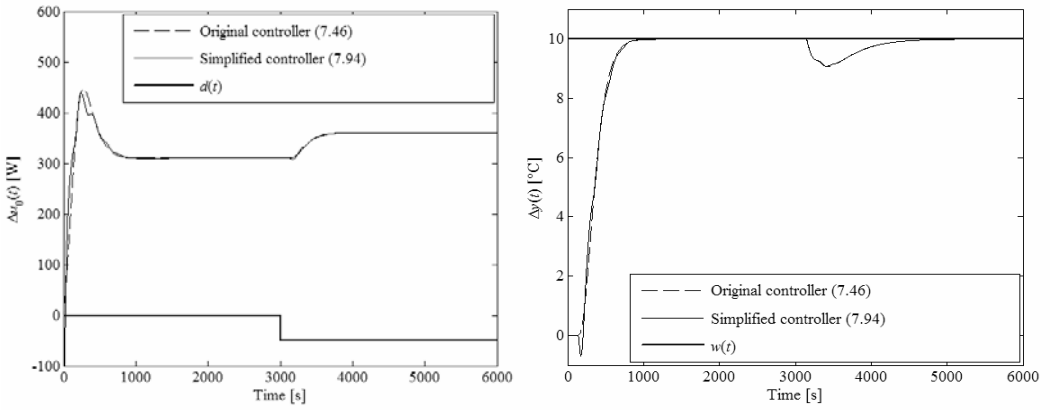

Fig. 7.32 Simulation control responses of $\Delta u_0(t)$ (left) and $\Delta y(t)$ (right) for the 1DoF structure with controllers (7.46) vs. (7.94)

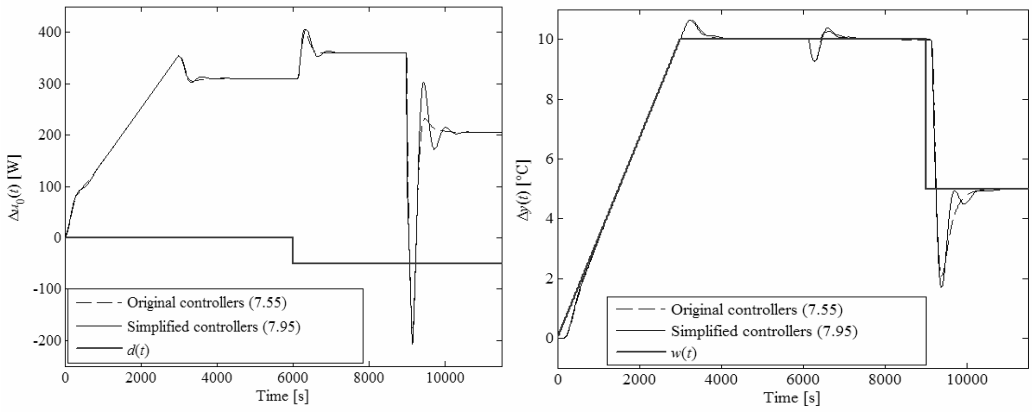

Fig. 7.33 Simulation control responses of $\Delta u_0(t)$ (left) and $\Delta y(t)$ (right) for TFC structure with controllers (7.55) vs. (7.95)

7.8 Discrete-time implementation

As mentioned in Subchapters 2.9 and 7.1, we initially intended to verify the results above via a PC equipped with RS232 and CTRL V3 unit [34] which can work with discrete-time samples only (approx. $T_s > 1s$); however, later, the PC has been enhanced by the data acquisition card AD622 and Real-Time Toolbox for Matlab, which enables to use quasi-continuous algorithms (e.g. $T_s \approx 0.01s$). Nevertheless, to demonstrate the usability of the discretization approach based on delta models introduced in Subchapter 2.9, namely by

(2.134), (2.151) – (2.153), the discrete-time versions of control algorithms follow. The reader is free to use them if necessary.

A general solution will not be presented mainly due to its complexity caused by the assumption of interpolation (2.134). Hence, set $T_s = 1s$, then the discrete-time rule of controller (7.46) reads

$$G_{RD}(z) = \frac{Q_D(z)}{P_D(z)} \tag{7.96}$$

where

$$\begin{aligned}
Q_D(z) &= q_0 + q_1 z^{-1} + q_2 z^{-2} + q_3 z^{-3} + q_{143} z^{-143} + q_{144} z^{-144} + q_{145} z^{-145} + q_{146} z^{-146} \\
P_D(z) &= p_0 + p_1 z^{-1} + p_2 z^{-2} + p_3 z^{-3} + p_{131} z^{-131} + p_{132} z^{-132} + p_{133} z^{-133} + p_{134} z^{-134} \\
&\quad + p_{135} z^{-135} + q_{136} z^{-136}
\end{aligned}$$

$$\begin{aligned}
&q_0 = m_0^3(8 + a_0 + 2a_1 + 4a_2), q_1 = m_0^3(-24 + 3a_0 + 2a_1 - 4a_2), \\
&q_2 = m_0^3(24 + 3a_0 - 2a_1 - 4a_2), q_3 = m_0^3(-8 + a_0 - 2a_1 + 4a_2), \\
&q_{143} = q_{146} = m_0^3 a_{0D}, q_{144} = q_{145} = 3m_0^3 a_{0D},
\end{aligned} \tag{7.97}$$

$$\begin{aligned}
&p_0 = (b_0 + b_{0D})(m_0^3 + 6m_0^2 + 12m_0 + 8), p_1 = (b_0 + b_{0D})(3m_0^3 + 6m_0^2 - 12m_0 - 24), \\
&p_2 = (b_0 + b_{0D})(3m_0^3 - 6m_0^2 - 12m_0 + 24), p_3 = (b_0 + b_{0D})(m_0^3 - 6m_0^2 + 12m_0 - 8), \\
&p_{131} = -b_0 m_0^3, p_{132} = m_0^3(-3b_0 - 0.5b_{0D}), p_{133} = m_0^3(-3b_0 - 2b_{0D}), \\
&p_{134} = m_0^3(-b_0 - 3b_{0D}), p_{135} = -2b_{0D} m_0^3, p_{136} = -0.5b_{0D} m_0^3
\end{aligned}$$

The discretization of controllers (7.55) yields a very intricate form of

$$G_{QD}(z) = \frac{Q_D(z)}{P_D(z)}, G_{RD}(z) = \frac{R_D(z)}{P_D(z)} \tag{7.98}$$

with

$$\begin{aligned}
Q_D(z) &= q_0 + q_1 z^{-1} + q_2 z^{-2} + q_3 z^{-3} + q_4 z^{-4} + q_5 z^{-5} + q_6 z^{-6} + q_{143} z^{-143} \\
&\quad + q_{144} z^{-144} + q_{145} z^{-145} + q_{146} z^{-146} + q_{147} z^{-147} + q_{148} z^{-148} + q_{149} z^{-149} \\
R_D(z) &= r_0 + r_1 z^{-1} + r_2 z^{-2} + r_3 z^{-3} + r_4 z^{-4} + r_5 z^{-5} + r_6 z^{-6} + r_{143} z^{-143} + r_{144} z^{-144} \\
&\quad + r_{145} z^{-145} + r_{146} z^{-146} + r_{147} z^{-147} + r_{148} z^{-148} + r_{149} z^{-149} \\
P_D(z) &= p_0 + p_1 z^{-1} + p_2 z^{-2} + p_3 z^{-3} + p_4 z^{-4} + p_5 z^{-5} + p_6 z^{-6} + p_{131} z^{-131} + p_{132} z^{-132} \\
&\quad + p_{133} z^{-133} + p_{134} z^{-134} + p_{135} z^{-135} + p_{136} z^{-136} + p_{137} z^{-137} + p_{138} z^{-138}
\end{aligned}$$

$$q_{149} = 2a_{0D}(1-\gamma)m_0^3(b_0(4+131m_0)+b_{0D}(4+132.5m_0)), q_{148} = 2q_{149},$$
$$q_{147} = -q_{149}, q_{146} = -4q_{149}, q_{145} = -q_{149}, q_{144} = 2q_{149}, q_{143} = q_{149},$$
$$q_6 = 2(-4+0.5a_0 - a_1 + 2a_2)q_{149}/a_{0D}, q_5 = 2(16+a_0-4a_2)q_{149}/a_{0D},$$
$$q_4 = 2(-20-0.5a_0+3a_1-2a_2)q_{149}/a_{0D}, q_3 = 2(2a_0+8a_2)q_{149}/a_{0D},$$
$$q_2 = 2(20-0.5a_0-3a_1-2a_2)q_{149}/a_{0D}, q_1 = 2(-16+a_0-4a_2)q_{149}/a_{0D},$$
$$q_0 = 2(4+0.5a_0+a_1+2a_2)q_{149}/a_{0D},$$

$$r_{149} = a_{0D}m_0^3\begin{pmatrix} b_{0D}(-m_0+\gamma(8+265m_0)-4m_1-132m_0m_1) \\ +b_0(-m_0+\gamma(8+262m_0)-4m_1-130.5m_0m_1)\end{pmatrix},$$
$$r_{148} = a_{0D}m_0^3\begin{pmatrix} b_{0D}(-4m_0+\gamma(16+530m_0)-16m_1-527m_0m_1) \\ +b_0(-4m_0+\gamma(16+524m_0)-16m_1-521m_0m_1)\end{pmatrix},$$
$$r_{147} = a_{0D}m_0^3\begin{pmatrix} b_{0D}(-5m_0+\gamma(-8-265m_0)-20m_1-655m_0m_1) \\ +b_0(-5m_0+\gamma(-8-262m_0)-20m_1-647.5m_0m_1)\end{pmatrix},$$
$$r_{146} = a_{0D}m_0^3\begin{pmatrix} b_{0D}(\gamma(-32-1060m_0)+10m_0m_1) \\ +b_0(\gamma(-32-1048m_0)+10m_0m_1)\end{pmatrix},$$
$$r_{145} = a_{0D}m_0^3\begin{pmatrix} b_{0D}(5m_0+\gamma(-8-265m_0)+20m_1+670m_0m_1) \\ +b_0(5m_0+\gamma(-8-262m_0)+20m_1+662.5m_0m_1)\end{pmatrix},$$
$$r_{144} = a_{0D}m_0^3\begin{pmatrix} b_{0D}(4m_0+\gamma(16+530m_0)+16m_1+533m_0m_1) \\ +b_0(4m_0+\gamma(16+524m_0)+16m_1+527m_0m_1)\end{pmatrix},$$
$$r_{143} = a_{0D}m_0^3\begin{pmatrix} b_{0D}(m_0+\gamma(8+265m_0)+4m_1+133m_0m_1) \\ +b_0(m_0+\gamma(8+262m_0)+4m_1+131.5m_0m_1)\end{pmatrix},$$

$$r_6 = m_0^3\begin{pmatrix} b_{0D}\begin{pmatrix}\gamma(-64-16a_1+32a_2-2120m_0-530a_1m_0+1060a_2m_0+a_0(8+265m_0)) \\ +m_1(32-4a_0+8a_1-16a_2)+m_0\begin{pmatrix}8-a_0+2a_1-4a_2+1056m_1 \\ -132a_0m_1+264a_1m_1-528a_2m_1\end{pmatrix}\end{pmatrix} \\ +b_0\begin{pmatrix}\gamma(-64-16a_1+32a_2-2096m_0-524a_1m_0+1048a_2m_0+a_0(8+262m_0)) \\ +m_1(32-4a_0+8a_1-16a_2)+m_0\begin{pmatrix}8-a_0+2a_1-4a_2+1044m_1 \\ -130.5a_0m_1+261a_1m_1-522a_2m_1\end{pmatrix}\end{pmatrix}\end{pmatrix}$$

$$r_5 = m_0^3\begin{pmatrix} b_{0D}\begin{pmatrix}\gamma(256-64a_2+8480m_0-2120a_2m_0+a_0(16+530m_0)) \\ +m_1(-64-16a_0+16a_1)+m_0\begin{pmatrix}-16-4a_0+4a_1-2120m_1 \\ -527a_0m_1+526a_1m_1+4a_2m_1\end{pmatrix}\end{pmatrix} \\ +b_0\begin{pmatrix}\gamma(256-64a_2+8384m_0-2096a_2m_0+a_0(16+524m_0)) \\ +m_1(-64-16a_0+16a_1)+m_0\begin{pmatrix}-16-4a_0+4a_1-2096m_1 \\ -521a_0m_1+520a_1m_1+4a_2m_1\end{pmatrix}\end{pmatrix}\end{pmatrix}$$

$$r_4 = m_0^3\left(\begin{array}{l} b_{0D}\left(\begin{array}{l}\gamma\left(-320+48a_1-32a_2-10600m_0+1590a_1m_0-1060a_2m_0-a_0\left(8+265m_0\right)\right)\\ +m_1\left(-32-20a_0-8a_1+48a_2\right)+m_0\left(\begin{array}{l}-8-5a_0-2a_1+12a_2-1048m_1\\ -655a_0m_1-270a_1m_1+1588a_2m_1\end{array}\right)\end{array}\right)\\ +b_0\left(\begin{array}{l}\gamma\left(-320+48a_1-32a_2-10480m_0+1570a_1m_0-1048a_2m_0-a_0\left(8+262m_0\right)\right)\\ +m_1\left(-32-20a_0-8a_1+48a_2\right)+m_0\left(\begin{array}{l}-8-5a_0-2a_1+12a_2-1036m_1\\ -647.5a_0m_1-267a_1m_1+1570a_2m_1\end{array}\right)\end{array}\right)\end{array}\right)$$

$$r_3 = m_0^3\left(\begin{array}{l} b_{0D}\left(\begin{array}{l}\gamma\left(128a_2+4240a_2m_0-a_0\left(32+1060m_0\right)\right)\\ +m_1\left(128-32a_1\right)+m_0\left(32-8a_1+4240m_1+10a_0m_1-1060a_1m_1-8a_2m_1\right)\end{array}\right)\\ +b_0\left(\begin{array}{l}\gamma\left(128a_2+4192a_2m_0-a_0\left(32+1048m_0\right)\right)\\ +m_1\left(128-32a_1\right)+m_0\left(32-8a_1+4192m_1+10a_0m_1-1048a_1m_1-8a_2m_1\right)\end{array}\right)\end{array}\right)$$

$$r_2 = m_0^3\left(\begin{array}{l} b_{0D}\left(\begin{array}{l}\gamma\left(320-48a_1-32a_2+10600m_0-1590a_1m_0-1060a_2m_0-a_0\left(8+265m_0\right)\right)\\ +m_1\left(-32+20a_0-8a_1-48a_2\right)+m_0\left(\begin{array}{l}-8+5a_0-2a_1-12a_2-1072m_1\\ +670a_0m_1-260a_1m_1-1592a_2m_1\end{array}\right)\end{array}\right)\\ +b_0\left(\begin{array}{l}\gamma\left(320-48a_1-32a_2+10480m_0-1572a_1m_0-1048a_2m_0-a_0\left(8+262m_0\right)\right)\\ +m_1\left(-32+20a_0-8a_1-48a_2\right)+m_0\left(\begin{array}{l}-8+5a_0-2a_1-12a_2-1060m_1\\ +662.5a_0m_1-257a_1m_1-1574a_2m_1\end{array}\right)\end{array}\right)\end{array}\right)$$

$$r_1 = m_0^3\left(\begin{array}{l} b_{0D}\left(\begin{array}{l}\gamma\left(-256-64a_2-8480m_0-2120a_2m_0+a_0\left(16+560m_0\right)\right)\\ +m_1\left(-64+16a_0+16a_1\right)+m_0\left(\begin{array}{l}-16+4a_0+4a_1-2120m_1\\ +533a_0m_1+534a_1m_1+4a_2m_1\end{array}\right)\end{array}\right)\\ +b_0\left(\begin{array}{l}\gamma\left(-256-64a_2-8384m_0-2096a_2m_0+a_0\left(16+524m_0\right)\right)\\ +m_1\left(-64+16a_0+16a_1\right)+m_0\left(\begin{array}{l}-16+4a_0+4a_1-2096m_1\\ +527a_0m_1+528a_1m_1+4a_2m_1\end{array}\right)\end{array}\right)\end{array}\right)$$

$$r_0 = m_0^3\left(\begin{array}{l} b_{0D}\left(\begin{array}{l}\gamma\left(64+16a_1+32a_2+2120m_0+530a_1m_0+1060a_2m_0+a_0\left(8+265m_0\right)\right)\\ +m_1\left(32+4a_0+8a_1+16a_2\right)+m_0\left(\begin{array}{l}8+a_0+2a_1+4a_2+1064m_1\\ +133a_0m_1+266a_1m_1+532a_2m_1\end{array}\right)\end{array}\right)\\ +b_0\left(\begin{array}{l}\gamma\left(64+16a_1+32a_2+2096m_0+524a_1m_0+1048a_2m_0+a_0\left(8+262m_0\right)\right)\\ +m_1\left(32+4a_0+8a_1+16a_2\right)+m_0\left(\begin{array}{l}8+a_0+2a_1+4a_2+1052m_1\\ +131.5a_0m_1+263a_1m_1+526a_2m_1\end{array}\right)\end{array}\right)\end{array}\right)$$

$$p_{138} = b_{0D}m_0^3\left(b_0\left(-16+8m_1+m_0\left(-522+261m_1\right)\right)+b_{0D}\left(-16+8m_1+m_0\left(-528+264m_1\right)\right)\right)$$

$$p_{137} = m_0^3\left(\begin{array}{l} b_0^2\left(-8+4m_1+m_0\left(-261+130.5m_1\right)\right)+b_{0D}^2\left(-16+24m_1+m_0\left(-524+790m_1\right)\right)\\ +b_0b_{0D}\left(-24+28m_1+m_0\left(-782+913m_1\right)\right)\end{array}\right)$$

$$p_{136} = m_0^3\left(\begin{array}{l} b_0^2\left(-16+16m_1+m_0\left(-520+521m_1\right)\right)+b_{0D}^2\left(32+16m_1+m_0\left(1064+520m_1\right)\right)\\ +b_0b_{0D}\left(16+32m_1+m_0\left(526+1041m_1\right)\right)\end{array}\right)$$

$$
\begin{aligned}
p_{135} &= m_0^3\begin{pmatrix} b_0^2(8+20m_1+m_0(267+647.5m_1))+b_{0D}^2(32-16m_1+m_0(1056-540m_1)) \\ +b_0b_{0D}(40+4m_1+m_0(1314+121m_1)) \end{pmatrix} \\
p_{134} &= m_0^3\begin{pmatrix} b_0^2(32+m_0(1048-10m_1))-b_{0D}^2(16+24m_1+m_0(536+800m_1)) \\ +b_0b_{0D}(16-24m_1+m_0(530+801m_1)) \end{pmatrix} \\
p_{133} &= m_0^3\begin{pmatrix} b_0^2(8-20m_1+m_0(257-662.5m_1))-b_{0D}^2(16+8m_1+m_0(532+266m_1)) \\ -b_0b_{0D}(8+28m_1+m_0(266+933m_1)) \end{pmatrix} \\
p_{132} &= -b_0m_0^3\left(b_0(16+16m_1+m_0(528+527m_1))+b_{0D}(16+16m_1+m_0(534+533m_1))\right) \\
p_{131} &= -b_0m_0^3\left(b_0(8+4m_1+m_0(263+131.5m_1))+b_{0D}(8+4m_1+m_0(266+133m_1))\right) \\
p_6 &= (b_0+b_{0D})^2\left(-16+8m_1+(16m_0-12m_0^2+4m_0^3-0.5m_0^4)(2-m_1)\right) \\
p_5 &= (b_0+b_{0D})^2\left(64-16m_1-64m_0+24m_0^2m_1+16m_0^3(1-m_1)+m_0^4(-4+3m_1)\right) \\
p_4 &= (b_0+b_{0D})^2\begin{pmatrix} -80-8m_1+(16m_0+2.5m_0^4)(-2+3m_1)+12m_0^2(6-m_1) \\ -4m_0^3(2+5m_1) \end{pmatrix} \\
p_3 &= (b_0+b_{0D})^2\left(32m_1+16(8m_0-3m_0^2m_1-2m_0^3)+10m_0^4m_1\right) \\
p_2 &= (b_0+b_{0D})^2\begin{pmatrix} -80-8m_1+(-16m_0+2.5m_0^4)(2+3m_1)-12m_0^2(6+m_1) \\ +4m_0^3(-2+5m_1) \end{pmatrix} \\
p_1 &= (b_0+b_{0D})^2\left(-64-16m_1-64m_0+24m_0^2m_1+16m_0^3(1+m_1)+m_0^4(4+3m_1)\right) \\
p_0 &= (b_0+b_{0D})^2\left(16+8m_1+(16m_0-12m_0^2+4m_0^3-0.5m_0^4)(2+m_1)\right)
\end{aligned}
\tag{7.99}
$$

Simulated control responses of original (continuous-time) controllers versus the discrete ones almost coincide, thus, these plots are not displayed here.

7.9 Feedback control applied to the laboratory plant

Last of all, selected simulated results from Subchapter 7.7 are going to be concisely verified by taking real measurements on the laboratory circuit heating plant. Namely, parameters of relay test based models (6.1) obtained by the use of a saturation relay with the time-domain solution and the relay transient, respectively, are identified. Then, controllers (7.46) and (7.55) derived by the algebraic approach in the R_{MS} ring for model (7.40) are compared with those designed for relay-based model, i.e. (7.59) and (7.60), and with the ones simplified by the Padé approximation, i.e. (7.94) and (7.95).

7.9.1 Original controllers using the R_{MS} ring

Control responses for the original controller (7.46) incorporated in the 1DoF structure are displayed in Figs. 7.34. and 7.35. As can be seen from the figures, both stepwise reference tracking and disturbance rejection are accomplished well. The measured control action is asymptotically lower then the expected one, likely due to an imperfect temperature sensors calibration (we suppose that $u = 300$ W implies $y = 36$ °C).

The use of the TFC control system with controllers (7.55) yields responses in Figs. 7.36 and 7.37. Contrariwise to the 1DoF test, the real manipulated input is higher then the simulated one. We suppose that this is because of very low temperature in a laboratory room during the measurement (approx. 18 °C), which causes a lower plant static gain and possibly incorrect sensors calibration. However, a new plant model (operation point) has not been calculated to demonstrate the robustness of the control system. Undisturbed stepwise and linearwise reference tracking is satisfied very well; nevertheless, the reaction to a stepwise disturbance introduces oscillating modes.

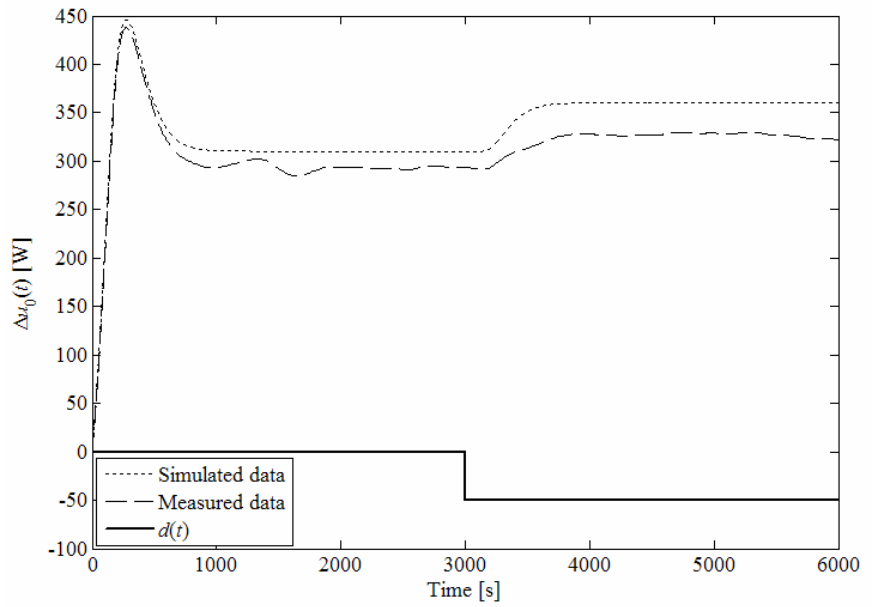

Fig. 7.34 Measured vs. simulated control responses of $\Delta u_0(t)$ for the 1DoF structure with controller (7.46)

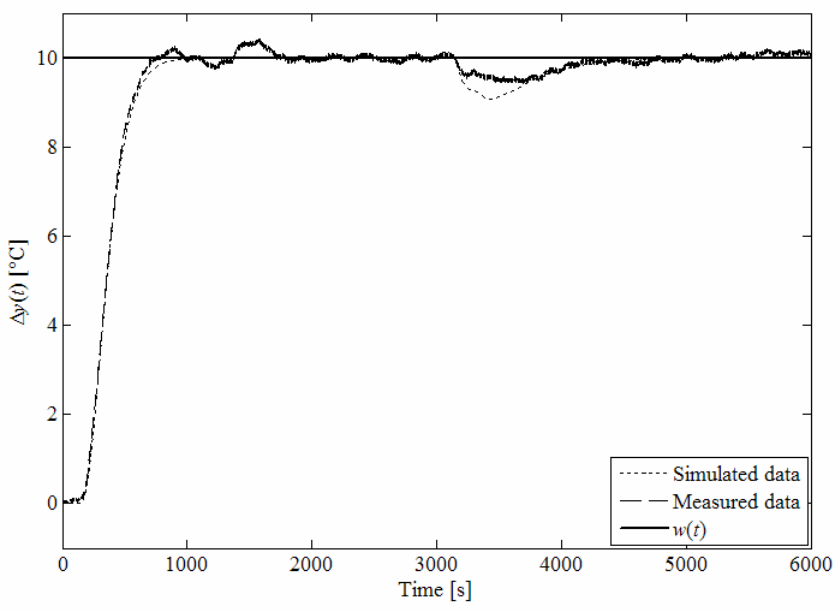

Fig. 7.35 Measured vs. simulated control responses of $\Delta y(t)$ for the 1DoF structure with controller (7.46)

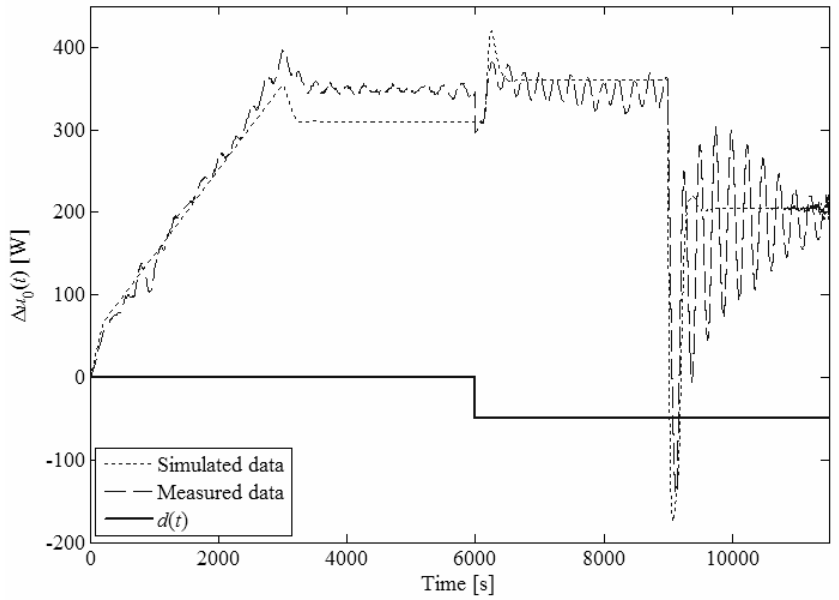

Fig. 7.36 Measured vs. simulated control responses of $\Delta u_0(t)$ for the TFC structure with controllers (7.55)

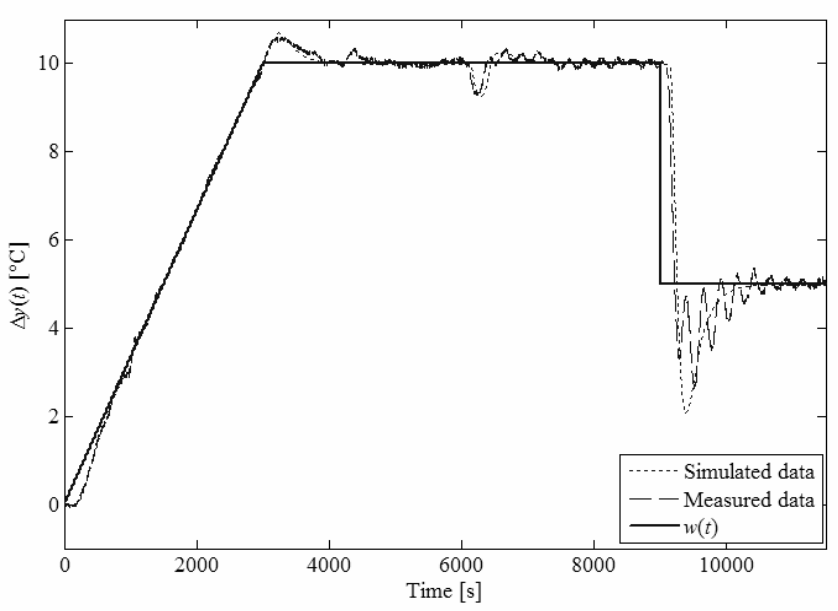

Fig. 7.37 Measured vs. simulated control responses of $\Delta y(t)$ for the TFC structure with controllers (7.55)

7.9.2 Relay test based controllers using the R_{MS} ring

Let us use the relay test to identify parameters of plant model (7.40). A comparison of simulated and measured data from the relay test with a symmetrical and biased on-off relay, saturation relay and those with an artificial delay element are presented in Tab. 7.15, see also Subchapter 7.4.1.

There emerges a problem of a shifted stationary component (y_0) of limit cycles, see Fig. 7.38, here that is caused likely by process nonlinearity. It brings about inconveniencies mainly for the static gain evaluation using a biased relay (Fig. 7.39) and for the relay transient test since it is not clear whether to take $y_0 = 36$ (i.e. the steady state before the entrance of a symmetrical relay output) or $y_0 = 35.38$ which is the arithmetical mean value of maximum and minimum outputs within the period of limit cycles. Both possibilities are benchmarked within the static gain evaluation and the relay transient procedure below.

Tab. 7.15 Comparison of simulated and measured relay tests data

Quantity	Measured data	Simulated data
A_1 [°C]	1.85	1.9975
$T_{u,1}$ [s]	377.9	364.8
$k_{u,1}$ [W·°C^{-1}]	137.65	127.48
τ [s]	129.6	136.7
$k_{u,2}$ [W·°C^{-1}]	151.42	140.23
$\overline{A}_2$ [°C]	1.32	1.426
A_2 [°C]	1.59	1.9245
$T_{u,2}$ [s]	380.6	373.4
τ^+ [s]	78.7	77.8
$\tilde{A}_1$ [°C]	2.72	3.1
$\tilde{T}_{u,1}$ [s]	579.9	555.3
$\tilde{k}_{u,1}$ [W·°C^{-1}]	93.62	82.14
$\tilde{k}_{u,2}$ [W·°C^{-1}]	131.07	115
$\overline{\tilde{A}}_2$ [°C]	2.55	2.52
$\tilde{A}_2$ [°C]	1.53	1.7391
$\tilde{T}_{u,2}$ [s]	616.7	597.8

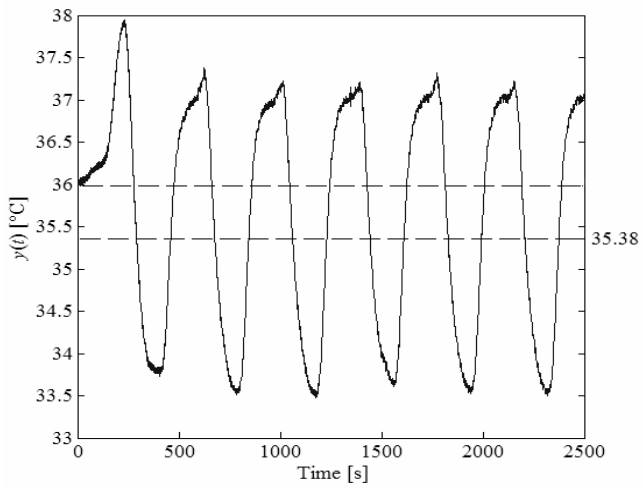

Fig. 7.38 Symmetrical on-off relay test

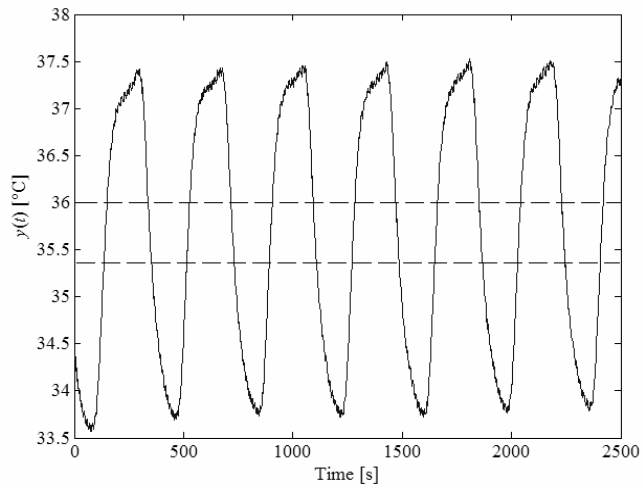

Fig. 7.39 Biased relay test

If $y_0 = 36$ is taken, the static gain according to (2.126) results in $k = -0.0133$, which is a physical nonsense. For $y_0 = 35.38$, $k = 0.0078$ is obtained, which is much closer to the reality, yet still too far from the "real" gain $k = 0.0325$. If this value were required to be reached, the value $y_0 = 34.65$ would be set.

Time-domain solution, see Subchapter 7.4.2, of limit cycles data via the NM method (starting from the initial parameters estimation $a_0 = a_1 = 0.5/T_{u,2} = 0.013$, $\tau = \vartheta = 129.6$) is introduced in Tab. 7.16, where i stands for the iteration step. These steps are chosen so that they provide substantially diverse model parameters estimations. Note that all parameters sets give stable models and $k = b_0/(a_0 + a_1) = 0.0325$ is taken from a step response.

Apparently, the estimation for $i = 40$ gives a better result than the converged one, see Fig. 7.40 for the comparison of step responses, that is comparable to the best simulated result (in Tab. 7.11).

Consider now the use of the relay transient with the same settings as in Subchapter 7.4.3. Data for $y_0 = 36$ then (using the NM optimization) provide parameters estimations that mostly give unstable plant models (e.g. for $i = 20, 40, 1800$). Exceptional "stable" values are presented in Tab. 7.16.

Tab. 7.16 Time domain solution via NM method

i	8	20	40	1800
a_0	$2.192334 \cdot 10^{-2}$	$1.6925505 \cdot 10^{-2}$	$1.570412 \cdot 10^{-2}$	$3.815484 \cdot 10^{-2}$
a_1	$-1.754199 \cdot 10^{-2}$	$-1.069627 \cdot 10^{-2}$	$-8.513952 \cdot 10^{-3}$	$-2.677777 \cdot 10^{-2}$
τ	137.71	134.59	134.45	78.88
ϑ	137.71	139.34	139.84	132.55
e	$1.04 \cdot 10^{-3}$	$8.03 \cdot 10^{-5}$	$3.56 \cdot 10^{-6}$	$1.47 \cdot 10^{-33}$
J_{ISE}	96.95	5.601	0.321	2.291
J_{ISTE}	82175	3341.2	183.85	1331.1

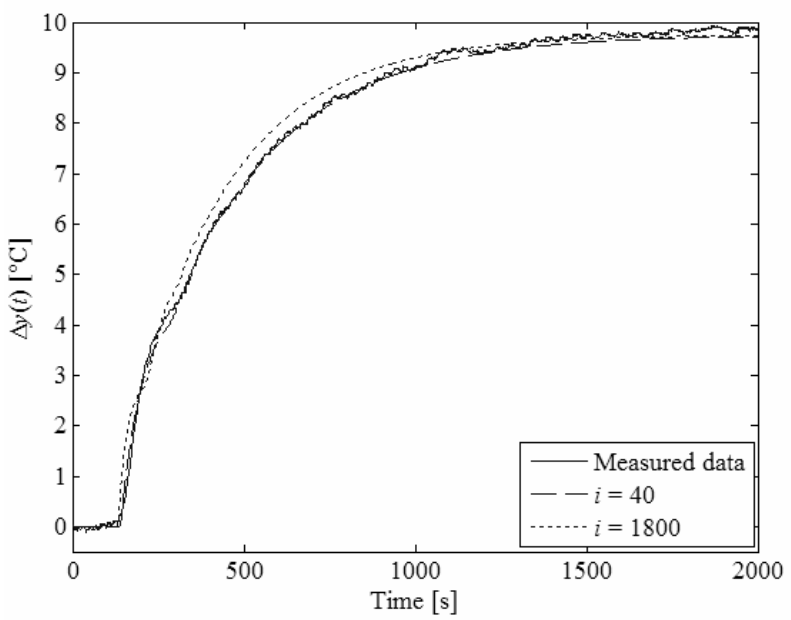

Fig. 7.40 Step responses comparison of measured data vs. relay based model using the time domain solution

If it is considered that $y_0 = 35.38$, the NM method converges as well; however, almost all estimations give unstable models except for $i = 12$, with $a_0 = 0.3007063$, $a_1 = -0.2233959$, $\tau = 157.15$, $\vartheta = 101.79$, $e = 1.64 \cdot 10^{-3}$, $J_{ISE} = 16.165$, $J_{ISTE} = 9900$.

Tab. 7.17 Results of the use of the relay transient with $y_0 = 36$

i	8	20
a_0	$9.396924 \cdot 10^{-2}$	$5.576783 \cdot 10^{-2}$
a_1	$-6.905566 \cdot 10^{-2}$	$-3.101127 \cdot 10^{-2}$
τ	177.95	165.2
ϑ	158.17	145.21
e	$1.09 \cdot 10^{-2}$	$6.69 \cdot 10^{-3}$
J_{ISE}	324.28	4.002
J_{ISTE}	26016	1591

Step responses for the best results of both variants ($y_0 = 36$ vs. $y_0 = 35.38$) compared to the measured response are pictured in Fig. 7.41. It seems that $y_0 = 36$ is a more suitable choice.

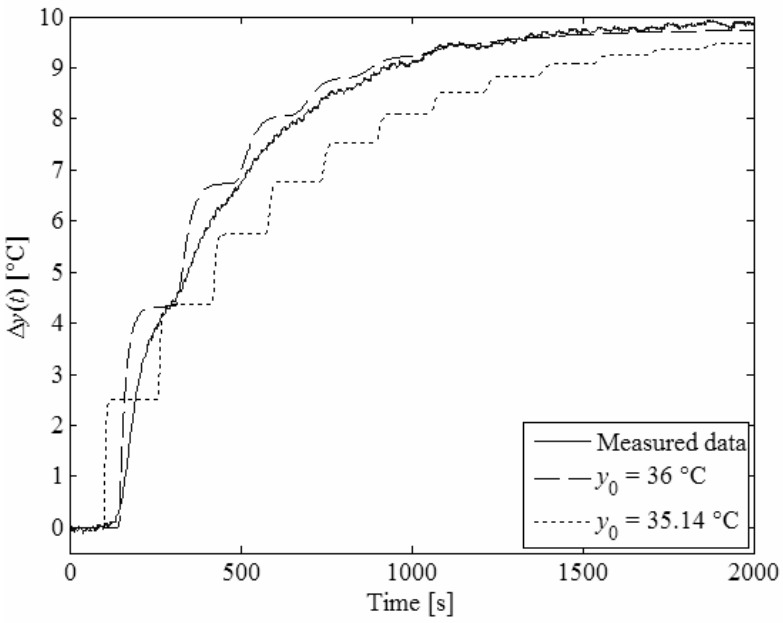

Fig. 7.41 Step responses comparison of measured data vs. relay based model using the time domain solution

As it is clear from Figs. 7.40 and 7.41, the time-domain evaluation of limit cycles from on-off and saturation relay tests gives better plant model parameters estimations in comparison with the use of relay transient, although simulation benchmark has given rather different results. The letter methodology is sensitive to signal noise and the estimation of a stationary component of the signal. Therefore, as plant model parameters, the data in the third column in Tab. 7.16 are taken. Control responses for the 1DoF system with controller (7.59) are presented in Figs. 7.42 and 7.43, whereas those for the TFC system with controllers (7.60) can be seen in Figs. 7.44 and 7.45. For particular controllers settings, see Subchapter 7.7.

Regarding to a peak of the real control response in Fig. 7.42 and output insufficiency in Fig. 7.43 within the time range approx. $t \in [1000,2000]$, these unsatisfactory data are caused probably by temporarily decreased room temperature. The same problem is apparent in other two figures. Amazingly, the real reaction to a step change in the reference signal is better then in the case of the original controllers (7.55) because of less oscillating output.

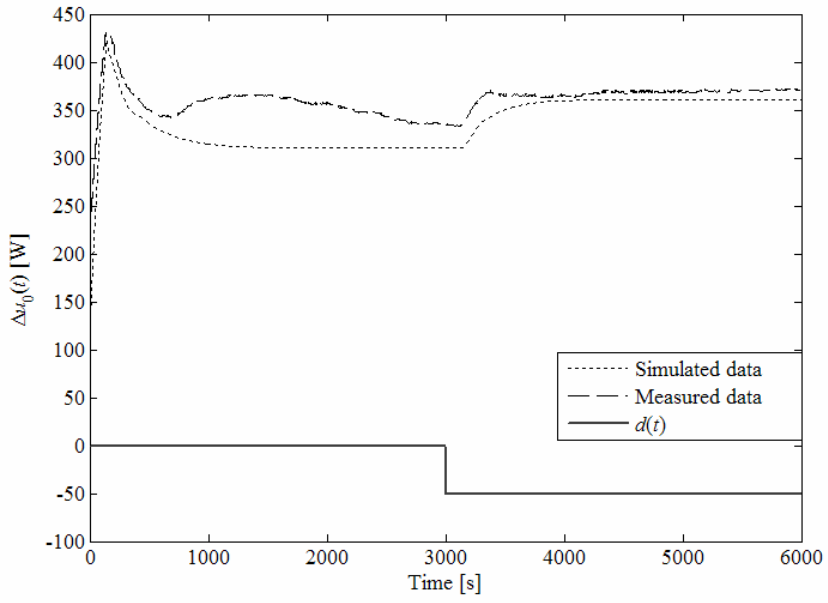

Fig. 7.42 Measured vs. simulated control responses of $\Delta u_0(t)$ for the 1DoF structure with controller (7.59)

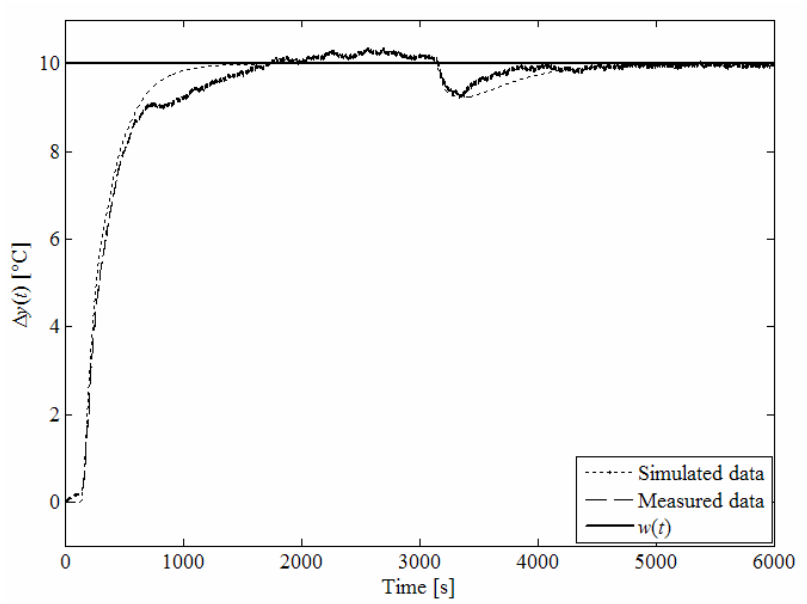

Fig. 7.43 Measured vs. simulated control responses of $y(t)$ for the 1DoF structure with controller (7.59)

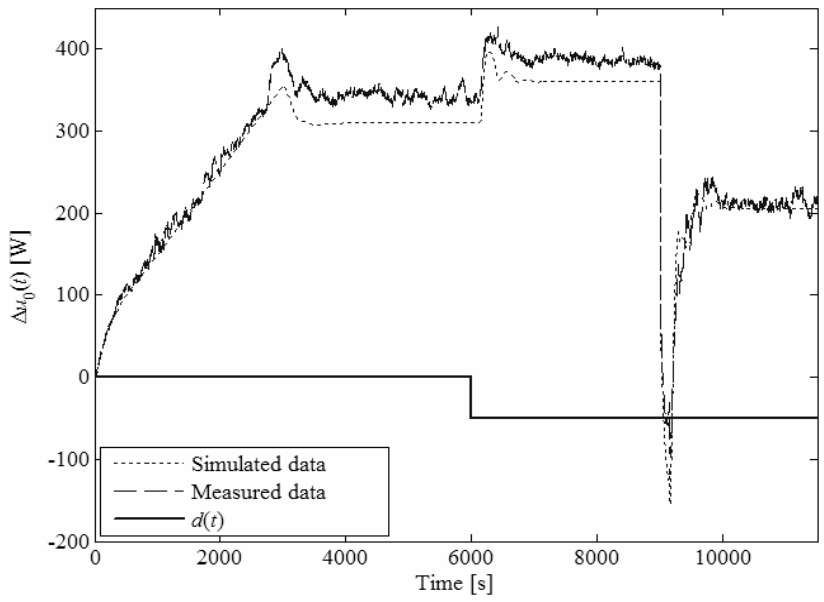

Fig. 7.44 Measured vs. simulated control responses of $\Delta u_0(t)$ for the TFC structure with controllers (7.60)

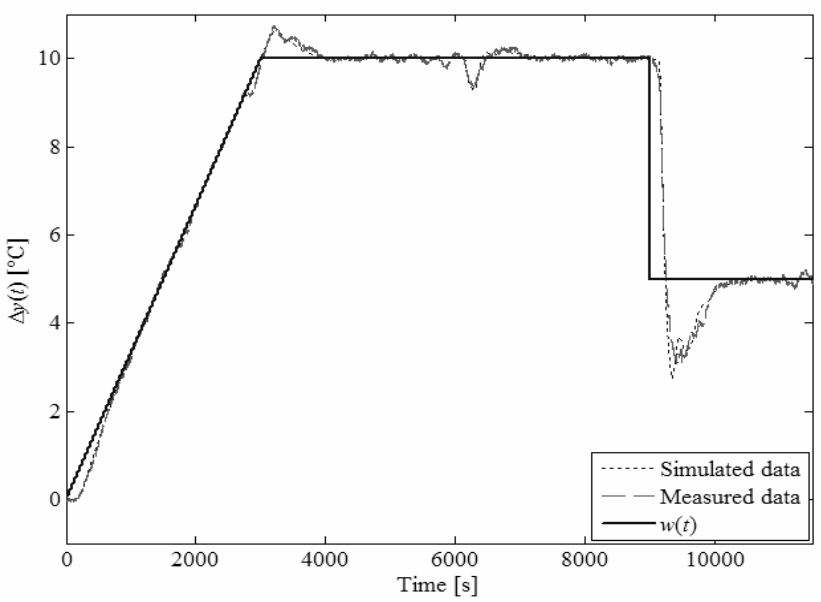

Fig. 7.45 Measured vs. simulated control responses of $y(t)$ for the TFC structure with controllers (7.60)

Overall, there is a very good agreement between simulated and measured data in the figures even though plant models (parameters) rather differ (compare Tabs. 7.10 and 7.16).

7.9.3 Simplified controllers using the Padé approximation

Finally, verify the usability of controllers (7.94) and (7.95) that has arisen from the simplification of controllers (7.46) and (7.55) using the Padé approximation. The corresponding comparison of simulated and measured control responses are displayed in Figs. 7.46 – 7.49.

To avoid the abrupt change in the control action at the beginning of Fig. 7.46, we would suggest using a low-pass filter on the reference signal (similarly as for the preceding subchapter). Other undesirable effect can be seen near the end of the measurement where due to rapidly decreasing ambient temperature the control action increases whereas controlled temperature can not reach the reference value.

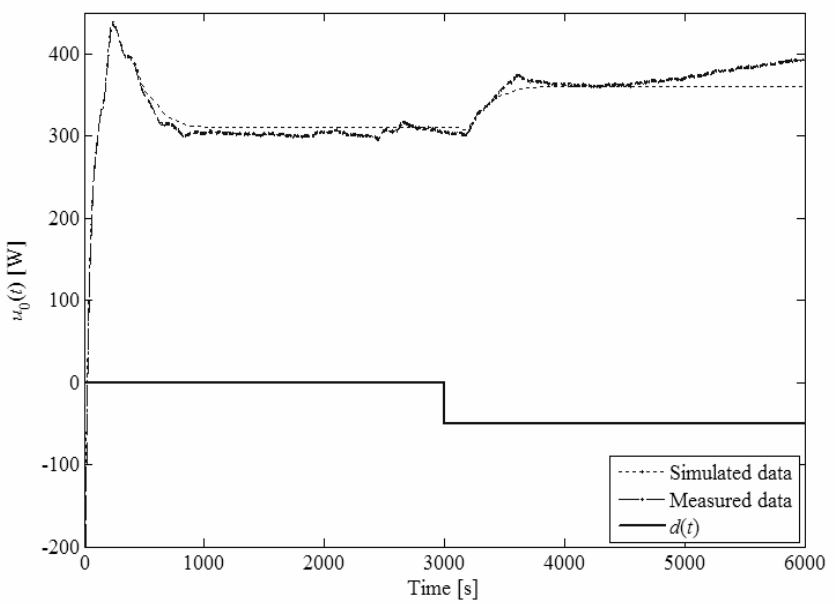

Fig. 7.46 Measured vs. simulated control responses of $\Delta u_0(t)$ for the 1DoF structure with controller (7.94)

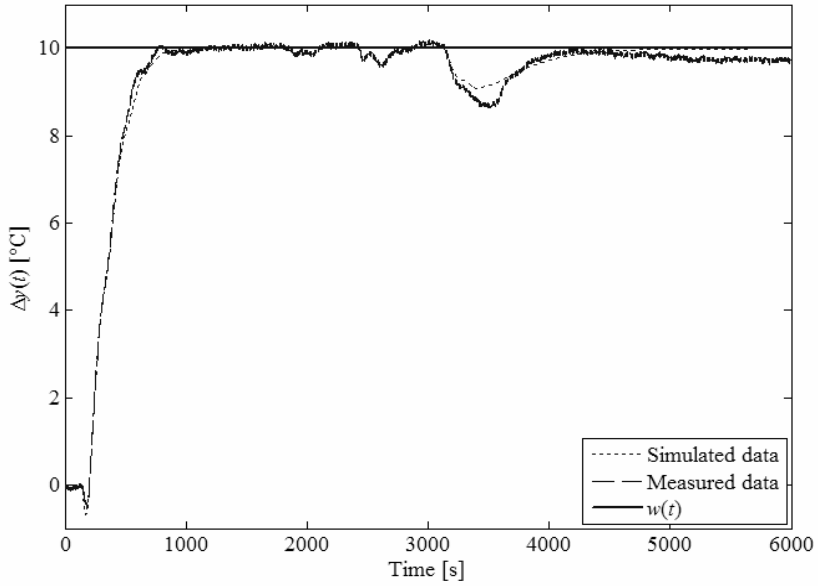

Fig. 7.47 Measured vs. simulated control responses of $y(t)$ for the 1DoF structure with controller (7.94)

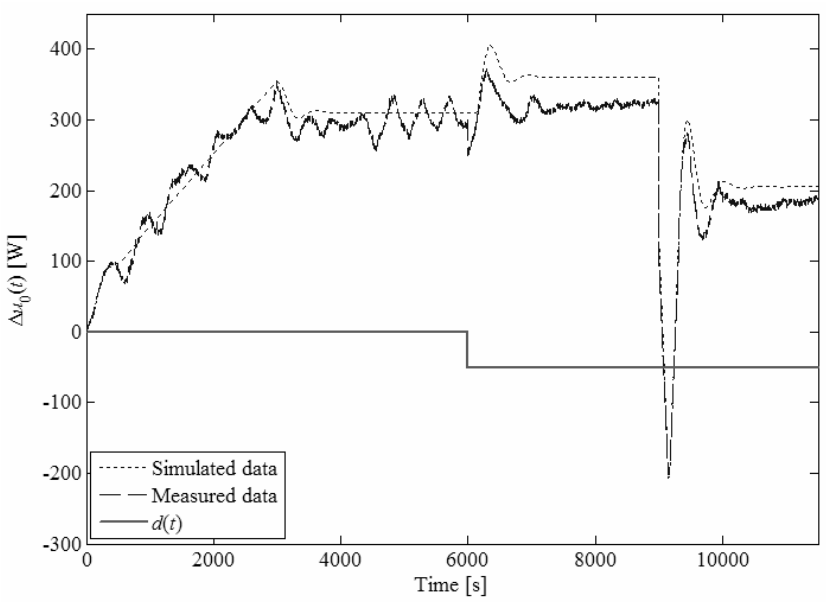

Fig. 7.48 Measured vs. simulated control responses of $\Delta u_0(t)$ *for the TFC structure with controllers (7.95)*

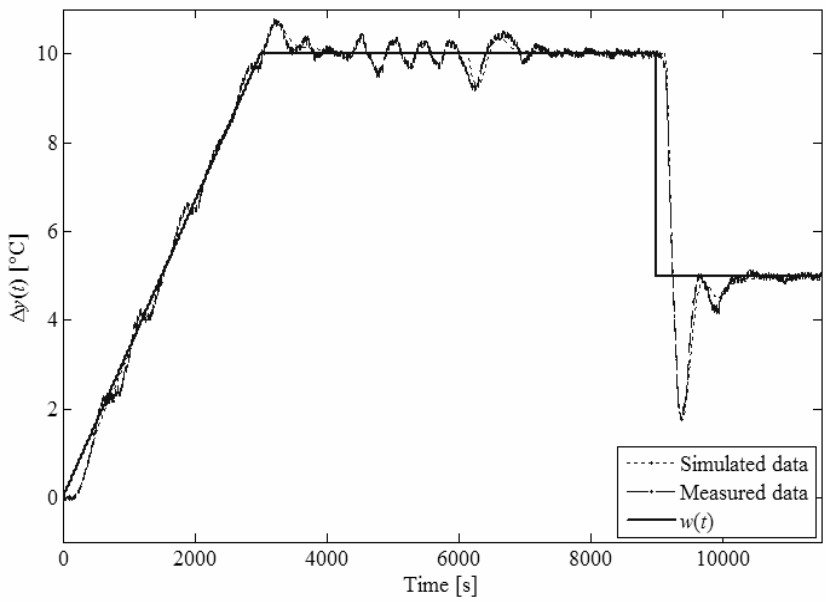

Fig. 7.49 Measured vs. simulated control responses of $y(t)$ *for the TFC structure with controllers (7.95)*

Although real control responses are not as satisfactory as in the case of original and relay-test based controllers derived using the R_{MS} ring, figures above prove the usability and applicability of simplified finite-dimensional controllers as well. Particularly, the reaction to the load disturbance when using the TFC structure is surprisingly good.

7.10 Discussion and summary

To sum up, the above presented practical experiment of control of a laboratory circuit heating plant (i.e. temperature driven by the heater power) has proven the usability and applicability of identification and control algorithms described in this thesis, in real conditions. Naturally, there emerge some problems related to the sensitivity to ambient temperature, measurements uncertainties, unexpected environmental influences or the estimation of a stationary component for relay-based model parameters identification. However, all the designed controllers and their performance have affirmed the robustness of the designed approaches, particularly, those based on the R_{MS} ring together with the Bézout identity and the Youla-Kučera parameterization.

8 CONTRIBUTIONS AND FURTHER DIRECTIONS

The primary contribution of this thesis has been a diminutive development and enhancement of some magnificent theoretical ideas of algebraic control of linear dynamic continuous systems with delays or latencies, regardless of whether in an input-output or internal relation. Practical aspects have not been omitted as well, as demonstrated in the final part of the thesis.

In the first part of the thesis, a concise classification of mathematical models of linear systems with delays has been presented. Dynamic properties of these models are an inseparable part of their description; therefore, poles, zeros, stability and related notions have followed the models classification. Without any attempt to be exhaustive, as the emphasis has been put to algebraic control approaches, an overview of their contemporary state supported by the enumeration of basic algebraic notions and their mutual relations has been introduced afterwards. The work has then also purveyed control system structures and controller tuning principles to be used, unstructured robust stability and performance analysis tools, fundamentals of relay-feedback autotuning and it has briefly outlined possibilities of anisochronic controller discretization as well.

This introductory survey part of the thesis has intended to familiarize the reader with basic and/or recent ideas and approaches which can be useful throughout the work. One of educational and didactic contributions consists in many examples, introduced here, elucidating presented facts to even non-experts.

The crucial section of the thesis which has brought about new ideas and enhanced existing ones about algebraic controller design in the ring of (retarded) quasipolynomial meromorphic functions, R_{MS}, then has followed. The extension of the ring to neutral delayed systems, proofs of some basic properties of the revised ring formulation, a constructive methodology for controller design, the investigation of a quasi-finite spectrum assignment procedure, stability analysis of selected retarded quasipolynomials, an original pole-placement-like optimal tuning algorithm or a generalization of the Nyquist criterion and robust stability and performance conditions belong to the most important and interesting results from the theoretical point of view.

A novel combination of the use of a saturation relay and an anisochronic plant model together with unordinary data evaluation for controlled system modelling and identification can be attributed to the theoretical merit of this thesis as well. Delayed controllers' simplification proposal has been a minor yet integral part of this work.

From the practical point of view, most of theoretically described and developed procedures and ideas have been verified on control of temperature of a laboratory appliance representing a circuit heating system with significant input-output as well as internal delays. The results and subsequent discussion indicate both pros and cones of introduced controller design and tuning. Practical test have proven the usability and applicability of controllers calculated using the R_{MS} ring for both original and relay-based plant models, and also of simplified versions of final controllers. Although there is a significant difference between simulated and real-measured control responses, all controllers have shown their robustness that was calculated before.

There are many possible ways how to utilize and extend the obtained results. For instance, proofs of other R_{MS} ring properties, a more constructive stabilizing procedure, the use of other control system structures or the development of efficient and optimal tuning algorithms can be some of further theoretical contributions. From the practical point of view, the assembling and programming of a compact embedded industrial controller interpreting the core of this thesis can be a challenging task.

9 CONCLUSION

Systems with delays or latencies of any type can be found all around us, in the everyday use, therefore there is a natural necessity to control them. However, delays depreciate control feedback performance due to the infinite spectrum of the control system that appears when using conventional finite-dimensional controllers, which can lead up to feedback instability. Thus, it is no wonder that problems of systems with delays have been considered in control theory for decades. There have been developed a great many algorithms and approaches dealing with this task; however, there is still a lack of those taking advantages of input-output models or dealing with internal delays. The use of algebraic structures, such as rings, can be fruitful in the effort to cope with this issue.

This doctoral thesis has been focused on issues of continuous-time algebraic control design for time-delay systems as well as relay-based identification of anisochronic models and controllers' parameters tuning, to name the main topics. First, it has provided a relatively detailed overview of analysis and control methods for linear time-invariant systems with delays concerning algebraic ones and related notions. Tuning of delayed controllers, their robustness as well as principal issues of relay-based identification and autotuning and possible controller discretization approaches have followed as a next descriptive part of the work.

A novel or beneficial section of the thesis has introduced a revision version of the R_{MS} ring accompanied by its basic properties, a detailed controller design procedure based on the Bézout identity and the Youla-Kučera parameterization for two distinct control system structures using the ring, some stability issues usable also for robust stability and performance analysis and supported by a relatively original relay-based identification idea for time-delay plant models. The approach provides a quasi-finite spectrum assignment for one of control structures. A suboptimal algorithm for controllers' parameters settings via poles shifting has been proposed in addition. For practical reasons, some suggestions of anisochronic controller's simplification have not been omitted. Many ideas and approaches have been supported by illustrative examples. The main disadvantages of the proposed controller design method can be considered in the fact that there it is not always possible to

perform Bézout coprime factorization. On the other side, the procedure is easy-to-handle, robust and applicable to a wide range of time-delay systems, including neutral ones.

The final, practical, part of the work has shown relay-based identification and algebraic control experiments on a circuit heating laboratory model. Although some of relay-based identification submethods has shown to be sensitive to the estimation of the stationary signal component, all designed controllers proved to be practically applicable and robust even to a very inaccurate estimation of ambient temperature.

REFERENCES

[1] ABDALLAH, C., DORATO, P., BENITEZ-READ, J., BYRNE, R. Delayed positive feedback can stabilize oscillatory system. In *Proceedings of the American Control Conference*. San Francisco, CA, USA. 1993, pp. 3106-3107. ISBN 0-7803-0860-3.

[2] ÅSTRÖM, K. J., HÄGGLUND, T. Automatic tuning of simple controllers with specification on phase and amplitude margins. *Automatica*, 1984, vol. 20, no. 5, pp. 645-651. ISSN 0005-1098.

[3] BARTKO, R. *MATLAB II. – Optimization* (in Slovak). Prague: VŠCHT Publishing, 2008. ISBN 978-80-7080-691-3.

[4] BATTLE, C., MIRALLES, A. On the approximation of delay elements by feedback. *Automatica*, 2000, vol. 36, no. 5, pp. 659-664. ISSN 0005-1098.

[5] BELLEN, A., MASET, S. Numerical solution of constant coefficient linear delay differential equations as abstract Cauchy problems. *Numerische Mathematik*, 2000, vol. 84, no. 3. ISSN 0029-599X.

[6] BELLMAN, R., COOKE, K. L. *Differential-Difference Equations*. New York: Academic Press, 1963. 462 p. ISBN 978-0-08-095514-8.

[7] BERETTA, E., KUANG, Y. Geometric stability switch criteria in delay differential systems with delay depended parameters. *SIAM Journal on Mathematical Analysis*, 2002, vol. 3, no. 5, pp. 1144-1165. ISSN 0036-1410.

[8] BOBÁL, V., BOHM, J., FESSL, J., MACHÁČEK, J. *Digital Self-tuning Controllers: Algorithms, Implementation and Applications*. United Kingdom: Springer, 2005. 318 p. ISBN 978-18-523-3980-7.

[9] BONNET, C., PARTINGTON, J. R. Stabilization of fractional exponential systems including delays. *Kybernetika*, 2001, vol. 37, no. 3, pp. 345-353. ISSN 0023-5954.

[10] BREDA, D. Solution operator approximation for characteristic roots of delay differential equations. *Applied Numerical Mathematics*, 2006, vol. 56, no. 3-4, pp. 305-317. ISSN 0168-9274.

[11] BREDA, D. Nonautonomous delay differential equations in Hilbert spaces and Lyapunov exponents. *Differential and Integral Equations*, 2010 vol. 23, no. 9-10, pp. 935-956. ISSN 0893-4983.

[12] BREDA, D., MASET, S., VERMIGLIO, R. Numerical computation of characteristic roots for delay differential equations. In *Time Delay Systems, Proceedings of the 3rd IFAC International Workshop on Time Delay System*, Santa Fe, New Mexico, USA. K. Gu, C. Abdullah, S.-I. Niculescu (Eds.), 2001. ISBN 978-0080440040.

[13] BREDA, D., MASET, S., VERMIGLIO, R. Computing the characteristic roots for delay differential equations. *IMA Journal of Numerical Analysis*. 2004, vol. 24, no. 1, pp. 1-19. ISSN 0272-4979.

[14] BREDA, D., MASET, S., VERMIGLIO, R. Pseudospectral differencing methods for characteristic roots of delay differential equations. *SIAM Journal on Scientific Computing*, 2005, vol. 27, no. 2, pp. 482-495. ISSN 1064-8275.

[15] BREDA, D., MASET, S., VERMIGLIO, R. Discretization of solution operators for linear time invariant - time delay systems in Hilbert spaces. In *Time Delay Systems: Methods, Applications and New Trends. Lecture Notes in Control and Information Sciences*, vol. 423. R. Sipahi, T. Vyhlídal, S.-I. Niculescu, P. Pepe (Eds.). Berlin: Springer, 2012, pp. 217-228. ISBN 978-3-642-25220-4.

[16] BRETHÉ, D., LOISEAU, J. J. An effective algorithm for finite spectrum assignment of single-input systems with delays. *Mathematics and Computers in Simulation*, 1998, vol. 45, no. 3-4, pp. 339-348. ISSN 0378-4754.

[17] BURKE, J., LEWIS, A., OVERTON, M. A robust gradient sampling algorithm for nonsmooth, nonconvex optimization. *SIAM Journal of Optimization*, 2005, vol. 15, no. 3, pp. 751-779. ISSN 1052-6234.

[18] BYRNES, C. I., SPONG, M. W., TARN, T. J. A several complex variables approach to feedback stabilization of neutral delay-differential systems. *Mathematical Systems Theory*, 1984, vol. 17, no. 1, pp. 97-133. ISSN 0025-5661.

[19] CALLIER, F. M., DESOER, C. A. An algebra of transfer function for distributed linear time-invariant systems. *IEEE Transactions on Circuits and Systems*, 1975, vol. 25, no. 9, pp. 651-662. ISSN 0098-4094.

[20] COHEN, G. H., COON, G. A. Theoretical consideration of retarded control. *Transactions of ASME*, 1953, vol. 75, pp. 827-834.

[21] COMEAU, A. R., HORI, N. State-space forms for higher-order discrete-time models. *Systems & Control Letters*, 1998, vol. 34, no. 1-2, pp. 23-31. ISSN 0167-6911.

[22] CONTE, G., PERDON, A. M. Systems over a principal ideal domain: A polynomial model approach. *SIAM Journal of Control and Optimization*, 1982, vol. 20, no. 1, pp. 112-124. ISSN 0363-0129.

[23] CONTE, G., PERDON, A. M. The block decoupling problem for systems over a ring. *IEEE Transactions on Automatic Control*, 1998, vol. 43, no. 11, pp. 1600-1604. ISSN 0018-9286.

[24] CONTE, G., PERDON, A. M. Systems over rings: Geometric theory and applications. *Annual Reviews in Control*, 2000, vol. 24, pp. 113-124. ISSN 1367-5788.

[25] COOKE, K. L., GROSSMAN, Z. Discrete delay, distributed delay and stability switches. *Journal of Mathematical Analysis and Applications*, 1982, vol. 86, pp. 592-627.

[26] DELICE, I. I., SIPAHI, R. Controller design for delay-independent stability of multiple time-delay systems via Déscartes's rule of signs. In *Proceedings of the 9th IFAC Workshop on Time Delay Systems (TDS 2010)* [online], vol. 9. Prague: IFAC, 2010. pp. 144-149. Available from: http://www.ifac-papersonline.net/Detailed/43707.html. ISBN 978-3-902661-71-5.

[27] DESOER, C. A., VIDYASAGAR, M. *Feedback Systems: Input-Output Properties*. New York: Academic Press, 1975. 264 p. ISBN 978-0122120503.

[28] DESOER, C. A., LIU, R. W., MURRAY, J., SEAKS, R. Feedback system design: the fractional representation approach to analysis and synthesis. *IEEE Transactions on Automatic Control*, 1980, vol. 25, no. 3, pp. 399-412. ISSN 0018-9286.

[29] DIEKMANN, O., VAN GILS, S. A., VERDUYN LUNEL, S. M., WALTHER, H.-O. *Delay Equations: Functional, Complex and Nonlinear Analysis*. *Applied Mahematical Sciences*, vol. 110. New York: Springer, 1995. ISBN 978-0387944166.

[30] DI LORETO, M., LAFAY, J.-F., LOISEAU, J. J., LU, H. On the structure at infinity for linear time-delay systems. In *Proceedings of the 9th IFAC Workshop on Time Delay Systems (TDS 2010)* [online], vol. 9. Prague: IFAC, 2010. pp. 156-161. Available from: http://www.ifac-papersonline.net/Detailed/43709.html. ISBN 978-3-902661-71-5.

[31] DLAPA, M., PROKOP, R. Algebraic approach to controller design using structured singular value. *Control Engineering Practice*, 2010, vol. 18, no. 4, pp. 358-382. ISBN 0967-0661.

[32] DOSTÁL, P., GAZDOŠ, F., BOBÁL, V. Design of controllers for processes with time delay by polynomial method. In *Proceedings of the IEEE European Control Conference*, Kos, Greece. 2007. pp. 4540-4545.

[33] DOSTÁL, P., MATUŠŮ, R. *State and Algebraic Control Theory* (in Czech). Tomas Bata Zlín: Tomas Bata University in Zlín, Czech Republic, 2010. 90 p. ISBN 978-80-7318-991-4.

[34] DOSTÁLEK, P., DOLINAY, J., VAŠEK, V. Design and implementation of portable data acquisition unit in process control and supervision applications. *WSEAS Transactions on Systems and Control*. 2008, vol. 3, no. 9, pp. 779-788. ISSN 1991-8763.

[35] DOYLE, J. C., FRANCIS, B. A., TANNENBAUM, A. R. *Feedback Control Theory*. New York: McMillan, 1992. ISBN 978-0486469331.

[36] EL'SGOL'TS, L. E., NORKIN, S. B. *Introduction to the Theory and Application of Differential Equations with Deviated Arguments*. New York: Academic Press, 1973. ISBN 978-0122377501.

[37] EMRE, E. On necessary and sufficient conditions for regulation of linear systems over rings. *SIAM Journal of Control and Optimization*, 1982, vol. 20, no. 2, pp. 150-160. ISSN 0363-0129.

[38] EMRE, E. Regulation of linear systems over rings by dynamic output feedback. *Systems & Control Letters*, 1983, vol. 3, no. 1, pp. 57-62. ISSN 0167-6911.

[39] ENGELBORGHS, K., ROOSE, D. On stability of LMS-methods and characteristic roots of delay differential equations. *SIAM Journal on Numerical Analysis*, 2002, vol. 40, no. 2, pp. 629-650. ISSN 0036-1429.

[40] ERGENC, A. F. A new method for delay-independent stability of time-delayed systems. In *Proceedings of the 9th IFAC Workshop on Time Delay Systems (TDS 2010)* [online], [online], vol. 9. Prague: IFAC, 2010. pp. 51-56. Available from: http://www.ifac-papersonline.net/Detailed/43691.html. ISBN 978-3-902661-71-5.

[41] FIORAVANTI, A. R., BONNET, C., ÖZBAY, H., NICULESCU, S.-I. A numerical method to find stability windows and unstable poles for linear neutral time-delay systems. In *Proceedings of the 9th IFAC Workshop on Time Delay Systems (TDS 2010)* [online], vol. 9. Prague: IFAC, 2010. pp. 183-188. Available from: http://www.ifac-papersonline.net/Detailed/43714.html. ISBN 978-3-902661-71-5.

[42] FINDENSEN, W., PULACZEWSKI, J., MANITIUS, A. Multilevel optimization and dynamic coordination of mass flows in a beet sugar plant. *Automatica*, 1970, vol. 6, no. 4, pp. 581-589. ISSN 0005-1098.

[43] FOIAS, C., ÖZBAY, H., TANNENBAUM, A. *Robust Control of Infinite Dimensional Systems – Frequency Domain Methods*. In *Lecture Notes in Control and Information Sciences*, vol. 209. New York: Springer, 1996. ISBN 3540199942.

[44] FORNASINI, E., MARCHESINI, G. State-space realization theory of two-dimensional filters. *IEEE Transactions on Automatic Control*, 1976, vol. 21, no. 4, pp. 484-492. ISSN 0018-9286.

[45] GIBSON, J. S. Linear-quadratic optimal control of hereditary differential systems: Infinite dimensional Riccati equations and numerical approximation. *SIAM Journal on Control and Optimization*, 1983, vol. 21, no. 1, pp. 95-139. ISSN 0363-0129.

[46] GLUESING-LUEERSSEN, H. A behavioral approach to delay-differential systems. *SIAM Journal of Control and Optimization*, 1997, vol. 35, no. 2, pp. 480-499. ISSN 0363-0129.

[47] GÓRECKI, H., FUKSA, S., GRABOWSKI, P., KORYTOWSKI, A. *Analysis and Synthesis of Time Delay Systems*. Warszawa: PWN – Polish Scientific Publishers, co-editor John Wiley & Sons, 1989. 369 p. ISBN 978-0471276227.

[48] GU, K., KHARITONOV, V. L., CHEN, J. *Stability of Time-Delay Systems*. Boston: Birghäuser, 2003. ISBN 978-0817642129.

[49] HABETS, L. *Algebraic and Computational Aspects of Time-Delay Systems*. Ph. D. thesis, Eindhoven, 1994.

[50] HALE, J. K., VERDUYN LUNEL, S. M. *Introduction to Functional Differential Equations*. In *Applied Math. Sciences*, vol. 99. New York: Springer, 1993. 464 p. ISBN 978-0387940762.

[51] HALE, J. K., VERDUYN LUNEL, S. M. Effects of small delays on stability and control. *Operator Theory; Advances and Applications*, vol. 122. Birghauser, 2001, pp. 275-301.

[52] HALE, J. K., VERDUYN LUNEL, S. M. Strong stabilization of neutral functional differential equations. *IMA Journal of Mathematical Control and Information*, 2002, vol. 19, no. 1-2, pp. 5-23. ISSN 0265-0754.

[53] HANG, C. C., ÅSTRÖM, K. J., WANG, Q. G. Relay feedback auto-tuning of process controllers – a tutorial review. *Journal of Process Control*, 2002, vol. 12, no. 1, pp. 143-162. ISSN 0959-1524.

[54] HANG, C. C., WANG, Q. G., CAO, L. S. Self-tuning Smith predictors for processes with long dead time. *International Journal of Adaptive Control and Signal Processing*, 1995, vol. 9., no. 3, pp. 255-270. ISSN 1099-1115.

[55] HAUTUS, M. J. L. *Controlled Invariance for Systems over a Ring*. In *Feedback Control of Linear and Nonlinear Systems*. *Lecture Notes on Control and Information Sciences*, vol. 39. Springer, 1982. ISBN 978-3-540-11749-0.

[56] HOFREITER, M. Discretization of continuous linear anisochronic models. *Studies in Informatics and Control*, 2003, vol. 12, no. 1, pp. 69-76. ISSN 1220-1766.

[57] INABA, H., WANG., W. Block decoupling for linear systems over rings. *Linear Algebra and its Applications*, 1996, vol. 241-243, pp. 619-634. ISSN 0024-3795.

[58] KALMAN, R. E., FALB, P. L., ARBIB, M. A. *Topics in Mathematical System Theory*, McGraw-Hill, 1969.

[59] KAMEN, E. W. On the algebraic theory of systems defined by convolution operations. *Mathematical Systems Theory*, 1975, vol. 9, pp. 57-74. ISSN 0025-5661.

[60] KAMEN, E. W. Ring models for delay differential systems. *Automatica*, 1976, vol. 12, no. 6, pp. 529-531. ISSN 0005-1098.

[61] KAMEN, E. W. Lectures on algebraic system theory: Linear systems over rings. *NASA Contractor Report 3016*, 1978. 73 p.

[62] KAMEN, E. W. KHARGONEKAR, P. P., TANNENBAUM, A. Stabilization of time-delay systems using finite-dimensional controllers. *IEEE Transactions on Automatic Control*, 1985, vol. 30, no. 1, pp. 75-78. ISSN 0018-9286.

[63] KAMEN, E. W. KHARGONEKAR, P. P., TANNENBAUM, A. Proper stable Bézout factorization and feedback control of linear time-delay systems. *International Journal of Control*, 1986, vol. 43, no. 3, pp. 837-857. ISSN 0020-7179.

[64] KHARITONOV, V., MONDIÉ, S., COLLADO, J. Exponential estimates for neutral time-delay systems: an LMI approach. *IEEE Transactions in Automatic Control*, 2005, vol. 50, no. 5, pp. 666-670. ISSN 0018-9286.

[65] KOLMANOVSKII, V. B., MYSHKIS, A. *Introduction to the Theory and Applications of Functional Differential Equations*. Dordrecht: Kluwer Academic Publishers, 1999. 648 p. ISBN 0-7923-5504-0.

[66] KOLMANOVSKII, V. B., NOSOV, V. R. *Stability of Functional Differential Equations*. London: Academic Press, 1986. ISBN 0-12-417940-1.

[67] KRASOVSKII, N. N. *Stability of Motion: Applications of Lyapunov's Second Method to Differential Systems and Equations with Delay*. Chicago: Standford University Press, 1963. 188 p. ISBN 978-0804700986.

[68] KRČMÁŘ, J. *Design and Realization of Hardware Interface Between Laboratory Heat Exchanger and Multifunction I/O Card* (in Czech). Master's thesis. Zlín: Faculty of Applied Informatics, Tomas Bata University in Zlín, 2012. Supervisor Prof. Ing. Vladimír Bobál, CSc.

[69] KUČERA, V. Diophantine equations in control - a survey. *Automatica*, 1993, vol. 29, no. 6, pp. 1361-1375. ISSN 0005-1098.

[70] KUČERA, V. Robust controllers. *Automa*, 2001, vol. 7, no. 6, pp. 43-45. ISSN 1210-9592. (in Czech)

[71] LEE, E. B., ZAK, S. H. On spectrum placement for linear time invariant delay systems. *IEEE Transactions on Automatic Control*, 1982, vol. 27, no. 2, pp. 446-449. ISSN 0018-9286.

[72] LI, W., ESKINAT, E., LUYBEN, W. L. An improved autotune identification method. *Industrial & Engineering Chemistry Research*, 1991, vol. 30, no. 7, pp. 1530-1541. ISSN 0888-5885.

[73] LI, Y., SHEN, A., QI, Q. Further results on guaranteed dominant pole placement with PID controllers. In *Proceedings of 30th Chinese Control Conference (CCC 2011)*, Yantai, China, 2011. IEEE. pp. 3756-3760. ISBN 978-1457706776.

[74] LOISEAU, J. J. Algebraic tools for the control and stabilization of time-delay systems. *Annual Reviews in Control*, 2000, vol. 24, pp. 135-149. ISSN 1367-5788.

[75] LOISEAU, J. J., CARDELLI, M., DUSSER, X. Neutral-type time-delay systems that are not formally stable are not BIBO stabilizable. *IMA Journal of Mathematical Control and Information*, 2002, vol. 19, no. 1-2, pp. 217-227. ISSN 0265-0754.

[76] LUYBEN W. L. Derivation of transfer functions for highly nonlinear distillation columns. *Industrial & Engineering Chemistry Research*, 1987, vol. 26, no. 12, pp. 2490-2495. ISSN 0888-5885.

[77] LUZYANINA, T., ENGELBORGHS, K., ROOSE, D. Computing stability of differential equations with bounded distributed delays. *Numerical Algorithms*, 2003, vol. 34, no. 1, pp. 41-66. ISSN 1017-1398.

[78] MADSEN, K., NIELSEN H. B., TINGLEFF, O. *Methods for Non-linear Least Square Problems*. *Informatics and Mathematical Modelling* [online]. Lyngby: Technical University of Denmark, 2004. Available from: http://www2.imm.dtu.dk/pubdb/view/edoc_download.php/3215/pdf/imm3215.pdf.

[79] MAJHI, S. Relay based identification of processes with time delay. *Journal of Process Control*, 2007, vol. 17, no. 2, pp. 93-101. ISSN 0959-1524.

[80] MAKILLA, P. M., PARTINGTON, J. R. Laguerre and Kautz shift approximations of delay systems. *International Journal of Control*, 1999a, vol. 72, no. 10, pp. 932-946. ISSN 0020-7179.

[81] MAKILLA, P. M., PARTINGTON, J. R. Shift operator induced approximations of delay systems. *SIAM Journal of Control and Optimization*, 1999b, vol. 37, no. 6, pp. 1897-1912. ISSN 0363-0129.

[82] MALEK-ZAVAREI, M., JAMSHIDI, M. *Time Delay System*s. *Analysis, Optimization and Applications*. In *North-Holland Systems and Control Series*, vol. 9. Amsterdam: North Holland, 1987. ISBN 978-0444702043.

[83] MANITIUS, A. Z., OLBROT, A. W. Finite spectrum assignment problem for systems with delays. *IEEE Transactions on Automatic Control*, 1979, vol. 24, no. 4, pp. 541-553. ISSN 0018-9286.

[84] MARCHETTI, G., SCALI, C. Use of modified relay techniques for the design of model-based controllers for chemical processes. *Industrial and Engineering Chemistry Research*, 2000, vol. 39, no. 9, pp. 3325-3334. ISSN 0888-5885.

[85] MAREŠ, J. Simplified first principle of thermal process. In *Proceedings of the XXXIIIrd Seminary ASR '08: Instruments and Control*. Ostrava: VŠB-TU in Ostrava, Czech Republic, 2008. pp. 213–220. ISBN 978-80-248-1727-9.

[86] MARSHALL, J. E., GÓRECKI, H., KORYTOWSKI, A., WALTON, K. *Time Delay Systems, Stability and Performance Criteria with Applications*. New York: Ellis Horwood, 1992. 244 p. ISBN 978-0134659237.

[87] MATUŠŮ, R., PROKOP, R. Single-parameter tuning of PI controllers: Theory and application. *Journal of the Franklin Institute*, 2011, vol. 348, no. 8, pp. 2059-2071. ISSN 0016-0032.

[88] MCGAHAN, P., VYHLÍDAL, T. Optimization based pole-placement of retarded systems using derivative feedback. In *Proceedings of the 8th International Scientific – Technical Conference Process Control* [CD-ROM], Kouty nad Desnou, Czech Republic, 2008.

[89] MICHIELS, W., ENGELBORGHS, K., ROOSE, D., DOCHAIN, D. Sensitivity to infinitesimal delays in neutral equations. *SIAM Journal on Control and Optimization*, 2001, vol. 40, no. 4. ISSN 0363-0129.

[90] MICHIELS, W., ENGELBORGHS, K., VANSEVEVANT, P., ROOSE, D. Continuous pole placement for delay equations. *Automatica*, 2002, vol. 38, no. 5, pp. 747-761. ISSN 0005-1098.

[91] MICHIELS, W., NICULESCU, S.-I. Characterization of delay-independent stability and delay interference phenomena. *SIAM Journal on Control and Optimization*, 2007a, vol. 45, no. 6, pp. 2138-2155. ISSN 0363-0129.

[92] MICHIELS, W., NICULESCU, S.-I. *Stability and Stabilization of Time-Delay Systems. An Eigenvalue Based Approach*. Philadelphia: SIAM Publications, 2007b. ISBN 978-0898716320.

[93] MICHIELS, W., ROOSE, D. An eigenvalue based approach for the robust stabilization of linear time-delay systems. *International Journal of Control*, 2003, vol. 76, no. 7, pp. 678-686. ISSN 0020-7179.

[94] MICHIELS, W., VYHLÍDAL, T. An eigenvalue based approach for the stabilization of linear time-delay systems of neutral type. *Automatica*, 2005, vol. 41, no. 6, pp. 991-998. ISSN 0005-1098.

[95] MICHIELS, W., VYHLÍDAL, T., HUIJBERTS, H., NIJMEIJER, H. Stabilizability and stability robustness of state derivative feedback controllers. *SIAM Journal on Control and Optimization*, 2009a, vol. 47, no. 6, pp. 3100-3117. ISSN 0363-0129.

[96] MICHIELS, W., VYHLÍDAL, T., ZÍTEK, P., NIJMEIJER, H., HENRION, D. Strong stability of neutral equations with an arbitrary delay dependency structure. *SIAM Journal on Control and Optimization*, 2009b, vol. 48, no. 2, pp. 763-786. ISSN 0363-0129.

[97] MICHIELS, W., VYHLÍDAL, T., ZÍTEK P. Control design for time-delay systems based on quasi-direct pole placement. *Journal of Process Control*, 2010, vol. 20, no. 3, pp. 337-343. ISSN 0959-1524.

[98] MIDDLETON, R. H., GOODWIN, G. C. *Digital Control and Estimation: A Unified Approach*. Detroit: Prentice Hall, 1990. ISBN 978-0132116657.

[99] MONDIÉ, S., KHARITONOV, V. Exponential estimates for retarded time-delay systems: an LMI approach. *IEEE Transactions in Automatic Control*, 2005, vol. 50, no. 2, pp. 666-670. ISSN 0018-9286.

[100] MORÁVKA, J., MICHÁLEK, K. Anisochronous model of the metallurgical RH Process. *Transactions of the VŠB – Technical University of Ostrava, Mechanical Series*, 2008, vol. 14, no. 2, pp. 91–96. ISSN 1210-0471.

[101] MORF, M., LÉVY, B. C., KUNG, S.-Y. New results in 2-D systems theory, part I: 2-D polynomial matrices, factorization and coprimeness. *Proceedings of the IEEE*, 1977, vol. 65, no. 6, pp. 861-872. ISSN 0018-9219.

[102] MORSE, A. S. Ring models for delay-differential systems. *Automatica*, 1976, vol. 12, no. 5, 1976, pp. 529-531. ISSN 0005-1098.

[103] MOUNIER, H. *Propriétes structurelles des systémes linéaires à retards: aspects théoreques et pratiques*. Ph.D. thesis. Paris: Supélec, 1995.

[104] MYSHKIS, A. D. *Linear Differential Equations with Delays Arguments*. Moskow: Nauka, 1972.

[105] NELDER, J. A., MEAD, R. A simplex method for function minimization. *The Computer Journal*, 1965, vol. 7, no. 4, pp. 308–313. ISSN 0010-4620.

[106] NICULESCU, S.-I. *Delay Effects on Stability: A Robust Control Approach. Lecture Notes in Control and Information Sciences*, vol. 269. Berlin: Springer, 2001. 403 p. ISBN 978-1852332914.

[107] NICULESCU, S.-I. On delay robustness analysis of a simple control algorithm in high-speed networks. *Automatica*, 2002, vol. 38, no. 5, pp. 885-889. ISSN 0005-1098.

[108] O'DWEYR, A. *Handbook of PI and PID Controller Tuning Rules*. 3rd edition. London: Imperial College Press, 2009. ISBN 978-1848162426.

[109] OLGAC, N., SIPAHI, R. An exact method for the stability analysis of time delay LTI systems. *IEEE Transaction on Automatic Control*, 2002, vol. 47, no. 5, pp. 793-797. ISSN 0018-9286.

[110] OLGAC, N., SIPAHI J., ERGENC, A. F. 'Delay scheduling' as unconventional use of time delay for trajectory tracking. *Mechatronics*, 2007, vol. 17, no. 4-5, pp. 199-206. ISSN 0957-4158.

[111] OLBROT, W. Stabilizability, detectability and spectrum assignment for linear autonomous systems with general time delays. *IEEE Transactions on Automatic Control*, 1978, vol. 23, no. 5, pp. 887-890. ISSN 0018-9286.

[112] ORTEGA, R., KELLY, R. PID self-tuners: Some theoretical and practical aspects. *IEEE Transactions on Industrial Electronics*, 1984, vol. IE-31, no. 4, pp. 332-338. ISSN 0278-0046.

[113] OSIPOV, Y. S. Stabilization of controlled systems with delay. *Differentsial'nye Uravneniya*, 1965, vol. 1, pp. 605–618. ISSN 0374-0641.

[114] PARTINGTON, J. R. Some frequency-domain approaches to the model reduction of delay systems. *Annual Reviews in Control*, 2004, vol. 28, no. 1, pp. 65-73. ISSN 1367-5788.

[115] PARTINGTON, J. R., BONNET, C. H_∞ and BIBO stabilization of delay systems of neutral type. *Systems & Control Letters*, 2004, vol. 52, no. 3-4, pp. 283-288. ISSN 0167-6911.

[116] PAZY, A. *Semigroups of Linear Operators and Applications to Partial Differential Equations*. In *Graduate Texts in Mathematics*. New York: Springer, 1992. ISBN 978-0387908458.

[117] PEKAŘ, L. Relay test for anisochronic models – time domain solution. *Transactions of the VŠB – Technical University of Ostrava, Mechanical Series*, 2008, vol. 54, no. 2, pp. 103-108. ISSN 1210-0471.

[118] PEKAŘ, L. Root locus analysis of a retarded quasipolynomial. *WSEAS Transaction on Systems and Control*, 2011, vol. 6, no. 3, pp. 79-91. ISSN 1991-8763.

[119] PEKAŘ, L. On the optimal pole assignment for time-delay systems. *International Journal of Mathematical Models in Applied Sciences* [online], 2013, vol. 7, no. 1, pp. 63-74. Available from: http://www.naun.org/multimedia/NAUN/m3as/16-603.pdf. ISSN 1998-0140.

[120] PEKAŘ, L., KURE ČKOVÁ, E. Does the higher order mean the better internal delay rational approximation?. *International Journal of Mathematics and Computers in Simulation* [online], 2012, vol. 6, no. 1, 2012, pp. 153-160. Available from: http://www.naun.org/multimedia/NAUN/mcs/17-742.pdf. ISSN 1998-0159.

[121] PEKAŘ, L., PROKOP, R. On some tuning principles for anisochronic controllers. In *2nd International Conference on Advanced Control Circuits & Systems - ACCS'07* [CD-ROM]. Cairo: National Authority for Remote Sensing & Space Sciences (NARSS), 2008a. Paper no. AST108.

[122] PEKAŘ, L., PROKOP, R. Algebraic control of integrating processes with dead time by two feedback controllers in the ring RMS. *International Journal of Circuits, Systems and Signal Processing* [online], 2008b, vol. 2, no. 4, pp. 249-263. Available from: http://www.naun.org/multimedia/NAUN/circuitssystemssignal/cssp-90.pdf. ISSN 1998-4464.

[123] PEKAŘ, L., PROKOP, R. An approach for relay based identification of anisochronic models. In *Proceedings of the 27th IASTED International Conference on Modelling, Identification and Control (MIC 2008)*, Innsbruck, Austria, 2008c. pp. 438-443. ISBN 978-0-88986-712-3.

[124] PEKAŘ, L., PROKOP, R. Some observations about the RMS ring for delayed systems. In *Proceedings of the 17th International Conference on Process Control '09*, Štrbské Pleso, Slovakia, 2009. pp. 28-36. ISBN 978-80-227-3081-5.

[125] PEKAŘ, L., PROKOP, R. Stability conditions for a retarded quasipolynomial and their applications. *International Journal of Mathematics and Computers in Simulations* [online], 2010a, vol. 4, no. 3, pp. 90-98. Available from: http://www.naun.org/multimedia/NAUN/mcs/19-453.pdf. ISSN 1998-0159.

[126] PEKAŘ, L., PROKOP, R. Stabilization of a delayed system by a proportional controller. *International Journal of Mathematical Models and Methods in Applied Sciences* [online], 2010b, vol. 4, no. 4, pp. 282-290. Available from: http://www.naun.org/multimedia/NAUN/m3as/19-432.pdf. ISSN 1998-0140.

[127] PEKAŘ, L., PROKOP, R. Implementation of a new quasi-optimal controller tuning algorithm for time-delay systems. In *MATLAB for Engineers – Applications in Control, Electrical Engineering, IT and Robotics*. K. Perůtka (Ed.). Rijeka, Croatia: Intech, 2011, pp. 3-26. ISBN 978-953-307-914-1.

[128] PEKAŘ, L., PROKOP, R., DOSTÁLEK, P. Circuit heating plant model with internal delays. *WSEAS Transaction on Systems*, 2009, vol. 8, no. 9, pp. 1093-1104. ISSN 1109-2777.

[129] PEKAŘ, L., PROKOP, R., DOSTÁLEK, P. Non-stepwise reference tracking for time delay systems. In *Proceedings of 12th International Carpathian Control Conference (ICCC '11)*. Velké Karlovice, Czech Republic, 2011. pp. 292-297. ISBN 978-1-61284-359-9.

[130] PEKAŘ, L., PROKOP, R., KORBEL, J. Autotuning for delay systems in meromorphic functions – a second order case. In *Proceedings of the European Control Conference*, Kos, Greece, 2007. pp. 1839 – 1845. ISBN 978-960-89028-5-5.

[131] PEKAŘ, L., PROKOP, R., MATUŠŮ, R. Algebraic control of unstable delayed first order systems using RQ-meromorphic functions. In *Proceedings of the 15th Mediterranean Conference on Control and Automation* [CD-ROM], Athens, Greece, 2007. ISBN 978-96-0254-664-2.

[132] PEKAŘ, L., PROKOP, R., MATUŠŮ, R. A stability test for control systems with delays based on the Nyquist criterion. *International Journal of Mathematical Models in Applied Sciences* [online], 2011, vol. 5, no. 6, pp. 1213-1224. Available from: http://www.naun.org/multimedia/NAUN/m3as/17-128.pdf. ISSN 1998-0140.

[133] PEKAŘ, L., PROKOP, R., NAVRÁTIL, P. Spectral abscissa minimization when algebraic control of unstable LTI-TDS. In *Proceedings of the IFAC Conference on Advances in PID Control (PID '12)*, Brescia, Italy, 2012. Paper no. ThB 1.1.

[134] PENROSE, R. A generalized inverse for matrices. *Mathematical Proceedings of the Cambridge Philosophical Society*, 1955, vol. 51, no. 3. ISSN 0305-0041.

[135] PICARD, P., LAFAY, J.-F., KUČERA, V. Feedback realization of non-singular precompensators for linear systems with delays. *IEEE Transactions on Automatic Control*, 1997, vol. 42, no. 6, pp. 848-853. ISSN 0018-9286.

[136] PICARD, P., LAFAY, J.-F., KUČERA, V. Model matching for linear systems with delays and 2D systems. *Automatica*, 1998, vol. 34, no. 2, pp. 183-191. ISSN 0005-1098.

[137] PONTRYAGIN, L. S. On the zeros of some elementary transcendental functions. *Izvestiya Akademii Nauk SSSR*, 1942, vol. 6, pp. 115-131. ISSN 0002-337X.

[138] PROKOP, R., CORRIOU, J. P. Design and analysis of simple robust controllers. *International Journal of Control*, 1997, vol. 66, no. 6, pp. 905-921. ISSN 0020-7179.

[139] PROKOP, R., PEKAŘ, L., KORBEL, J. Autotuning for delay systems using meromorphic functions. In *Proceedings of the 9th IFAC Workshop on Time Delay Systems (TDS 2010)* [online], vol. 9. Prague: IFAC, 2010. pp. 331-336. Available from: http://www.ifac-papersonline.net/Detailed/43739.html. ISBN 978-3-902661-71-5.

[140] REKASIUS, Z. V. A stability test for systems with delays. In *Proceedings Joint Automatic Control Conference*, San Francisco, 1980. Paper no. TP9-A.

[141] RICHARD J. P. Time-delay systems: an overview of some recent advances and open problems. *Automatica*, 2003, vol. 39, no. 10, pp. 1667-1694. ISSN 0005-1098.

[142] RODUNER, C., GEERING, H. P. Modellbasierte Mehrgroessen-Regulung eines Ottomotors unter Berueckichtigung der Totzeiten. *Automatisierungstechnik,* 1996, vol. 44, no. 7, pp. 314-321. ISSN 0178-2312.

[143] ROOSE, D., LUZYANINA, T., ENGELBORGHS, K., MICHIELS, W. Software for stability and bifurcation analysis of delay differential equations and applications to stabilization. In S.-I. Niculescu and K. Gu (Eds.), *Advances in Time-Delay Systems*, vol. 38, New York: Springer, 2004, pp. 167-182. ISBN 978-3540208907.

[144] ROSICKÝ, J. *Algebra I*. 2nd ed. Brno: Masaryk University in Brno, Czech Republic, 1994. ISBN 80-210-0990-.

[145] ROUCHALEAU, Y. *Linear, Discrete Time, Finite Dimensional Dynamical Systems over Some Classes of Commutative Rings*. Ph.D. thesis. Stanford: Stanford University, 1972.

[146] ROUCHALEAU, Y., WYMAN, B. F., KALMAN, R. E. Algebraic structure of linear dynamical systems. III. Realization theory over a commutative ring. *Proceedings of the National Academy of Sciences of the United States of America,* 1972, vol. 69, no. 11, pp. 3404-3406. ISSN 0027-8424.

[147] ROWAN, T. H. *Functional Stability Analysis of Numerical Algorithms*. Ph.D. thesis. Austin: University of Texas, 1990.

[148] SCALI, C., MARCHETTI, G., SEMINO, D. Relay and additional delay for identification and autotuning of completely unknown processes. *Industrial and Engineering Chemistry Research*, 1999, vol. 38, no. 5, pp. 1987-1997. ISSN 0888-5885.

[149] SHEN, S.-H., YU, H.-D., YU, CH.-CH. Use of saturation-relay feedback for autotune identification. *Chemical Engineering Science*, 1996, vol. 51, no. 8, pp. 1187-1198. ISSN 0009-2509.

[150] SILVA, G. J., DATTA, A., BHATTACHARYYA, S. P. *PID Controllers for Time-Delay Systems*. Boston: Birkhäuser, 2005. 400 p. ISBN 978-0817642662.

[151] SIMUENOVIC, G. *Separate Identification of Coefficients and Delays in Time-Delay Systems.* Ph.D. thesis. Prague: Faculty of Mechanical Engineering, Czech Technical University in Prague, 2011.

[152] SINGER, S., NELDER, J. Nelder-Mead algorithm. *Scholarpedia* [online], 2009, vol. 4, no. 7, pp. 2928. Available from: http://www.scholarpedia.org/article/Nelder-Mead_algorithm. ISSN 1941-6016.

[153] SIPAHI, R., OLGAC, N. Complete stability robustness of third-order LTI multiple time-delay systems. *Automatica*, 2005, vol. 41, no. 8, pp. 1413-1422. ISSN 0005-1098.

[154] SKOGESTAD, S., POSTLETHWAITE, I. *Multivariable Feedback Control: Analysis and Design*. Chichester, UK: John Wiley & Sons, 2005. ISBN 978-0470011683.

[155] SMITH, M. C. On stabilization and the existence of coprime factorization. *IEEE Transactions on Automatic Control*, 1989, vol. 34, no. 9, pp. 1005-1007. ISSN 0018-9286.

[156] SONTAG, E. D. Linear systems over commutative rings: A survey. *Ricerche di Automatica*, 1976, vol. 7, no. 1, 1976, pp. 1-34. ISSN 0048-8291.

[157] SONTAG, E. D. Linear systems over commutative rings: a (partial) updated survey. In *Control Science and Technology for the Progress of Society, vol. 1, Kyoto, 1981*. Laxenburg: IFAC, 1982. pp. 325-330. ISBN 978-0080275802.

[158] SPONG, M. W., TARN, T. J. On the spectral controllability of delay-differential equations. *IEEE Transactions on Automatic Control*, 1981, vol. 26, no. 2, pp. 527-528. ISSN 0018-9286.

[159] STÉPÁN, G. *Retarded Dynamical Systems: Stability and Characteristic Functions*. In *Pitman Research Notes in Mathematical Series*, vol. 120. New York: Longman Scientific & Technical, 1989. ISBN 978-0582039322.

[160] ŠEBEK, M. Characteristic polynomial assignment for delay-differential systems via 2-D polynomial equations. *Kybernetika*, 1987, vol. 23, no. 5. ISSN 0023-5954.

[161] ŠEBEK, M. Asymptotic tracking for 2-D and delay-differential systems. *Automatica*, 1988, vol. 24, no. 5, pp. 711-713. ISSN 0005-1098.

[162] ŠVEHLÍKOVÁ, M. *Heating Plant Mathematical Model Verification*. Bachelor's thesis. Zlín: Faculty of Applied Informatics, Tomas Bata University in Zlín, 2009. Supervisor Ing. Libor Pekař.

[163] TAN, K. K., LEE, T. H., WANG, Q. G. An enhanced automatic tuning procedure for PI/PID controllers for process control. *AIChE Journal*, 1996, vol. 42, no. 9, pp. 2555-2562. ISSN 0001-1541.

[164] TAN, K. K., WANG, Q.-G., LEE, T. H. Finite spectrum assignment control of unstable time delay processes with relay tuning. *Industrial & Engineering Chemistry Research*, 1998, vol. 37, no. 4, pp. 1351-1357. ISSN 0888-5885.

[165] VANASSCHE, V., DAMBRINE, M., LAFAY, J. F., RICHARD, J. P. Some problems arising in the implementation of distributed-delay control laws. In *Proceedings of the 38th Conference on Decision and Control*, Phoenix, AZ, 1999. pp. 4668-4672. ISBN 978-0780352506.

[166] VANBIERVLIET, T., VERHEYDEN, K., MICHIELS, W., VANDEWALLE, S. A nonsmooth optimization approach for the stabilization of time-delay systems. *ESIAM: Control, Optimisation and Calculus of Variations*, 2008, vol. 14, no. 3, pp. 478-493. ISSN 1292-8119.

[167] VIDYASAGAR, M. *Control System Synthesis: A Factorization Approach*. Cambridge, M.A.: MIT Press, 1985. ISBN 978-0262220279.

[168] VILLAFUERTE, R., MONDIÉ, S. Tuning the leading roots of a second order DC servomotor with proportional retarded control. In *Proceedings of the 9th IFAC*

Workshop on Time Delay Systems (TDS 2010) [online], vol. 9. Prague: IFAC, 2010. pp. 337-342. Available from: http://www.ifac-papersonline.net/Detailed/43740.html. ISBN 978-3-902661-71-5.

[169] VÍTEČKOVÁ, M., VÍTEČEK, A. 2DOF PI and PID controllers tuning. In *Proceedings of the 9th IFAC Workshop on Time Delay Systems (TDS 2010)* [online], vol. 9. Prague: IFAC, 2010. pp. 343-348. Available from: http://www.ifac-papersonline.net/Detailed/43741.html. ISBN 978-3-902661-71-5.

[170] VOLTERRA, V. Sur la théorie mathématique des phénomenès héreditaires. *Journal des Mathématiques Pures et Appliquées*, 1928, vol. 7, pp. 249-298. ISSN 0021-7824.

[171] VYHLÍDAL, T. *Analysis and Synthesis of Time Delay System Spectrum*. Ph.D. thesis. Prague: Faculty of Mechanical Engineering, Czech Technical University in Prague, 2003.

[172] VYHLÍDAL, T., MICHIELS, W., MCGAHAN, P. Synthesis of a strongly stable state-derivative controller for a time delay system using constrained nonsmooth optimization. *IMA Journal of Mathematical Control and Information*, 2010, vol. 27, no. 4, pp. 437-455. ISSN 0265-0754.

[173] VYHLÍDAL, T., ZÍTEK, P. Control system design based on a universal first order model with time delays. *Acta Polytechnica*, 2001, vol. 44, no. 4-5, pp. 49-53. ISSN 1210-2709.

[174] VYHLÍDAL, T., ZÍTEK, P. Quasipolynomial mapping based rootfinder for analysis of time delay systems. In *Proceedings of the 4th IFAC Workshop on Time-Delay systems (TDS 2003)*, Rocquencourt, France, 2003. pp. 227-232. ISBN 978-0080442389.

[175] VYHLÍDAL, T., ZÍTEK, P. Discrete approximation of a time delay system and delta model spectrum. In *Proceedings of the 16th IFAC World Congress* [online], vol. 16, Prague, 2005. Available from: http://www.ifac-papersonline.net/Detailed/27918.html. ISBN 978-3-902661-75-3.

[176] VYHLÍDAL, T., ZÍTEK, P. Mapping based algorithm for large-scale computation of quasi-polynomial zeros. *IEEE Transactions on Automatic Control*, 2009, vol. 54, no. 1, 2009, pp. 171-177. ISSN 0018-9286.

[177] WANG, Q. G., HANG, C. C., ZOU, B. Low-order modelling from relay feedback. *Industrial & Engineering Chemistry Research*, 1997a, vol. 36, no. 2, pp. 375-381. ISSN 0888-5885.

[178] WANG, Q. G., HANG, C. C., BI, Q. Process frequency response estimation from relay feedback. *Control Engineering Practice*, 1997b, vol. 5, no. 9, pp. 1293-1302. ISSN 0967-0661.

[179] WANG, Q. G., HANG, C. C., BI, Q. A technique for frequency response identification from relay feedback. *IEEE Transactions on Control Systems Technology*, 1999a, vol. 7, no. 1, pp. 122-128. ISSN 1063-6536.

[180] WANG, Q.-G., LEE, T. H, TAN, K. K. *Finite Spectrum Assignment for Time Delay Systems*. In *Lecture Notes in Control and Information Sciences*, vol. 239. London: Springer, 1999b. ISBN 978-1-85233-065-1.

[181] WANG, Q.-G., YE., Z., HANG, C.C. Tuning of phase-lead compensators for exact gain and phase margins. *Automatica*, 2006, vol. 42, no. 2, pp. 349-352. ISSN 0005-1098.

[182] WANG, Q.-G., ZHANG, Z., ÅSTRÖM, K. J., CHEK, L. S. Guaranteed dominant pole placement with PID controllers. *Journal of Process Control*, 2009, vol. 19, no. 2, pp. 349-352. ISSN 0959-1524.

[183] WATANABE, K., NOBUYAMA, E., KOJIMA, A. Recent advances in control of time-delay systems – A tutorial review. In *Proceedings of the 35th IEEE Conference on Decision and Control*, Kobe, Japan, 1996. pp. 2083-2089. ISBN 978-0780335905.

[184] WATANABE, K., NOBUYAMA, E., KITAMORI, T., ITO, M. A new algorithm for finite spectrum assignment for single-input systems with time-delays. *IEEE Transactions on Automatic Control*, 1992, vol. 37, no. 9, pp. 1377-1383.

[185] WEISSTEIN, E. W. *MathWorld – A Wolfram Web Resource* [online]. Wolfram Research, 1995 [updated Dec 1, 2012; cited Dec 7, 2012]. Available from: http://mathworld.wolfram.com/.

[186] WILLEMS, J. C. *Models for dynamics*. In *Dynamics Reported. A Series in Dynamical Systems and Their Applications*, vol. 2. U. Kirchgraber, H. O. Walther (Eds.). Chichester: John Wiley & Sons, 1989, pp. 171-269. ISBN 978-0471919582.

[187] WU, J. *Theory and Applications of Partial Functional Differential Equation*s. In *Applied Mathematical Sciences*, vol. 199. New York: Springer, 1996. ISBN 978-0387947716.

[188] WU, M., HE, Y., SHE, J.-H. *Stability Analysis and Robust Control of Time-Delay Systems*. Heidelberg: Science Press Beijing, co-editor Springer, 2010. ISBN 978-3642030369.

[189] XU, B. Stability criteria for linear systems with uncertain delays. *Journal of Mathematical Analysis and Applications*, 2003, vol. 284, no. 2, pp. 455-470. ISSN 0022-247X.

[190] YOULA, D. C. *The synthesis of networks containing lumped and distributed elements, Part I*. In *Network and Switching Theory*, vol. 11. New York: Academic Press, 1968, pp. 73-133.

[191] YU, CH.-CH. *Autotuning of Pid Controllers: A Relay Feedback Approach*. 2nd edition. London: Springer, 2006. 261 p. ISBN 978-1-84628-036-8.

[192] ZELINKA, I. SOMA-Self Organizing Migrating Algorithm. In *New Optimization Techniques in Engineering*. G. C. Onwubolu, B. V. Babu (Eds.). Berlin: Springer, 2004. pp. 167-218. ISBN 978-3540201670.

[193] ZIEGLER, J. G., NICHOLS, N. B. Optimum settings for automatic controllers. *Transactions of ASME*, 1942, vol. 64, pp. 759-768.

[194] ZHANG, W., ALLGOWER, F., LIU, T. Controller parameterization for SISO and MIMO plants with time delay. *Systems & Control Letters*, 2006, vol. 55, no. 10, pp. 794-802. ISSN 0167-6911.

[195] ZÍTEK, P. Anisochronic state theory of dynamic systems. *Acta Technica ČSAV*, 1983, vol. 4. ISSN 0001-7043.

[196] ZÍTEK, P. Anisochronic modelling and stability criterion of hereditary systems. *Problems of Control and Information Theory*, 1986, vol. 15, no. 6, pp. 413-423. ISSN 0370-2529.

[197] ZÍTEK, P. Frequency domain synthesis of hereditary control systems via anisochronic state space. *International Journal of Control*, 1997, vol. 66, no. 4, pp. 539-556. ISSN 0020-7179.

[198] ZÍTEK, P., HLAVA, J. Anisochronic internal model control of time-delay systems. *Control Engineering Practice*, 2001, vol. 9, no. 5, pp. 501-516. ISSN 0967-0661.

[199] ZÍTEK, P., KUČERA, V. Algebraic design of anisochronic controllers for time delay systems. *International Journal of Control*, 2003, vol. 76, no. 16, pp. 1654-1665. ISSN 0020-7179.

[200] ZÍTEK, P., FIŠER, J., VYHLÍDAL, T. Ultimate-frequency based dominant pole placement. In *Proceedings of the 9th IFAC Workshop on Time Delay Systems (TDS 2010)* [online], vol. 9. Prague: IFAC, 2010a. pp. 87-92. Available from: http://www.ifac-papersonline.net/Detailed/43697.html. ISBN 978-3-902661-71-5.

[201] ZÍTEK, P., KUČERA, V., VYHLÍDAL, T. Meromorphic stabilization and control of time delay systems. In *Proceedings of the 16th IFAC World Congress*. Oxford: Elsevier Ltd., 2005. ISBN 0-08-045108-X.

[202] ZÍTEK, P., KUČERA, V., VYHLÍDAL, T. Meromorphic observer-based pole assignment in time delay systems. *Kybernetika*, 2008, vol. 44, no. 5, pp. 633-648. ISSN 0023-5954.

[203] ZÍTEK, P., KUČERA, V., VYHLÍDAL, T. Affine parameterization of cascade control with time delays. In *Proceedings of the 9th IFAC Workshop on Time Delay Systems (TDS 2010)* [online], vol. 9. Prague: IFAC, 2010b. pp. 162-167. Available from: http://www.ifac-papersonline.net/Detailed/43710.html. ISBN 978-3-902661-71-5.

[204] ZÍTEK, P., PETROVÁ, R. Discrete approximation of anisochronic systems using delta transform. In *Proceedings of 5th International Conference on Process Control (RIP '02)*, Kouty nad Desnou, Czech Republic, 2002. ISBN 80-7194-452-1.

[205] ZÍTEK, P., VÍTEČEK, A. *Control of systems with delays and nonlinearities* (in Czech). Prague: ČVUT Publishing, 1999. ISBN 80-0101939X.

[206] ZÍTEK, P., VYHLÍDAL, T. Dominant eigenvalue placement for time delay systems. In *Proceedings of the 5th Portuguese Conference on Automatic Control (Controlo 2002)*, Aveiro, Portugal, 2002. pp. 605-610. ISBN 972-789-072-5.

[207] ZÍTEK, P., VYHLÍDAL, T. Low order time delay approximation of conventional linear model. In *Proceedings of the 4th MathMod Conference*, Vienna, Austria, 2003.

[208] ZÍTEK, P., VYHLÍDAL, T. Argument-increment based stability criterion for neutral time delay systems. In *Proceedings of the 16th Mediterranean Conference on Control and Automation*, Ajaccio, France, 2008. pp. 824-829.

LIST OF AUTHOR'S RELATED PUBLICATIONS

Book chapters

I. PEKAŘ, L., KURECČKOVÁ, E., PROKOP, R. On finite-dimensional transformations of anisochronic controllers designed by algebraic means: A user interface. In *MATLAB - A Fundamental Tool for Scientific Computing and Engineering Applications - Volume 2*. Vasilios N. Katsikis (ed.), Rijeka, Croatia: InTech, 2012, pp. 91-118. ISBN 978-953-51-0751-4.

II. PEKAŘ, L., PROKOP, R. Implementation of a new quasi-optimal controller tuning algorithm for time-delay systems. In *MATLAB for Engineers – Applications in Control, Electrical Engineering, IT and Robotics*. K. Perůtka (Ed.). Rijeka, Croatia: Intech, 2011, pp. 3-26. ISBN 978-953-307-914-1.

Journal papers

I. PEKAŘ, L., PROKOP, R. Algebraic optimal control in RMS ring: A case study. *International Journal of Mathematics and Computers in Simulation* [online], 2013, vol. 7, no. 1, 2013, pp. 59-68. Available from: http://www.naun.org/multimedia/NAUN/mcs/16-645.pdf. ISSN 1998-0159.

II. PEKAŘ, L. On the optimal pole assignment for time-delay systems. *International Journal of Mathematical Models in Applied Sciences* [online], 2013, vol. 7, no. 1, pp. 63-74. Available from: http://www.naun.org/multimedia/NAUN/m3as/16-603.pdf. ISSN 1998-0140.

III. PEKAŘ, L. A ring for description and control of time-delay systems. *WSEAS Transactions on Systems, Special Issue: Modelling, Identification, Stability, Control and Applications*, 2012, vol. 11, no. 10, pp. 539-540. ISSN 2224-2678.

IV. PROKOP, R., PEKAŘ, L., MATUŠŮ, R., KORBEL, J. Autotuning principles for delayed systems. *International Journal of Mathematical Models in Applied Sciences* [online], 2012, vol. 6, no. 2, pp. 273-280. Available from: http://www.naun.org/multimedia/NAUN/m3as/17-738.pdf. ISSN 1998-0140.

V. PEKAŘ, L., KUREČKOVÁ, E. Does the higher order mean the better internal delay rational approximation?. *International Journal of Mathematics and Computers in Simulation* [online], 2012, vol. 6, no. 1, 2012, pp. 153-160. Available from: http://www.naun.org/multimedia/NAUN/mcs/17-742.pdf. ISSN 1998-0159.

VI. PEKAŘ, L., PROKOP, R., MATUŠŮ, R. A stability test for control systems with delays based on the Nyquist criterion. *International Journal of Mathematical Models in Applied Sciences* [online], 2011, vol. 5, no. 6, pp. 1213-1224. Available from: http://www.naun.org/multimedia/NAUN/m3as/17-128.pdf. ISSN 1998-0140.

VII. PEKAŘ, L. Root locus analysis of a retarded quasipolynomial. *WSEAS Transaction on Systems and Control*, 2011, vol. 6, no. 3, pp. 79-91. ISSN 1991-8763.

VIII. PEKAŘ, L., PROKOP, R. Stabilization of a delayed system by a proportional controller. *International Journal of Mathematical Models and Methods in Applied Sciences* [online], 2010, vol. 4, no. 4, pp. 282-290. Available from: http://www.naun.org/multimedia/NAUN/m3as/19-432.pdf. ISSN 1998-0140.

IX. PEKAŘ, L., PROKOP, R. Stability conditions for a retarded quasipolynomial and their applications. *International Journal of Mathematics and Computers in Simulations* [online], 2010, vol. 4, no. 3, pp. 90-98. Available from: http://www.naun.org/multimedia/NAUN/mcs/19-453.pdf. ISSN 1998-0159.

X. PROKOP, R., PEKAŘ, L. Control of delay systems – A meromorphic function approach. *Journal of Cybernetics and Informatics*, 2010, vol. 9, no. 1, pp. 41-49. ISSN 1336-4774.

XI. PROKOP, R., PEKAŘ, L. Systémy se zpožděním – kvazipolynomiální přístup. *Automatizace*, 2009, vol. 52, no. 7-8, pp. 414-420. ISSN 0005-125X.

XII. PEKAŘ, L., PROKOP, R., DOSTÁLEK, P. Circuit heating plant model with internal delays. *WSEAS Transaction on Systems*, 2009, vol. 8, no. 9, pp. 1093-1104. ISSN 1109-2777.

XIII. PEKAŘ, L. Relay test for anisochronic models – time domain solution. *Transactions of the VŠB – Technical University of Ostrava, Mechanical Series*, 2008, vol. 54, no. 2, pp. 103-108. ISSN 1210-0471.

XIV. PEKAŘ, L., PROKOP, R. Algebraic control of integrating processes with dead time by two feedback controllers in the ring RMS. *International Journal of Circuits, Systems and Signal Processing* [online], 2008, vol. 2, no. 4, pp. 249-263. Available from: http://www.naun.org/multimedia/NAUN/circuitssystemssignal/cssp-90.pdf. ISSN 1998-4464.

XV. PEKAŘ, L. Parameterization-based control of anisochronic systems using RMS ring. *Transactions of the VŠB – Technical University of Ostrava, Mechanical Series*, 2007, vol. 53, no. 2, pp. 93-100. ISSN 1210-0471.

XVI. PEKAŘ, L., PROKOP, R. Využití meromorfních funkcí při řízení systémů s dopravním zpožděním. *Automa*, 2007, vol. 13, no. 11, pp. 76-79. ISSN 1210-9592.

Conference contributions

I. PEKAŘ, L., PROKOP, R., NAVRÁTIL, P. Spectral abscissa minimization when algebraic control of unstable LTI-TDS. In *Proceedings of the IFAC Conference on Advances in PID Control*, Brescia, Italy, 2012. Paper no. ThB 1.1.

II. PEKAŘ, L., PROKOP, R. A revised ring of stable and proper quasipolynomial meromorphic functions for LTI-TDS. In *Advances in Mathematical and Computational Methods. Proceedings of the 14th WSEAS International Conference on Mathematical and Computational Methods in Science and Engineering*, Sliema, Malta, 2012. pp. 281-285. ISBN 978-1-61804-117-3.

III. PEKAŘ, L., VALENTA, P. Algebraic 1DoF control of heating process with internal delays. In *Advances in Mathematical and Computational Methods. Proceedings of the 14th WSEAS International Conference on Mathematical and Computational Methods in Science and Engineering*, Sliema, Malta, 2012. pp. 115-120. ISBN 978-1-61804-117-3.

IV. PEKAŘ, L., PROKOP, R. Optimal pole placement for LTI-TDS via some advanced iterative algorithms - Part II: application. In *Recent Researches in Circuits and Systems. Proceedings of the 16th WSEAS International Conference on Systems*, Kos, Kos Island, Greece, 2012. pp. 202-206. ISBN 978-1-61804-108-1.

V. PEKAŘ, L., PROKOP, R. Optimal pole placement for LTI-TDS via some advanced iterative algorithms - Part I: theory. In *Recent Researches in Circuits and Systems. Proceedings of the 16th WSEAS International Conference on Systems*, Kos, Kos Island, Greece, 2012. pp. 196-201. ISBN 978-1-61804-108-1.

VI. PEKAŘ, L., PROKOP, R., DOSTÁLEK, P. Non-stepwise reference tracking for time delay systems. In *Proceedings of 12th International Carpathian Control Conference (ICCC '11)*, Velké Karlovice, Czech Republic, 2011. pp. 292-297. ISBN 978-1-61284-359-9.

VII. PEKAŘ, L., MATUŠŮ, R., DOSTÁLEK, P., DOLINAY, J. The Nyquist criterion for LTI time-delay systems. In *Recent Researches in Automatic Control. Proceedings of the 13th WSEAS International Conference on Automatic Control, Modelling & Simulation*, Lanzarote, Canary Islands, Spain, 2011. pp. 80-85. ISBN 978-1-61804-004-6.

VIII. PEKAŘ, L., PROKOP, R. Analysis of a simple quasipolynomial of degree one. In *Recent Researches in Automatic Control. Proceedings of the 13th WSEAS International Conference on Automatic Control, Modelling & Simulation*, Lanzarote, Canary Islands, Spain, 2011. pp. 86-91. ISBN 978-1-61804-004-6.

IX. PROKOP, R. PEKAŘ, L., MATUŠŮ, R., KORBEL, J. Autotuning of anisochronic controllers for delay systems. In *Mathematical Methods and Techniques in Engineering & Environmental Science. Proceedings of the 13th WSEAS International Conference on Mathematical and Computational Methods in Science and Engineering*, Catania, Sicily, Italy, 2011. pp. 210-216. ISBN 978-1-61804-046-6.

X. PEKAŘ, L., KUREČKOVÁ, E. Rational approximation for time-delay systems: Case studies. In *Mathematical Methods and Techniques in Engineering & Environmental Science. Proceedings of the 13th WSEAS International Conference on Mathematical and Computational Methods in Science and Engineering*, Catania, Sicily, Italy, 2011. pp. 217-222. ISBN 978-1-61804-046-6.

XI. PEKAŘ, L. Nyquist criterion for systems with distributed delays. In *Annals of DAAAM for 2011 & Proceedings of the 22nd International DAAAM Symposium*, Vienna, Austria, 2011. pp. 0485-0486. ISBN 978-3-901509-83-4.

XII. PEKAŘ, L., KUREČKOVÁ, E. Comparison of transfer function rational approximations for LTI-TDS. In *Annals of DAAAM for 2011 & Proceedings of the 22nd International DAAAM Symposium*, Vienna, Austria, 2011. pp. 0483-0484. ISBN 978-3-901509-83-4.

XIII. PEKAŘ, L., PROKOP, R. On reference tracking and disturbance rejection for time delay systems. In *Proceedings of the 31st IASTED International Conference on Modelling, Identification and Control (MIC 2011)*, Innsbruck, Austria, 2011. pp. 327-333. ISBN 978-088986863-2.

XIV. PEKAŘ, L. Control of stable delayed systems using algebraic tools and the modified Nyquist criterion. In *Proceedings of the XXXVth Seminary ASR '10: Instruments and Control*. Ostrava: VŠB-TU in Ostrava, Czech Republic, 2010. pp. 303-312. ISBN 978-80-248-2191-7.

XV. PEKAŘ, L. Anisochronic modelling: A study case. In *Mezinárodní Baťova konference pro doktorandy a mladé vědecké pracovníky 2010* [CD-ROM]. Zlín: Tomas Bata University in Zlín, 2010. 9 p. ISBN 978-80-7318-922-8.

XVI. PEKAŘ, L., PROKOP, R. Closed-loop stability for delayed systems: A case study. In *Annals of DAAAM for 2010 & Proceedings of the 21st International DAAAM Symposium*, Vienna, Austria, 2010. pp. 0663-0664. ISBN 978-3-901509-73-5.

XVII. PEKAŘ, L., PROKOP, R. On a stability of a quasipolynomial. In *Annals of DAAAM for 2010 & Proceedings of the 21st International DAAAM Symposium*, Vienna, Austria, 2010. pp. 0665-0666. ISBN 978-3-901509-73-5.

XVIII. PEKAŘ, L., PROKOP, R. Argument principle based stability conditions of a retarded quasipolynomial with two delays. In *Last Trends on Systems. Proceedings of the 14th WSEAS International Conference on Systems*, vol. 1, Corfu Island, Greece, 2010. pp. 276-281. ISBN 978-960-474-199-1.

XIX. PEKAŘ, L., PROKOP, R. Non-delay depending stability of a time-delay system. In *Last Trends on Systems. Proceedings of the 14th WSEAS International Conference on Systems*, vol. 1, Corfu Island, Greece, 2010. pp. 271-275. ISBN 978-960-474-199-1.

XX. PROKOP, R., PEKAŘ, L., KORBEL, J. Autotuning for delay systems using meromorphic functions. In *Proceedings of the 9th IFAC Workshop on Time Delay Systems (TDS 2010)* [online], vol. 9. Prague: IFAC, 2010. pp. 331-336. Available from: http://www.ifac-papersonline.net/Detailed/43739.html. ISBN 978-3-902661-71-5.

XXI. PEKAŘ, L., PROKOP, R. An approach for relay based identification of anisochronic models. In *Proceedings of the 29th IASTED International Conference on Modelling, Identification and Control (MIC 2010)*, Innsbruck, Austria, 2010. pp. 400-407. ISBN 978-0-88986-833-5.

XXII. PROKOP, R., PEKAŘ, L. Control of delay systems – A meromorphic function approach. In P*roceedings of the International Conference Cybernetics and Informatics 2010*, Vyšná Boča, Slovakia, 2010. 9 p. ISBN 978-80-227-3241-3.

XXIII. PEKAŘ, L., DOSTÁLEK, P., PROKOP, R. An anisochronic model of a thermal circuit process. In *Proceedings of the XXXIVth Seminary ASR '09: Instruments and Control*. Ostrava: VŠB-TU in Ostrava, Czech Republic, 2009. pp. 259-271. ISBN 978-8-248-1953-2.

XXIV. PEKAŘ, L., PROKOP, R. Some observations about the RMS ring for delayed systems. In *Proceedings of the 17th International Conference on Process Control '09*, Štrbské Pleso, Slovakia, 2009. pp. 28-36. ISBN 978-80-227-3081-5.

XXV. PEKAŘ, L., MATUŠŮ, R., DOSTÁLEK, P. A model of a laboratory plant with internal delays. In *Annals of DAAAM for 2009 & Proceedings of the 20th International DAAAM Symposium*, Vienna, Austria, 2009. pp. 0447-0449. ISBN 978-3-901509-70-4.

XXVI. PEKAŘ, L., PROKOP, R., DOSTÁLEK, P. An anisochronic model of a laboratory heating system. *Proceedings of the 13th WSEAS International Conference on Systems*, Rhodos, Greece. Athens: WSEAS, 2009. pp. 165-172. ISBN 978-960-474-097-0.

XXVII. PEKAŘ, L., PROKOP, R. On the limit cycle parameter identification of anisochronic models. In *Proceedings of the 8th International Scientific - Technical Conference Process Control '08* [CD-ROM], Kouty nad Desnou, Czech Republic, 2008. Paper No. 113a. ISBN 978-80-7395-077-4.

XXVIII. PEKAŘ, L. Anisochronní modely a systémy. In *Sborník z Mezinárodní Baťovy konference pro doktorandy a mladé vědecké pracovníky 2008* [CD-ROM]. Zlín: Tomas Bata University in Zlín, 2008. Paper No. 515. ISBN 978-80-7318-664-7.

XXIX. PEKAŘ, L. Relay feedback identification of anisochronic models. In *Proceedings of the XXXIIIrd Seminary ASR '08: Instruments and Control*. Ostrava: VŠB-TU in Ostrava, Czech Republic, 2008. pp. 247-258. ISBN 978-80-248-1727-9.

XXX. PEKAŘ, L., PROKOP, R. Control of delayed integrating processes using two feedback controllers – RMS approach. In *Proceedings of the 7th WSEAS International Conference on System Science and Simulation in Engineering (ICOSSSE '08)*, Venice, Italy, 2008. pp. 35-40. ISBN 978-960-474-027-7.

XXXI. PEKAŘ, L., PROKOP, R. Design of controllers for delayed integration processes using RMS ring. In *16th Mediterranean Conference on Control and Automation*, Ajaccio-Corsica, France. Mediterranean Control Association, 2008. pp. 146-151. ISBN 978-1-4244-2505-1.

XXXII. PEKAŘ, L., PROKOP, R. On some tuning principles for anisochronic controllers. In *2nd International Conference on Advanced Control Circuits & Systems - ACCS'07* [CD-ROM]. Cairo: National Authority for Remote Sensing & Space Sciences (NARSS), 2008a. Paper no. AST108.

XXXIII. PEKAŘ, L., PROKOP, R. An approach for relay based identification of anisochronic models. In *Proceedings of the 27th IASTED International Conference on Modelling, Identification and Control (MIC 2008)*, Innsbruck, Austria, 2008. pp. 438-443. ISBN 978-0-88986-712-3.

XXXIV. PEKAŘ, L. RQ-meromorphic functions control approach for delayed systems. In *Proceedings of the XXXIInd Seminary ASR '07: Instruments and Control*. Ostrava: VŠB-TU in Ostrava, Czech Republic, 2007. pp. 197-207. ISBN 978-80-248-1272-4.

XXXV. PEKAŘ, L., PROKOP, R. Anisochronic controllers for high order systems. In *Proceedings of the 16th International Conference on Process Control '07* [CD-ROM], Štrbské Pleso, Slovakia, 2007. ISBN 978-80-227-3081-5.

XXXVI. PEKAŘ, L., PROKOP, R. Time delay systems – meromorphic function control approach. In *Proceedings of the IFAC CEA'07 Conference*, Monterrey, Mexico, 2007. ISBN 978-3-902661-32-6.

XXXVII. PEKAŘ, L., PROKOP, R., KORBEL, J. Autotuning for delay systems in meromorphic functions – a second order case. In *Proceedings of the European Control Conference*, Kos, Greece, 2007. pp. 1839 – 1845. ISBN 978-960-89028-5-5.

XXXVIII. PEKAŘ, L., PROKOP, R., MATUŠŮ, R. Algebraic control of unstable delayed first order systems using RQ-meromorphic functions. In *Proceedings of the 15th Mediterranean Conference on Control and Automation* [CD-ROM], Athens, Greece, 2007. ISBN 978-96-0254-664-2.

XXXIX. PEKAŘ, L., PROKOP, R. A simple stabilization and algebraic control design of unstable delayed systems using meromorphic functions. In *Proceedings of the 26th IASTED International Conference on Modelling, Identification and Control (MIC 2007)*, Innsbruck, Austria, 2007. pp. 183-188. ISBN 978-0-88986-633-1.

XL. PEKAŘ, L., PROKOP, R. Use of meromorphic functions in the control design for delayed systems. In *Proceedings of the 7th International Scientific - Technical Conference Process Control '06*, Kouty nad Desnou, Czech Republic, 2006. p. 50. ISBN 80-7194-860-8.

Publications not related to the topic of the thesis

I. NAVRÁTIL, P., PEKAŘ, L. Combined production of heat and electric energy – Linear mathematical model. In *Recent Researches in Circuits and Systems*. *Proceedings of the 16th WSEAS International Conference on Systems*, Kos, Kos Island, Greece, 2012. pp. 207-212. ISBN 978-1-61804-108-1.

II. NAVRÁTIL, P., PEKAŘ, L. Possible approach to creation and utilization of linear mathematical model of heat source for optimization of combined production of

heat and electric energy. *International Journal of Mathematical Models in Applied Sciences* [online], 2012, vol. 6, no. 8, pp. 943-954. Available from: http://www.naun.org/multimedia/NAUN/m3as/16-499.pdf.

III. PEKAŘ, L., NERI, P. An introduction to the Special Issue on Time Delay Systems: Modelling, Identification, Stability, Control and Applications. *WSEAS Transactions on Systems, Special Issue: Modelling, Identification, Stability, Control and Applications*, 2012, vol. 11, no. 10, pp. 539-540. ISSN 2224-2678.

IV. NAVRÁTIL, P., PEKAŘ, L. One of possible methods of control of multivariable control loop. In *Recent Researches in Automatic Control. Proceedings of the 13th WSEAS International Conference on Automatic Control, Modelling & Simulation*, Lanzarote, Canary Islands, Spain, 2011. pp. 140-144. ISBN 978-1-61804-004-6.

V. MATUŠŮ, R., PROKOP, R., PEKAŘ, L. Uncertainty modelling in time-delay systems: Parametric vs. unstructured approach. In *Recent Researches in Automatic Control. Proceedings of the 13th WSEAS International Conference on Automatic Control, Modelling & Simulation*, Lanzarote, Canary Islands, Spain, 2011. pp. 310-313. ISBN 978-1-61804-004-6.

VI. NAVRÁTIL, P., PEKAŘ, L. Possible solution of decoupling and invariance of multi-variable control loop by using binding and correction members. *WSEAS Transaction on Circuits and Systems*, 2011, vol. 10, no. 6, pp. 209-219. ISSN 1109-2734.

VII. MATUŠŮ, R., PROKOP, R., PEKAŘ, L. Parametric and unstructured approach to uncertainty modelling and robust stability analysis. *International Journal of Mathematical Models in Applied Sciences* [online], 2011, vol. 5, no. 6, pp. 1011-1018. Available from: http://www.naun.org/multimedia/NAUN/m3as/20-844.pdf.

VIII. DOSTÁLEK, P., PEKAŘ, L., VAŠEK, V., DOLINAY, J. Microcontroller based self-tuning digital PID controller. In *Last Trends on Systems. Proceedings of the 14th WSEAS International Conference on Systems*, vol. 1, Corfu Island, Greece, 2010. pp. 248-251. ISBN 978-960-474-199-1.

IX. DOSTÁLEK, P., DOLINAY, J., VAŠEK, V., PEKAŘ, L. Self-tuning digital PID controller implemented on 8–bit Freescale microcontroller. *International Journal of Mathematical Models in Applied Sciences* [online], 2010, vol. 4, no. 4, pp. 274-281. Available from: http://www.naun.org/multimedia/NAUN/m3as/19-425.pdf.

X. MATUŠŮ, R., PROKOP, R., PEKAŘ, L. Approach to discrete-time adaptive control: Software implementation for industrial application. In *Annals of DAAAM for 2009 & Proceedings of the 20th International DAAAM Symposium*, Vienna, Austria, 2009. pp. 0523-0525. ISBN 978-3-901509-70-4.

XI. MATUŠŮ, R., PROKOP, R., PEKAŘ, L. Control of systems with periodic time-varying parameters: an algebraic approach. In *Proceedings of the 15th Mediterranean Conference on Control and Automation* [CD-ROM], Athens, Greece, 2007. Paper No. T31-008. ISBN 978-96-0254-664-2.

AUTHOR'S CURRICULUM VITAE

Personal Information

First name	Libor
Last name	Pekař
E-mail	pekar@fai.utb.cz
Website	http://web.fai.utb.cz/ ?id=0_2_2_7&iid=11&lang=cs&type=0
Phone (office)	(+420) 57 603 5261
Citizenship	Czech Rep.
Birth date	October 11th, 1979
Birth place	Zlín, Czech Rep.
Address (office)	Nad Stráněmi 4511, 76005 Zlín

Current

2006 – today	Teaching and Research Assistant, Faculty of Applied Informatics, Tomas Bata University in Zlín.
	Given courses: Automation, System Theory, Optimization (for Engineering Informatics).
2005 – today	Ph. D. Student, Faculty of Applied Informatics, Tomas Bata University in Zlín. Study programme:

Chemical and Process Engineering. Study course: Technical Cybernetics.

Education

2002 – 2005	Master of Science, Faculty of Applied Informatics, Tomas Bata University in Zlín. Study programme: Chemical and Process Engineering. Study course: Automation and Control in Consumer Industry.
1999 – 2002	Bachelor of Science, Faculty of Technology in Zlín, Technical University of Brno. Study programme: Chemical and Process Engineering. Study course: Automation and Informatics.

Working Experiences and Internships

07/2009	Slovak Technical University, Bratislava, Slovakia. KONTAKT programme (study stay). Lecture: Anisochronic Systems – Analysis and Synthesis in the RMS Ring.
09/2008	Slovak Technical University, Bratislava, Slovakia. KONTAKT programme (study stay).
05/2008	Akademia Techniczno-Humanistyczna, Bielsko-Biala, Poland. ERASMUS programme (teaching stay). Lectures: Analysis and Synthesis of Anisochronic Systems. Relay Identification and Control of Anisochronic Systems in RMS Ring.

04/2006 – 07/2006	Universidade Técnica de Lisboa, Instituto Superior Técnico, Lisboa, Portugal. SOCRATES – ERASMUS programme (Ph.D. study stay).
07/2005 – 09/2005	Split University, Split, Croatia. IAESTE programme. Work contents: Design and assembling of a laboratory model of a second order system.
09/2004 – 09/2006	Computer study room administrator, Library of Tomas Bata University in Zlín.
06/2004 – 08/2004	Hochschule Zittau/Görlitz, Zittau, Germany. IAESTE programme. Work contents: Programming of Kohonen neural networks in Matlab and Delphi.

Languages

Czech	Mother language
Slovak	Fluent
English	Fair (B2)
German	Basic

Grants and Projects

01/2012 – today	Grant of European Regional Development Fund, No. CZ.1.05/2.1.00/03.0089 – The Centre of Safety, Information and Advanced Technologies (CEBIA-Tech). (Co-solver)
10/2011 – today	Project of European Social Fund and Ministry of Education, Sports and Youth of the Czech Republic,

	No. CZ.1.07/2.2.00/15.0463 – Modernization of Educational Material and Didactic Methods. (Co-solver)
09/2011 – 03/2012	Project of Academy of Sciences of the Czech Republic, No. CZ.1.07/2.3.00/09.0034 – Open Science II. Topic: Electronic Database and a Key to Genus Russula (Brittlegill).
03/2010 – 06/2010	Project of Academy of Sciences of the Czech Republic, No. CZ.1.07/2.3.00/09.0034 – Open Science II. Topic: Design of SW for Operating and Control of a Heating Model.
2007 – 2011	Grant of Ministry of Education, Sports and Youth of the Czech Republic, No. MSM 7088352102 – Modeling and Control of Manufacturing Processes of Natural and Synthetic Polymers. (Co-solver)

Honors

2007, 2010	Laureate of Seminary ASR "Instruments and Control", Ostrava, Czech Republic.

Computer Skills

OSs	Microsoft operating systems
Languages	Delphi, (Turbo) Pascal, HTML, CSS, SQL, Matlab, Mathematica
IDE and editors	MS Office, Adobe Acrobat

More

Scientific activities	Co-editor of WSEAS Trans. Systems, Co-organizer of WSEAS conference special sessions (CSCC 2010, ACMOS 2011, CSCC 2012), reviewer of several scientific conferences and journals.
Scientific interests	Analysis and control of time delay systems, algebraic control methods, relay-based autotuning, systems modeling
Associations	Member of MENSA, member of the Czech Mycological Society
Sports	cycling, floorball, cross-country skiing, hiking
Hobbies	mycology, family, brewing